

Advances

in Clinical and Experimental Medicine

MONTHLY ISSN 1899-5276 (PRINT) ISSN 2451-2680 (ONLINE)

advances.umw.edu.pl

2023, Vol. 32, No. 6 (June)

Impact Factor (IF) – 1.736
Ministry of Science and Higher Education – 70 pts
Index Copernicus (ICV) – 168.52 pts



WROCLAW
MEDICAL UNIVERSITY

Advances
in Clinical and Experimental
Medicine



Advances in Clinical and Experimental Medicine

ISSN 1899-5276 (PRINT)

ISSN 2451-2680 (ONLINE)

advances.umw.edu.pl

MONTHLY 2023
Vol. 32, No. 6
(June)

Advances in Clinical and Experimental Medicine (*Adv Clin Exp Med*) publishes high-quality original articles, research-in-progress, research letters and systematic reviews and meta-analyses of recognized scientists that deal with all clinical and experimental medicine.

Editorial Office

ul. Marcinkowskiego 2–6
50-368 Wrocław, Poland
Tel.: +48 71 784 12 05
E-mail: redakcja@umw.edu.pl

Publisher

Wrocław Medical University
Wybrzeże L. Pasteura 1
50-367 Wrocław, Poland

Online edition is the original version
of the journal

Editor-in-Chief

Prof. Donata Kurpas

Deputy Editor

Prof. Wojciech Kosmala

Managing Editor

Marek Misiak, MA

Statistical Editors

Wojciech Bombała, MSc
Anna Kopszak, MSc
Dr. Krzysztof Kujawa

Manuscript editing

Marek Misiak, MA, Jolanta Krzyżak, MA

Scientific Committee

Prof. Sabine Bährer-Kohler
Prof. Antonio Cano
Prof. Breno Diniz
Prof. Erwan Donal
Prof. Chris Fox
Prof. Naomi Hachiya
Prof. Carol Holland
Prof. Markku Kurkinen
Prof. Christos Lionis

Prof. Raimundo Mateos
Prof. Zbigniew W. Raś
Prof. Jerzy W. Rozenblit
Prof. Silvina Santana
Prof. James Sharman
Prof. Jamil Shibli
Prof. Michał Toborek
Prof. László Vécsei
Prof. Cristiana Vitale

Section Editors

Anesthesiology

Prof. Marzena Zielińska

Basic Sciences

Prof. Iwona Bil-Lula
Prof. Bartosz Kempisty
Dr. Wiesława Kranc
Dr. Anna Lebedeva
Dr. Maciej Sobczyński

Clinical Anatomy, Legal Medicine, Innovative Technologies

Prof. Rafael Boscolo-Berto

Dentistry

Prof. Marzena Dominiak
Prof. Tomasz Gedrange
Prof. Jamil Shibli

Laser Dentistry

Assoc. Prof. Kinga Grzech-Leśniak

Dermatology

Prof. Jacek Szepietowski

Emergency Medicine, Innovative Technologies

Prof. Jacek Smereka

Gynecology and Obstetrics

Prof. Olimpia Sipak-Szmigiel

Histology and Embryology

Dr. Mateusz Olbromski

Internal Medicine

Angiology

Dr. Angelika Chachaj

Cardiology

Prof. Wojciech Kosmala
Dr. Daniel Morris

Endocrinology

Prof. Marek Bolanowski

Gastroenterology

Assoc. Prof. Katarzyna Neubauer

Hematology

Prof. Andrzej Deptała

Prof. Dariusz Wołowicz

Nephrology and Transplantology

Assoc. Prof. Dorota Kamińska

Assoc. Prof. Krzysztof Letachowicz

Pulmonology

Prof. Anna Brzecka

Microbiology

Prof. Marzenna Bartoszewicz

Assoc. Prof. Adam Junka

Molecular Biology

Dr. Monika Bielecka

Prof. Jolanta Saczko

Neurology

Assoc. Prof. Magdalena Koszewicz

Assoc. Prof. Anna Pokryszko-Dragan

Dr. Masaru Tanaka

Neuroscience

Dr. Simone Battaglia

Oncology

Prof. Andrzej Deptała

Dr. Marcin Jędryka

Gynecological Oncology

Dr. Marcin Jędryka

Orthopedics

Prof. Paweł Reichert

Otolaryngology

Assoc. Prof. Tomasz Zatoński

Pediatrics

Pediatrics, Metabolic Pediatrics, Clinical Genetics, Neonatology, Rare Disorders

Prof. Robert Śmigiel

Pediatric Nephrology

Prof. Katarzyna Kiliś-Pstrusińska

Pediatric Oncology and Hematology

Assoc. Prof. Marek Ussowicz

Pharmaceutical Sciences

Assoc. Prof. Marta Kepinska

Prof. Adam Matkowski

Pharmacoeconomics, Rheumatology

Dr. Sylwia Szafraniec-Buryło

Psychiatry

Prof. Jerzy Leszek

Assoc. Prof. Bartłomiej Stańczykiewicz

Public Health

Prof. Monika Sawhney

Prof. Izabella Uchmanowicz

Qualitative Studies, Quality of Care

Prof. Ludmiła Marcinowicz

Radiology

Prof. Marek Sądadek

Rehabilitation

Dr. Elżbieta Rajkowska-Labon

Surgery

Assoc. Prof. Mariusz Chabowski

Prof. Renata Taboła

Telemedicine, Geriatrics, Multimorbidity

Assoc. Prof. Maria Magdalena

Bujnowska-Fedak

Editorial Policy

Advances in Clinical and Experimental Medicine (Adv Clin Exp Med) is an independent multidisciplinary forum for exchange of scientific and clinical information, publishing original research and news encompassing all aspects of medicine, including molecular biology, biochemistry, genetics, biotechnology and other areas. During the review process, the Editorial Board conforms to the "Uniform Requirements for Manuscripts Submitted to Biomedical Journals: Writing and Editing for Biomedical Publication" approved by the International Committee of Medical Journal Editors (www.ICMJE.org). The journal publishes (in English only) original papers and reviews. Short works considered original, novel and significant are given priority. Experimental studies must include a statement that the experimental protocol and informed consent procedure were in compliance with the Helsinki Convention and were approved by an ethics committee.

For all subscription-related queries please contact our Editorial Office: redakcja@umw.edu.pl

For more information visit the journal's website: advances.umw.edu.pl

Pursuant to the ordinance of the Rector of Wrocław Medical University No. 12/XVI R/2023, from February 1, 2023, authors are required to pay a fee for each manuscript accepted for publication in the journal Advances in Clinical and Experimental Medicine. The fee amounts to 990 EUR for original papers and meta-analyses, 700 EUR for reviews, and 350 EUR for research-in-progress (RIP) papers and research letters.

Advances in Clinical and Experimental Medicine has received financial support from the resources of Ministry of Science and Higher Education within the "Social Responsibility of Science – Support for Academic Publishing" project based on agreement No. RCN/SP/0584/2021.



Ministry of Education and Science
Republic of Poland

Czasopismo Advances in Clinical and Experimental Medicine korzysta ze wsparcia finansowego ze środków Ministerstwa Edukacji i Nauki w ramach programu „Społeczna Odpowiedzialność Nauki – Rozwój Czasopism Naukowych” na podstawie umowy nr RCN/SP/0584/2021.



Ministerstwo
Edukacji i Nauki

Indexed in: MEDLINE, Science Citation Index Expanded, Journal Citation Reports/Science Edition, Scopus, EMBASE/Excerpta Medica, Ulrich's™ International Periodicals Directory, Index Copernicus

Typographic design: Piotr Gil, Monika Kołęda

DTP: Wydawnictwo UMW

Cover: Monika Kołęda

Printing and binding: Drukarnia I-BiS Bierońscy Sp.k.

Contents

Editorials

- 607 Francesco Di Gregorio, Simone Battaglia
Advances in EEG-based functional connectivity approaches to the study of the central nervous system in health and disease

Meta-analyses

- 613 Shengqiang Zhou, Bo Li, Yihui Deng, Jian Yi, Guo Mao, Ruizhen Wang, Wen Zeng, Baiyan Liu, Dahua Wu, Fang Liu
Meta-analysis of the relations between gut microbiota and pathogens and Parkinson's disease
- 623 Ting Li, Xiumei Zou, Yujuan Kang, Mingzhu Sun, Xi Huang, Xiaoyan Duan
A meta-analysis of the effect of multidisciplinary comprehensive care on health-related quality of life and Unified Parkinson's Disease Rating Scale in Parkinson's disease
- 633 Bo Wang, Ji Xie, Yao Teng
A meta-analysis of the effects of probiotics on various parameters in critically ill ventilated individuals

Original papers

- 643 Tianjiu Zhang, Yifa Ji, Song Yu, Nankai Wang, Qixiao Zhang, Kaicheng Guo
Rspo1 inhibited apoptosis of glucocorticoid-induced osteoblasts via Wnt/ β -catenin pathway in Legg–Calve–Perthes disease
- 655 Li Sun, Guangsheng Gao, Xingsheng Wang, Xinxin Zhang, Yun Li
Protective effect of basic helix-loop-helix family member e40 on cerebral ischemia/reperfusion injury: Inhibition of apoptosis via repressing the transcription of pleckstrin homology-like domain family A, member 1
- 667 Małgorzata Grotowska, Piotr Harbut, Claes Frostell, Waldemar Goździk
Fluid resuscitation, but not inhaled nitric oxide, improves microcirculation in septic pigs
- 677 Xianyi Cheng, Xiulan Deng, Huiping Zeng, Tao Zhou, Dezhi Li, Wei V. Zheng
Silencing of TMED5 inhibits proliferation, migration and invasion, and enhances apoptosis of hepatocellular carcinoma cells
- 689 Yunfei Cheng
Hsa-circ-0000098 promotes the progression of hepatocellular carcinoma by regulation of miR-136-5p/MMP2 axis

Reviews

- 701 Fei Xue, Xin Liu, Xiao Qi, Jiajing Zhou, Yongjun Liu
The clinical research study for fosaprepitant to prevent chemotherapy-induced nausea and vomiting: A review
- 707 Yeshun Wu, Hongqing Xu, Xiaoming Tu, Zhenyan Gao
Review of the epidemiology, pathogenesis and prevention of atrial fibrillation after pacemaker implantation

Advances in EEG-based functional connectivity approaches to the study of the central nervous system in health and disease

Francesco Di Gregorio^{1,2,A,D–F}, Simone Battaglia^{2,A,D–F}

¹ Azienda Unità Sanitaria Locale, UOC Rehabilitative Medicine and Neurorehabilitation, Bologna, Italy

² Center for Studies and Research in Cognitive Neuroscience, Department of Psychology “Renzo Canestrari”, Cesena Campus, University of Bologna, Italy

A – research concept and design; B – collection and/or assembly of data; C – data analysis and interpretation;

D – writing the article; E – critical revision of the article; F – final approval of the article

Advances in Clinical and Experimental Medicine, ISSN 1899–5276 (print), ISSN 2451–2680 (online)

Adv Clin Exp Med. 2023;32(6):607–612

Address for correspondence

Simone Battaglia

E-mail: simone.battaglia@unibo.it

Funding sources

This work was supported by #NEXTGENERATIONEU (NGEU) and funded by the Ministry of University and Research (MUR), National Recovery and Resilience Plan (NRRP), project MNESYS (PE0000006) – A multiscale integrated approach to the study of the nervous system in health and disease (DN. 1553 11.10.2022).

Conflict of interest

None declared

Received on April 28, 2023

Reviewed on May 17, 2023

Accepted on May 24, 2023

Published online on June 6, 2023

Abstract

Functional brain connectivity is closely linked to the complex interactions between brain networks. In the last two decades, measures of functional connectivity based on electroencephalogram (EEG) data have proved to be an important tool for neurologists and clinical and non-clinical neuroscientists. Indeed, EEG-based functional connectivity may reveal the neurophysiological processes and networks underlying human cognition and the pathophysiology of neuropsychiatric disorders. This editorial discusses recent advances and future prospects in the study of EEG-based functional connectivity, with a focus on the main methodological approaches to studying brain networks in health and disease.

Key words: EEG, brain connectivity, brain oscillations, central nervous system, clinical neuroscience

Cite as

Di Gregorio F, Battaglia S. Advances in EEG-based functional connectivity approaches to the study of the central nervous system in health and disease. *Adv Clin Exp Med.* 2023;32(6):607–612. doi:10.17219/acem/166476

DOI

10.17219/acem/166476

Copyright

Copyright by Author(s)

This is an article distributed under the terms of the Creative Commons Attribution 3.0 Unported (CC BY 3.0) (<https://creativecommons.org/licenses/by/3.0/>)

The “old but gold” electroencephalogram

Ever since the German psychiatrist Hans Berger discovered human brainwaves in 1920, the electroencephalogram (EEG) has remained an essential tool for assessing the pathophysiology and brain functions associated with cognitive processes and behavior, as well as brain disorders. The EEG is one of the most frequently used high-temporal resolution techniques in different but convergent scientific fields, including neuroscience, neurology and psychiatry.¹ Indeed, EEG systems are low-cost, non-invasive, can be implemented at the bedside of patients, and have been shown to have high test–retest reliability, sensitivity and specificity.^{2–6} Thus, EEG is considered a valuable method for studying temporal hierarchy and dynamics of neurocognitive processes and the central nervous system in health and disease.^{7–11} In particular, EEG-based measurements can capture fast cognitive dynamics and the temporal progression of cognitive events in the time-frame in which cognition occurs.^{12–19}

Although the use of the EEG in humans for research and clinical purposes is dated, thousands of studies are now described in the scientific literature, and today we can firmly state that EEG is a valuable tool among the neurotechniques that allow the study of brain functions and cognition, as well as their complex interactions. Indeed, due to technological advancements, EEG still represents a valid technique that constantly presents new theoretical, functional and computational challenges. Therefore, in our opinion, we can define it as the ‘old but gold’ neuroscientific methodology.

EEG technical and methodological promises and pitfalls

Over the last two decades, a growing interest has emerged in quantitative measures of EEG-based connectivity. These quantitative analyses allow for the evaluation of interdependencies between brain signals recorded from the scalp level (i.e., sensor space) or between neural nodes (i.e., source space). Different methodological procedures can be applied to the study of EEG-based connectivity.²⁰ Nevertheless, many methodological and theoretical problems may arise. For example, volume conduction represents a primary issue when analyzing sensor–space connectivity.^{21–23} In this regard, the low spatial resolution of the EEG makes it challenging to interpret connectivity results in relation to brain areas. In particular, common neural sources can influence contiguous electrode activity, which may increase the risk of false positive connectivity for contiguous electrodes.^{4,21,24,25} Thus, it is possible to calculate source-level connectivity to reduce the effect of volume conduction.^{4,21} However, source-level methods also have some limitations. While connectivity measures from

sensor-level EEG recordings have low spatial precision, source-level analysis requires a large number of electrodes or accurate head models to infer how electrical fields propagate through the head at a reasonable spatial resolution.²⁶ This process is called the inverse problem.²⁷ Recent studies propose new methodological advances and recommendations to reduce technical and theoretical issues related to EEG analyses.^{3,28} Furthermore, the consensus on using EEG-based measurements may have crucial implications for their application in clinical research.

In a clinical context, the ad hoc visual evaluation of EEG data is still an important criterion for the assessment of epilepsies and disorders of consciousness.^{29–33} However, new computational advances would allow for a more objective and quantitative EEG data analysis. Indeed, scalp-level EEG visual analysis does not allow estimates of the interconnections between distant brain areas and quantitative data, which differs from visual evaluation, as the latter can be compared with normative data.⁷ Finally, these quantitative analyses of EEG data can be used as biomarkers for classifying neuropsychiatric disorders and identifying the psychophysiological correlates of cognition.^{20,34–37}

EEG-based functional connectivity

Empirical research and mathematical models in neuroscience propose oscillatory synchronization between brain nodes and networks as a key mechanism for information sharing within neural networks.^{38–40} However, complex neural networks implicated in cognitive functions communicate at multiple spatial and temporal scales.⁴¹ Indeed, EEG-based measures of connectivity may reflect diverse aspects of these spatiotemporal relationships between electrodes at the scalp level or between nodes at the source space.³ In general, EEG-based connectivity can describe either the statistical linear or non-linear covariation between signals (i.e., functional connectivity) or the causal influence of the activity of one signal over another as effective connectivity.^{42–44} These computational models may unveil intrinsic brain networks and functional mechanisms underlying sensorimotor, cognitive and affective processes in healthy participants and patients with neurological and psychiatric disorders.

There are several methods for quantifying and evaluating functional connectivity using EEG-recorded data,⁴⁵ and each method has its advantages and limitations. Different measures are better suited for specific purposes or assumptions about underlying neurophysiological processes.⁴⁶ In particular, functional connectivity measurements can be based on associations between phases (e.g., phase lag index, phase locking values and phase coherence),^{25,47,48} between the amplitude of the oscillations in specific frequency bands (e.g., power-based coherence and cross-frequency coupling),^{49–52} and in the complexity

of the EEG signal (e.g., mutual information and transfer entropy).^{20,53} In the subsequent sections, we will briefly describe some of the EEG functional connectivity analyses and recent advances, in the use of these analyses, for the study of the brain functioning in health and disease.

(a) The functional connectivity measures based on the phase of brain oscillatory activity rely on the phase angle distribution between 2 signals. For instance, the phase lag index (PLI) and the similar evolutions, namely weighted PLI and squared weighted PLI) evaluates the consistency of the phase differences between 2 EEG signals recorded over specific electrodes or neural nodes.⁴⁷ The PLI has been shown to be less influenced by spurious correlations than power coherence measures because of common sources.⁴⁷

(b) Power-based connectivity analyses involve the correlation between 2 signals over time and across frequency amplitudes. These correlations can be computed between activity in the same or different frequency bands (i.e., power coherence (PC)) and between different events (i.e., inter-trial coherence).^{49,50} For instance, PC calculates the absolute correlation between amplitudes in specific frequency bands over time.

(c) Mutual information (MI) and related measures such as transfer entropy and joint entropy are based on the concept of entropy, which can be defined as the amount of information within a variable.²⁴ Mutual information is a functional connectivity index that estimates the level of information shared between 2 variables or time series, and is calculated by adding the individual entropies of the time series and subtracting the joint entropy.

Therefore, EEG functional connectivity measures can provide multidimensional data and largely independent information. However, the cross-validation of results using more than 1 technique is rare in the literature.³ These evidence-based approaches highlight neural mechanisms of brain plasticity and connectivity in healthy individuals,^{54,55} but more importantly, they could also lead to adequate prediction and evaluation of clinical symptoms or treatment improvements.^{10,20,30,36,56–60} In particular, a recent study compared different measures to predict clinical outcomes in patients with traumatic or non-traumatic acquired brain injuries.²⁰ While the PLI connectivity may reflect the typical diffuse axonal damage in trauma patients, the MI and PC predicted long-term clinical outcomes in all patients. Moreover, a larger PC within the fronto-parietal motor network in the first weeks after stroke correlated positively with subsequent motor and cognitive improvements, while connectivity increases were associated with poorer clinical outcomes.⁶¹

Impaired PLI connectivity within the fronto-parieto-occipital areas can be an accurate biomarker for predicting the future development of psychiatric disorders in subclinical populations.^{60,62,63} In addition, large-scale connectivity impairments within the alpha range have been directly associated with the severity of the positive

symptoms of schizophrenia.⁶⁴ Furthermore, several studies report a decrease in long-range connectivity among the autism spectrum disorder population using different measures,^{65–68} while results regarding short-range connectivity are not as clear.⁶⁴ Moreover, abnormal lateralization and inter-hemispheric connectivity in autism spectrum disorders have been consistently reported across studies.⁶⁴

Conclusions and future insights

As discussed, EEG-based connectivity is a multifaceted world comprising various methodological approaches with different advantages and limitations.^{69,70} There is no optimal brain connectivity measurement, and using one measure should be based on the study hypotheses and the neurophysiological and/or neurological mechanisms behind the specific connectivity. Many recent studies have focused on modeling and estimating EEG-based connectivity, and increasing evidence shows that it can be helpful in investigating and understanding human cognition as well as psychiatric and neurological conditions.^{3,45}

After decades of intensive use, there is no doubt that EEG-based research has a great potential, and the study of EEG functional connectivity can have a massive impact with decisive repercussions in research and clinical practice. However, to use connectivity measures in a clinical context, one of the major advances should be the ability to collect normative data to reduce biases and better understand the link between functional networks and cognition.³ Moreover, although algorithms were implemented to compute functional connectivity measures, technical advances are needed to make those measures reliable and easy to implement in a clinical context. In this view, international cooperation and open data repositories with strict methodological standards should be encouraged among scientists.⁷¹

In recent years, quantitative EEG measurements, brain connectivity data and clinical data were combined using machine learning algorithms in multicenter studies to improve accuracy in the clinical classification of neuropsychiatric diseases and brain diseases as well as to study complex cognitive functions.^{20,57,72} Advances in the application of machine learning algorithms in a clinical context may help with clinical decision-making and the implementation of brain–computer interfaces in neurorehabilitation. Moreover, integrating psychophysiological, structural and functional imaging data with behavioral data using causative statistics can create models of cognitive functions⁷³ and neuropsychiatric diseases,^{10,74–76} and advance our understanding of human cognition.

In the near future, EEG-based connectivity could provide crucial information about neural network functioning in health and disease with high temporal resolution and precision. These EEG measurements may help characterize

the psychophysiological correlates of brain diseases and cognitive functions as well as monitor the psychophysiological effects of neurorehabilitative treatments over time. However, current international guidelines do not endorse the use of EEG biomarkers in clinical trials performed in patients, for example, in Alzheimer's disease,⁷⁷ autism spectrum disorders,⁷⁸ depression,⁷⁹ and other neuropsychiatric disorders, despite increasing evidence.⁸⁰ Thus, it is currently reasonable, timely and relevant to make a concerted effort to translate scientific advances into clinical practice.

ORCID iDs

Francesco Di Gregorio  <https://orcid.org/0000-0002-3587-3149>

Simone Battaglia  <https://orcid.org/0000-0003-4133-654X>

References

1. Biasucci A, Franceschiello B, Murray MM. Electroencephalography. *Curr Biol*. 2019;29(3):R80–R85. doi:10.1016/j.cub.2018.11.052
2. Brienza M, Mecarelli O. Neurophysiological basis of EEG. In: Mecarelli O, ed. *Clinical Electroencephalography*. Cham, Switzerland: Springer International Publishing; 2019:9–21. doi:10.1007/978-3-030-04573-9_2
3. Babiloni C, Barry RJ, Başar E, et al. International Federation of Clinical Neurophysiology (IFCN); EEG research workgroup. Recommendations on frequency and topographic analysis of resting state EEG rhythms. Part 1: Applications in clinical research studies. *Clin Neurophysiol*. 2020;131(1):285–307. doi:10.1016/j.clinph.2019.06.234
4. Mahjoory K, Nikulin VV, Botrel L, Linkenkaer-Hansen K, Fato MM, Haufe S. Consistency of EEG source localization and connectivity estimates. *Neuroimage*. 2017;152:590–601. doi:10.1016/j.neuroimage.2017.02.076
5. Cocquyt E, Van Laeken H, Van Mierlo P, De Letter M. Test–retest reliability of electroencephalographic and magnetoencephalographic measures elicited during language tasks: A literature review. *Eur J Neurosci*. 2023;57(8):1353–1367. doi:10.1111/ejn.15948
6. Bareham CA, Roberts N, Allanson J, et al. Bedside EEG predicts longitudinal behavioural changes in disorders of consciousness. *Neuroimage Clin*. 2020;28:102372. doi:10.1016/j.nicl.2020.102372
7. Bolwig TG. EEG and psychiatry: Time for a resurrection. *Acta Psychiatr Scand*. 2008;117(4):241–243. doi:10.1111/j.1600-0447.2008.01172.x
8. Buzsáki G, Wang XJ. Mechanisms of gamma oscillations. *Annu Rev Neurosci*. 2012;35(1):203–225. doi:10.1146/annurev-neuro-062111-150444
9. Gerez M, Tello A. Selected quantitative EEG (QEEG) and event-related potential (ERP) variables as discriminators for positive and negative schizophrenia. *Biol Psychiatry*. 1995;38(1):34–49. doi:10.1016/0006-3223(94)00205-H
10. Di Gregorio F, Petrone V, Casanova E, et al. Hierarchical psychophysiological pathways subtend perceptual asymmetries in neglect. *Neuroimage*. 2023;270:119942. doi:10.1016/j.neuroimage.2023.119942
11. Al-Qazzaz NK, Ali SHBM, Ahmad SA, Islam MS, Escudero J. Discrimination of stroke-related mild cognitive impairment and vascular dementia using EEG signal analysis. *Med Biol Eng Comput*. 2018;56(1):137–157. doi:10.1007/s11517-017-1734-7
12. Di Gregorio F, Maier ME, Steinhäuser M. Are errors detected before they occur? Early error sensations revealed by metacognitive judgments on the timing of error awareness. *Conscious Cogn*. 2020;77:102857. doi:10.1016/j.concog.2019.102857
13. Di Gregorio F, Maier ME, Steinhäuser M. Early correlates of error-related brain activity predict subjective timing of error awareness. *Psychophysiology*. 2022;59(7):e14020. doi:10.1111/psyp.14020
14. O'Reilly RC. Six principles for biologically based computational models of cortical cognition. *Trends Cogn Sci*. 1998;2(11):455–462. doi:10.1016/S1364-6613(98)01241-8
15. Kahneman D. *Thinking, Fast and Slow*. New York, USA: Farrar, Straus and Giroux; 2013. ISBN:978-0-374-53355-7.
16. Battaglia S, Cardellicchio P, Di Fazio C, Nazzi C, Fracasso A, Borgomaneri S. Stopping in (e)motion: Reactive action inhibition when facing valence-independent emotional stimuli. *Front Behav Neurosci*. 2022;16:998714. doi:10.3389/fnbeh.2022.998714
17. Battaglia S, Thayer JF. Functional interplay between central and autonomic nervous systems in human fear conditioning. *Trends Neurosci*. 2022;45(7):504–506. doi:10.1016/j.tins.2022.04.003
18. Battaglia S, Orsolini S, Borgomaneri S, Barbieri R, Diciotti S, Di Pellegrino G. Characterizing cardiac autonomic dynamics of fear learning in humans. *Psychophysiology*. 2022;59(12):e14122. doi:10.1111/psyp.14122
19. Battaglia S, Cardellicchio P, Di Fazio C, Nazzi C, Fracasso A, Borgomaneri S. The influence of vicarious fear-learning in “infecting” reactive action inhibition. *Front Behav Neurosci*. 2022;16:946263. doi:10.3389/fnbeh.2022.946263
20. Di Gregorio F, La Porta F, Petrone V, et al. Accuracy of EEG biomarkers in the detection of clinical outcome in disorders of consciousness after severe acquired brain injury: Preliminary results of a pilot study using a machine learning approach. *Biomedicine*. 2022;10(8):1897. doi:10.3390/biomedicine10081897
21. Palva JM, Wang SH, Palva S, et al. Ghost interactions in MEG/EEG source space: A note of caution on inter-areal coupling measures. *Neuroimage*. 2018;173:632–643. doi:10.1016/j.neuroimage.2018.02.032
22. Haufe S, Meinecke F, Görgen K, et al. On the interpretation of weight vectors of linear models in multivariate neuroimaging. *Neuroimage*. 2014;87:96–110. doi:10.1016/j.neuroimage.2013.10.067
23. Hipp JF, Siegel M. Accounting for linear transformations of EEG and MEG data in source analysis. *PLoS One*. 2015;10(4):e0121048. doi:10.1371/journal.pone.0121048
24. Cohen MX. *Analyzing Neural Time Series Data: Theory and Practice*. Cambridge, USA: MIT Press; 2014. ISBN:978-0-262-01987-3.
25. Vinck M, Oostenveld R, Van Wingerden M, Battaglia F, Pennartz CMA. An improved index of phase-synchronization for electrophysiological data in the presence of volume-conduction, noise and sample-size bias. *Neuroimage*. 2011;55(4):1548–1565. doi:10.1016/j.neuroimage.2011.01.055
26. Moezzi B, Goldworthy MR. Commentary: Consistency of EEG source localization and connectivity estimates. *Front Neurosci*. 2018;12:147. doi:10.3389/fnins.2018.00147
27. Van Diessen E, Numan T, Van Dellen E, et al. Opportunities and methodological challenges in EEG and MEG resting state functional brain network research. *Clin Neurophysiol*. 2015;126(8):1468–1481. doi:10.1016/j.clinph.2014.11.018
28. Hallett M, De Haan W, Deco G, et al. Human brain connectivity: Clinical applications for clinical neurophysiology. *Clin Neurophysiol*. 2020;131(7):1621–1651. doi:10.1016/j.clinph.2020.03.031
29. Isaksson A, Wennberg A. Visual evaluation and computer analysis of the EEG: A comparison. *Electroencephalogr Clin Neurophysiol*. 1975;38(1):79–86. doi:10.1016/0013-4694(75)90212-6
30. Bagnato S, Boccagni C, Prestandrea C, Sant'Angelo A, Castiglione A, Galardi G. Prognostic value of standard EEG in traumatic and non-traumatic disorders of consciousness following coma. *Clin Neurophysiol*. 2010;121(3):274–280. doi:10.1016/j.clinph.2009.11.008
31. Duszyk-Bogorodzka A, Zieleniewska M, Jankowiak-Siuda K. Brain activity characteristics of patients with disorders of consciousness in the EEG resting state paradigm: A review. *Front Syst Neurosci*. 2022;16:654541. doi:10.3389/fnsys.2022.654541
32. Smith SJM. EEG in the diagnosis, classification, and management of patients with epilepsy. *J Neurol Neurosurg Psychiatry*. 2005;76(Suppl 2):ii2–ii7. doi:10.1136/jnnp.2005.069245
33. Rossi Sebastiano D, Varotto G, Sattin D, Franceschetti S. EEG assessment in patients with disorders of consciousness: Aims, advantages, limits, and pitfalls. *Front Neurol*. 2021;12:649849. doi:10.3389/fneur.2021.649849
34. Di Gregorio F, Ernst B, Steinhäuser M. Differential effects of instructed and objective feedback reliability on feedback-related brain activity. *Psychophysiology*. 2019;56(9):e13399. doi:10.1111/psyp.13399
35. Keser Z, Buchl SC, Seven NA, et al. Electroencephalogram (EEG) with or without transcranial magnetic stimulation (TMS) as biomarkers for post-stroke recovery: A narrative review. *Front Neurol*. 2022;13:827866. doi:10.3389/fneur.2022.827866
36. Kim B, Winstein C. Can neurological biomarkers of brain impairment be used to predict poststroke motor recovery? A systematic review. *Neurorehabil Neural Repair*. 2017;31(1):3–24. doi:10.1177/1545968316662708
37. Al-Qazzaz NK, Ali SHBM, Ahmad SA, Chellappan K, Islam MdS, Escudero J. Role of EEG as biomarker in the early detection and classification of dementia. *ScientificWorldJournal*. 2014;2014:906038. doi:10.1155/2014/906038

38. Fries P. A mechanism for cognitive dynamics: Neuronal communication through neuronal coherence. *Trends Cogn Sci.* 2005;9(10): 474–480. doi:10.1016/j.tics.2005.08.011
39. Salinas E, Sejnowski TJ. Correlated neuronal activity and the flow of neural information. *Nat Rev Neurosci.* 2001;2(8):539–550. doi:10.1038/35086012
40. Singer W. Synchronization of cortical activity and its putative role in information processing and learning. *Annu Rev Physiol.* 1993;55(1): 349–374. doi:10.1146/annurev.ph.55.030193.002025
41. Varela F, Lachaux JP, Rodriguez E, Martinerie J. The brainweb: Phase synchronization and large-scale integration. *Nat Rev Neurosci.* 2001; 2(4):229–239. doi:10.1038/35067550
42. Valdes-Sosa PA, Roebroeck A, Daunizeau J, Friston K. Effective connectivity: Influence, causality and biophysical modeling. *Neuroimage.* 2011;58(2):339–361. doi:10.1016/j.neuroimage.2011.03.058
43. Friston KJ. Functional and effective connectivity: A review. *Brain Connect.* 2011;1(1):13–36. doi:10.1089/brain.2011.0008
44. Dietz MJ, Friston KJ, Mattingley JB, Roepstorff A, Garrido MI. Effective connectivity reveals right-hemisphere dominance in audiospatial perception: Implications for models of spatial neglect. *J Neurosci.* 2014;34(14):5003–5011. doi:10.1523/JNEUROSCI.3765-13.2014
45. Cao J, Zhao Y, Shan X, et al. Brain functional and effective connectivity based on electroencephalography recordings: A review. *Hum Brain Mapp.* 2022;43(2):860–879. doi:10.1002/hbm.25683
46. Imperatori LS, Betta M, Cecchetti L, et al. EEG functional connectivity metrics wPLI and wSML account for distinct types of brain functional interactions. *Sci Rep.* 2019;9(1):8894. doi:10.1038/s41598-019-45289-7
47. Stam CJ, Nolte G, Daffertshofer A. Phase lag index: Assessment of functional connectivity from multi channel EEG and MEG with diminished bias from common sources. *Hum Brain Mapp.* 2007;28(11): 1178–1193. doi:10.1002/hbm.20346
48. Nolte G, Ziehe A, Nikulin VV, et al. Robustly estimating the flow direction of information in complex physical systems. *Phys Rev Lett.* 2008; 100(23):234101. doi:10.1103/PhysRevLett.100.234101
49. Bruns A, Eckhorn R, Jokeit H, Ebner A. Amplitude envelope correlation detects coupling among incoherent brain signals. *Neuroreport.* 2000;11(7):1509–1514. PMID:10841367.
50. Hipp JF, Hawellek DJ, Corbetta M, Siegel M, Engel AK. Large-scale cortical correlation structure of spontaneous oscillatory activity. *Nat Neurosci.* 2012;15(6):884–890. doi:10.1038/nn.3101
51. Canolty RT, Knight RT. The functional role of cross-frequency coupling. *Trends Cogn Sci.* 2010;14(11):506–515. doi:10.1016/j.tics.2010.09.001
52. Allen EA, Liu J, Kiehl KA, et al. Components of cross-frequency modulation in health and disease. *Front Syst Neurosci.* 2011;5:59. doi:10.3389/fnsys.2011.00059
53. King JR, Sitt JD, Faugeras F, et al. Information sharing in the brain indexes consciousness in noncommunicative patients. *Curr Biol.* 2013; 23(19):1914–1919. doi:10.1016/j.cub.2013.07.075
54. Battaglia S, Nazzi C, Thayer JF. Fear-induced bradycardia in mental disorders: Foundations, current advances, future perspectives. *Neurosci Biobehav Rev.* 2023;149:105163. doi:10.1016/j.neubiorev.2023.105163
55. Battaglia S, Di Fazio C, Vicario CM, Avenanti A. Neuropharmacological modulation of N-methyl-D-aspartate, noradrenaline and endocannabinoid receptors in fear extinction learning: Synaptic transmission and plasticity. *Int J Mol Sci.* 2023;24(6):5926. doi:10.3390/ijms24065926
56. Bagnato S, Boccagni C, Sant'Angelo A, Fingelkurts AA, Fingelkurts AA, Galardi G. Longitudinal assessment of clinical signs of recovery in patients with unresponsive wakefulness syndrome after traumatic or nontraumatic brain injury. *J Neurotrauma.* 2017;34(2):535–539. doi:10.1089/neu.2016.4418
57. Chennu S, Annen J, Wannez S, et al. Brain networks predict metabolism, diagnosis and prognosis at the bedside in disorders of consciousness. *Brain.* 2017;140(8):2120–2132. doi:10.1093/brain/awx163
58. Di Gregorio F, La Porta F, Casanova E, et al. Efficacy of repetitive transcranial magnetic stimulation combined with visual scanning treatment on cognitive and behavioral symptoms of left hemispatial neglect in right hemispheric stroke patients: Study protocol for a randomized controlled trial. *Trials.* 2021;22(1):24. doi:10.1186/s13063-020-04943-6
59. Di Gregorio F, La Porta F, Lullini G, et al. Efficacy of repetitive transcranial magnetic stimulation combined with visual scanning treatment on cognitive-behavioral symptoms of unilateral spatial neglect in patients with traumatic brain injury: Study protocol for a randomized controlled trial. *Front Neurol.* 2021;12:702649. doi:10.3389/fneur.2021.702649
60. Trajkovic J, Di Gregorio F, Ferri F, Marzi C, Diciotti S, Romei V. Resting state alpha oscillatory activity is a valid and reliable marker of schizotypy. *Sci Rep.* 2021;11(1):10379. doi:10.1038/s41598-021-89690-7
61. Nicolo P, Rizk S, Magnin C, Pietro MD, Schnider A, Guggisberg AG. Coherent neural oscillations predict future motor and language improvement after stroke. *Brain.* 2015;138(10):3048–3060. doi:10.1093/brain/awv200
62. Liu T, Zhang J, Dong X, et al. Occipital alpha connectivity during resting-state electroencephalography in patients with ultra-high risk for psychosis and schizophrenia. *Front Psychiatry.* 2019;10:553. doi:10.3389/fpsy.2019.00553
63. King S, Holleran L, Mothersill D, et al. Early life adversity, functional connectivity and cognitive performance in schizophrenia: The mediating role of IL-6. *Brain Behav Immun.* 2021;98:388–396. doi:10.1016/j.bbi.2021.06.016
64. Ippolito G, Bertaccini R, Tarasi L, et al. The role of alpha oscillations among the main neuropsychiatric disorders in the adult and developing human brain: Evidence from the last 10 years of research. *Biomedicines.* 2022;10(12):3189. doi:10.3390/biomedicines10123189
65. O'Reilly C, Lewis JD, Elsabbagh M. Is functional brain connectivity atypical in autism? A systematic review of EEG and MEG studies. *PLoS One.* 2017;12(5):e0175870. doi:10.1371/journal.pone.0175870
66. Han J, Zeng K, Kang J, et al. Development of brain network in children with autism from early childhood to late childhood. *Neuroscience.* 2017;367:134–146. doi:10.1016/j.neuroscience.2017.10.015
67. Dickinson A, DiStefano C, Lin YY, Scheffler AW, Senturk D, Jeste SS. Interhemispheric alpha-band hypoconnectivity in children with autism spectrum disorder. *Behav Brain Res.* 2018;348:227–234. doi:10.1016/j.bbr.2018.04.026
68. Zhou T, Kang J, Cong F, Li DrX. Early childhood developmental functional connectivity of autistic brains with non-negative matrix factorization. *Neuroimage Clin.* 2020;26:102251. doi:10.1016/j.nicl.2020.102251
69. Balogh L, Tanaka M, Török N, Vécsei L, Taguchi S. Crosstalk between existential phenomenological psychotherapy and neurological sciences in mood and anxiety disorders. *Biomedicines.* 2021;9(4):340. doi:10.3390/biomedicines9040340
70. Tanaka M, Vécsei L. Editorial of Special Issue 'Dissecting Neurological and Neuropsychiatric Diseases: Neurodegeneration and Neuroprotection.' *Int J Mol Sci.* 2022;23(13):6991. doi:10.3390/ijms23136991
71. Tanaka M, Szabó Á, Vécsei L. Integrating armchair, bench, and bedside research for behavioral neurology and neuropsychiatry: Editorial. *Biomedicines.* 2022;10(12):2999. doi:10.3390/biomedicines10122999
72. Engemann DA, Raimondo F, King JR, et al. Robust EEG-based cross-site and cross-protocol classification of states of consciousness. *Brain.* 2018;141(11):3179–3192. doi:10.1093/brain/awy251
73. Casey CP, Tanabe S, Farahbakhsh Z, et al. Dynamic causal modelling of auditory surprise during disconnected consciousness: The role of feedback connectivity. *Neuroimage.* 2022;263:119657. doi:10.1016/j.neuroimage.2022.119657
74. Tanaka M, Toldi J, Vécsei L. Exploring the etiological links behind neurodegenerative diseases: Inflammatory cytokines and bioactive kynurenines. *Int J Mol Sci.* 2020;21(7):2431. doi:10.3390/ijms21072431
75. Tanaka M, Tóth F, Polyák H, Szabó Á, Mándi Y, Vécsei L. Immune influencers in action: Metabolites and enzymes of the tryptophan–kynurenine metabolic pathway. *Biomedicines.* 2021;9(7):734. doi:10.3390/biomedicines9070734
76. Tanaka M, Szabó Á, Spekter E, Polyák H, Tóth F, Vécsei L. Mitochondrial impairment: A common motif in neuropsychiatric presentation? The link to the tryptophan–kynurenine metabolic system. *Cells.* 2022;11(16):2607. doi:10.3390/cells11162607
77. McKhann GM, Knopman DS, Chertkow H, et al. The diagnosis of dementia due to Alzheimer's disease: Recommendations from the National Institute on Aging–Alzheimer's Association workgroups on diagnostic guidelines for Alzheimer's disease. *Alzheimers Dement.* 2011;7(3):263–269. doi:10.1016/j.jalz.2011.03.005

78. Howes OD, Rogdaki M, Findon JL, et al. Autism spectrum disorder: Consensus guidelines on assessment, treatment and research from the British Association for Psychopharmacology. *J Psychopharmacol*. 2018;32(1):3–29. doi:10.1177/0269881117741766
79. Davidson JRT. Major depressive disorder treatment guidelines in America and Europe. *J Clin Psychiatry*. 2010;71(Suppl E1):e04. doi:10.4088/JCP.9058se1c.04gry
80. Babiloni C, Arakaki X, Azami H, et al. Measures of resting state EEG rhythms for clinical trials in Alzheimer's disease: Recommendations of an expert panel. *Alzheimers Dement*. 2021;17(9):1528–1553. doi:10.1002/alz.12311

Meta-analysis of the relations between gut microbiota and pathogens and Parkinson's disease

Shengqiang Zhou^{1,A-D,F}, Bo Li^{2,A-D,F}, Yihui Deng^{3,A-D,F}, Jian Yi^{4,A-D,F}, Guo Mao^{5,A-F},
Ruizhen Wang^{6,A,B,D-F}, Wen Zeng^{6,A-D,F}, Baiyan Liu^{7,A-F}, Dahua Wu^{8,A-C,E,F}, Fang Liu^{1,A-C,E,F}

¹ National TCM Master Liu Zuyi Inheritance Studio, The Affiliated Hospital of Hunan Academy of Chinese Medicine, Changsha, China

² Department of Pediatrics, The First Hospital of Hunan University of Chinese Medicine, Changsha, China

³ Key Laboratory of Hunan Province for Integrated Traditional Chinese and Western Medicine on Prevention and Treatment of Cardio-Cerebral Diseases, Hunan University of Chinese Medicine, Changsha, China

⁴ Key Laboratory of Ministry of Education on Prevention and Treatment of Major Diseases in Internal Medicine of Traditional Chinese Medicine, The First Hospital of Hunan University of Chinese Medicine, Changsha, China

⁵ Key Project Office, The Affiliated Hospital of Hunan Academy of Chinese Medicine, Changsha, China

⁶ Graduate School, Hunan University of Chinese Medicine, Changsha, China

⁷ College of Integrated Traditional Chinese and Western Medicine, Hunan University of Chinese Medicine, Changsha, China

⁸ Department of Neurology, The Affiliated Hospital of Hunan Academy of Chinese Medicine, Changsha, China

A – research concept and design; B – collection and/or assembly of data; C – data analysis and interpretation;

D – writing the article; E – critical revision of the article; F – final approval of the article

Advances in Clinical and Experimental Medicine, ISSN 1899–5276 (print), ISSN 2451–2680 (online)

Adv Clin Exp Med. 2023;32(6):613–621

Address for correspondence

Fang Liu

E-mail: 15874952352@163.com

Funding sources

This work was supported by the Clinical Medical Technology Innovation Guidance Project of Hunan Provincial Department of Science and Technology (grant No. 2021SK51010), the Natural Science Foundation Project of Changsha City (grant No. kq2208144) and the Scientific Research Project of Hunan Provincial Administration of Traditional Chinese Medicine (grant No. 2021083, No.C2022011).

Conflict of interest

None declared

Received on October 11, 2022

Reviewed on November 23, 2022

Accepted on December 6, 2022

Published online on March 7, 2023

Cite as

Zhou S, Li B, Deng Y, et al. Meta-analysis of the relations between gut microbiota and pathogens and Parkinson's disease. *Adv Clin Exp Med.* 2023;32(6):613–621. doi:10.17219/acem/157193

DOI

10.17219/acem/157193

Copyright

Copyright by Author(s)

This is an article distributed under the terms of the Creative Commons Attribution 3.0 Unported (CC BY 3.0) (<https://creativecommons.org/licenses/by/3.0/>)

Abstract

Background. The motor symptoms in patients with Parkinson's disease (PD) are commonly preceded by gastrointestinal (GI) symptoms. The enteric nervous system (ENS) has also been reported to exhibit neuropathological characteristics of PD.

Objectives. To evaluate the relationship between the incidence of parkinsonism and alteration in gut microbiota and pathogens.

Materials and methods. Studies in different languages that evaluate the relationship between gut microorganisms and PD were included into this meta-analysis. The outcomes of these studies were analyzed using a random effects model; it was also used to calculate the mean difference (MD) with 95% confidence interval (95% CI) in order to quantify the impact of different rehabilitation techniques on clinical parameters. Dichotomous and continuous models were used for the analysis of extracted data.

Results. A total of 28 studies were included in our analysis. The analysis of small intestinal bacterial overgrowth showed a significant correlation with Parkinson's subjects compared with controls ($p < 0.001$). In addition, the presence of *Helicobacter pylori* (HP) infection was significantly related to the Parkinson's group ($p < 0.001$). On the other hand, there was a significantly higher abundance level of Bifidobacteriaceae ($p = 0.008$), Verrucomicrobiaceae ($p < 0.001$) and Christensenellaceae ($p = 0.003$) in Parkinson's subjects. In contrast, a significantly lower abundance levels in Parkinson's subjects were found in *Faecalibacterium* ($p = 0.03$), Lachnospiraceae ($p = 0.005$) and Prevotellaceae ($p = 0.005$). No significant difference was related to Ruminococcaceae.

Conclusion. Parkinson's subjects showed a higher degree of alteration of gut microbiota and pathogens compared with normal human subjects. Future multicenter randomized trials are needed.

Key words: intestinal bacteria, *Helicobacter pylori*, microbiota, Parkinson's, gut

Introduction

Parkinson's disease (PD) is a neurological movement illness that affects multiple systems and worsens over time.¹ Patient with PD has both motor and nonmotor symptoms, such as hyposmia, sleep difficulties, depression, and gastrointestinal (GI) symptoms. Motor symptoms include resting tremors, bradykinesia, rigidity, and gait abnormalities.² The most prevalent GI symptom in PD is constipation, which may be present in up to 80% of patients before the appearance of motor symptoms.³ Therefore, constipation is considered a clinical indicator for the diagnosis of prodromal PD.⁴ The loss of dopaminergic neurons in the substantia nigra pars compacta and the appearance of Lewy bodies (LBs) or Lewy neurites, which consist of aberrant α -synuclein aggregates, are the major neuropathological hallmarks of PD.⁵ According to Braak's pathological staging, the development of PD begins with the ingestion or inhalation of a pathogen, which then causes the creation of LBs and their subsequent migration from the GI tract to the central nervous system via the vagus nerve.⁶ As a result, researchers began to pay more attention to the "gut-brain axis" as a potential player in the pathogenic mechanism of PD.

The presence of an intestinal infection has been associated with a higher risk of developing PD,^{7,8} which may then lead to PD-like symptoms.⁹ The gut microbiota of PD patients has been shown to exacerbate α -synuclein-mediated motor impairments and brain disease in a PD mouse model, whereas a germ-free PD mouse model had less severe α -synuclein pathology.¹⁰ Accordingly, a disruption in the gut flora may be a risk factor for PD. The gut microbiota is an intricate system that produces several antimicrobial chemicals and serves as a physical barrier against invading infections.¹¹ There is mounting evidence that LB development in the enteric nervous system (ENS) may be triggered by abnormalities in the gut microbiota and their metabolic products.

Intestinal epithelial *Helicobacter pylori* (HP) is a Gram-negative bacteria that, in the absence of eradication drug therapy, causes chronic mucosal inflammation and persistent infection.¹² Studies conducted in the 1980s proved the causative association of this bacterium with peptic ulcers and stomach cancer.¹² Subsequent research with varying levels of evidence confirmed the association between HP infection and several extra GI diseases, such as idiopathic thrombocytopenic purpura, unexplained iron deficiency anemia, ischemic heart diseases, and neurological disorders (such as stroke, Alzheimer's disease and PD).¹³ Moreover, it has been investigated whether or not HP infection is linked to PD. Patients with PD, for instance, have been found to have a greater frequency of HP infections than the general population.⁸ In several case-control studies, patients with PD have been shown to have greater titers of antibodies to HP than controls.¹⁴ In addition, motor performance is worse in PD patients with HP infection compared to PD patients without HP infection,¹⁵ but motor function can be improved by changing levodopa absorption in PD patients who undergo HP eradication therapy.¹⁶ However,

there has been a dearth of research on whether HP infection is linked to PD in the general population.

Objectives

The current meta-analysis aims to evaluate the relationship between the incidence of parkinsonism and alteration in gut microbiota and pathogens.

Materials and methods

Study design

Meta-analyses of clinical studies were included in the epidemiological declaration and had a set study protocol. For data collection and analysis, a wide variety of databases were consulted, including Google Scholar, Cochrane Library, Embase, OVID, and PubMed, in search of paper published between 1996 to 2020.

Data pooling

Evaluating the association between the occurrence of parkinsonism and alterations in the gut microbiota and pathogens is the subject of prospective and retrospective investigations. There was no language limitation for study inclusion; only human-related research was included regardless of the sample size. In the current meta-analysis, non-interventional studies such as reviews, editorials and research letters were excluded. Figure 1 depicts the comprehensive study identification procedure.

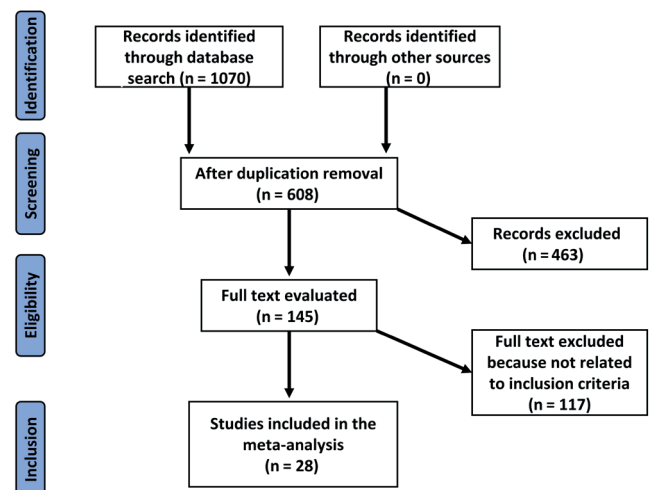


Fig. 1. Schematic diagram of the study procedure and inclusion of trials

Eligibility and inclusion criteria

An evaluation of the association between the incidence of parkinsonism and alterations in the gut microbiota and infections was performed to compile this summary.

The study of sensitivity was limited to articles reporting the association between the occurrence of parkinsonism and alterations in the gut microbiota and pathogens. In addition to examining the impact of the occurrence of infections in PD patients compared to healthy controls, this study also examined the relationship between the two. Various subject types were compared to the interventional groups for subclass and sensitivity analyses.

For an article to be considered for inclusion in our meta-analysis, it had to satisfy the following inclusion criteria:

1. Only clinical trials involving humans were included.
2. Subjects with PD were the intervention population examined against a control group.
3. Intestinal microorganisms, including microbiota, discovered in stool samples, were the main point of research in recruited studies.

The exclusion criteria were:

1. Studies that did not evaluate the relationship between specific microorganisms found in the gut microbiota with the risk of PD.
2. Review articles, research letters, books, or book chapters.

Identification

Under the PICOS principle, the following protocol of search tactics was established: P (population) – subjects with PD; I (intervention/exposure) – stool samples for detection of intestinal bacteria; C (comparison) – quantity and incidence of gut microorganisms in PD compared to controls; O (outcome) – incidence levels of HP and intestinal microorganisms in PD against the control group; S (design of the study) – prospective or retrospective clinical studies.

Relevant articles published till August 2022 were searched through a comprehensive search of Cochrane Library, Embase, PubMed, OVID, and Google Scholar databases, using the key words and associated phrases given in Table 1. The titles and abstracts of all the articles that had been compiled in a reference management program were reviewed, and all studies that did not correlate postoperative results with rehabilitation strategies were excluded. The 2 authors (BL and YD) served as reviewers for the selection of appropriate studies.

Screening

According to the following criteria, data from different studies were collected to include: study- and subject-related features in a standard format; the surname of the first author; the length of the study; the year of publication; the country of the study; the design of the study; the population type recruited in the study; the total number of subjects; qualitative and quantitative evaluation method; demographic data; clinical and treatment characteristics; information source; outcome evaluation; and statistical

Table 1. Search strategy for each database

Database	Search strategy
PubMed	#1 "Parkinsonism"[MeSH terms] OR "Microbiota"[all fields] #2 "Gut"[MeSH terms] OR "H.Pylori"[all fields] #3 #1 AND #2 (word variations have been searched)
Embase	#1 "Parkinsonism"/exp OR "Microbiota" #2 "Gut"/exp OR "H.Pylori" #3 #1 AND #2 (word variations have been searched)
Cochrane Library	#1 "Parkinsonism": ti,ab,kw OR "Microbiota": ti,ab,kw (word variations have been searched) #2 "Gut": ti,ab,kw OR "H.Pylori": ti,ab,kw (word variations have been searched) #3 #1 AND #2
OVID	#1 "Parkinsonism"[all fields] OR "Microbiota"[all fields] #2 "Gut"[all fields] OR "H.Pylori"[all fields] #3 #1 AND #2 (word variations have been searched)
Google Scholar	#1 "Parkinsonism" OR "Microbiota" #2 "Gut" OR "H.Pylori" #3 #1 AND #2 (word variations have been searched)

ti,ab,kw – terms in either title or abstract or keyword fields;
exp – exploded indexing term.

analysis methods. Each study was assessed for bias, and the methodological quality of the chosen studies was evaluated by 2 of the authors in a blinded fashion.

Statistical analyses

Mean difference (MD) and 95% confidence interval (95% CI) were determined using a random effects model. Due to a substantial heterogeneity in certain groups and inconsistent technique in other groups, all groups were evaluated using the random model. Utilizing the fixed models required proof of high similarity between the included studies and low heterogeneity (I^2) level. The I^2 index was calculated as a percentage value ranging from 0% to 100%. The absence of heterogeneity was indicated by I^2 of 0%. The I^2 values ranged from >0% to <25%, 25% to <75% and \geq 75% indicating low, moderate and high heterogeneity, respectively. As indicated previously, the subcategory analysis was performed by stratifying the first evaluation into result categories. The publication bias was analyzed statistically using the Begg's test and the Egger's tests, and it was deemed to exist when $p < 0.05$. The p-values were determined using a two-tailed test. Statistical analyses and graphs were produced using Jamovi 2.3 software (<https://www.jamovi.org/download.html>).

Results

After a review of 1070 relevant studies, 28 studies published between 1996 and 2019 were included

Table 2. Characteristics of included studies

Study	Year	Country	Intervention group, n	Control group, n	Total number of subjects	Intervention
Huang et al. ⁷	2018	Greece	9105	9105	18,210	relation between HP and incidence of parkinsonism
Aho et al. ¹⁷	2019	Finland	64	64	128	relation between gut microbiota and parkinsonism
Barichella et al. ¹⁸	2018	Italy	193	113	306	relation between gut microbiota and parkinsonism
Bedarf et al. ¹⁹	2017	Germany	31	28	59	relation between gut microbiota and parkinsonism
Blaecher et al. ²⁰	2013	Italy	60	256	316	relation between HP and incidence of parkinsonism
Bu et al. ²¹	2015	UK	131	141	272	relation between HP and incidence of parkinsonism
Charlett et al. ²²	1999	Japan	33	78	111	relation between HP and incidence of parkinsonism
Charlett et al. ²³	2009	UK	120	196	316	relation between HP and incidence of parkinsonism
Davies et al. ²⁴	1996	Taiwan	15	15	30	small intestine bacteria overgrowth impact on the incidence of parkinsonism
Dobbs et al. ²⁵	2000	UK	105	210	315	relation between HP and incidence of parkinsonism
Efthymiou et al. ²⁶	2017	Greece	39	68	107	relation between HP and incidence of parkinsonism
Fasano et al. ²⁷	2013	Malaysia	33	30	63	relation between HP and incidence of parkinsonism
Fasano et al. ²⁷	2013	Malaysia	33	30	63	small intestine bacteria overgrowth impact on the incidence of parkinsonism
Gabrielli et al. ²⁸	2011	UK	48	36	84	small intestine bacteria overgrowth impact on the incidence of parkinsonism
Hasegawa et al. ²⁹	2015	USA	52	36	88	relation between gut microbiota and parkinsonism
Hill-Burns et al. ³⁰	2017	China	197	130	327	relation between gut microbiota and parkinsonism
Hopfner et al. ³¹	2017	Germany	29	29	58	relation between gut microbiota and parkinsonism
Li et al. ³²	2019	China	51	48	99	relation between gut microbiota and parkinsonism
Li et al. ³³	2019	China	10	10	20	relation between gut microbiota and parkinsonism
Li et al. ³⁴	2017	China	24	14	38	relation between gut microbiota and parkinsonism
Lin et al. ³⁵	2018	China	75	45	120	relation between gut microbiota and parkinsonism
Nafisah et al. ³⁶	2013	Denmark	29	23	52	relation between HP and incidence of parkinsonism
Nielsen et al. ³⁷	2012	UK	4484	22,416	26,900	relation between HP and incidence of parkinsonism
Niu et al. ³⁸	2012	Italy	182	200	382	small intestine bacteria overgrowth impact on the incidence of parkinsonism
Petrov et al. ³⁹	2017	Russia	89	66	155	relation between gut microbiota and parkinsonism
Ren et al. ⁴⁰	2020	China	14	13	27	relation between gut microbiota and parkinsonism
Scheperjans et al. ⁴¹	2015	Finland	72	72	144	relation between gut microbiota and parkinsonism
Tsolaki et al. ⁴²	2015	China	9	31	40	relation between HP and incidence of parkinsonism
Unger et al. ⁴³	2016	Germany	34	34	68	relation between gut microbiota and parkinsonism

in the meta-analysis because they fit the inclusion criteria.^{7,17–43} Table 2 (characteristics of included studies: year, country, number of subjects, and study quality) summarizes the findings of these investigations.

Small intestinal bacterial overgrowth

The analysis included 4 studies that showed significantly increased growth of small intestinal bacteria in PD subjects compared with controls ($p < 0.001$, MD = 1.66 (95% CI: 1.1623–2.15), $I^2 = 7.1\%$). Neither the rank correlation nor the regression test showed funnel plot asymmetry ($p = 0.33$ and $p = 0.18$, respectively) (Fig. 2A).

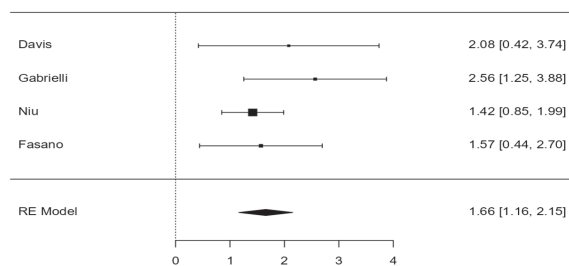
Helicobacter pylori

The analysis comprised 11 studies that found a significantly higher incidence of HP among PD subjects compared with controls ($p < 0.001$, MD = 0.51 (95% CI: 0.27–0.74), $I^2 = 44.5\%$). Neither the rank correlation nor the regression test showed funnel plot asymmetry ($p = 0.44$ and $p = 0.4$, respectively) (Fig. 2B).

Bifidobacteriaceae

The analysis included 8 studies that showed significant abundant levels of Bifidobacteriaceae in PD subjects compared with controls ($p = 0.002$, MD = 0.35 (95% CI: 0.09–0.61), $I^2 = 76\%$). Neither the rank correlation nor

A Incidence of small intestine bacteria overgrowth



B Incidence of *Helicobacter pylori* infection

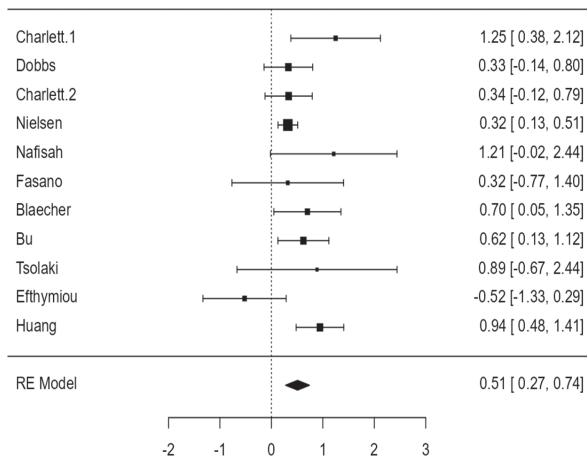


Fig. 2. Forest plot showing the incidence of small intestinal bacterial overgrowth and the incidence of *Helicobacter pylori* (HP) infection for Parkinson's subjects compared with controls

the regression test showed funnel plot asymmetry ($p = 0.11$ and $p = 0.22$, respectively) (Fig. 3A).

Christensenellaceae

Five studies included in this analysis showed significantly higher levels of Christensenellaceae in PD subjects compared with controls ($p = 0.003$, MD = 0.20 (95% CI: 0.07–0.34), $I^2 = 0.67\%$). Neither the rank correlation nor the regression test revealed any funnel plot asymmetries ($p = 0.81$ and $p = 0.85$, respectively) (Fig. 3B).

Faecalibacterium

Five studies included in this analysis showed significantly lower levels of *Faecalibacterium* in PD subjects compared with controls ($p = 0.01$, MD = -0.33 (95% CI: -0.65--0.02), $I^2 = 72.2\%$). Neither the rank correlation nor the regression test indicated any asymmetry in the funnel plot ($p = 1.00$ and $p = 0.52$, respectively) (Fig. 3C).

Lachnospiraceae

The analysis of 7 studies that met the inclusion criteria showed significantly lower levels of Lachnospiraceae in PD subjects compared with controls ($p = 0.005$, MD = -0.34

(95% CI: -0.58--0.1), $I^2 = 62.7\%$). No significant asymmetry was found using either the rank correlation or the regression test ($p = 0.77$ and $p = 0.44$, respectively) (Fig. 3D).

Prevotellaceae

Nine studies included in this analysis showed significantly lower levels of Prevotellaceae in PD subjects compared with controls ($p < 0.001$, MD = -0.37 (95% CI: -0.62--0.11), $I^2 = 72.4\%$). There was no significant bias according to the rank correlation or the regression test ($p = 0.92$ and $p = 0.85$, respectively) (Fig. 3E).

Ruminococcaceae

The analysis included 10 studies that showed a non-significant difference between PD subjects and controls ($p = 0.1$, MD = 0.66 (95% CI: -0.19–1.51), $I^2 = 96.8\%$) regarding Ruminococcaceae levels. The regression test revealed a significant publication bias ($p = 0.001$), although the rank correlation test did not ($p = 0.12$) (Fig. 3F).

Verrucomicrobiaceae

The analysis included 7 studies using the random effects model that showed significant levels of Verrucomicrobiaceae ($p < 0.001$, MD = 0.45 (95% CI: 0.21–0.69), $I^2 = 67.9\%$). Neither rank correlation nor regression test suggested a publication bias ($p = 1.00$ and $p = 0.6279$, respectively) (Fig. 3G).

Discussion

Patients with PD were found to have significantly lower levels of numerous metabolic products secreted by their gut bacteria, which may lead to constipation.⁴³ Functional differences between PD patients and controls were found in the glucuronate and tryptophan degradation pathways.¹⁹ Several bioactive molecules with putative neuroprotective effects, including short-chain fatty acids (SCFAs), ubiquinone and salicylate, were modified in PD, as were the substances associated with neurodegeneration, including ceramides, sphingosine and trimethylamine N-oxide.⁴⁴ Disease duration, motor symptom severity and non-motor symptom severity were all observed to correspond with several gut bacteria.⁴⁵ Changes in the composition of the metabolome, such as the decrease in SCFAs, have also been linked to impairments in cognition. In PD, decreased butyrate levels have been linked to increased levels of postural instability and gait disorder.⁴⁴ Total counts of gut microbiota declined over the course of PD progression and differed between worsening and stable PD groups, according to a 2-year follow-up study that suggested they could be utilized as a diagnostic tool for monitoring the course of PD.^{46,47} The levels

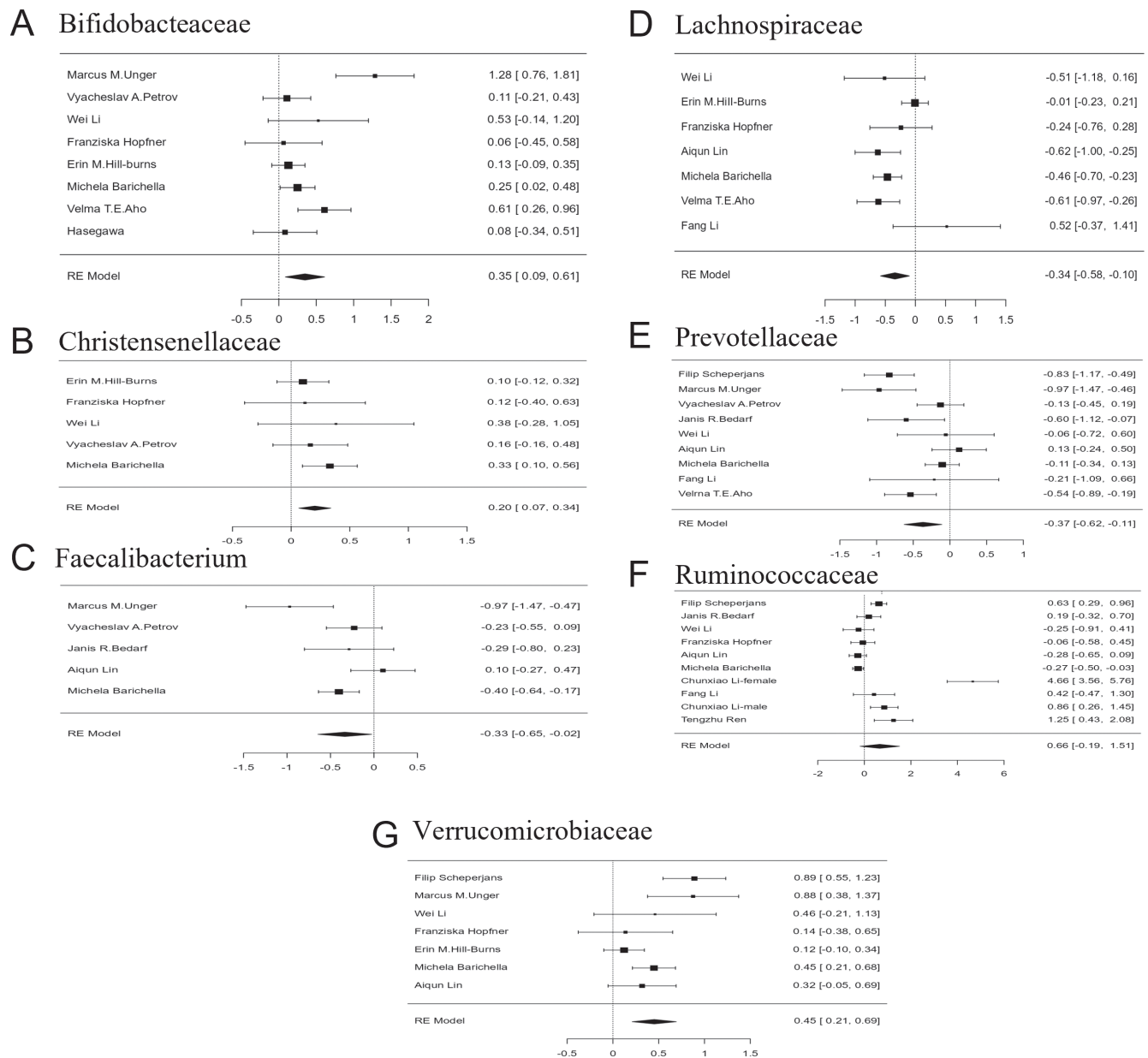


Fig. 3. Forest plot showing alteration in gut microbiota for Parkinson's subjects compared with controls

of Bifidobacteriaceae were found to be lower in the severe case of PD compared with the stable case and they were linked to the delusional symptoms and hallucination.⁴⁷ These manifestations could be a result of a lower antioxidant effect associated with a lower Bifidobacteriaceae count.⁴⁶ In the current study, the level of Bifidobacteriaceae was compared between PD subjects and healthy controls, and was higher in PD subjects. Some studies indicated a lower abundance of Bifidobacteriaceae, while the majority indicated a higher abundance.⁴⁸

Twenty-five genetic markers from the gut microbiota were found to be significantly altered in PD, and an index was developed from these changes; this index could differentiate between individuals with PD and those with multiple system atrophy.⁴⁵ Heterogeneous reactions to levodopa, such as diminished efficacy and unpleasant side

effects, are reported among patients with PD. This may be due, in part, to variations in the gut microbial activity.⁴⁹

Delivery method, newborn feeding, nutrition, lifestyle, culture, geography, age, gender, and other factors all contribute to the unique composition of each person's gut microbiota.⁵⁰ However, even when we controlled for these variables, we still discovered that the quantity of Prevotellaceae, *Faecalibacterium*, Lachnospiraceae, Bifidobacteriaceae, Verrucomicrobiaceae, and Christensenellaceae all varied in a PD patient's gut, regardless of where the study was conducted. These shifts in gut microbiota were mostly associated with PD clinical markers or may have operated as PD progression promoters. It is now well established that inflammation contributes to the onset of PD, activating microglia that play a critical role in the destruction of dopaminergic neurons and the accumulation of α -synuclein.⁵¹ Short-chain fatty acids may have

neuroprotective effects due to their anti-inflammatory and antioxidant properties, which could aid in the regulation of neuroinflammation and gut permeability.⁵² Microglial activation and an uptick in the risk of α -synuclein deposition in PD have been linked to an imbalance in the bacteria that produce SCFAs. In terms of the lipid metabolism pathway, oxidative stress and inflammatory reaction may be facilitated by lipid dysregulation, hence contributing to PD pathophysiological process.⁵³ In synucleinopathy, lipids influence α -synuclein aggregation and transit.^{53,54} This suggests that alterations in the gut microbiota that have a role in lipid metabolism may also contribute to the pathophysiology of PD. A previous review showed results similar to the current study, expressed as the higher abundance of Verrucomicrobiaceae, Christensenellaceae and Bifidobacteriaceae in PD subjects compared with controls.⁵⁵ In addition, it was reported that the abundance of Prevotellaceae is lower in PD subjects compared with controls. While the mentioned review showed different results regarding Ruminococcaceae which have been reported to be highly abundant in PD subjects in 3 studies,⁵⁵ in the current research, 10 studies have been selected and analyzed to reflect the conclusion of a non-significant difference between PD and controls. Another study by Romano et al. showed the results similar to the current studies regarding the abundance of *Bifidobacteriaceae*, *Lachnospiraceae* and *Faecalibacterium* in PD subjects compared with controls.⁵⁶

Various hypotheses have been proposed in order to explain the mechanism(s) connecting HP and eventual PD. For example, endotoxins from Gram-negative bacteria may cause microglia to produce inflammatory markers via the humoral or vagal afferent pathways, leading to the notion of microglia-mediated neuroinflammation. Nitric oxide can be transferred via the vagal pathway⁵⁷ and lead to α -synuclein misfolding,^{58,59} and interleukin (IL)-1 and tumor necrosis factor alpha (TNF- α) can pass the blood–brain barrier and harm the dopaminergic neurons via the humoral pathway.²¹ The α -synuclein is thought to be a prion-like protein that is improperly deposited in the ENS of PD patients and may acquire the access to the central nervous system via the vagus nerve.^{60,61} In its soluble state, the protein would be able to pass the blood–brain barrier.⁶² It has also been suggested that apoptosis may play a role in the link between HP infection and eventual PD,⁶³ with the infection entering the brain via the oral–nasal olfactory route, activating apoptosis via the mitochondrial apoptotic pathway and causing dopaminergic neuron degeneration. The HP infection may promote α -synuclein-mediated neuroinflammation⁶⁴ by disrupting gut microbiota and host homeostasis,⁶⁴ possibly via effects on microbial SCFA signaling and microglial activation. Furthermore, small intestinal bacterial overgrowth may perform an alternate or synergistic role to HP, activating degenerative processes in the ENS.²⁸ Bacterial overgrowth in the small intestine has been linked to an increased risk for developing PD^{28,65} and has been shown to predict motor impairment in PD

on its own. Increased levels of *Enterococcus* spp. and *Staphylococcus aureus* were observed in the stomach and duodenum in other investigations evaluating the impact of HP infection on the digestive tract.⁶⁶ Increased levels of *E. coli* and Enterococci were also found in the cecum, and *Bacteroides/Prevotella* spp. were found in the colon, according to another study.⁶⁷

Limitations

Many studies discussing a similar topic were excluded as they did not meet the inclusion criteria. Furthermore, the influence of race on the shown outcomes was not assessed in all of the included research. In addition, patients with GI symptoms were most commonly diagnosed using endoscopic mucosal biopsy due to the limited funding for ¹³C urea breath testing. This may suggest that the HP infection had been prevalent for some time. Similar difficulties were encountered when attempting to differentiate between HP infection and gastritis or peptic ulcers.

Conclusions

Parkinson's subjects showed a higher degree of alteration of gut microbiota and pathogens compared with healthy subjects. Higher incidence of small intestinal bacteria overgrowth and HP were significantly related to parkinsonism. Future multicenter randomized trials are still needed.

ORCID iDs

Shengqiang Zhou  <https://orcid.org/0000-0002-0786-6419>
 Bo Li  <https://orcid.org/0000-0002-3647-5193>
 Yihui Deng  <https://orcid.org/0000-0003-3073-1982>
 Jian Yi  <https://orcid.org/0000-0002-4198-9631>
 Guo Mao  <https://orcid.org/0000-0003-0293-8273>
 Ruizhen Wang  <https://orcid.org/0000-0001-6178-0096>
 Wen Zeng  <https://orcid.org/0000-0001-8350-982X>
 Baiyan Liu  <https://orcid.org/0000-0002-5469-4402>
 Dahua Wu  <https://www.orcid.org/0000-0002-0510-7072>
 Fang Liu  <https://orcid.org/0000-0002-5089-9697>

References

- Poewe W, Seppi K, Tanner CM, et al. Parkinson disease. *Nat Rev Dis Primers*. 2017;3(1):17013. doi:10.1038/nrdp.2017.13
- Kalia LV, Lang AE. Parkinson's disease. *Lancet*. 2015;386(9996):896–912. doi:10.1016/S0140-6736(14)61393-3
- Su A, Gandhi R, Barlow C, Triadafilopoulos G. A practical review of gastrointestinal manifestations in Parkinson's disease. *Parkinsonism Relat Disord*. 2017;39:17–26. doi:10.1016/j.parkrel.2017.02.029
- Berg D, Postuma RB, Adler CH, et al. MDS research criteria for prodromal Parkinson's disease. *Mov Disord*. 2015;30(12):1600–1611. doi:10.1002/mds.26431
- Abeliovich A, Gitler AD. Defects in trafficking bridge Parkinson's disease pathology and genetics. *Nature*. 2016;539(7628):207–216. doi:10.1038/nature20414
- Rietdijk CD, Perez-Pardo P, Garssen J, van Wezel RJA, Kraneveld AD. Exploring Braak's hypothesis of Parkinson's disease. *Front Neurol*. 2017;8:37. doi:10.3389/fneur.2017.00037
- Huang HK, Wang JH, Lei WY, Chen CL, Chang CY, Liou LS. *Helicobacter pylori* infection is associated with an increased risk of Parkinson's disease: A population-based retrospective cohort study. *Parkinsonism Relat Disord*. 2018;47:26–31. doi:10.1016/j.parkrel.2017.11.331

8. Brudek T. Inflammatory bowel diseases and Parkinson's disease. *J Parkinsons Dis.* 2019;9(S2):S331–S344. doi:10.3233/JPD-191729
9. Matheoud D, Cannon T, Voisin A, et al. Intestinal infection triggers Parkinson's disease-like symptoms in Pink1^{-/-} mice. *Nature.* 2019; 571(7766):565–569. doi:10.1038/s41586-019-1405-y
10. Bhogaraju S, Kalayil S, Liu Y, et al. Phosphoribosylation of ubiquitin promotes serine ubiquitination and impairs conventional ubiquitination. *Cell.* 2016;167(6):1636–1649.e13. doi:10.1016/j.cell.2016.11.019
11. Nair AT, Ramachandran V, Joghee NM, Antony S, Ramalingam G. Gut microbiota dysfunction as reliable non-invasive early diagnostic biomarkers in the pathophysiology of Parkinson's disease: A critical review. *J Neurogastroenterol Motil.* 2018;24(1):30–42. doi:10.5056/jnm17105
12. McColl KEL. *Helicobacter pylori* infection. *N Engl J Med.* 2010;362(17):1597–1604. doi:10.1056/NEJMcp1001110
13. Tan HJ, Goh KL. Extragastrintestinal manifestations of *Helicobacter pylori* infection: Facts or myth? A critical review. *J Digest Dis.* 2012; 13(7):342–349. doi:10.1111/j.1751-2980.2012.00599.x
14. Çamcı G, Oğuz S. Association between Parkinson's disease and *Helicobacter pylori*. *J Clin Neurol.* 2016;12(2):147. doi:10.3988/jcn.2016.12.2.147
15. Tan AH, Mahadeva S, Marras C, et al. *Helicobacter pylori* infection is associated with worse severity of Parkinson's disease. *Parkinsonism Relat Disord.* 2015;21(3):221–225. doi:10.1016/j.parkreldis.2014.12.009
16. Lahner E, Annibale B, Delle Fave G. Systematic review: *Helicobacter pylori* infection and impaired drug absorption. *Aliment Pharmacol Ther.* 2009;29(4):379–386. doi:10.1111/j.1365-2036.2008.03906.x
17. Aho VTE, Pereira PAB, Voutilainen S, et al. Gut microbiota in Parkinson's disease: Temporal stability and relations to disease progression. *EBioMedicine.* 2019;44:691–707. doi:10.1016/j.ebiom.2019.05.064
18. Barichella M, Severgnini M, Cilia R, et al. Unraveling gut microbiota in Parkinson's disease and atypical parkinsonism. *Mov Disord.* 2019;34(3):396–405. doi:10.1002/mds.27581
19. Bedarf JR, Hildebrand F, Coelho LP, et al. Functional implications of microbial and viral gut metagenome changes in early stage L-DOPA naïve Parkinson's disease patients. *Genome Med.* 2017;9(1):39. doi:10.1186/s13073-017-0428-y
20. Blaecher C, Smet A, Flahou B, et al. Significantly higher frequency of *Helicobacter suis* in patients with idiopathic parkinsonism than in control patients. *Aliment Pharmacol Ther.* 2013;38(11–12):1347–1353. doi:10.1111/apt.12520
21. Bu XL, Wang X, Xiang Y, et al. The association between infectious burden and Parkinson's disease: A case-control study. *Parkinsonism Relat Disord.* 2015;21(8):877–881. doi:10.1016/j.parkreldis.2015.05.015
22. Charlett A, Dobbs RJ, Dobbs SM, Weller C, Brady P, Peterson DW. Parkinsonism: Siblings share *Helicobacter pylori* seropositivity and facets of syndrome. *Acta Neurol Scand.* 2009;99(1):26–35. doi:10.1111/j.1600-0404.1999.tb00654.x
23. Charlett A, Dobbs RJ, Dobbs SM, et al. Blood profile holds clues to role of infection in a premonitory state for idiopathic parkinsonism and of gastrointestinal infection in established disease. *Gut Pathog.* 2009;1(1):20. doi:10.1186/1757-4749-1-20
24. Davies KN, King D, Billington D, Barrett JA. Intestinal permeability and oro-caecal transit time in elderly patients with Parkinson's disease. *Postgrad Med J.* 1996;72(845):164–167. doi:10.1136/pgmj.72.845.164
25. Dobbs RJ, Charlett A, Dobbs SM, Weller C, Peterson DW. Parkinsonism: Differential age-trend in *Helicobacter pylori* antibody. *Aliment Pharmacol Ther.* 2000;14(9):1199–1205. doi:10.1046/j.1365-2036.2000.00815.x
26. Efthymiou G, Dardiotis E, Liaskos C, et al. Immune responses against *Helicobacter pylori*-specific antigens differentiate relapsing–remitting from secondary progressive multiple sclerosis. *Sci Rep.* 2017;7(1):7929. doi:10.1038/s41598-017-07801-9
27. Fasano A, Bove F, Gabrielli M, et al. The role of small intestinal bacterial overgrowth in Parkinson's disease. *Mov Disord.* 2013;28(9):1241–1249. doi:10.1002/mds.25522
28. Gabrielli M, Bonazzi P, Scarpellini E, et al. Prevalence of small intestinal bacterial overgrowth in Parkinson's disease. *Mov Disord.* 2011;26(5):889–892. doi:10.1002/mds.23566
29. Hasegawa S, Goto S, Tsuji H, et al. Intestinal dysbiosis and lowered serum lipopolysaccharide-binding protein in Parkinson's disease. *PLoS One.* 2015;10(11):e0142164. doi:10.1371/journal.pone.0142164
30. Hill-Burns EM, Debelius JW, Morton JT, et al. Parkinson's disease and Parkinson's disease medications have distinct signatures of the gut microbiome. *Mov Disord.* 2017;32(5):739–749. doi:10.1002/mds.26942
31. Hopfner F, Künstner A, Müller SH, et al. Gut microbiota in Parkinson disease in a Northern German cohort. *Brain Res.* 2017;1667:41–45. doi:10.1016/j.brainres.2017.04.019
32. Li C, Cui L, Yang Y, et al. Gut microbiota differs between Parkinson's disease patients and healthy controls in northeast China. *Front Mol Neurosci.* 2019;12:171. doi:10.3389/fnmol.2019.00171
33. Li F, Wang P, Chen Z, Sui X, Xie X, Zhang J. Alteration of the fecal microbiota in northeastern Han Chinese population with sporadic Parkinson's disease. *Neurosci Lett.* 2019;707:134297. doi:10.1016/j.neulet.2019.134297
34. Li W, Wu X, Hu X, et al. Structural changes of gut microbiota in Parkinson's disease and its correlation with clinical features. *Sci China Life Sci.* 2017;60(11):1223–1233. doi:10.1007/s11427-016-9001-4
35. Lin A, Zheng W, He Y, et al. Gut microbiota in patients with Parkinson's disease in southern China. *Parkinsonism Relat Disord.* 2018;53:82–88. doi:10.1016/j.parkreldis.2018.05.007
36. Nafisah WY, Mohamed Ibrahim N, Najman Achok H, et al. High prevalence of *Helicobacter pylori* infection in Malaysian Parkinson's disease patients. *J Parkinsonism Restless Legs Syndrome.* 2013;2013:63–67. doi:10.2147/JPRLS.S50491
37. Nielsen HH, Qiu J, Friis S, Wermuth L, Ritz B. Treatment for *Helicobacter pylori* infection and risk of Parkinson's disease in Denmark. *Eur J Neurol.* 2012;19(6):864–869. doi:10.1111/j.1468-1331.2011.03643.x
38. Niu XL, Liu L, Song ZX, et al. Prevalence of small intestinal bacterial overgrowth in Chinese patients with Parkinson's disease. *J Neural Transm.* 2016;123(12):1381–1386. doi:10.1007/s00702-016-1612-8
39. Petrov VA, Saltykova IV, Zhukova IA, et al. Analysis of gut microbiota in patients with Parkinson's disease. *Bull Exp Biol Med.* 2017;162(6):734–737. doi:10.1007/s10517-017-3700-7
40. Ren T, Gao Y, Qiu Y, et al. Gut microbiota altered in mild cognitive impairment compared with normal cognition in sporadic Parkinson's disease. *Front Neurol.* 2020;11:137. doi:10.3389/fneur.2020.00137
41. Scheperjans F, Aho V, Pereira PAB, et al. Gut microbiota are related to Parkinson's disease and clinical phenotype. *Mov Disord.* 2015;30(3):350–358. doi:10.1002/mds.26069
42. Tsolaki F, Kountouras J, Topouzis F, Tsolaki M. *Helicobacter pylori* infection, dementia and primary open-angle glaucoma: Are they connected? *BMC Ophthalmol.* 2015;15(1):24. doi:10.1186/s12886-015-0006-2
43. Unger MM, Spiegel J, Dillmann KU, et al. Short chain fatty acids and gut microbiota differ between patients with Parkinson's disease and age-matched controls. *Parkinsonism Relat Disord.* 2016;32:66–72. doi:10.1016/j.parkreldis.2016.08.019
44. Tan AH, Chong CW, Lim S, et al. Gut microbial ecosystem in Parkinson disease: New clinicobiological insights from multi-omics. *Ann Neurol.* 2021;89(3):546–559. doi:10.1002/ana.25982
45. Qian Y, Yang X, Xu S, et al. Alteration of the fecal microbiota in Chinese patients with Parkinson's disease. *Brain Behav Immun.* 2018;70:194–202. doi:10.1016/j.bbi.2018.02.016
46. Minato T, Maeda T, Fujisawa Y, et al. Progression of Parkinson's disease is associated with gut dysbiosis: Two-year follow-up study. *PLoS One.* 2017;12(11):e0187307. doi:10.1371/journal.pone.0187307
47. Dutta SK, Verma S, Jain V, et al. Parkinson's disease: The emerging role of gut dysbiosis, antibiotics, probiotics, and fecal microbiota transplantation. *J Neurogastroenterol Motil.* 2019;25(3):363–376. doi:10.5056/jnm19044
48. Pietrucci D, Teofani A, Unida V, et al. Can gut microbiota be a good predictor for Parkinson's disease? A machine learning approach. *Brain Sci.* 2020;10(4):242. doi:10.3390/brainsci10040242
49. Maini Rekdal V, Bess EN, Bisanz JE, Turnbaugh PJ, Balskus EP. Discovery and inhibition of an interspecies gut bacterial pathway for levodopa metabolism. *Science.* 2019;364(6445):eaau6323. doi:10.1126/science.aau6323
50. Zhuang X, Xiong L, Li L, Li M, Chen M. Alterations of gut microbiota in patients with irritable bowel syndrome: A systematic review and meta-analysis. *J Gastroenterol Hepatol.* 2017;32(1):28–38. doi:10.1111/jgh.13471
51. Baizabal-Carvalho JF, Alonso-Juarez M. The link between gut dysbiosis and neuroinflammation in Parkinson's disease. *Neuroscience.* 2020;432:160–173. doi:10.1016/j.neuroscience.2020.02.030

52. Bullich C, Keshavarzian A, Garssen J, Kraneveld A, Perez-Pardo P. Gut vibes in Parkinson's disease: The microbiota–gut–brain axis. *Mov Disord Clin Pract*. 2019;6(8):639–651. doi:10.1002/mdc3.12840
53. Hu L, Dong MX, Huang YL, et al. Integrated metabolomics and proteomics analysis reveals plasma lipid metabolic disturbance in patients with Parkinson's disease. *Front Mol Neurosci*. 2020;13:80. doi:10.3389/fnmol.2020.00080
54. Mori A, Imai Y, Hattori N. Lipids: Key players that modulate α -synuclein toxicity and neurodegeneration in Parkinson's disease. *Int J Mol Sci*. 2020;21(9):3301. doi:10.3390/ijms21093301
55. Li Z, Liang H, Hu Y, et al. Gut bacterial profiles in Parkinson's disease: A systematic review [published online as ahead of print on October 25, 2022]. *CNS Neurosci Ther*. 2022. doi:10.1111/cns.13990
56. Romano S, Savva GM, Bedarf JR, Charles IG, Hildebrand F, Narbad A. Meta-analysis of the Parkinson's disease gut microbiome suggests alterations linked to intestinal inflammation. *NPJ Parkinsons Dis*. 2021; 7(1):27. doi:10.1038/s41531-021-00156-z
57. Danzer M, Samberger C, Schicho R, Lippe ITH, Holzer P. Immunocytochemical characterization of rat brainstem neurons with vagal afferent input from the stomach challenged by acid or ammonia. *Eur J Neurosci*. 2004;19(1):85–92. doi:10.1111/j.1460-9568.2004.03109.x
58. Nakamura T, Lipton SA. Redox regulation of mitochondrial fission, protein misfolding, synaptic damage, and neuronal cell death: Potential implications for Alzheimer's and Parkinson's diseases. *Apoptosis*. 2010;15(11):1354–1363. doi:10.1007/s10495-010-0476-x
59. Lema Tomé CM, Tyson T, Rey NL, Grathwohl S, Britschgi M, Brundin P. Inflammation and α -synuclein's prion-like behavior in Parkinson's disease: Is there a link? *Mol Neurobiol*. 2013;47(2):561–574. doi:10.1007/s12035-012-8267-8
60. Visanji NP, Brooks PL, Hazrati LN, Lang AE. The prion hypothesis in Parkinson's disease: Braak to the future. *Acta Neuropathol Commun*. 2013;1(1):2. doi:10.1186/2051-5960-1-2
61. Braak H, Rüb U, Gai WP, Del Tredici K. Idiopathic Parkinson's disease: Possible routes by which vulnerable neuronal types may be subject to neuroinvasion by an unknown pathogen. *J Neural Transm*. 2003;110(5):517–536. doi:10.1007/s00702-002-0808-2
62. Fasano A, Visanji NP, Liu LWC, Lang AE, Pfeiffer RF. Gastrointestinal dysfunction in Parkinson's disease. *Lancet Neurol*. 2015;14(6):625–639. doi:10.1016/S1474-4422(15)00007-1
63. Kountouras J, Zavos C, Polyzos SA, et al. *Helicobacter pylori* infection and Parkinson's disease: Apoptosis as an underlying common contributor. *Eur J Neurol*. 2012;19(6):e56. doi:10.1111/j.1468-1331.2012.03695.x
64. Yang YJ, Sheu BS. Metabolic interaction of *Helicobacter pylori* infection and gut microbiota. *Microorganisms*. 2016;4(1):15. doi:10.3390/microorganisms4010015
65. Dukowicz AC, Lacy BE, Levine GM. Small intestinal bacterial overgrowth: A comprehensive review. *Gastroenterol Hepatol (N Y)*. 2007; 3(2):112–122. PMID:21960820.
66. Yin YN, Wang CL, Liu XW, et al. Gastric and duodenum microflora analysis after long-term *Helicobacter pylori* infection in Mongolian gerbils. *Helicobacter*. 2011;16(5):389–397. doi:10.1111/j.1523-5378.2011.00862.x
67. Heimesaat MM, Fischer A, Plickert R, et al. *Helicobacter pylori* induced gastric immunopathology is associated with distinct microbiota changes in the large intestines of long-term infected Mongolian gerbils. *PLoS One*. 2014;9(6):e100362. doi:10.1371/journal.pone.0100362

A meta-analysis of the effect of multidisciplinary comprehensive care on health-related quality of life and Unified Parkinson's Disease Rating Scale in Parkinson's disease

Ting Li^{1,B,C}, Xiumei Zou^{2,C,D}, Yujuan Kang^{3,B,D,E}, Mingzhu Sun^{1,B,C}, Xi Huang^{1,B,C}, Xiaoyan Duan^{4,A,E,F}

¹ School of Nursing, Shaanxi University of Chinese Medicine, Xianyang, China

² Emergency Department, The Affiliated Traditional Chinese Medicine Hospital of Southwest Medical University, Luzhou, China

³ Nursing Department, Affiliated Hospital of Shaanxi University of Chinese Medicine, Xianyang, China

⁴ Outpatient Department, Affiliated Hospital of Shaanxi University of Chinese Medicine, Xianyang, China

A – research concept and design; B – collection and/or assembly of data; C – data analysis and interpretation;

D – writing the article; E – critical revision of the article; F – final approval of the article

Advances in Clinical and Experimental Medicine, ISSN 1899–5276 (print), ISSN 2451–2680 (online)

Adv Clin Exp Med. 2023;32(6):623–631

Address for correspondence

Xiaoyan Duan

E-mail: lt870027959@163.com

Funding sources

Scientific Research Task Statement of Affiliated Hospital of Shaanxi University of Chinese Medicine Project Name: To explore the effect of auricular acupoint pressing on improvement of sleep disorder in patients with Parkinson's disease based on meridian flow theory (project No. 2022LCJD004).

Conflict of interest

None declared

Received on October 19, 2022

Reviewed on October 29, 2022

Accepted on December 7, 2022

Published online on March 15, 2023

Cite as

Li T, Zou X, Kang Y, Sun M, Huang X, Duan X. A meta-analysis of the effect of multidisciplinary comprehensive care on health-related quality of life and Unified Parkinson's Disease Rating Scale in Parkinson's disease.

Adv Clin Exp Med. 2023;32(6):623–631.

doi:10.17219/acem/157241

DOI

10.17219/acem/157241

Copyright

Copyright by Author(s)

This is an article distributed under the terms of the Creative Commons Attribution 3.0 Unported (CC BY 3.0) (<https://creativecommons.org/licenses/by/3.0/>)

Abstract

Introduction. According to many reports, multidisciplinary comprehensive care alleviates Parkinson's disease (PD) more frequently than any other standard care, though the results were found to vary greatly.

Materials and methods. A systematic literature search up to July 2022 was performed and 1234 related studies were evaluated. The chosen studies comprised 1115 subjects with PD who participated in baseline trials; 633 of them were under multidisciplinary comprehensive care, while 482 were under standard care. Odds ratios (ORs) and mean differences (MDs) with 95% confidence intervals (95% CIs) were calculated to measure the results of multidisciplinary comprehensive care for PD by the contentious and dichotomous approaches with a random or fixed influence model employed.

Results. The use of multidisciplinary comprehensive care resulted in significantly better health-related quality of life (HRQL) (MD: -3.17 ; 95% CI: -5.98 – -0.35 , $p = 0.03$) and Unified Parkinson's Disease Rating Scale (UPDRS) score (MD: -5.25 ; 95% CI: -10.14 – -0.37 , $p = 0.04$) compared to the standard care for subjects with PD. Nevertheless, no significant difference was found between multidisciplinary comprehensive care and standard care for subjects with PD regarding medication dosage (MD: 0.31 ; 95% CI: -0.72 – 1.34 , $p = 0.56$) and caregiver strain (MD: -0.51 ; 95% CI: -1.69 – 0.67 , $p = 0.40$).

Conclusions. Outpatient multidisciplinary comprehensive care models may improve patient-reported HRQL and UPDRS score; nevertheless, no significant difference was found in terms of medication dosage and caregiver strain compared to the standard care for subjects with PD. The small sample size of 2 out of 7 analyzed studies and the small number of studies in certain comparisons requires attention when analyzing the results.

Key words: Parkinson's disease, integrated care, health-related quality of life, Unified Parkinson's Disease Rating Scale

Background

Parkinson's disease (PD) is a progressive neurological condition with bradykinesia, tremor, stiffness, and postural instability as its hallmarks. These clinical symptoms can be present in several illnesses, and the clinical syndrome is known as parkinsonism. Parkinsonian disorders are conditions where parkinsonism is a dominant feature. Parkinson's disease has toxic, traumatic and degenerative vascular etiologies.¹ In autopsy series, synucleinopathies (Lewy body disease and multiple system atrophy) and tauopathies (progressive supranuclear palsy and corticobasal degeneration) are the most prevalent neurological causes of PD.² Because the above causes include additional symptoms, some of these are regarded as atypical PD.^{3,4} Parkinson's disease is characterized by irregularities of movement, including tremors, gait and balance issues, and slowness of movement.⁵ The abnormalities of neuronal and muscular activity that are associated with these symptoms are well understood.⁶ Motor symptoms can also be described in terms of motor control, a level of description that explains how movement variables, such as a limb's position and speed, are controlled and coordinated.⁷ Understanding motor symptoms as motor control abnormalities means identifying how the disease disrupts normal control processes.^{8–14} In the case of PD, movement slowness, for example, would be explained by a disruption of the control processes that determine normal movement speed.^{15–23} The capacity to manage behaviors can be impacted by emotions.²⁴ The valence of emotional cues may have a varied impact on certain motor skills; however, it is unclear whether emotions have a positive or negative impact on action control.²⁵ The stop-signal task, which calculates the ability to completely cancel a response to the presentation of a stop signal using the stop signal reaction times, is a method for measuring reactive inhibitory control.²⁶ When challenged with emotional stimuli, such as stop signals in stop-signal tasks, action control is both impaired and assisted, with conflicting outcomes for positive compared to negative stimuli.²⁷

Since the beginning of cognitive neuroscience, it has been known that emotions have an impact on several executive functions, including the inhibition of action; however, the intricate interplay between emotional stimuli and action regulation is still not fully comprehended.²⁸ The stop-signal task is a method of assessing inhibitory control.²⁹ Regarding internal emotional stimuli such as stop signals in stop-signal tasks, it has been discovered that action control is both aided and impaired.³⁰

Currently, the most effective medical care available for patients with PD entails a medical professional applying cutting-edge diagnostic and therapeutic knowledge acquired from cohort studies and clinical trials.³¹ The ability, experience and intuition of medical professionals to translate knowledge based on collective decision-making to individual decision-making is crucial to the much-needed

customization of medicine.³² Within 20 years, such individual therapeutic decisions will be substantially backed by digital technologies, creating a new healthcare ecosystem that is frequently referred to as "digital medicine."³³ New "digital health pathways" or data-driven personalized decision support, which is based on a combination of multimodal data sources, including evidence-based medical knowledge, is anticipated to be part of the next phase of digitalization (e.g., clinical guidelines).³⁴ Currently, PD can only be treated with symptomatic medications.³⁵ Both motor and a wide range of nonmotor symptoms in PD contribute to the general disease problem.³⁶ This complexity calls for a personalized, all-encompassing therapeutic strategy. Given the variety of symptoms of the disease, PD nurses or care coordinators who specialize in the condition can support patients in achieving their unique therapeutic objectives.³⁷ Better self-management information, adequate interdisciplinary collaboration amongst various healthcare professionals, appropriate amount of time to discuss potential future scenarios, and a specific healthcare professional guiding and support are among the reported core needs from the patient's point of view.³⁸ With widely differing degrees and intensities, several distinct multidisciplinary comprehensive care models have been formed globally to meet these needs.³⁹ All of these models strive to provide PD patients with structured, individually tailored treatment programs. Until now, programs' venues, team makeup or degree of clinical integration have not been consistent. The majority of programs do, nevertheless, adhere to some common disciplines. Additionally, the outcomes of published data vary in terms of study design and findings (including improvement in HRQL). The nomenclature employed is also not uniform, with care models most frequently being referred to as "multidisciplinary", "interprofessional", "interdisciplinary", or "integrated". The phrase "multidisciplinary comprehensive care" is consistently used. The delivery of multidisciplinary comprehensive care involves at least 1 patient and numerous healthcare workers from various specialties. The accessible data and evidence on present multidisciplinary comprehensive care models and their results concerning the improvements in the HRQL of PD patients are synthesized in the current meta-analysis and systematic review, along with Unified Parkinson's Disease Rating Scale (UPDRS), medication dosage and caregiver strain. The most often used rating tool for PD is the UPDRS.^{40,41} Three subscales, namely (I) Mentation, Behavior, and Mood; (II) Activities of Daily Living; and (III) Motor Examination, make up the total UPDRS score, which consists of 31 items.⁴⁰ Although this information might provide help in clinical decision-making, the UPDRS does not evaluate general cardiovascular fitness and offers only scant details on functional performance relevant to daily activities. Therefore, it is important to assess the UPDRS's ability to predict outcomes for time- and resource-intensive tests, such as ambulatory function.

Objectives

The objective of the study was to determine the outcomes of multidisciplinary comprehensive care for PD, e.g., HRQL, UPDRS, medication dosage, and caregiver strain.

Materials and methods

Information sources

All studies included in the analysis involved humans as research participants. Language or study scope were not among the inclusion or exclusion criteria. The list of publications did not include commentaries, review papers and papers that did not present any relationship between the studied phenomena. The complete course of the study is shown in Fig. 1. The studies were chosen for the meta-analysis when the following inclusion criteria were met:

1. The study was either a controlled trial, observational, prospective, or retrospective study.
2. The selected subjects were subjects with PD.
3. The intervention program included multidisciplinary comprehensive care.
4. The study was the consequence of multidisciplinary comprehensive care for PD.

The studies which did not present any comparison of outcomes within its protocol, studies that did not examine multidisciplinary comprehensive care in subjects with PD, and research papers on subjects with no PD or without multidisciplinary comprehensive care were excluded from the study.

Search strategy

A protocol regarding search strategy was developed following the PICOS concept, and was characterized as follows: population (P) – subjects with PD; intervention (I) – multidisciplinary comprehensive care technique; comparison (C) – multidisciplinary comprehensive care compared to standard care; outcomes (O) – HRQL, UPDRS, medication dosages, and caregiver strain; study design (S) – no restrictions.^{42,43}

A thorough search of the OVID, Embase, Cochrane Library, PubMed, and Google Scholar databases up to June 2022 was conducted, using an arrangement of key words and correlated terms regarding multidisciplinary comprehensive care, HRQL, PD, and UPDRS (as shown in Fig. 1 and Table 1). To single out studies that did not examine the relationship between multidisciplinary comprehensive care and standard care in subjects with PD, all included papers were listed in an EndNote file, duplicates were eliminated, and the titles and abstracts were assessed.

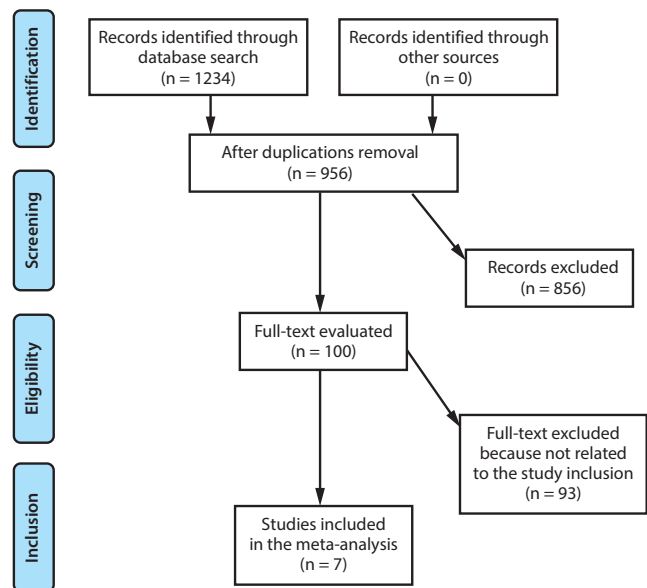


Fig. 1. Flowchart of the study

Table 1. Search strategy for each database

Database	Search strategy
PubMed	#1 "multidisciplinary comprehensive care" [MeSH terms] OR "subjects with Parkinson's disease" [all fields] OR "standard care" [all fields] #2 "Unified Parkinson's Disease Rating Scale" [MeSH terms] OR "Health Related Quality of Life new" [all fields] #3 #1 AND #2
Embase	#1 "multidisciplinary comprehensive care"/exp OR "subjects with Parkinson's disease"/exp OR "standard care" #2 "Unified Parkinson's Disease Rating Scale"/exp OR "Health Related Quality of Life" #3 #1 AND #2
Cochrane Library	#1 "multidisciplinary comprehensive care": ti,ab,kw OR "subjects with Parkinson's disease": ti,ab,kw OR "standard care": ti,ab,kw (word variations have been searched) #2 "Unified Parkinson's Disease Rating Scale": ti,ab,kw OR "Health Related Quality of Life": ti,ab,kw (word variations have been searched) #3 #1 AND #2

MeSH – medical subject headings; ti,ab,kw – terms in either title or abstract or keyword fields; exp – exploded indexing term.

Data collection process

The data collected for the purpose of the study included the last name of the first author, country, quantitative and qualitative assessment technique, the information source, the results of the assessment, and statistical analysis results.⁴⁴

Study risk of bias assessment

Two authors individually evaluated the methodology of the 7 chosen papers to ascertain the possibility of bias in each study. The procedural quality was assessed using

the “risk of bias instrument” from the Cochrane Handbook for Systematic Reviews of Interventions v. 5.1.0.⁴⁵ Each study was assessed according to the evaluation criteria and assigned one of 3 levels of bias risk. A study was rated as having a low risk of bias if all the quality standards were met. If one or more requirements were not met, a study was rated as having a moderate risk of bias. High risk of bias occurred if one or more quality criteria were not met at all or were only partially met. The original article was revised to remove any inconsistencies.

Effect measures

Only the studies that reported and assessed the influence of multidisciplinary comprehensive care in comparison to standard care underwent sensitivity assessment. Sensitivity and subclass analyses were utilized to compare the consequences of multidisciplinary comprehensive care for PD.

Statistical analyses

The current meta-analysis used a fixed- or random-effects model with dichotomous and continuous techniques to compute the odds ratio (OR) and mean difference (MD) with a 95% confidence interval (95% CI). The heterogeneity (I^2) index was calculated using a range of 0–100%. The values were around 0%, 25%, 50%, and 75%, respectively, and showed no, low, moderate, and high heterogeneity.⁴⁶ Additional characteristics that show a high degree of similarity between the included studies were analyzed to confirm the employment of the correct model. The random-effects model was considered if I^2 was 50% or above; if I^2 was less than 50%, the likelihood of employing the fixed-effects model increased.⁴⁶ By stratifying the initial evaluation according to the previously mentioned outcome categories, the subclass analysis was finished. The value of $p = 0.05$ indicated statistical significance for differences between the subcategories.

Reporting bias assessment

Publication bias was measured both qualitatively and statistically using the funnel plots and the Egger's regression test, which display the logarithm of ORs or MDs compared to their standard errors (publication bias was considered for $p = 0.05$).⁴⁷

Certainty assessment

Two-tailed tests were used to analyze all p -values. The graphs were created and the statistical analysis was conducted using Reviewer Manager v. 5.3 (The Cochrane Collaboration, Copenhagen, Denmark).

Results

From a total of 1234 examined studies, 7 articles published between 2003 and 2021 that met the requirements and were included in the meta-analysis were selected.^{48–54} Table 2 presents the findings from these studies. A total of 1115 subjects with PD participated in the selected studies' baseline trials; 633 of them underwent multidisciplinary comprehensive care, while 482 were provided with standard care. Sample size of the analyzed studies was between 79 and 269. Six studies presented data organized according to the HRQL, 4 studies presented data organized according to UPDRS, 3 studies presented data organized according to the medication dosage, and 2 studies presented data organized according to caregiver strain.

The use of multidisciplinary comprehensive care resulted in significantly better HRQL (MD: -3.17 ; 95% CI: -5.98 – -0.35 , $p = 0.03$, $Z = 2.21$, degrees of freedom (df) = 5) with moderate heterogeneity ($I^2 = 55\%$), and UPDRS (MD: -5.25 ; 95% CI: -10.14 – -0.37 , $p = 0.04$, $Z = 2.11$, df = 3) with moderate heterogeneity ($I^2 = 71\%$) compared to the standard care for subjects with PD (Fig. 2,3). Nevertheless, no significant difference was found between multidisciplinary comprehensive care and standard care for subjects with PD in terms of medication dosage (MD: 0.31 ; 95% CI: -0.72 – 1.34 , $p = 0.56$, $Z = 0.59$, df = 2) with no heterogeneity ($I^2 = 0\%$), and caregiver strain (MD: -0.51 ; 95% CI: -1.69 – 0.67 , $p = 0.40$, $Z = 0.85$, df = 1) with low heterogeneity ($I^2 = 28\%$) (Fig. 4,5).

Stratified models could not be utilized to examine the influence of some factors on comparison outcomes, such as gender, age and ethnicity, due to scarcity of data on these parameters. After performing quantitative evaluations using the Egger's regression test and visual inspection of the funnel plot, there was no evidence of publication bias ($p = 0.85$, $p = 0.83$, $p = 0.89$, and $p = 0.91$, respectively, for HRQL, UPDRS, medication dosage, and caregiver strain) (Fig. 6–9). Nevertheless, the bulk of the included randomized controlled trials were found to have subpar methodological quality, no bias in selective reporting, and scant outcome data.

Discussion

In the trials included in this meta-analysis, 1115 subjects with PD participated in baseline trials; 633 of them received multidisciplinary comprehensive care, while 482 were provided with standard care.^{48–54} The use of multidisciplinary comprehensive care resulted in significantly better HRQL and UPDRS compared to the standard care for subjects with PD. Nevertheless, no significant difference was found between multidisciplinary comprehensive care and standard care for subjects with PD in terms of medication dosage and caregiver strain. Caution should be taken when evaluating the results due to the modest sample size of 2 studies ($n = 100$)

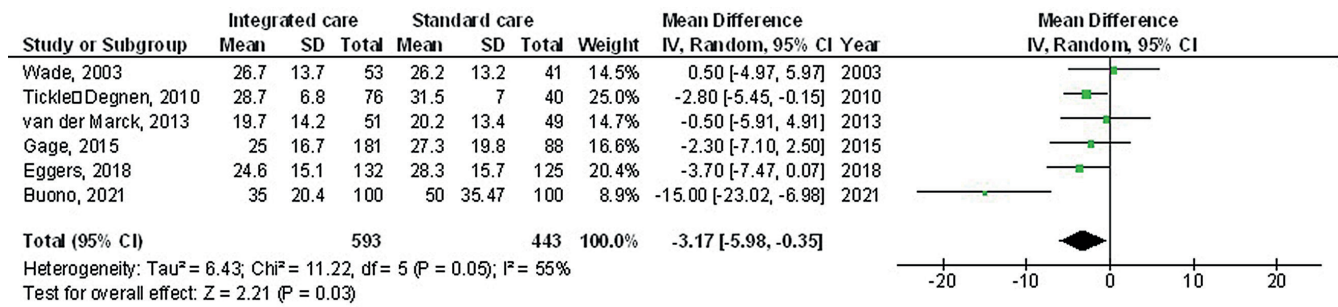


Fig. 2. The forest plot of multidisciplinary comprehensive care compared to standard care regarding the health-related quality of life (HRQL) outcomes in subjects with Parkinson's disease (PD)

df – degrees of freedom; 95% CI – 95% confidence interval; SD – standard deviation.

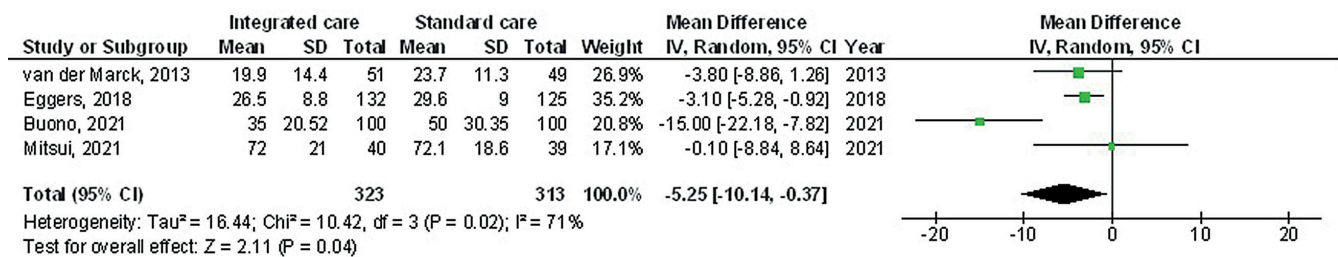


Fig. 3. The forest plot of multidisciplinary comprehensive care compared to standard care regarding the Unified Parkinson's Disease Rating Scale (UPDRS) results in subjects with Parkinson's disease (PD)

df – degrees of freedom; 95% CI – 95% confidence interval; SD – standard deviation.

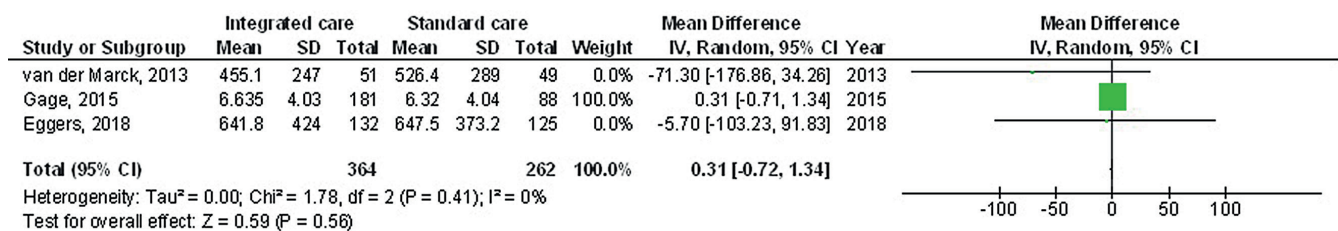


Fig. 4. The forest plot of multidisciplinary comprehensive care compared to standard care regarding the medication dosage outcomes in subjects with Parkinson's disease (PD)

df – degrees of freedom; 95% CI – 95% confidence interval; SD – standard deviation.

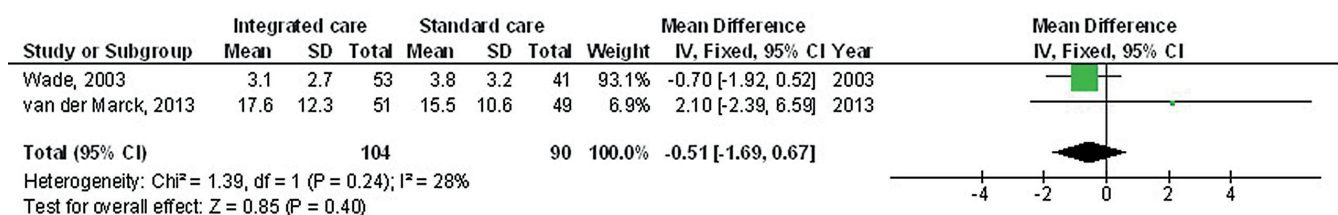


Fig. 5. The forest plot of multidisciplinary comprehensive care compared to standard care regarding the caregiver strain outcomes in subjects with Parkinson's disease (PD)

df – degrees of freedom; 95% CI – 95% confidence interval; SD – standard deviation.

and the small number of studies including the comparisons, e.g., medication dosage and caregiver strain.

This systematic review identified several healthcare delivery models that provide PD patients with multidisciplinary comprehensive care. For a better understanding of the advantages and disadvantages of the various

individual models, further information from head-to-head comparisons could be needed. Nevertheless, despite individual variations in the models, earlier studies on other topics, such as chronic lung illness, cancer treatment and chronic renal disease, have effectively analyzed the impact of multidisciplinary comprehensive care.^{55–58} Although

Table 2. Characteristics of the studies selected for the meta-analysis

Study, year	Country	Total	Multidisciplinary comprehensive care	Standard care	Intervention application	Setting	Time	Control
Wade et al., 2003 ⁴⁸	UK	94	53	41	PD nurse physical therapist occupational therapist social worker (program coordinator)	specialist center and general neurology clinic	baseline, 24 weeks	standard care
Tickle-Degnen et al., 2010 ⁴⁹	USA	116	76	40	movement disorder specialist	outpatient specialist center and home visits	post-treatment, 2 months, 4 months	standard care
van der Marck et al., 2013 ⁵⁰	Netherlands	100	51	49	movement disorder specialist PD nurse general neurologist social worker (program coordinator)	outpatient specialist center and general neurology clinic	baseline, 4 months, 8 months	standard care with general neurology
Gage et al., 2014 ⁵¹	UK	269	181	88	general neurologist PD nurse gerontologist physical therapist occupational therapist speech therapist non-nurse coordinator	community	baseline, 6 weeks, 24 weeks, 36 weeks	standard care
Eggers et al., 2018 ⁵²	Germany	257	132	125	movement disorders specialist general neurologist PD nurse	outpatient neurology clinic and home visits	baseline, 3 months, 6 months	standard care
Lo Buono et al., 2021 ⁵³	Italy	200	100	100	60 days of hospitalization rehabilitative program	neurorehabilitation unit	baseline, 2 months	standard care
Mitsui et al., 2021 ⁵⁴	Japan	79	40	39	physical therapist occupational therapist speech-language-hearing therapist; 2 categories of training: multidisciplinary rehabilitation consisting of conventional training of passive and active movements	Tokushima National Hospital, Japan	post-treatment, 32 months, 6 months	standard care
Total		1115	633	482		–		

PD – Parkinson's disease.

many concerns are still not answered, there are some important discoveries that might be taken into account for the application of present or future multidisciplinary comprehensive care models in PD.⁵⁹ Some significant endorsements for the organization of integrated clinical care teams in PD have recently been made using a practice-based evidence approach.⁶⁰ Additionally, some team members, such as the vascular medicine specialist,⁶¹ gastroenterologists,⁶² pulmonologist, neuro-ophthalmologist, urologist, geriatrician, palliative care specialist, and dentist, have not been recognized as “classic” candidates of a multidisciplinary comprehensive care model for PD.⁶³ The inclusion of these specialties may raise awareness of the complexity of non-motor symptoms linked to PD and encourage the commencement of more effective referrals to the appropriate healthcare providers.^{64,65} According to a recent randomized controlled trial, extended multidisciplinary care is superior to conventional multidisciplinary rehabilitation in PD.⁶⁶ Multidisciplinary comprehensive care models

offer a probability to harmonize healthcare pathways, personalize healthcare utilization based on individual requirements, and improve patient–provider communication as digital infrastructures continue to develop.⁶⁵ Nevertheless, there are few comprehensive statistics on these novel methods and their use. It is crucial to note that the fundamental objectives of multidisciplinary comprehensive care models might change in the future as researchers continue to look for disease-modifying treatments to slow down, halt or even reverse the neurodegenerative process linked to PD. The team makeup and overall design of multidisciplinary comprehensive care programs may need to be reviewed whenever major advancements in this area are made and some method of disease modification is truly available.

This meta-analysis assessed the results of multidisciplinary comprehensive care for PD. More homogeneous and larger study samples are necessary in such investigation. This was likewise emphasized in a previous work that

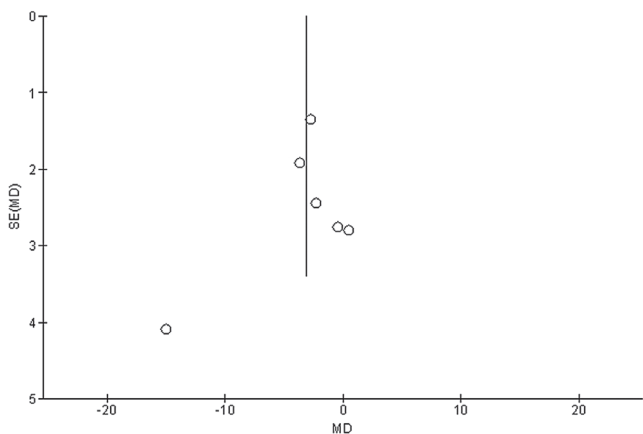


Fig. 6. Health-related quality of life (HRQL) outcomes funnel plot
SE – standard error; MD – mean difference.

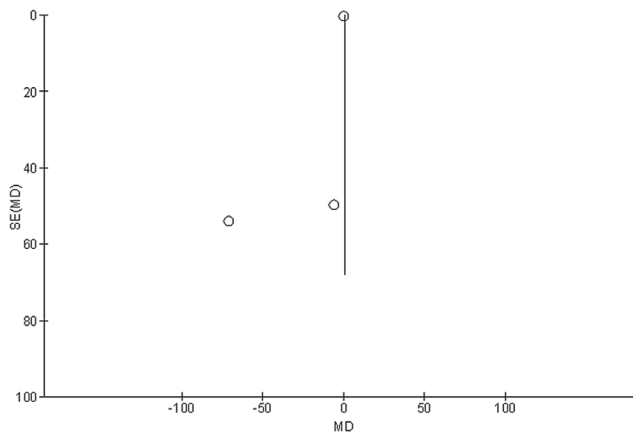


Fig. 8. Medication dosage outcomes funnel plot
SE – standard error; MD – mean difference.

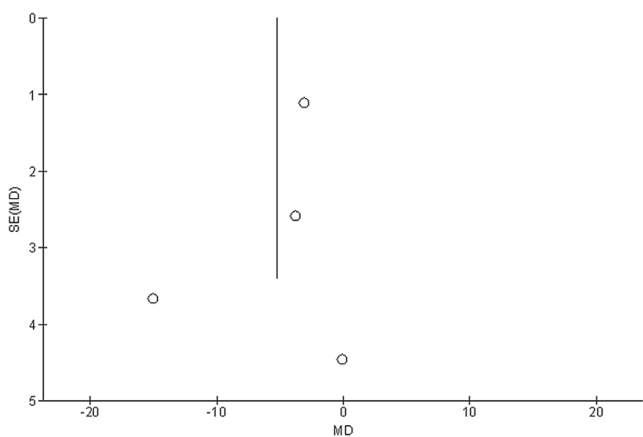


Fig. 7. Unified Parkinson's Disease Rating Scale (UPDRS) outcomes funnel plot
SE – standard error; MD – mean difference.

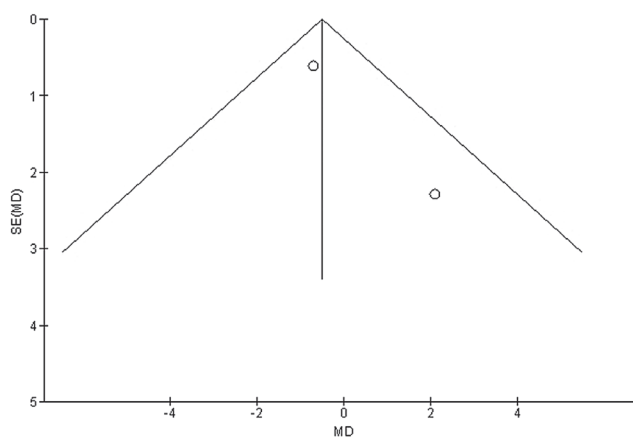


Fig. 9. Caregiver strain outcomes funnel plot
SE – standard error; MD – mean difference.

employed a similar meta-analysis technique and yielded advantageous outcomes for multidisciplinary comprehensive care and standard care for subjects with PD.^{66,67} Since in the present meta-analysis it was impossible to define whether the differences in gender, age and ethnicity are related to the outcomes, future randomized controlled trials are needed to evaluate these factors.

Limitations

Since several studies identified during the search were not included in the systemic review, there might have been a selection bias. However, the removed publications did not meet the necessary inclusion criteria. The sample size for 2 of the 7 chosen papers was less than 100. Furthermore, we were incapable to determine whether factors such as age, gender or ethnicity affected the outcomes of the study. The meta-analysis aimed to compare the outcomes of the standard care group with the multidisciplinary comprehensive care group for subjects with PD. The incorporation of data from earlier studies could have added bias due to incomplete or inaccurate data. Potential

sources of bias included the nutritional status of the participants as well as their age and gender characteristics. Regrettably, some unpublished papers and missing data can bias the studied results.

Conclusions

The use of multidisciplinary comprehensive care resulted in significantly better HRQL and UPDRS compared to the standard care for subjects with PD. Nevertheless, no significant difference was found between multidisciplinary comprehensive care and standard care for subjects with PD in terms of medication dosage and caregiver strain. Thus, we encourage the use of multidisciplinary comprehensive care for PD subjects. Communication between team members is an important constituent of multidisciplinary comprehensive care and might need tailored solutions. Above all, maintaining the subject-centered approach in any care model requires constant feedback and availability of modification mechanism in which the subjects and caregiver play equally vital roles.

Availability of data

The corresponding author agrees to make the meta-analysis database available upon reasonable request.

ORCID iDs

Xiaoyan Duan  <https://orcid.org/0000-0002-9775-9851>

References

- Litvan I. What is the accuracy of the clinical diagnosis of multiple system atrophy? A clinicopathologic study. *Arch Neurol.* 1997;54(8):937–944. doi:10.1001/archneur.1997.00550200007003
- Espay AJ. What the VaP? The meaning of “vascular parkinsonism.” *Parkinsonism Relat Disord.* 2022;94:132–134. doi:10.1016/j.parkreldis.2021.12.008
- Caproni S, Colosimo C. Diagnosis and differential diagnosis of Parkinson disease. *Clinics Geriatr Med.* 2020;36(1):13–24. doi:10.1016/j.cger.2019.09.014
- Zijlmans JCM, Daniel SE, Hughes AJ, Révész T, Lees AJ. Clinicopathological investigation of vascular parkinsonism, including clinical criteria for diagnosis. *Mov Disord.* 2004;19(6):630–640. doi:10.1002/mds.20083
- Liaqat H, Parveen A, Kim SY. Neuroprotective natural products' regulatory effects on depression via gut–brain axis targeting tryptophan. *Nutrients.* 2022;14(16):3270. doi:10.3390/nu14163270
- Wang Z, Pi YL, Wu Y, et al. Selective effects of exercise on reactive and proactive inhibition in Parkinson's disease. *PeerJ.* 2022;10:e13628. doi:10.7717/peerj.13628
- Wang C, Chen L, Zhang M, Yang Y, Wong G. PDmethDB: A curated Parkinson's disease associated methylation information database. *Comput Struct Biotechnol J.* 2020;18:3745–3749. doi:10.1016/j.csbj.2020.11.015
- Török N, Maszlag-Török R, Molnár K, et al. Single nucleotide polymorphisms of indoleamine 2,3-dioxygenase 1 influenced the age onset of Parkinson's disease. *Front Biosci (Landmark Ed).* 2022;27(9):265. doi:10.31083/j.fbl2709265
- Holland C, Garner I, Simpson J, et al. Impacts of COVID-19 lockdowns on frailty and wellbeing in older people and those living with long-term conditions. *Adv Clin Exp Med.* 2021;30(11):1111–1114. doi:10.17219/acem/144135
- Tanaka M, Szabó Á, Spekker E, Polyák H, Tóth F, Vécsei L. Mitochondrial impairment: A common motif in neuropsychiatric presentation? The link to the tryptophan–kynurenine metabolic system. *Cells.* 2022;11(16):2607. doi:10.3390/cells11162607
- Tanaka M, Toldi J, Vécsei L. Exploring the etiological links behind neurodegenerative diseases: Inflammatory cytokines and bioactive kynurenines. *Int J Mol Sci.* 2020;21(7):2431. doi:10.3390/ijms21072431
- Zhang YJ, Zhu WK, Qi FY, Che FY. CirHIPK3 promotes neuroinflammation through regulation of the miR-124-3p/STAT3/NLRP3 signaling pathway in Parkinson's disease [published online ahead of print on October 28, 2022]. *Adv Clin Exp Med.* 2022. doi:10.17219/acem/154658
- Sini P, Dang TBC, Fais M, et al. Cyanobacteria, cyanotoxins, and neurodegenerative diseases: Dangerous liaisons. *Int J Mol Sci.* 2021;22(16):8726. doi:10.3390/ijms22168726
- Tanaka M, Spekker E, Szabó Á, Polyák H, Vécsei L. Modelling the neurodevelopmental pathogenesis in neuropsychiatric disorders: Bioactive kynurenines and their analogues as neuroprotective agents. In celebration of 80th birthday of Professor Peter Riederer. *J Neural Transm.* 2022;129(5–6):627–642. doi:10.1007/s00702-022-02513-5
- Nyatega CO, Qiang L, Adamu MJ, Kawuwa HB. Gray matter, white matter and cerebrospinal fluid abnormalities in Parkinson's disease: A voxel-based morphometry study. *Front Psychiatry.* 2022;13:1027907. doi:10.3389/fpsy.2022.1027907
- Battaglia S. Neurobiological advances of learned fear in humans. *Adv Clin Exp Med.* 2022;31(3):217–221. doi:10.17219/acem/146756
- Carrera-González M del P, Cantón-Habas V, Rich-Ruiz M. Aging, depression and dementia: The inflammatory process. *Adv Clin Exp Med.* 2022;31(5):469–473. doi:10.17219/acem/149897
- Hsu YL, Hung HS, Tsai CW, et al. Peiminine reduces ARTS-mediated degradation of XIAP by modulating the PINK1/parkin pathway to ameliorate 6-hydroxydopamine toxicity and α -synuclein accumulation in Parkinson's disease models in vivo and in vitro. *Int J Mol Sci.* 2021;22(19):10240. doi:10.3390/ijms221910240
- Tanaka M, Vécsei L. Editorial of Special Issue 'Dissecting Neurological and Neuropsychiatric Diseases: Neurodegeneration and Neuroprotection.' *Int J Mol Sci.* 2022;23(13):6991. doi:10.3390/ijms23136991
- Török N, Tanaka M, Vécsei L. Searching for peripheral biomarkers in neurodegenerative diseases: The tryptophan–kynurenine metabolic pathway. *Int J Mol Sci.* 2020;21(24):9338. doi:10.3390/ijms21249338
- Chen C. Recent advances in the study of the comorbidity of depressive and anxiety disorders. *Adv Clin Exp Med.* 2022;31(4):355–358. doi:10.17219/acem/147441
- Cao X, Yang F, Zheng J, Wang X, Huang Q. Aberrant structure MRI in Parkinson's disease and comorbidity with depression based on multinomial tensor regression analysis. *J Pers Med.* 2022;12(1):89. doi:10.3390/jpm12010089
- Mazzoni P, Shabbott B, Cortes JC. Motor control abnormalities in Parkinson's disease. *Cold Spring Harb Perspect Med.* 2012;2(6):a009282. doi:10.1101/cshperspect.a009282
- Battaglia S, Cardellicchio P, Di Fazio C, Nazzi C, Fracasso A, Borgomaneri S. Stopping in (e)motion: Reactive action inhibition when facing valence-independent emotional stimuli. *Front Behav Neurosci.* 2022;16:998714. doi:10.3389/fnbeh.2022.998714
- Chung EJ, Cho HJ, Hur DY, Kim YS, Lee KH, Kim SJ. One autopsy proved neocortical Lewy body disease without the involvement of the olfactory bulb and brainstem. *J Korean Med Sci.* 2022;37(23):e195. doi:10.3346/jkms.2022.37.e195
- Lee SH, Kim M, Lee J, et al. Clinical factors and dopamine transporter availability for the prediction of outcomes after globus pallidus deep brain stimulation in Parkinson's disease. *Sci Rep.* 2022;12(1):16870. doi:10.1038/s41598-022-19150-3
- Dickson DW. Neuropathology of Parkinson disease. *Parkinsonism Relat Disord.* 2018;46(Suppl 1):S30–S33. doi:10.1016/j.parkreldis.2017.07.033
- Karni L, Jusufi I, Nyholm D, Klein GO, Memedi M. Toward improved treatment and empowerment of individuals with Parkinson disease: Design and evaluation of an Internet of things system. *JMIR Form Res.* 2022;6(6):e31485. doi:10.2196/31485
- Riggare S, Stamford J, Hägglund M. A long way to go: Patient perspectives on digital health for Parkinson's disease. *J Parkinsons Dis.* 2021;11(Suppl 1):S5–S10. doi:10.3233/JPD-202408
- Dunn D, Williams A, Giust J, Kronenberger W. Epilepsy and attention-deficit hyperactivity disorder: Links, risks, and challenges. *Neuropsychiatr Dis Treat.* 2016;12:287–296. doi:10.2147/NDT.S81549
- Simonet C, Noyce AJ. Domotics, smart homes, and Parkinson's disease. *J Parkinsons Dis.* 2021;11(Suppl 1):S55–S63. doi:10.3233/JPD-202398
- Spreadbury JH, Young A, Kipps CM. A comprehensive literature search of digital health technology use in neurological conditions: Review of digital tools to promote self-management and support. *J Med Internet Res.* 2022;24(7):e31929. doi:10.2196/31929
- Battaglia S, Cardellicchio P, Di Fazio C, Nazzi C, Fracasso A, Borgomaneri S. The influence of vicarious fear-learning in “infecting” reactive action inhibition. *Front Behav Neurosci.* 2022;16:946263. doi:10.3389/fnbeh.2022.946263
- Klucken J, Krüger R, Schmidt P, Bloem BR. Management of Parkinson's disease 20 years from now: Towards digital health pathways. *J Parkinsons Dis.* 2018;8(Suppl 1):S85–S94. doi:10.3233/JPD-181519
- Bloem BR, Okun MS, Klein C. Parkinson's disease. *Lancet.* 2021;397(10291):2284–2303. doi:10.1016/S0140-6736(21)00218-X
- Borgomaneri S, Serio G, Battaglia S. Please, don't do it! Fifteen years of progress of non-invasive brain stimulation in action inhibition. *Cortex.* 2020;132:404–422. doi:10.1016/j.cortex.2020.09.002
- Mai T. Stand und Entwicklung der Rolle als Parkinson Nurse in Deutschland: Eine Online-Befragung. *Pflege.* 2018;31(4):181–189. doi:10.1024/1012-5302/a000617
- Vlaanderen FP, Rompen L, Munneke M, Stoffer M, Bloem BR, Faber MJ. The voice of the Parkinson customer. *J Parkinsons Dis.* 2019;9(1):197–201. doi:10.3233/JPD-181431

39. Battaglia S, Fabius JH, Moravkova K, Fracasso A, Borgomaneri S. The neurobiological correlates of gaze perception in healthy individuals and neurologic patients. *Biomedicines*. 2022;10(3):627. doi:10.3390/biomedicines10030627
40. Poewe W. Clinical measures of progression in Parkinson's disease. *Mov Disord*. 2009;24(Suppl 2):S671–S676. doi:10.1002/mds.22600
41. Ebersbach G, Baas H, Csoti I, Müngersdorf M, Deuschl G. Scales in Parkinson's disease. *J Neurol*. 2006;253(Suppl 4):iv32–iv35. doi:10.1007/s00415-006-4008-0
42. Stroup DF. Meta-analysis of observational studies in epidemiology: A proposal for reporting. *JAMA*. 2000;283(15):2008. doi:10.1001/jama.283.15.2008
43. Liberati A, Altman DG, Tetzlaff J, et al. The PRISMA statement for reporting systematic reviews and meta-analyses of studies that evaluate health care interventions: Explanation and elaboration. *J Clin Epidemiol*. 2009;62(10):e1–e34. doi:10.1016/j.jclinepi.2009.06.006
44. Gupta A, Das A, Majumder K, et al. Obesity is independently associated with increased risk of hepatocellular cancer-related mortality: A systematic review and meta-analysis. *Am J Clin Oncol*. 2018;41(9):874–881. doi:10.1097/COC.0000000000000388
45. Higgins JPT, Green S, eds. *Cochrane Handbook for Systematic Reviews of Interventions Version 5.1.0* (updated March 2011). Cochrane Collaboration, 2011. <https://handbook-5-1.cochrane.org/>.
46. Sheikhabahaei S, Trahan TJ, Xiao J, et al. FDG-PET/CT and MRI for evaluation of pathologic response to neoadjuvant chemotherapy in patients with breast cancer: A meta-analysis of diagnostic accuracy studies. *Oncologist*. 2016;21(8):931–939. doi:10.1634/theoncologist.2015-0353
47. Higgins JPT. Measuring inconsistency in meta-analyses. *BMJ*. 2003;327(7414):557–560. doi:10.1136/bmj.327.7414.557
48. Wade DT, Gage H, Owen C, Trend P, Grossmith C, Kaye J. Multidisciplinary rehabilitation for people with Parkinson's disease: A randomised controlled study. *J Neurol Neurosurg Psychiatry*. 2003;74(2):158–162. doi:10.1136/jnnp.74.2.158
49. Tickle-Degnen L, Ellis T, Saint-Hilaire MH, Thomas CA, Wagenaar RC. Self-management rehabilitation and health-related quality of life in Parkinson's disease: A randomized controlled trial. *Mov Disord*. 2010;25(2):194–204. doi:10.1002/mds.22940
50. van der Marck MA, Bloem BR, Borm GF, Overeem S, Munneke M, Guttman M. Effectiveness of multidisciplinary care for Parkinson's disease: A randomized, controlled trial. *Mov Disord*. 2013;28(5):605–611. doi:10.1002/mds.25194
51. Gage H, Grainger L, Ting S, et al. Specialist rehabilitation for people with Parkinson's disease in the community: A randomised controlled trial. *Health Serv Deliv Res*. 2014;2(51):1–376. doi:10.3310/hsdr02510
52. Eggers C, Dano R, Schill J, Fink GR, Hellmich M, Timmermann L; CPN study group. Patient-centered integrated healthcare improves quality of life in Parkinson's disease patients: A randomized controlled trial. *J Neurol*. 2018;265(4):764–773. doi:10.1007/s00415-018-8761-7
53. Lo Buono V, Palmeri R, De Salvo S, et al. Anxiety, depression, and quality of life in Parkinson's disease: The implications of multidisciplinary treatment. *Neural Regen Res*. 2021;16(3):587–590. doi:10.4103/1673-5374.293151
54. Mitsui T, Arai Y, Tsukamoto A, et al. Sociability-based fitness approach in Parkinson's disease: Comparison with conventional rehabilitation. *Eur J Neurol*. 2021;28(6):1893–1900. doi:10.1111/ene.14798
55. Krus AL, Smidt N, Assendelft WJ, et al. Integrated disease management interventions for patients with chronic obstructive pulmonary disease. *Cochrane Database Syst Rev*. 2013;9(9):CD009437. doi:10.1002/14651858.CD009437.pub2
56. Wang SM, Hsiao LC, Ting IW, et al. Multidisciplinary care in patients with chronic kidney disease: A systematic review and meta-analysis. *Eur J Intern Med*. 2015;26(8):640–645. doi:10.1016/j.ejim.2015.07.002
57. Hoerger M, Wayser GR, Schwing G, Suzuki A, Perry LM. Impact of interdisciplinary outpatient specialty palliative care on survival and quality of life in adults with advanced cancer: A meta-analysis of randomized controlled trials. *Ann Behav Med*. 2019;53(7):674–685. doi:10.1093/abm/kay077
58. Galbraith L, Jacobs C, Hemmelgarn BR, Donald M, Manns B, Jun M. Chronic disease management interventions for people with chronic kidney disease in primary care: A systematic review and meta-analysis. *Nephrol Dial Transplant*. 2017;33(1):112–121. doi:10.1093/ndt/gfw359
59. Üstün TB, Kostanjsek N, Chatterji S, Rehm J, eds. *Measuring Health and Disability: Manual for WHO Disability Assessment Schedule (WHODAS 2.0)*. Geneva, Switzerland: World Health Organization; 2010. <https://apps.who.int/iris/handle/10665/43974>. ISBN:978-92-4-154759-8.
60. Valentijn PP, Vrijhoef HJM, Ruwaard D, Boesveld I, Arends RY, Bruijnzeels MA. Towards an international taxonomy of integrated primary care: A Delphi consensus approach. *BMC Fam Pract*. 2015;16(1):64. doi:10.1186/s12875-015-0278-x
61. Valentijn PP, Pereira F, Sterner CW, et al. Validation of the Rainbow Model of Integrated Care Measurement Tools (RMIC-MTs) in renal care for patient and care providers. *PLoS One*. 2019;14(9):e0222593. doi:10.1371/journal.pone.0222593
62. Stemmer M. Advancing the social sciences through the interdisciplinary enterprise. *Soc Sci J*. 1991;28(1):1–14. doi:10.1016/0362-3319(91)90040-B
63. World Health Organization. Regional Office for Europe. Roadmap: Strengthening people-centred health systems in the WHO European Region. A framework for action towards Coordinated/Integrated Health Services Delivery (CIHSD). 2013. <https://apps.who.int/iris/bitstream/handle/10665/108628/WHO-EURO-2013-4492-44255-62514-eng.pdf?sequence=1&isAllowed=y>. Accessed March 1, 2022.
64. Radder DLM, de Vries NM, Riksen NP, et al. Multidisciplinary care for people with Parkinson's disease: The new kids on the block! *Exp Rev Neurother*. 2019;19(2):145–157. doi:10.1080/14737175.2019.1561285
65. Marumoto K, Yokoyama K, Inoue T, et al. Inpatient enhanced multidisciplinary care effects on the quality of life for Parkinson disease: A quasi-randomized controlled trial. *J Geriatr Psychiatry Neurol*. 2019;32(4):186–194. doi:10.1177/0891988719841721
66. Rajan R, Brennan L, Bloem BR, et al. Integrated care in Parkinson's disease: A systematic review and meta-analysis. *Mov Disord*. 2020;35(9):1509–1531. doi:10.1002/mds.28097
67. Seid AA, Demirdel E, Aychiluhm SB, Mohammed AA. Multidisciplinary rehabilitation for people with Parkinson's disease: A systematic review and meta-analysis. *Parkinson's Dis*. 2022;2022:2355781. doi:10.1155/2022/2355781

A meta-analysis of the effects of probiotics on various parameters in critically ill ventilated individuals

Bo Wang^{1,A}, Ji Xie^{2,B}, Yao Teng^{3,D,F}

¹ Department of Intensive Care Medicine, No. 903 Hospital of PLA Joint Logistic Support Force, Hangzhou, China

² Department of Emergency Medicine, Jinling Hospital, Medical School of Nanjing University, China

³ Department of Emergency Medicine, The Fourth Affiliated Hospital of Nanjing Medical University, China

A – research concept and design; B – collection and/or assembly of data; C – data analysis and interpretation;

D – writing the article; E – critical revision of the article; F – final approval of the article

Advances in Clinical and Experimental Medicine, ISSN 1899–5276 (print), ISSN 2451–2680 (online)

Adv Clin Exp Med. 2023;32(6):633–642

Address for correspondence

Yao Teng

E-mail: tengyao_sci@outlook.com

Funding sources

None declared

Conflict of interest

None declared

Received on September 16, 2022

Reviewed on October 28, 2022

Accepted on December 12, 2022

Published online on March 16, 2023

Abstract

Background. According to reports, ventilator-associated pneumonia affects critically ill patients more frequently than any other nosocomial infection. Probiotic usage as a prophylactic intervention has shown promising results in numerous studies.

Objectives. We performed a meta-analysis to evaluate the effect of probiotics on different parameters in critically ill ventilated subjects.

Materials and methods. A systematic literature search up to June 2022 was performed and 5893 critically ill ventilated subjects at the baseline of the studies were identified; 2912 of them were using the probiotics, and there were 2981 controls. Odds ratio (OR) and mean difference (MD) with 95% confidence interval (95% CI) were calculated to assess the effect of probiotics on different parameters in critically ill ventilated subjects using the dichotomous and contentious methods with a random or fixed effects model.

Results. The probiotics caused a significantly lower incidence of ventilator-associated pneumonia (OR = 0.52; 95% CI: 0.40–0.68, $p < 0.001$), shorter duration of mechanical ventilation (MD = -2.22 ; 95% CI: -3.33 – -1.11 , $p < 0.001$), shorter intensive care unit (ICU) stay (MD = -2.09 ; 95% CI: -3.41 – -0.77 , $p = 0.002$), shorter hospital stay (MD = -2.36 ; 95% CI: -4.54 – -0.19 , $p = 0.03$), and lower oropharyngeal colonization (OR = 0.59; 95% CI: 0.36–0.96, $p = 0.03$) in critically ill ventilated subjects compared with controls. However, probiotic use had no significant difference in terms of diarrhea incidence (OR = 0.74; 95% CI: 0.52–1.07, $p = 0.11$) and in-hospital mortality (OR = 0.90; 95% CI: 0.79–1.03, $p = 0.14$) in critically ill ventilated subjects compared with controls.

Conclusions. Probiotics caused a significantly lower ventilator-associated pneumonia incidence, shorter duration of mechanical ventilation, shorter ICU and hospital stay, and lower oropharyngeal colonization. However, there was no significant difference in terms of diarrhea incidence and in-hospital mortality in subjects who used probiotics compared with controls. The low sample size of 9 out of 27 researches and the small number of studies in several comparisons requires attention when analyzing the results.

Key words: probiotic, ventilator-associated pneumonia, length of hospital stay, critically ill ventilated adult, oropharyngeal colonization

Cite as

Wang B, Xie J, Teng Y. A meta-analysis of the effects of probiotics on various parameters in critically ill ventilated individuals. *Adv Clin Exp Med.* 2023;32(6):633–642. doi:10.17219/acem/157407

DOI

10.17219/acem/157407

Copyright

Copyright by Author(s)

This is an article distributed under the terms of the Creative Commons Attribution 3.0 Unported (CC BY 3.0) (<https://creativecommons.org/licenses/by/3.0/>)

Introduction

According to reports, ventilator-related pneumonia affects critically ill subjects more frequently than any other nosocomial infection,¹ with a frequency of 2–16 sessions per 1000 ventilator days.² Ventilator-related pneumonia is said to be the most common cause of mortality among nosocomial infections.³ Although the pathophysiology of ventilator-related pneumonia is extremely complex, pathogenic bacterial colonization of the aerodigestive tract and bacterial translocation are the main contributing factors of the disease.⁴ Several trials and investigations have been conducted to determine the most effective pharmacological preventative techniques, including the use of probiotics or antibiotics for specific gastrointestinal or oral disinfection. Numerous studies have revealed that using probiotics as a preventative measure offers promising outcomes⁵; however, antibiotic resistance and price have been connected to the use of antibiotics for specific gastrointestinal or oral disinfection, respectively.⁶ Probiotics are living, nonpathogenic microorganisms that have been demonstrated to decrease bacterial translocation by promoting mucosal immunity and regulating the release of pro-inflammatory cytokines.⁴ They prevent the growth of pathogenic bacteria through a number of ways, such as the production of different chemicals, e.g., organic acid, hydrogen peroxide and bacteriocins, competition for nutrients, prevention of pathogen attachment, and inhibition of the effect of microbial toxins. Probiotics similarly contribute to maintaining the mucosal protective barrier by stimulating the formation of the normal epithelium.⁷ Prebiotics are indigestible sugars that promote the development of particular bacterial colonies through synbiotics that are a concoction of probiotics and prebiotics.⁸ In recent years, numerous randomized controlled trials (RCTs) have been carried out to assess the efficacy of probiotics in the inhibition of ventilator-related pneumonia, due to their promising nature in critically ill subjects. Latest meta-analyses demonstrated the effectiveness of probiotics in reducing the incidence of ventilator-related pneumonia.^{1,4} However, it is worth noting that some of the trials included in the study were of poor quality.

Objectives

The goal of the study was to assess the impact of probiotic use on the incidence of ventilator-related pneumonia, length of hospital stay, length of stay in an intensive care unit (ICU), duration of mechanical ventilation, incidence of diarrhea, frequency of oropharyngeal colonization, and in-hospital mortality in critically ill ventilated subjects.

Materials and methods

Eligibility criteria

Studies included in the analysis evaluated the impact of probiotics on different parameters in critically ill ventilated subjects. The analyses regarding the influence of the probiotics compared with controls were summarized.⁹

All studies involved humans as participants. Inclusion was unaffected by language or study size. Review articles, comments and research that failed to provide a measure of an association were all eliminated from the list of analyzed publications. Figure 1 depicts the entire course of the study. The inclusion criteria were as follows:

1. The research was either prospective, observational, retrospective, or a controlled trial.
2. The intended subjects were critically ill ventilated individuals.
3. The intervention regimen relied on probiotics.
4. The study compared probiotic use with controls.

The exclusion criteria were: 1) studies that did not examine the influence of probiotics compared to controls in critically ill ventilated subjects, 2) research on subjects treated without probiotics or controls, and 3) studies without the emphasis on the significance of comparison outcomes.

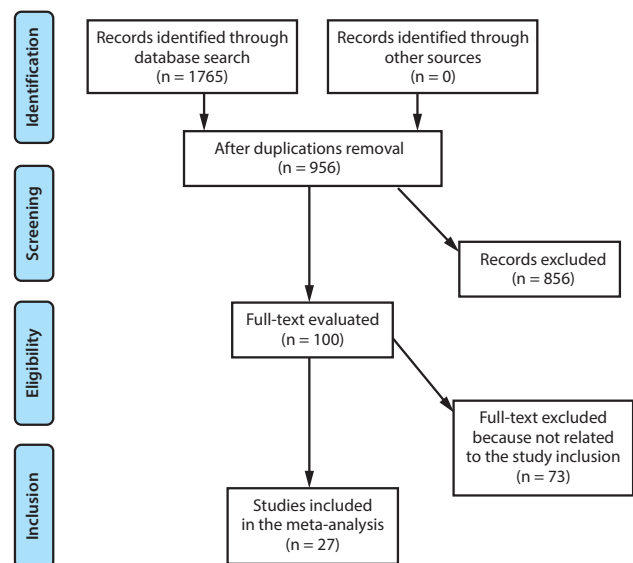


Fig. 1. Flowchart of the study process

Search strategy

According to the PICOS concept,¹⁰ a protocol of search strategy was created and defined as follows: P (population) – critically ill ventilated subjects; I (intervention/exposure) – probiotics; C (comparison) – probiotic use compared with controls; O (outcome) – ventilator-related pneumonia incidence, mechanical-ventilation period, length of ICU stay, length of hospital stay, oropharyngeal colonization, diarrhea incidence, and in-hospital mortality; S (study design) – no restrictions.¹¹

Table 1. Search strategy for each database

Database	Search strategy
PubMed	#1 "critically ill ventilated adult" [MeSH terms] OR "probiotic" [all fields] OR "length of hospital stay" [all fields] OR "diarrhea" [all fields] #2 "oro-pharyngeal colonization" [MeSH terms] OR "critically ill ventilated adult" [all fields] OR "length of hospital stay" [all fields] OR "ventilator-related pneumonia" [all fields] OR "in-hospital mortality" [all fields] #3 #1 AND #2
Embase	#1 "critically ill ventilated adult"/exp OR "probiotic"/exp OR "length of hospital stay"/exp OR "diarrhea" #2 "oro-pharyngeal colonization"/exp OR "length of hospital stay"/exp OR "ventilator-related pneumonia"/exp OR "in-hospital mortality" #3 #1 AND #2
Cochrane Library	#1 "critically ill ventilated adult": ti,ab,kw OR "probiotic": ti,ab,kw OR "length of hospital stay": ti,ab,kw (word variations have been searched) #2 "diarrhea": ti,ab,kw OR "oro-pharyngeal colonization": ti,ab,kw OR "length of hospital stay": ti,ab,kw OR "ventilator-related pneumonia": ti,ab,kw OR "in-hospital mortality": ti,ab,kw (word variations have been searched) #3 #1 AND #2

MeSH – medical subject headings; ti,ab,kw – terms in either title or abstract or keyword fields; exp – exploded indexing term.

First, using the arrangement of key words and correlated terms presented in Table 1, we conducted a thorough search of the OVID, Embase, Cochrane Library, PubMed, and Google Scholar databases for studies published until June 2022. All found papers were listed in an EndNote file (EndNote; Clarivate Analytics, London, UK), duplicates were removed, and the titles and abstracts were examined in order to exclude studies that did not show a relationship between probiotics and controls in critically ill ventilated people.

Data collection process

The data were gathered using the following criteria: last name of the first author, study period, publication year, country or region where the study was performed, population type, clinical and management characteristics, qualitative and quantitative technique of assessment, information source, results assessment, and statistical analysis.¹²

Data items

When there were various results from a single study, data were collected independently, based on the evaluation of the impact of complications of probiotics compared to controls in critically ill ventilated subjects.

Study risk of bias assessment

Two authors independently assessed the methods used in chosen publications in order to determine the likelihood of bias in each study. The methodological quality was

evaluated using the "risk of bias instrument" from the Cochrane Handbook for Systematic Reviews of Interventions v. 5.1.0.¹³

In terms of the assessment criteria, each study was rated and assigned to one of the 3 risk of bias levels: low – if all quality criteria were met; moderate – if one or more of the quality criteria were partially met or unclear; or high – if one or more of the criteria were not met or not included. Any inconsistencies were addressed after a re-evaluation of the original article.

Effect measures

Sensitivity studies were only performed on research that reported and examined the influence of the probiotics compared with controls. Other comparisons between probiotics and controls were used for sensitivity and subclass analysis.

Statistical analyses

Odds ratio (OR) and mean difference (MD) with a 95% confidence interval (95% CI) were calculated using a random or fixed effects model with dichotomous and contentious methods. The heterogeneity (I^2) index was calculated, with a range of 0–100%. No, low, moderate, and high heterogeneity were indicated by values around 0%, 25%, 50%, and 75%, respectively.¹⁴ When I^2 was higher than 50%, the random effects model was selected, and when it was lower than 50%, the fixed effects model was selected. The subclass analysis was completed by stratifying the first evaluation based on the previously specified outcome categories. The value of $p < 0.05$ was used in the analysis to indicate statistical significance for differences across subcategories.

Reporting the assessment of bias

Using the Egger's regression test and funnel plots showing the logarithm of ORs compared to their standard errors, the publication bias was evaluated both intuitively and quantitatively (the publication bias was considered present when $p \geq 0.05$).¹⁰

Certainty assessment

All p-values were calculated using two-tailed tests. The statistical analysis was conducted and the graphs were obtained using Review Manager v. 5.3 (The Cochrane Collaboration, Copenhagen, Denmark).

Results

A total of 27 articles published between 2006 and 2022 that matched the inclusion criteria were chosen from a total of 1765 evaluated studies.^{6,15–40} Table 2 displays

Table 2. Characteristics of the selected studies for the meta-analysis

Study, year	Country	Total	Probiotic	Controls
Kotzampassi et al., 2006 ¹⁵	Greece	65	35	30
Spindler-Vesel et al., 2007 ¹⁶	Slovenia	113	26	87
Forestier et al., 2008 ¹⁷	France	202	99	103
Knight et al., 2009 ¹⁸	UK	259	130	129
Giamarellos-Bourboulis et al., 2009 ¹⁹	Greece	72	36	36
Morrow et al., 2010 ⁶	USA	138	68	70
Barraud et al., 2010 ²⁰	France	149	78	71
Oudhuis et al., 2011 ²¹	Netherlands	248	129	119
Tan et al., 2011 ²²	China	35	16	19
Li et al., 2012 ²³	China	165	82	83
Banupriya et al., 2015 ²⁴	India	142	70	72
Rongrungruang et al., 2015 ²⁵	Thailand	150	75	75
Malik et al., 2016 ²⁶	Malaysia	49	24	25
Zeng et al., 2016 ²⁷	China	235	118	117
Amiri, 2016 ²⁸	Iran	60	30	30
Shimizu et al., 2018 ²⁹	Japan	72	35	37
Angurana et al., 2018 ³⁰	India	100	50	50
Kooshki et al., 2018 ³¹	Iran	80	40	40
Klarin et al., 2018 ³²	Sweden	137	69	68
Anandaraj et al., 2019 ³³	India	146	72	74
Mahmoodpoor et al., 2019 ³⁴	Iran	102	48	54
Habib et al., 2020 ³⁵	Egypt	65	32	33
Nazari et al., 2020 ³⁶	Iran	147	73	74
Johnstone et al., 2021 ³⁷	Canada	2650	1318	1332
Boraey et al., 2021 ³⁸	Egypt	80	40	40
Tsilika et al., 2022 ³⁹	Greece	112	59	53
Prasoon et al., 2022 ⁴⁰	India	120	60	60
Total		5893	2912	2981

the data from these publications. The chosen studies comprised 5893 critically ill ventilated participants in the trials' baseline; 2912 of them were using probiotics and there were 2981 controls. At the commencement of the trials, there were between 35 and 2650 individuals under study in total. Twenty-five studies presented data grouped according to the incidence of ventilator-related pneumonia, 16 studies presented data grouped according to the mechanical ventilation period, 17 according to the length of ICU stay, 8 according to the length of hospital stay, 5 according to oropharyngeal colonization rate, 6 according to diarrhea incidence, and 15 according to in-hospital mortality.

The probiotic use resulted in a significantly lower ventilator-related pneumonia incidence (OR = 0.52; 95% CI: 0.40–0.68, $p < 0.00001$) with moderate heterogeneity ($I^2 = 65\%$), shorter mechanical ventilation period (MD = -2.22; 95% CI: -3.33–-1.11, $p < 0.00001$) with high heterogeneity ($I^2 = 92\%$), shorter ICU stay (MD = -2.09; 95% CI: -3.41–-0.77, $p = 0.002$) with high heterogeneity ($I^2 = 89\%$), shorter hospital stay (MD = -2.36; 95% CI:

-4.54–-0.19, $p = 0.03$) with high heterogeneity ($I^2 = 83\%$), and lower rate of oropharyngeal colonization (OR = 0.59; 95% CI: 0.36–0.96, $p = 0.03$) with moderate heterogeneity ($I^2 = 63\%$) in critically ill ventilated subjects compared with controls (Fig. 2–6).

However, probiotics caused no significant difference in terms of diarrhea incidence (OR = 0.74; 95% CI: 0.52–1.07, $p = 0.11$) with low heterogeneity ($I^2 = 45\%$), and in-hospital mortality (OR = 0.90; 95% CI: 0.79–1.03, $p = 0.14$) with no heterogeneity ($I^2 = 0\%$) in critically ill ventilated subjects compared with controls (Fig. 7,8).

Due to the lack of available data on certain factors, such as gender, age and ethnicity, stratified models could not be used to investigate their impact on comparison outcomes. The visual assessment of the funnel plot and quantitative measurements using the Egger's regression test revealed no evidence of publication bias, as shown in Supplementary Fig. 1–7. However, it was shown that the majority of the included RCTs had poor methodological quality, no bias in selective reporting and only minimal outcome data, as shown in Fig. 9.

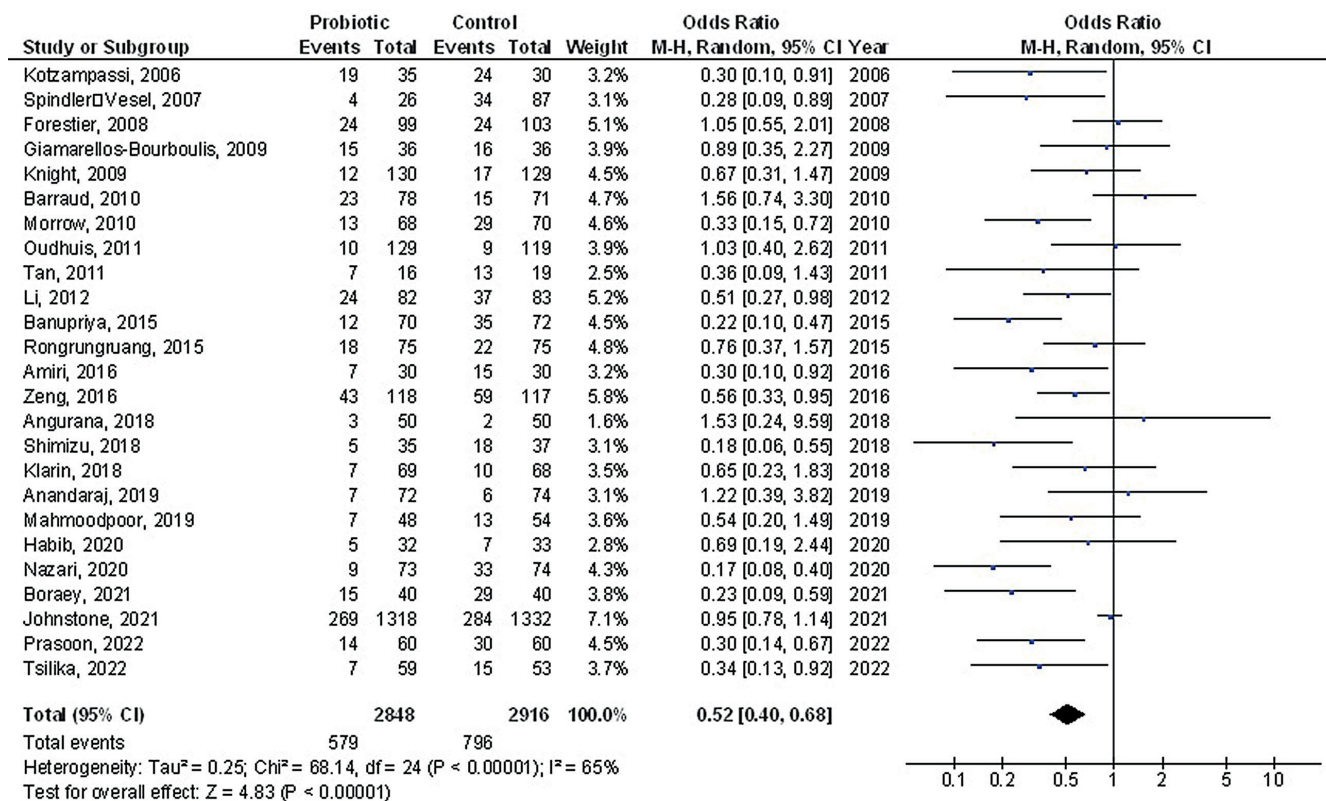


Fig. 2. Forest plot of the influence of probiotic use compared to controls on the frequency of the ventilator-related pneumonia incidence outcomes in critically ill ventilated subjects

95% CI – 95% confidence interval; df – degrees of freedom.

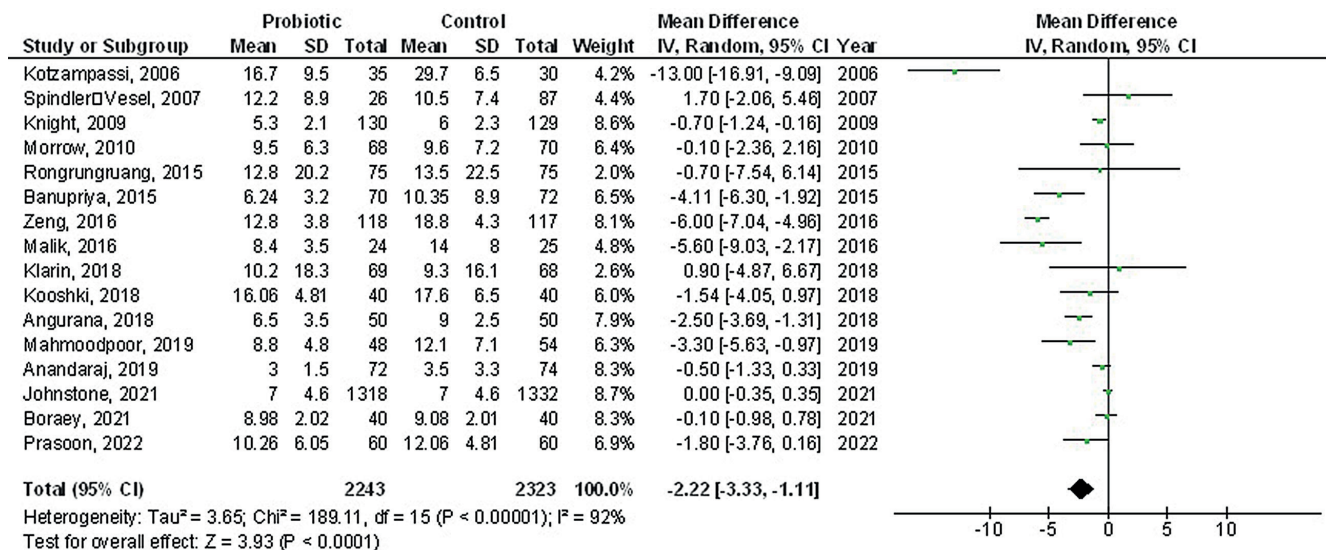


Fig. 3. Forest plot of the influence of probiotic use compared to controls on the mechanical ventilation period outcomes in critically ill ventilated subjects

95% CI – 95% confidence interval; df – degrees of freedom; SD – standard deviation.

Discussion

This meta-analysis had 5893 critically ill ventilated participants in the trials’ baseline; 2912 of them were using probiotics and there were 2981 controls.^{6,15–40} The probiotic use resulted in a significantly lower ventilator-related pneumonia

incidence, shorter mechanical ventilation period, shorter ICU and hospital stay, and lower oropharyngeal colonization rate in critically ill ventilated subjects compared with controls. However, probiotics had caused no significant difference in diarrhea incidence and in-hospital mortality in critically ill ventilated subjects compared with controls.

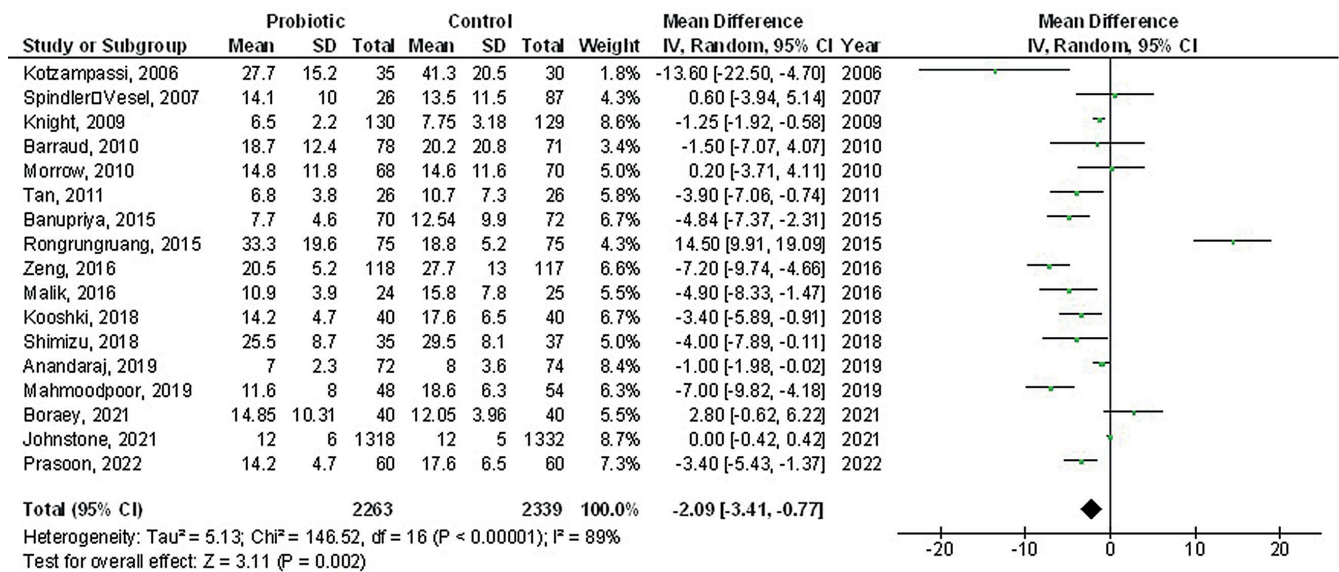


Fig. 4. Forest plot of the influence of probiotic use compared to controls on the length of intensive care unit stay outcomes in critically ill ventilated subjects
95% CI – 95% confidence interval; df – degrees of freedom; SD – standard deviation.

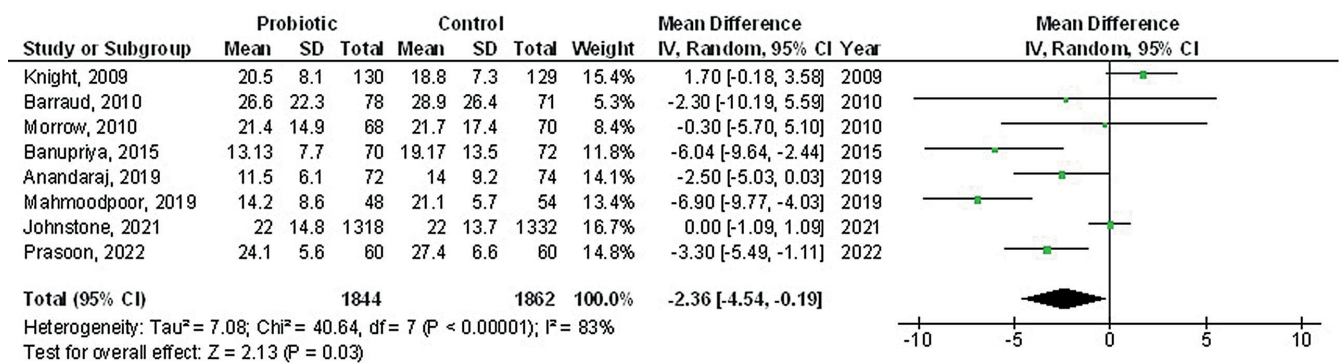


Fig. 5. Forest plot of the influence of probiotic use compared to controls on the length of hospital stay outcomes in critically ill ventilated subjects
95% CI – 95% confidence interval; df – degrees of freedom; SD – standard deviation.

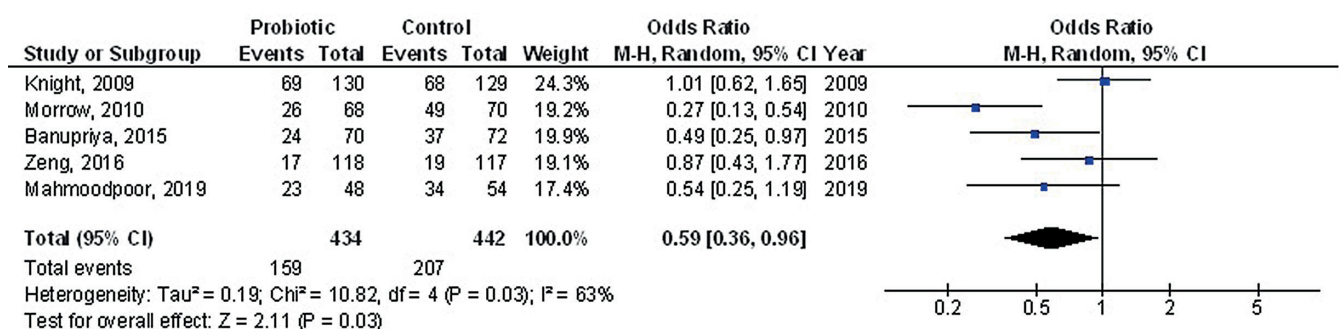


Fig. 6. Forest plot of the influence of probiotic use compared to controls on the oropharyngeal colonization outcomes in critically ill ventilated subjects
95% CI – 95% confidence interval; df – degrees of freedom.

The meta-analysis performed by Bo et al. also demonstrated that probiotics had a favorable impact on the incidence of ventilator-related pneumonia, even after studies with a high risk of bias were eliminated.⁴¹ Probiotic use was related to a statistically significant decline in the incidence of ventilator-related pneumonia and a decrease in the duration

of antibiotic treatment, according to the latest meta-analysis by Song et al.⁴² Our meta-analysis has shown that administering probiotics significantly lowers the risk of ventilator-related pneumonia occurrence, shortens the duration of mechanical ventilation and the time spent in the ICU, and reduces in-hospital mortality when compared to using a placebo.

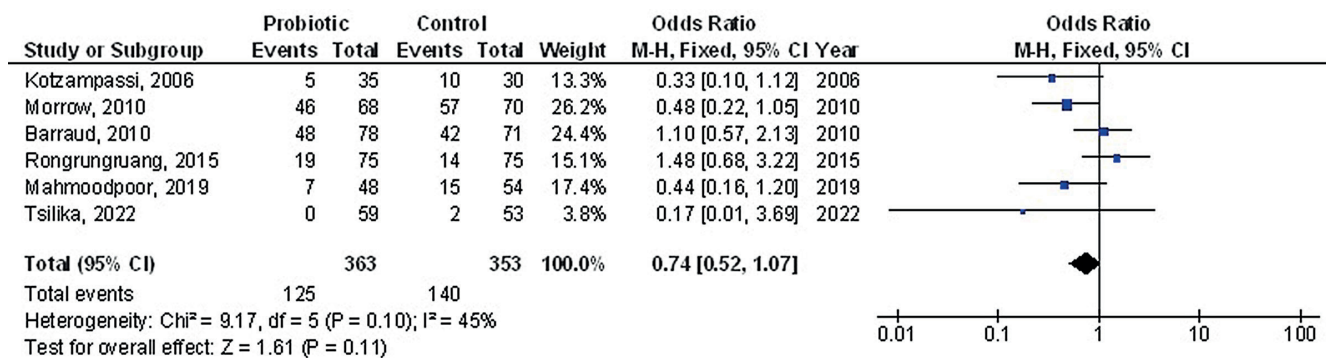


Fig. 7. Forest plot of the influence of probiotic use compared to controls on the diarrhea incidence outcomes in critically ill ventilated subjects
95% CI – 95% confidence interval; df – degrees of freedom.

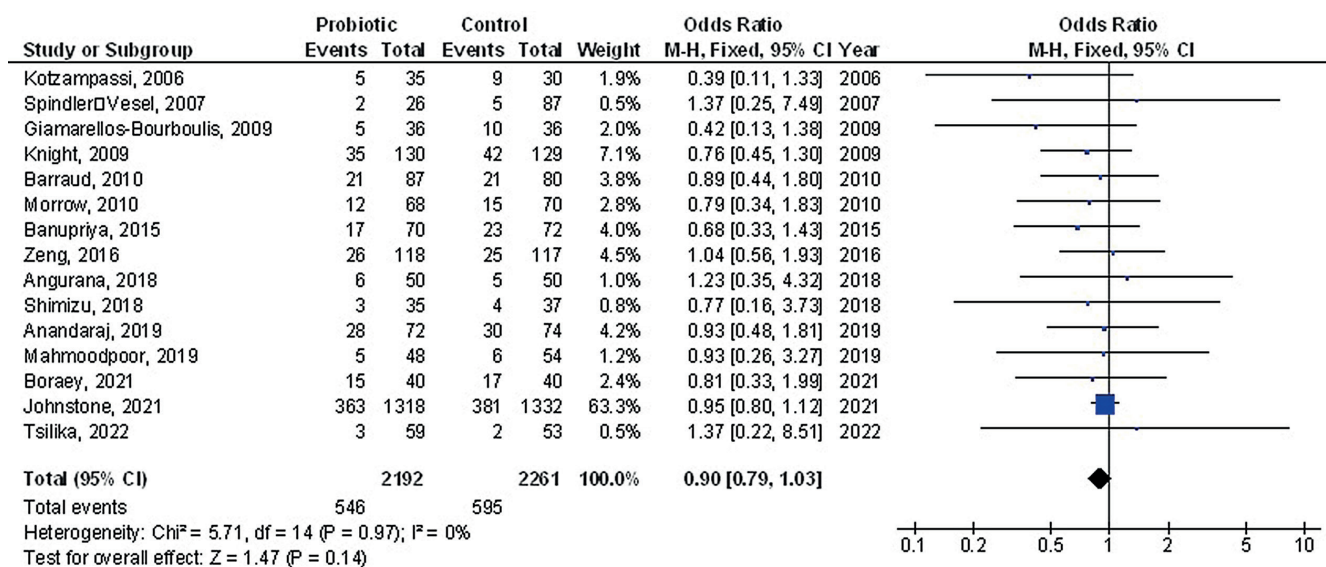


Fig. 8. Forest plot of the influence of probiotic use compared to controls on the in-hospital mortality outcomes in critically ill ventilated subjects
95% CI – 95% confidence interval; df – degrees of freedom.

According to previous meta-analyses,^{42–48} the incidence of ventilator-related pneumonia decreased after the probiotic treatment. The incidence of ventilator-related pneumonia did not, however, statistically significantly decline after probiotic delivery, according to 2 meta-analyses by Gu et al.⁴⁹ and Wang et al.⁵⁰ In our meta-analysis, there was no statistically significant reduction in diarrhea incidence or in-hospital mortality. However, our investigation found a statistically significant decrease in the incidence of ventilator-related pneumonia, length of the ICU stay and mechanical-ventilation period that was not described in prior meta-analyses.^{42–48} According to the meta-analysis by Siempos et al. published in 2010, the *Pseudomonas aeruginosa* colonization of the respiratory tract and the length of the ICU stay decreased following the probiotic administration.⁵¹ Probiotic administration was shown to shorten the ICU stay, as described by Gu et al.⁵² However, the study by Siempos et al.⁵¹ is outdated, and several new RCTs have since been published. The meta-analysis by Gu et al. included 2 papers only, which is a statistically insignificant quantity to describe the length of ICU stay.⁵²

The RCTs included in the present meta-analysis employed varying definitions of ventilator-related pneumonia. Two ventilator-related pneumonia rates (one for microbiological and one for clinical cases) were provided in 2 of the RCTs.^{6,27} For our meta-analysis, we chose the microbiological definition of ventilator-related pneumonia because it has been adopted by the majority of authors in different RCTs and meta-analyses. Since we relied on the stated definitions and since there is no standard definition provided in the RCTs, the ventilator-related pneumonia definition is a significant drawback to our meta-analysis. To precisely assess the impact of probiotics on ventilator-related pneumonia incidence, a sizable multicenter RCT with a standardized objective definition of a ventilator-related incident is required. According to Centers for Disease Control and Prevention (CDC), a ventilator-related incident happens when the subject’s oxygenation declines after a period of stability or improvement. The colonization rate on day 7 of the ICU stay was chosen to calculate the frequency of oropharyngeal colonization. The majority of studies defined diarrhea as 3 or more liquid stools per day.^{6,20,34}

	Random sequence generation (selection bias)	Allocation concealment (selection bias)	Blinding of participants and personnel (performance bias)	Blinding of outcome assessment (detection bias)	Incomplete outcome data (attrition bias)	Selective reporting (reporting bias)	Other bias
Kotzampassi, 2006	+	+	?	+	+	+	?
Spindler-Vesel, 2007	-	?	-	-	+	?	+
Forestier, 2008	-	?	-	-	+	?	+
Knight, 2009	+	+	-	+	+	?	?
Giamarellos-Bourboulis, 2009	+	?	-	-	+	?	+
Morrow, 2010	+	?	-	-	-	?	+
Barraud, 2010	+	-	?	+	+	?	?
Oudhuis, 2011	?	?	-	-	-	?	+
Tan, 2011	-	?	-	-	-	?	+
Li, 2012	-	?	-	-	-	?	+
Banupriya, 2015	+	?	-	-	+	?	+
Rongrungruang, 2015	?	?	-	-	+	?	+
Malik, 2016	+	?	?	+	+	+	?
Zeng, 2016	?	?	-	-	-	?	+
Amiri, 2016	?	?	-	-	-	?	+
Shimizu, 2018	+	+	-	+	+	?	?
Angurana, 2018	+	?	-	-	+	?	+
Kooshki, 2018	+	?	-	-	-	?	+
Klarin, 2018	+	-	?	+	+	?	?
Anandaraj, 2019	?	?	-	-	-	?	+
Mahmoodpoor, 2019	-	?	-	-	-	?	+
Habib, 2020	-	?	-	-	-	?	+
Nazari, 2020	+	?	-	-	+	?	+
Johnstone, 2021	?	?	-	-	+	?	+
Boraey, 2021	+	?	?	+	+	+	?
Tsilika, 2022	?	?	-	-	-	?	+
Prasoon, 2022	?	?	-	-	-	?	+

Fig. 9. Risk of bias assessment

This meta-analysis had few restrictions. First, there were differences in the probiotics' type, dosage and manner of delivery throughout RCTs. In a few studies, the length of the treatment was too brief to provide any conclusive data. Second, various definitions of ventilator-related pneumonia were used in the RCTs, including a subjective component. Although the most recent definition of a ventilator-related event from the CDC is more objective, none of the published RCTs on probiotics have applied it. The effects of probiotics on 2 additional clinically significant endpoints – the duration of antibiotic treatment and antibiotic use – is due to variable and sparse reporting of the aforementioned endpoints across trials. Next, immunocompromised subjects were not included in the RCTs that were part of the meta-analysis. Therefore, it is impossible to determine how probiotics are used by this particular subject population. Furthermore, no study found any negative consequences of probiotic use. The use of probiotics (best type, dose and method of administration) for ventilator-related pneumonia in an immunocompromised subject population is therefore in need of a large, multicenter RCT that would additionally assess the potential negative effects of probiotics.

This meta-analysis demonstrated how probiotics affect critically ill ventilated subjects.⁵³⁻⁶⁰ Further research is still required to clarify these potential connections as well as to assess the impact of probiotics on the outcomes under investigation. Larger, more homogeneous samples are required for such research. This was also mentioned in a previous study that employed a similar meta-analysis technique and found comparable favorable outcomes for probiotic benefits.⁴²⁻⁴⁸ Because our meta-analysis was unable to determine whether the differences in gender, age and ethnicity are related to the outcomes, meticulously conducted RCTs are required to evaluate these factors as well as the combination of different gender, age, ethnicities, and other variants.

Limitations

There may have been a selection bias since several papers identified through the database search were excluded. However, the omitted publications did not adhere to the inclusion criteria. Nine out of 27 papers that were selected had sample size <100. Furthermore, we were unable to ascertain whether age and ethnicity had an impact on the results. The purpose of this study was to compare the effects of probiotics compared to the controls in critically ill ventilated patients. Data from prior studies were used, which may have introduced bias due to missing or incorrect information. The subjects' nutritional states as well as the characteristics of age, sex and gender were all potential sources of bias. There may be some unpublished articles and missing data that could skew the results.

Conclusions

Critically ill ventilated participants treated with probiotics had significantly reduced incidence of ventilator-related pneumonia, shorter duration of mechanical ventilation, shorter ICU and stay, and decreased oropharyngeal colonization rate. Patients who were administered probiotics did not significantly differ from controls in terms of diarrhea incidence or in-hospital mortality in critically ill ventilated individuals. Analyzing the results requires caution due to the small sample size of 9 out of 27 studies included in the meta-analysis and the lack of studies in numerous comparisons.

Availability of data

The corresponding author agrees to make the meta-analysis database available upon reasonable request.

Supplementary materials

Supplementary figures are available at <https://doi.org/10.5281/zenodo.7340993>. The package consists of the following files:

Supplementary Fig. 1. Ventilator-associated pneumonia incidence funnel plot (Egger's test, $p = 0.86$).

Supplementary Fig. 2. Mechanical ventilation duration funnel plot (Egger's test, $p = 0.84$).

Supplementary Fig. 3. Length of ICU stay funnel plot (Egger's test, $p = 0.86$).

Supplementary Fig. 4. Length of hospital stay funnel plot (Egger's test, $p = 0.85$).

Supplementary Fig. 5. Oropharyngeal colonization funnel plot (Egger's test, $p = 0.91$).

Supplementary Fig. 6. Diarrhea incidence funnel plot (Egger's test, $p = 0.87$).

Supplementary Fig. 7. In-hospital mortality funnel plot (Egger's test, $p = 0.92$).

ORCID iDs

Yao Teng  <https://orcid.org/0000-0001-7548-1361>

References

1. Timsit JF, Esaied W, Neuville M, Bouadma L, Mourvillier B. Update on ventilator-associated pneumonia. *F1000Res*. 2017;6:2061. doi:10.12688/f1000research.12222.1
2. Rosenthal VD, Bijie H, Maki DG, et al. International Nosocomial Infection Control Consortium (INICC) report, data summary of 36 countries, for 2004–2009. *Am J Infect Control*. 2012;40(5):396–407. doi:10.1016/j.ajic.2011.05.020
3. Warren DK, Shukla SJ, Olsen MA, et al. Outcome and attributable cost of ventilator-associated pneumonia among intensive care unit patients in a suburban medical center. *Crit Care Med*. 2003;31(5):1312–1317. doi:10.1097/01.CCM.0000063087.93157.06
4. Torres A, Niederman MS, Chastre J, et al. International ERS/ESICM/ESCMID/ALAT guidelines for the management of hospital-acquired pneumonia and ventilator-associated pneumonia: Guidelines for the management of hospital-acquired pneumonia (HAP)/ventilator-associated pneumonia (VAP) of the European Respiratory Society (ERS), European Society of Intensive Care Medicine (ESICM), European Society of Clinical Microbiology and Infectious Diseases (ESCMID) and Asociación Latinoamericana del Tórax (ALAT). *Eur Respir J*. 2017;50(3):1700582. doi:10.1183/13993003.00582-2017
5. de Smet AMGA, Kluytmans JAJW, Cooper BS, et al. Decontamination of the digestive tract and oropharynx in ICU patients. *N Engl J Med*. 2009;360(1):20–31. doi:10.1056/NEJMoa0800394
6. Morrow LE, Kollef MH, Casale TB. Probiotic prophylaxis of ventilator-associated pneumonia: A blinded, randomized, controlled trial. *Am J Respir Crit Care Med*. 2010;182(8):1058–1064. doi:10.1164/rccm.200912-1853OC
7. Singhi SC, Kumar S. Probiotics in critically ill children. *F1000Res*. 2016;5:F1000 Faculty Rev-407. doi:10.12688/f1000research.7630.1
8. Pandey KR, Naik SR, Vakil BV. Probiotics, prebiotics and synbiotics: A review. *J Food Sci Technol*. 2015;52(12):7577–7587. doi:10.1007/s13197-015-1921-1
9. Stroup DF. Meta-analysis of observational studies in epidemiology: A proposal for reporting. *JAMA*. 2000;283(15):2008–2012. doi:10.1001/jama.283.15.2008
10. Higgins JPT. Measuring inconsistency in meta-analyses. *BMJ*. 2003;327(7414):557–560. doi:10.1136/bmj.327.7414.557
11. Liberati A, Altman DG, Tetzlaff J, et al. The PRISMA statement for reporting systematic reviews and meta-analyses of studies that evaluate health care interventions: Explanation and elaboration. *J Clin Epidemiol*. 2009;62(10):e1–e34. doi:10.1016/j.jclinepi.2009.06.006
12. Gupta A, Das A, Majumder K, et al. Obesity is independently associated with increased risk of hepatocellular cancer-related mortality: A systematic review and meta-analysis. *Am J Clin Oncol*. 2018;41(9):874–881. doi:10.1097/COC.0000000000000388
13. Higgins JPT, Altman DG, Gotzsche PC, et al. The Cochrane Collaboration's tool for assessing risk of bias in randomised trials. *BMJ*. 2011;343:d5928. doi:10.1136/bmj.d5928
14. Sheikhabaehi S, Trahan TJ, Xiao J, et al. FDG-PET/CT and MRI for evaluation of pathologic response to neoadjuvant chemotherapy in patients with breast cancer: A meta-analysis of diagnostic accuracy studies. *Oncologist*. 2016;21(8):931–939. doi:10.1634/theoncologist.2015-0353
15. Kotzampassi K, Giamarellos-Bourboulis EJ, Voudouris A, Kazamias P, Eleftheriadis E. Benefits of a synbiotic formula (Synbiotic 2000Forte®) in critically ill trauma patients: Early results of a randomized controlled trial. *World J Surg*. 2006;30(10):1848–1855. doi:10.1007/s00268-005-0653-1
16. Spindler-Vesel A, Bengmark S, Vovk I, Cerovic O, Kompan L. Synbiotics, prebiotics, glutamine, or peptide in early enteral nutrition: A randomized study in trauma patients. *JPEN J Parenter Enteral Nutr*. 2007;31(2):119–126. doi:10.1177/0148607107031002119
17. Forestier C, Guelon D, Cluytens V, Gillart T, Sirot J, De Champs C. Oral probiotic and prevention of *Pseudomonas aeruginosa* infections: A randomized, double-blind, placebo-controlled pilot study in intensive care unit patients. *Crit Care*. 2008;12(3):R69. doi:10.1186/cc6907
18. Knight DJW, Gardiner D, Banks A, et al. Effect of synbiotic therapy on the incidence of ventilator associated pneumonia in critically ill patients: A randomised, double-blind, placebo-controlled trial. *Intensive Care Med*. 2009;35(5):854–861. doi:10.1007/s00134-008-1368-1
19. Giamarellos-Bourboulis EJ, Bengmark S, Kanellakopoulou K, Kotzampassi K. Pro- and synbiotics to control inflammation and infection in patients with multiple injuries. *J Trauma*. 2009;67(4):815–821. doi:10.1097/TA.0b013e31819d979e
20. Barraud D, Blard C, Hein F, et al. Probiotics in the critically ill patient: A double blind, randomized, placebo-controlled trial. *Intensive Care Med*. 2010;36(9):1540–1547. doi:10.1007/s00134-010-1927-0
21. Oudhuis GJ, Bergmans DC, Dormans T, et al. Probiotics versus antibiotic decontamination of the digestive tract: Infection and mortality. *Intensive Care Med*. 2011;37(1):110–117. doi:10.1007/s00134-010-2002-6
22. Tan M, Zhu JC, Du J, Zhang LM, Yin HH. Effects of probiotics on serum levels of Th1/Th2 cytokine and clinical outcomes in severe traumatic brain-injured patients: A prospective randomized pilot study. *Crit Care*. 2011;15(6):R290. doi:10.1186/cc10579
23. Li XC, Wang JZ, Liu YH. Effect of probiotics on respiratory tract pathogen colonization in neonates undergoing mechanical ventilation [in Chinese]. *Zhongguo Dang Dai Er Ke Za Zhi*. 2012;14(6):406–408. PMID:22738443.

24. Banupriya B, Biswal N, Srinivasaraghavan R, Narayanan P, Mandal J. Probiotic prophylaxis to prevent ventilator associated pneumonia (VAP) in children on mechanical ventilation: An open-label randomized controlled trial. *Intensive Care Med.* 2015;41(4):677–685. doi:10.1007/s00134-015-3694-4
25. Rongrungruang Y, Krajangwittaya D, Pholtawornkulchai K, Tiengrim S, Thamlikitkul V. Randomized controlled study of probiotics containing *Lactobacillus casei* (Shirota strain) for prevention of ventilator-associated pneumonia. *J Med Assoc Thai.* 2015;98(3):253–259. PMID:25920295.
26. Malik AA, Rajandram R, Tah PC, Hakumat-Rai VR, Chin KF. Microbial cell preparation in enteral feeding in critically ill patients: A randomized, double-blind, placebo-controlled clinical trial. *J Crit Care.* 2016;32:182–188. doi:10.1016/j.jcrr.2015.12.008
27. Zeng J, Wang CT, Zhang FS, et al. Effect of probiotics on the incidence of ventilator-associated pneumonia in critically ill patients: A randomized controlled multicenter trial. *Intensive Care Med.* 2016;42(6):1018–1028. doi:10.1007/s00134-016-4303-x
28. Amiri M, Rafeie M, Probiotic effects in prevention from ventilator-associated pneumonia. *Koomesh.* 2016;17(4):803–813. <http://koomeshjournal.semums.ac.ir/article-1-2707-en.html>. Accessed August 16, 2022.
29. Shimizu K, Yamada T, Ogura H, et al. Synbiotics modulate gut microbiota and reduce enteritis and ventilator-associated pneumonia in patients with sepsis: A randomized controlled trial. *Crit Care.* 2018;22(1):239. doi:10.1186/s13054-018-2167-x
30. Angurana SK, Bansal A, Singhi S, et al. Evaluation of effect of probiotics on cytokine levels in critically ill children with severe sepsis: A double-blind, placebo-controlled trial. *Crit Care Med.* 2018;46(10):1656–1664. doi:10.1097/CCM.00000000000003279
31. Kooshki A, Khazaei Z, Zarghi A, Rad M, Tabaraie Y. Prebiotic prophylaxis of ventilator-associated pneumonia: A randomized clinical trial. *Biomed Res Ther.* 2018;5(5):2287–2295. doi:10.15419/bmr.v5i5.442
32. Klarin B, Adolffson A, Torstensson A, Larsson A. Can probiotics be an alternative to chlorhexidine for oral care in the mechanically ventilated patient? A multicentre, prospective, randomised controlled open trial. *Crit Care.* 2018;22(1):272. doi:10.1186/s13054-018-2209-4
33. Anandaraj AM, Pichamuthu KK, Hansdak SG, et al. A randomised controlled trial of *Lactobacillus* in the prevention of ventilator associated pneumonia. *J Clin Diagn Res.* 2019;13(8):OC21–OC24. doi:10.7860/JCDR/2019/42325.13084
34. Mahmoodpoor A, Hamishehkar H, Asghari R, Abri R, Shadvar K, Sanaie S. Effect of a probiotic preparation on ventilator-associated pneumonia in critically ill patients admitted to the intensive care unit: A prospective double-blind randomized controlled trial. *Nutr Clin Pract.* 2019;34(1):156–162. doi:10.1002/ncp.10191
35. Habib T, Kassem AB, Ahmed I. Early probiotics in preventing ventilator-associated pneumonia after multiple trauma. *Asian J Pharm Clin Res.* 2020;13(10):83–85. doi:10.22159/ajpcr.2020.v13i10.38114
36. Nazari B, Amani L, Ghaderi L, Khanbabayi Gol M. Effects of probiotics on prevalence of ventilator-associated pneumonia in multitrauma patients hospitalized in neurosurgical intensive care unit: A randomized clinical trial. *Trauma Mon.* 2020;25(6):262–268. doi:10.30491/tm.2021.250469.1176
37. Johnstone J, Meade M, Lauzier F, et al. Effect of probiotics on incident ventilator-associated pneumonia in critically ill patients: A randomized clinical trial. *JAMA.* 2021;326(11):1024–1033. doi:10.1001/jama.2021.13355
38. Boraey N, Atiyah TR, Ghonaim R, Deraz R, Abdulrahman D. Probiotics can reduce ventilator-associated pneumonia in mechanically ventilated children. *Ann Romanian Soc Cell Biol.* 2021;25(6):14726–14735. <https://annalsofrscb.ro/index.php/journal/article/view/8423/6192>.
39. Tsilika M, Thoma G, Aidoni Z, et al. A four-probiotic preparation for ventilator-associated pneumonia in multi-trauma patients: Results of a randomized clinical trial. *Int J Antimicrob Agents.* 2022;59(1):106471. doi:10.1016/j.ijantimicag.2021.106471
40. Prasoon A, Singh R, Anand R, Kumar S, Singh S, Singh A. A randomized controlled trial to evaluate the use of probiotics in prevention of ventilator-associated pneumonia in critically ill ICU patients. *J Cardiac Crit Care.* 2022;06(2):108–113. doi:10.1055/s-0042-1754161
41. Bo L, Li J, Tao T, et al. Probiotics for preventing ventilator-associated pneumonia. *Cochrane Database Syst Rev.* 2014;10(10):CD009066. doi:10.1002/14651858.CD009066.pub2
42. Song H, Hu W, Zhou X, et al. Clinical benefits from administering probiotics to mechanical ventilated patients in intensive care unit: A PRISMA-guided meta-analysis. *Front Nutr.* 2022;8:798827. doi:10.3389/fnut.2021.798827
43. Wang K, Zeng Q, Li KX, et al. Efficacy of probiotics or synbiotics for critically ill adult patients: A systematic review and meta-analysis of randomized controlled trials. *Burns Trauma.* 2022;10:tkac004. doi:10.1093/burnst/tkac004
44. Sharif S, Greer A, Skorupski C, et al. Probiotics in critical illness: A systematic review and meta-analysis of randomized controlled trials. *Crit Care Med.* 2022;50(8):1175–1186. doi:10.1097/CCM.0000000000005580
45. Ji T, Zhu X, Shang F, Zhang X. Preventive effect of probiotics on ventilator-associated pneumonia: A meta-analysis of 2428 patients. *Ann Pharmacother.* 2021;55(8):949–962. doi:10.1177/1060028020983021
46. Zhao J, Li LQ, Chen CY, Zhang GS, Cui W, Tian BP. Do probiotics help prevent ventilator-associated pneumonia in critically ill patients? A systematic review with meta-analysis. *ERJ Open Res.* 2021;7(1):00302–02020. doi:10.1183/23120541.00302-2020
47. Li C, Lu F, Chen J, Ma J, Xu N. Probiotic supplementation prevents the development of ventilator-associated pneumonia for mechanically ventilated ICU patients: A systematic review and network meta-analysis of randomized controlled trials. *Front Nutr.* 2022;9:919156. doi:10.3389/fnut.2022.919156
48. Cheema HA, Shahid A, Ayyan M, et al. Probiotics for the prevention of ventilator-associated pneumonia: An updated systematic review and meta-analysis of randomised controlled trials. *Nutrients.* 2022;14(8):1600. doi:10.3390/nu14081600
49. Gu WJ, Wei CY, Yin RX. Lack of efficacy of probiotics in preventing ventilator-associated pneumonia. *Chest.* 2012;142(4):859–868. doi:10.1378/chest.12-0679
50. Wang J, Liu KX, Ariani F, Tao LL, Zhang J, Qu JM. Probiotics for preventing ventilator-associated pneumonia: A systematic review and meta-analysis of high-quality randomized controlled trials. *PLoS One.* 2013;8(12):e83934. doi:10.1371/journal.pone.0083934
51. Siempos II, Ntaidou TK, Falagas ME. Impact of the administration of probiotics on the incidence of ventilator-associated pneumonia: A meta-analysis of randomized controlled trials. *Crit Care Med.* 2010;38(3):954–962. doi:10.1097/CCM.0b013e3181c8fe4b
52. Gu WJ, Deng T, Gong YZ, Jing R, Liu JC. The effects of probiotics in early enteral nutrition on the outcomes of trauma: A meta-analysis of randomized controlled trials. *JPN J Parenter Enteral Nutr.* 2013;37(3):310–317. doi:10.1177/0148607112463245
53. Elgendy MO, Hassan AH, Saeed H, Abdelrahim ME, Eldin RS. Asthmatic children and MDI verbal inhalation technique counseling. *Pulm Pharmacol Ther.* 2020;61:101900. doi:10.1016/j.pupt.2020.101900
54. Osama H, Abdullah A, Gamal B, et al. Effect of honey and royal jelly against cisplatin-induced nephrotoxicity in patients with cancer. *J Am Coll Nutr.* 2017;36(5):342–346. doi:10.1080/07315724.2017.1292157
55. Sayed AM, Khalaf AM, Abdelrahim MEA, Elgendy MO. Repurposing of some anti-infective drugs for COVID-19 treatment: A surveillance study supported by an in silico investigation. *Int J Clin Pract.* 2021;75(4):e13877. doi:10.1111/ijcp.13877
56. Saeed H, Elberry AA, Eldin AS, Rabea H, Abdelrahim MEA. Effect of nebulizer designs on aerosol delivery during non-invasive mechanical ventilation: A modeling study of in vitro data. *Pulm Ther.* 2017;3(1):233–241. doi:10.1007/s41030-017-0033-7
57. Saeed H, Abdelrahim ME, Rabea H, Salem HF. Impact of advanced patient counseling using a training device and smartphone application on asthma control. *Respir Care.* 2020;65(3):326–332. doi:10.4187/respcare.06903
58. Madney YM, Ibrahim Laz N, Elberry AA, Rabea H, Abdelrahim MEA. The impact of changing patient interfaces on delivering aerosol with titrated oxygen in the high flow system. *Int J Clin Pract.* 2021;75(4):e13898. doi:10.1111/ijcp.13898
59. Hassan A, Rabea H, Hussein RRS, et al. In-vitro characterization of the aerosolized dose during non-invasive automatic continuous positive airway pressure ventilation. *Pulm Ther.* 2016;2(1):115–126. doi:10.1007/s41030-015-0010-y
60. Harb HS, Laz NI, Rabea H, Abdelrahim MEA. First-time handling of different inhalers by chronic obstructive lung disease patients. *Exp Lung Res.* 2020;46(7):258–269. doi:10.1080/01902148.2020.1789903

Rspo1 inhibited apoptosis of glucocorticoid-induced osteoblasts via Wnt/ β -catenin pathway in Legg–Calve–Perthes disease

Tianjiu Zhang^{1,A–F}, Yifa Ji^{2,A,F}, Song Yu^{1,A–F}, Nankai Wang^{3,A,F}, Qixiao Zhang^{3,B–D,F}, Kaicheng Guo^{3,A–D,F}

¹ School of Clinical Medicine, Guizhou Medical University, Guiyang, China

² Fengtai YouAnMen Hospital, Beijing, China

³ Department of Pediatric Orthopaedics, Affiliated Hospital of Zunyi Medical University, China

A – research concept and design; B – collection and/or assembly of data; C – data analysis and interpretation;

D – writing the article; E – critical revision of the article; F – final approval of the article

Advances in Clinical and Experimental Medicine, ISSN 1899–5276 (print), ISSN 2451–2680 (online)

Adv Clin Exp Med. 2023;32(6):643–654

Address for correspondence

Song Yu

E-mail: yusongabc@126.com

Funding sources

This work was supported by the Guizhou Province's Science and Technology Plan Project (Basis (2018) 1430) and Guizhou Province's Science and Technology Plan Project (Support (2021) General 076).

Conflict of interest

None declared

Received on April 15, 2022

Reviewed on July 17, 2022

Accepted on November 28, 2022

Published online on March 7, 2023

Abstract

Background. The pathogenesis of Legg–Calve–Perthes disease (LCPD), a juvenile form of avascular necrosis of the femoral head (ANFH), is not fully understood.

Objectives. The purpose of this work was to study the regulatory effect of *R-spondin 1* (*Rspo1*) on osteoblastic apoptosis and evaluate the pre-clinical efficacy of recombinant human protein *Rspo1* (rh*Rspo1*) in treatment of LCPD.

Materials and methods. This is an experimental study. In vivo rabbit ANFH model was established. Human osteoblast cell line hFOB1.19 (hFOB) was used to overexpress and silence *Rspo1* in vitro. Additionally, hFOB cells were induced with glucocorticoid (GC) and methylprednisolone (MP), and treated with rh*Rspo1*. The expressions of *Rspo1*, β -catenin, *Dkk-1*, *Bcl-2*, and caspase-3, and the apoptosis rate of hFOB cells were examined.

Results. The expressions of *Rspo1* and β -catenin were lower in ANFH rabbits. The expression of *Rspo1* was decreased in GC-induced hFOB cells. Compared to the control group, after 1 μ M MP induction for 72 h, the expressions of β -catenin and *Bcl-2* were higher, while *Dkk-1*, caspase-3 and cleaved caspase-3 expressions were lower in *Rspo1* overexpression and rh*Rspo1*-treated groups. The apoptosis rate of GC-induced hFOB cells was decreased in *Rspo1* overexpression and rh*Rspo1*-treated groups compared to the control group.

Conclusions. *R-spondin 1* inhibited GC-induced osteoblast apoptosis via Wnt/ β -catenin pathway, which might be associated with the development of ANFH. Moreover, rh*Rspo1* had a potential pre-clinical therapeutic effect on LCPD.

Key words: apoptosis, Wnt/ β -catenin pathway, osteoblast, *R-spondin 1*, Perthes disease

Cite as

Zhang T, Ji Y, Yu S, Wang N, Zhang Q, Guo K. *Rspo1* inhibited apoptosis of glucocorticoid-induced osteoblasts via Wnt/ β -catenin pathway in Legg–Calve–Perthes disease. *Adv Clin Exp Med.* 2023;32(6):643–654. doi:10.17219/acem/156958

DOI

10.17219/acem/156958

Copyright

Copyright by Author(s)

This is an article distributed under the terms of the Creative Commons Attribution 3.0 Unported (CC BY 3.0) (<https://creativecommons.org/licenses/by/3.0/>)

Background

Legg–Calve–Perthes disease (LCPD) is a juvenile form of avascular necrosis of the femoral head (ANFH) that usually occurs between 2 and 14 years of age, and is associated with a permanent deformity of the femoral head and early osteoarthritis.^{1,2} The etiology of LCPD is not well understood, and it may be related to multiple factors. Its main pathogenesis is thought to be blood supply disturbance of the femoral head, leading to ischemic necrosis of the epiphysis and adjacent tissues.^{3,4} Many studies have confirmed that glucocorticoid (GC) can induce vascular endothelial cell injury, thrombosis, increased intraosseous pressure, and osteocyte apoptosis. This in turn results in avascular necrosis and blood flow disturbance in the femoral head,⁵ which is similar to the pathological process of LCPD, suggesting that GC may be one of the causes of this disease.

The Wnt/ β -catenin pathway, established in many human tissues, is a canonical signal transduction pathway, which controls many cellular activities during embryonic development and adult homeostasis, such as stem cell renewal, and cell proliferation and differentiation.^{6,7} Furthermore, the activation of this signaling pathway can stimulate cell proliferation, induce cell differentiation and inhibit apoptosis of osteoblasts.^{8,9} In addition, Wnt/ β -catenin pathway is essential in normal bone homeostasis, and has an important role in mediating the signaling coupled with osteoblastic bone formation and resorption. Moreover, Wnt/ β -catenin signaling maintains the dynamic balance of bone metabolism, and its dysregulation may lead to various osteoarticular diseases.⁶

R-spondin (Rspo) is a secretory protein composed of 4 family members (Rspo1–4), which can bind to the leucine-rich repeat-containing G protein-coupled receptors (LGR4–6), regulating cell differentiation, stem cell maintenance and angiogenesis. The R-spondin is expressed in both embryonic and adult tissues, and its proper expression is essential for the normal development of organisms and maintaining body homeostasis.^{10–12} As an agonist of the Wnt/ β -catenin pathway, Rspo1 plays a role in regulating the human skeletal system.^{13–15} The R-spondin and Wnt3a cooperate to induce osteoblastic differentiation and osteoprotegerin expression, thereby promoting bone remodeling.¹⁶ Therapeutic application of recombinant human protein Rspo1 (rhRspo1) has already shown beneficial effects in animal models of intestinal inflammatory diseases and mucositis.¹⁷ The administration of rhRspo1 can alleviate radiation-induced bone loss through maintaining bone homeostasis via the Rspo1–LGR4 axis.¹⁸

Currently, there are no relevant reports on the involvement of Rspo1 in the pathogenesis of LCPD.

Objectives

The etiology of LCPD is not clear. It is speculated that Rspo1 and Wnt/ β -catenin are involved in the pathogenesis of LCPD. The purpose of this study was to verify whether

Rspo1 is involved in the development of GC-induced ANFH in immature rabbits via Wnt/ β -catenin pathway *in vivo* and *in vitro*.

Materials and methods

Animals

Sixty healthy 8-week-old New Zealand white rabbits weighing 1300–1800 g were obtained from the Animal Research Center of Zunyi Medical College, Zunyi, China. All animal studies (including the rabbit euthanasia procedure) were performed in compliance with the regulations and guidelines of Zunyi Medical College institutional animal care and conducted according to the Association for Assessment and Accreditation of Laboratory Animal Care (AAALAC) and Institutional Animal Care and Use Committee (IACUC) guidelines (approval No. KLL-2020-008 of the ethics committee of Affiliated Hospital of Zunyi Medical College).

The immature rabbits were randomly divided into 2 groups: GC group (n = 48) and control group (n = 12). Rabbits in the GC group were given methylprednisolone (MP) (7.5 mg/kg⁻¹) in buttocks twice a week for 8 weeks, and those in the control group were injected with saline. Afterwards, all rabbits were euthanized by air embolism, and their bilateral femoral heads were quickly removed and evaluated with gross morphology and X-ray photography. The specimens were maintained at a constant distance from the X-ray source to minimize any effects of magnification.

One part of the femoral head was fixed in 4% formaldehyde solution for 36 h, followed by soaking in ethylenediaminetetraacetic acid (EDTA) to remove calcium; the other parts were put into a Eppendorf (EP) tube, snap-frozen in liquid nitrogen and stored at –80°C.

The ANFH was assessed by 3 doctors (specialists in imaging) using evaluation criteria as previous study.¹⁹ The experimental scheme was approved by the Animal Use and Care Committee of Zunyi Medical College.

Cell culture

Human osteoblast cell line hFOB1.19 (hFOB), provided by the Cell Bank of Chinese Academy of Sciences (Shanghai, China), was cultured in Dulbecco's modified Eagle's medium (DMEM0 (Gibco, Waltham, USA) supplemented with 10% fetal bovine serum (FBS) and G418 (Yuanye Corp., Shanghai, China) at 37°C with 5% CO₂. The morphology of hFOB cells was observed under an inverted phase contrast microscope (model CKX53; Olympus Corp., Tokyo, Japan), and cells after passage 3 were used for subsequent analysis.

The hFOB cells were inoculated on a 6-well plate, and different concentrations of MP (Pfizer, New York, USA) were added to the culture medium (0 μ M, 0.01 μ M, 0.1 μ M, and 1 μ M) for 24 h, 48 h and 72 h. In addition, cells grown

in a 6-well plate were treated with 500 ng/mL of rhRspo1 (Biolegend, San Diego, USA) for 72 h.^{20,21} The cells were divided into rhRspo1, MP, rhRspo1+MP, and control groups.

Lentivirus transfection

R-spondin 1 overexpression mRNA (Rspo1), non-coding Rspo1 mRNA negative control (Rspo1-NC) and Rspo1 silencing mRNA (shRNA) were encoded by lentivirus vectors (Hanheng Biotechnology Co., Ltd., Shanghai, China). The experiments were classified into the Rspo1+1 μ M MP, Rspo1-NC+1 μ M MP, Rspo1 silencing mRNA with short hairpin RNA (shRspo1), and control (1 μ M MP) groups. Briefly, approx. 2×10^4 cells were inoculated in a 24-well plate, and transfection was performed using the lentivirus vector at a multiplicity of infection (MOI) of 30, when cells were grown to a confluence of 30%. The infection efficiency was assessed using the frequency of green fluorescent protein (GFP)-positive cells and the expression level of Rspo1 after 72 h. Stably transfected cells were screened with 3 μ g/mL puromycin (Gibco).

Flow cytometry

The apoptosis rate of hFOB cells was detected with flow cytometry according to the manufacturer's instructions (Beyotime Biotechnology, Shanghai, China). Cells were collected by centrifugation at 2000 rpm for 5 min after digestion with trypsin, and washed with phosphate-buffered saline (PBS). Then, 5 μ L of Annexin V-APC and 5 μ L of 7-aminoactinomycin D (7-AAD) dye solution were added into the cell suspension at room temperature for 10 min in the dark. Apoptotic detection of the cells double stained with acridine orange and ethidium bromide (AO-EB) was also performed using a FACScalibur flow cytometer (BD Biosciences, Franklin Lakes, USA).

TUNEL assay

The apoptosis rate of hFOB cells was detected using the In Situ Cell Death Detection Kit (Roche, Basel, Switzerland). The treated cells were fixed using 4% paraformaldehyde for 1 h, followed by incubation with 3% H₂O₂ and 0.1% Triton X-100 for 20 min. Phosphate-buffered saline

cleaning was required between all the above steps. After that, the terminal deoxynucleotidyl transferase dUTP nick end labeling (TUNEL) staining was carried out according to the manufacturer's protocol. After completion of staining, 3 independent researchers counted the TUNEL-positive cells under a fluorescence microscope (model E8400; Nikon Corp., Tokyo, Japan).

Quantitative real-time polymerase chain reaction

Total RNA was extracted from the cells with RNAiso Plus (Takara, Shiga, Japan), and converted to cDNA using the high capacity cDNA RT Kit (MBI Fermentas Inc., Burlington, Canada), following the manufacturer's instructions. Relative mRNA expression levels were estimated based on the $2^{-\Delta\Delta CT}$ method, with *GAPDH* as the reference housekeeping gene for normalization. The quantitative real-time polymerase chain reaction (q-PCR) primers used are listed in Table 1.

Western blot

Immunoblotting was performed according to the manufacturer's instructions (Proteintech, Rosemont, USA). The hFOB cells were washed and lysed with radioimmunoprecipitation assay (RIPA) lysis buffer (Beyotime Biotechnology) supplemented with 1 mM protease inhibitor, and incubated on ice for 30 min. The supernatant was collected after the lysate was centrifuged at $12000 \times g$ for 5 min at 4°C. Proteins were separated using sodium dodecyl sulfate-polyacrylamide gel electrophoresis (SDS-PAGE) and then transferred to a polyvinylidene difluoride (PVDF) membrane (Millipore, Burlington, USA). The membrane was blocked with 5% bovine serum albumin (BSA) in tris-buffered saline with Tween (TBST) and then incubated with a primary antibody (anti-Rspo1, 1:1000; anti- β -catenin, 1:5000; anti-Dkk-1, 1:1000; anti-caspase-3, 1:2000; anti-cleaved caspase-3, 1:1000; and anti-bcl-2, 1:1000; all from Proteintech) at 4°C overnight. Subsequently, the TBST PVDF membrane was washed and incubated with the corresponding secondary antibody for 1 h at room temperature. Finally, the proteins were detected using an enhanced chemiluminescent (ECL) reaction, and the band's intensity was analyzed using ImageJ software (National Institutes of Health, Bethesda, USA).

Table 1. Primers used for quantitative real-time polymerase chain reaction (q-PCR)

Primer	Forward sequence	Reverse sequence
Rspo1	5'-TGTGAAATGAGCGAGTGGTC-3'	5'-GAGCAGTTGGTTTGGTCTCC-3'
β -catenin	5'-GCAGTGAAGAATGCACACGA-3'	5'-CAAGCAAAGTCAGCACCCT-3'
Dkk-1	5'-CTTGGACCAGAAGTGTCTAGCAC-3'	5'-GATTCCCTGGACCTAAAGGTGC-3'
Bcl-2	5'-GGTGGGGTCATGTGTGTGG-3'	5'-CGGTTACGGTACTCAGTCATCC-3'
Caspase-3	5'-CATGGAAGCGAATCAATGGACT-3'	5'-CTGTACCAGACCGAGATGTCA-3'
GAPDH	5'-GGAGCGAGATCCCTCCAAAT-3'	5'-GGCTGTTGTACTACTCTCATGG-3'
β -actin	5'-CTCCATCCTGGCCTCGTGT-3'	5'-GCTGTCACCTTACCCTTCC-3'

Statistical analyses

All experiments were repeated 3 times. All data were tested for normal distribution using the Shapiro–Wilk method, and normally distributed data were expressed as mean \pm standard deviation ($M \pm SD$), while non-normally distributed data were expressed as median and percentiles (25th percentile (P25) and 75th percentile (P75)). The homogeneity of variance was analyzed using Levene's test. The t-test and analysis of variance (ANOVA) were used to compare 2 groups and multiple groups, and non-parametric test was used to compare the data of non-normal distribution using Kruskal–Wallis test. A p-value <0.05 was considered statistically significant. All calculations were conducted using IBM SPSS v. 25.0 software (IBM Corp., Armonk, USA).

Results

Animal model

Twelve immature rabbits from the GC group died during the experiment because of diarrhea, while there were no deaths in the control group. Ten rabbits were confirmed as ANFH according to the diagnostic criteria of osteonecrosis of the femoral head (all unilateral).¹⁹ The gross morphology showed that the femoral head of ANFH became smaller, pale and collapsed, with

a non-spherical appearance, and the femoral neck became shorter. The X-ray images revealed a decreased density of femoral head epiphysis, with irregular shape, reduced size, partial necrosis, and collapse (Supplementary Fig. 1).

Downregulation of Rspo1 and β -catenin, and upregulation of Dkk-1 in the bony epiphysis of ANFH in vivo

Compared to the control group, the expressions of Rspo1 and β -catenin in the bony epiphysis of the femoral head were significantly lower, while Dkk-1 level was significantly higher in ANFH rabbits (all $p < 0.05$, Fig. 1, Table 2). These findings suggested that Rspo1 was negatively regulated by GC, which could reduce the activation of the Wnt/ β -catenin pathway and promote the occurrence of ANFH in immature rabbits.

Downregulation of Rspo1 and increased apoptosis rate of GC-induced hFOB cells in vitro

The apoptosis rate of GC-induced hFOB cells treated with different concentrations of MP (0 μ M, 0.01 μ M, 0.1 μ M, 1 μ M) was gradually increased in a time- and dose-dependent manner, as measured with flow cytometry analysis at 24 h, 48 h and 72 h. It was the highest in the 1 μ M MP group at 72 h. The expression of Rspo1 was the lowest in the 1 μ M MP group at 72 h, which also showed a dose-dependent tendency (Fig. 2, Table 3).

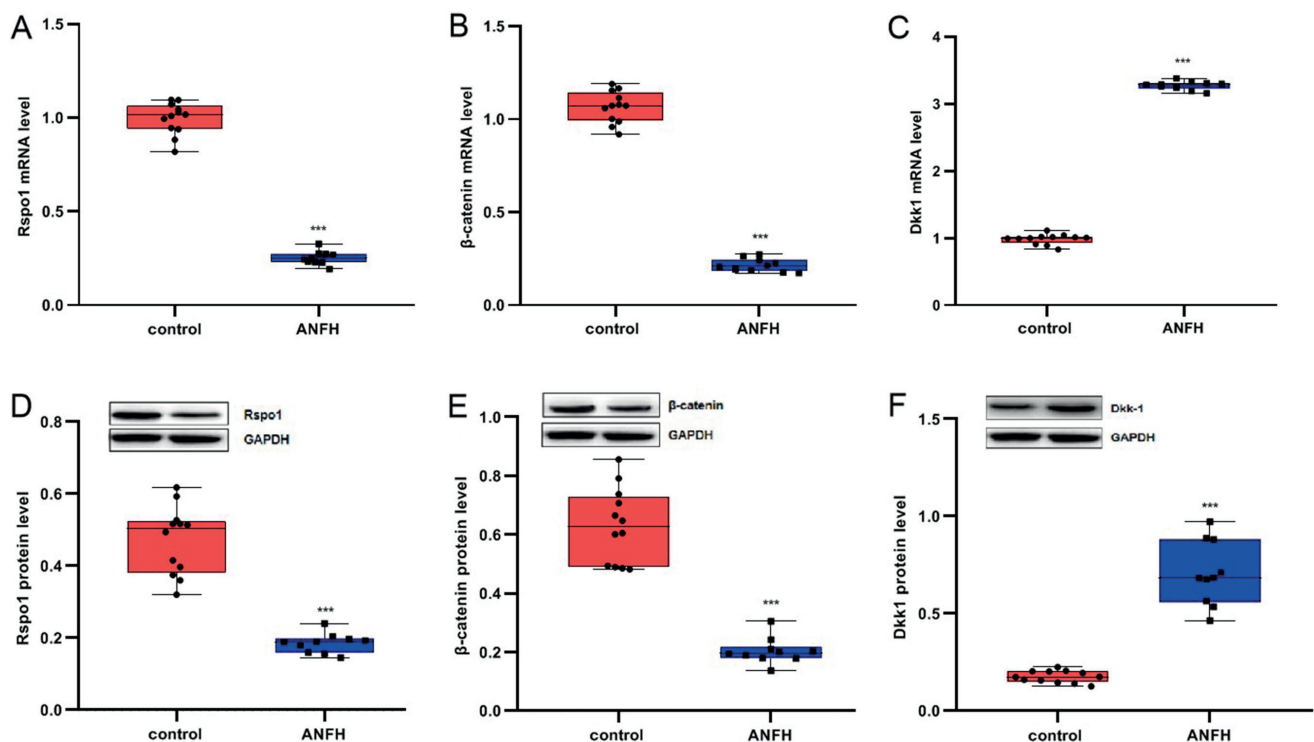


Fig. 1. Expressions of R-spondin 1 (Rspo1), β -catenin and Dkk-1 in the bony epiphysis of the femoral head in immature rabbits. A–C. The mRNA level of Rspo1 (A), β -catenin (B) and Dkk-1 (C) detected with quantitative real-time polymerase chain reaction (q-PCR); D–F. The protein level of Rspo1 (D), β -catenin (E) and Dkk-1 (F) analyzed with western blot

*** $p < 0.001$. ANFH – avascular necrosis of the femoral head.

Table 2. The normality test and statistical analysis of multiple dependent variable of Fig. 1

Dependent variable		Control					ANFH					t-test	
		mean	SD	n	Shapiro–Wilk		mean	SD	n	Shapiro–Wilk		statistics	Sig.
					statistics	Sig.				statistics	Sig.		
Rspo1	mRNA	0.999	0.085	12	0.934	0.423	0.253	0.036	10	0.957	0.748	25.072	0.000
	protein	0.471	0.095	12	0.940	0.500	0.185	0.027	10	0.948	0.640	9.165	0.000
β-catenin	mRNA	1.065	0.085	12	0.962	0.806	0.215	0.035	10	0.938	0.527	29.519	0.000
	protein	0.630	0.128	12	0.921	0.291	0.203	0.045	10	0.887	0.156	10.042	0.000
Dkk-1	mRNA	0.985	0.075	12	0.900	0.159	3.275	0.065	10	0.967	0.863	75.582	0.000
	protein	0.175	0.031	12	0.958	0.751	0.705	0.165	10	0.942	0.575	10.961	0.000

Rspo1 – R-spondin 1; ANFH – avascular necrosis of the femoral head; SD – standard deviation.

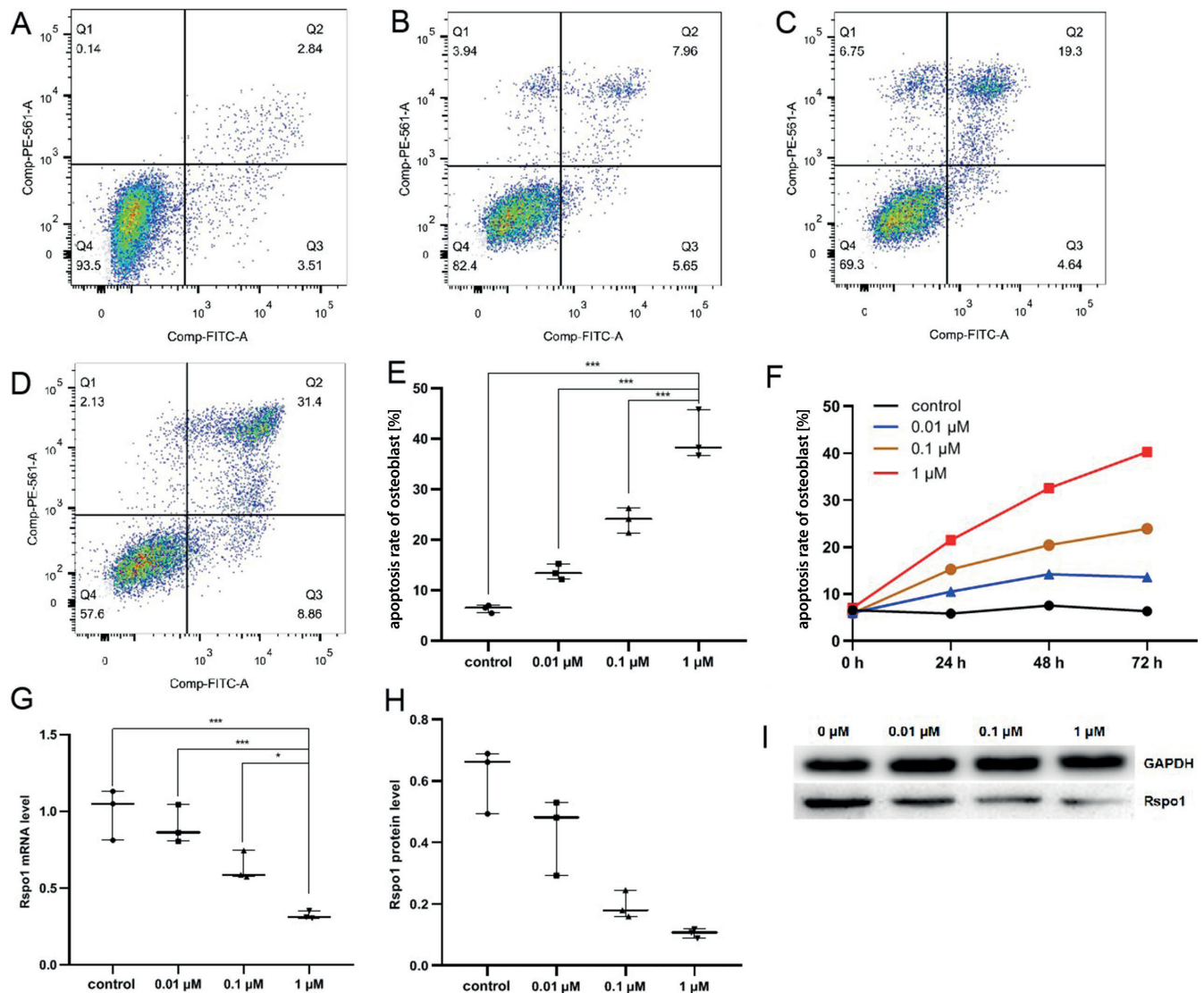


Fig. 2. Apoptosis rate and expression of R-spondin 1 (Rspo1) in glucocorticoid (GC)-induced human osteoblast cell line hFOB1.19 (hFOB). A–D. The photograph of apoptosis presented using flow cytometry with different doses of methylprednisolone (MP) (A: 0 μM; B: 0.01 μM; C: 0.1 μM; D: 1 μM) at 72 h; E,F. The apoptosis rate in different groups; G,H. The mRNA and protein level of Rspo1

* p < 0.05; ** p < 0.01; *** p < 0.001 (compared at the same time (F), n = 3/group). control group – 0 μM; FITC – fluorescein isothiocyanate.

Our findings suggested that GC promoted the apoptosis of osteoblasts and downregulated the expression of Rspo1.

R-spondin 1 inhibited apoptosis of GC-induced hFOB cells through the Wnt/ β -catenin pathway

The hFOB cells transfected with lentiviral vectors were observed under a fluorescence microscope after 72 h, and the successful transfection ratio was defined as 80%. The cell apoptosis rate was significantly higher in the 1 μ M

MP group compared with the shRspo1 group, while it was slightly lower in the Rspo1+1 μ M MP group compared with the Rspo1-NC+1 μ M MP group, without descending to the normal level (Fig. 3, Table 4). The expression levels of Rspo1, β -catenin and Bcl-2 were significantly higher, while Dkk-1, caspase-3 and cleaved caspase-3 levels were significantly lower in the Rspo1+1 μ M MP group compared with the Rspo1-NC+1 μ M MP group (Fig. 4, Table 4). These findings suggested that Rspo1 mRNA could reduce the apoptosis rate of osteoblasts and GC-induced hFOB cells via the Wnt/ β -catenin pathway.

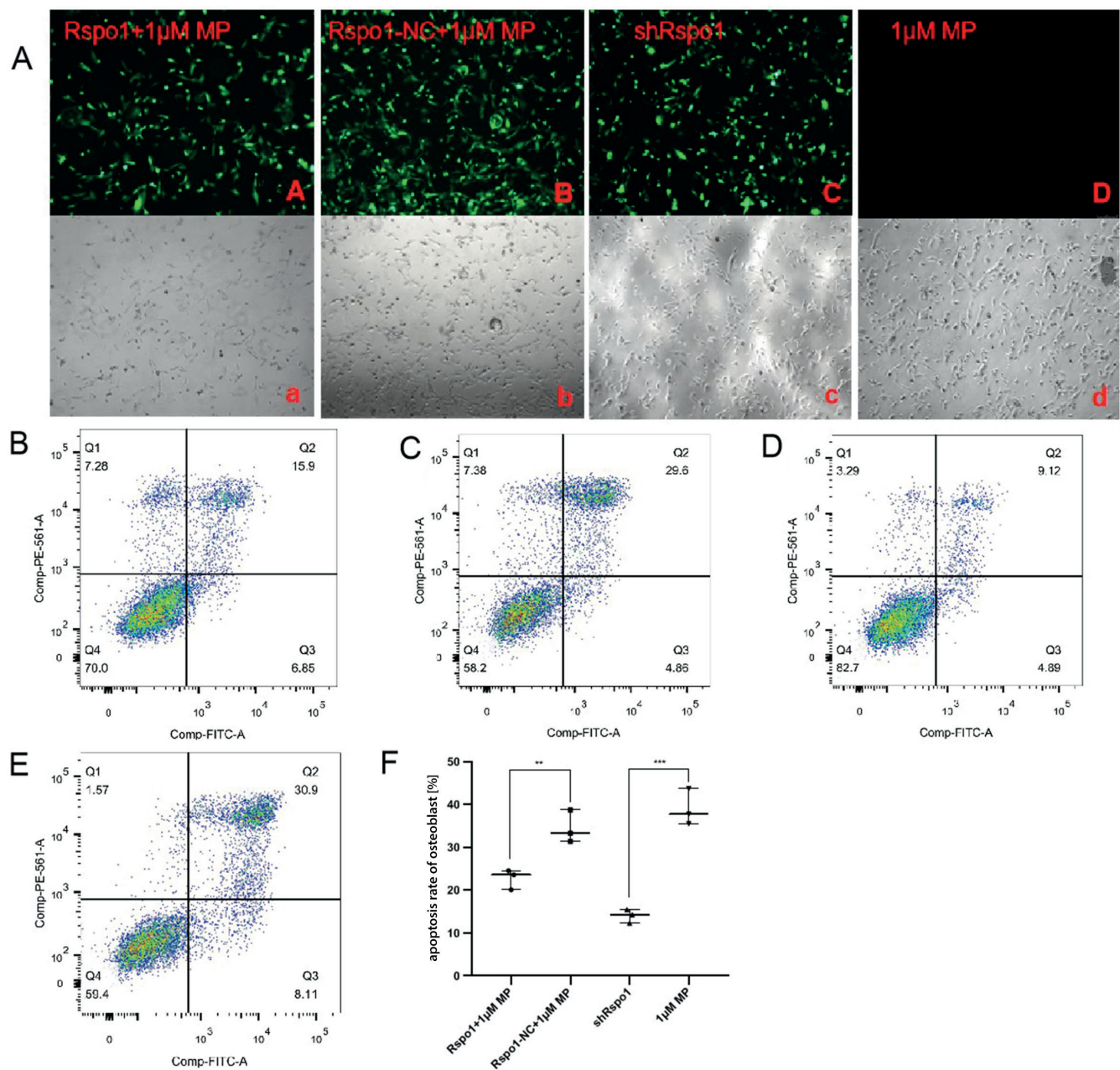


Fig. 3. Lentivirus vectors with green fluorescent protein (GFP) are successfully transfected into human osteoblast cell line hFOB1.19 (hFOB) confirmed using fluorescence microscopy (original magnification $\times 40$). A. The fluorescence and white light results. B–E. The apoptotic rate of (B) R-spondin 1 (Rspo1)+1 μ M MP group, (C) Rspo1-NC+1 μ M MP group, (D) shRspo1 group, and (E) 1 μ M MP group using flow cytometry; F. Histogram of the apoptotic rate

** $p < 0.01$; *** $p < 0.001$; $n = 3$ /group. Rspo1-NC – non-coding Rspo1 mRNA negative control; shRspo1 – Rspo1 silencing mRNA with short hairpin RNA; FITC – fluorescein isothiocyanate; MP – methylprednisolone.

Table 3. The normality test and statistical analysis of multiple dependent variable of Fig. 2

Dependent variable	Control				0.01 μM				0.1 μM				1 μM				THV		ANOVA/NPT		Sig ^b	Sig ^c		
	Shapiro-Wilk statistics		mean/median	SD/ (P25,P75)	Shapiro-Wilk statistics		mean	SD	Shapiro-Wilk statistics		mean	SD	Shapiro-Wilk statistics		mean	SD	statistics	Sig.	statistics	Sig.				
	stat.	Sig.			stat.	Sig.			stat.	Sig.			stat.	Sig.										
0 h	0.962	0.624	6.585	0.775	0.928	0.481	6.015	0.755	1.000	0.975	5.955	0.675	1.000	0.997	0.898	7.085	0.815	0.064 [§]	0.977	1.483	0.291	–	–	
24 h	0.771	0.047	6.195	5.669, 6.210	1.000	0.993	10.535	1.125	0.779	0.065	15.255	1.375	0.779	0.968	0.659	21.475	2.815	–	–	10.385 [®]	0.016	0.308	0.042	0.002
48 h	0.945	0.547	7.565	0.855	1.000	0.995	14.215	1.515	0.853	0.247	20.445	2.845	0.853	0.953	0.581	32.565	3.775	2.571 [®]	0.127	53.505	0.000	0.000	0.000	0.000
72 h	0.943	0.542	6.355	0.784	0.985	0.763	13.615	1.545	0.994	0.852	23.935	2.455	0.994	0.878	0.317	40.255	4.866	4.005 [®]	0.052	79.308	0.000	0.000	0.000	0.000
mRNA	0.927	0.478	0.998	0.166	0.916	0.438	0.905	0.125	0.807	0.131	0.635	0.095	0.807	0.857	0.259	0.323	0.026	2.822 [®]	0.107	20.879	0.000	0.010	0.000	0.000
Protein	0.852	0.245	0.615	0.106	0.894	0.368	0.435	0.125	0.915	0.433	0.195	0.044	0.915	0.977	0.708	0.105	0.015	4.625 [®]	0.037	–	–	0.312	0.233	0.074

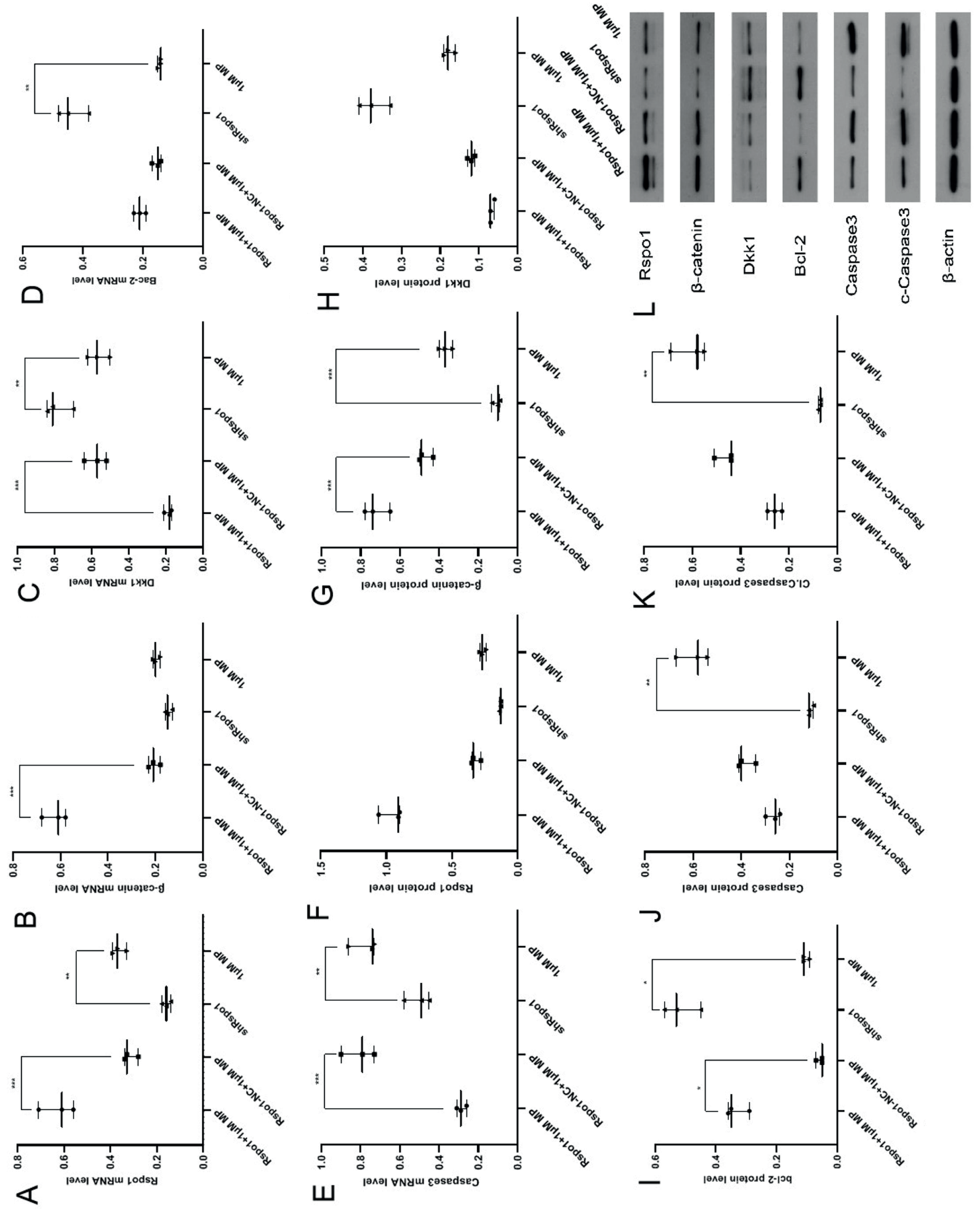
The Shapiro-Wilk test was used as normality test. ^a 1 μM group compared with 0.1 μM group; ^b 1 μM group compared with 0.01 μM group; ^c 1 μM group compared with control group. Other tests used: [®] Kruskal–Wallis test; [§] least significance difference test (LSD); [#] Tamhane's test. THV – test for homogeneity of variance; ANOVA – analysis of variance; NPT – non-parametric test; SD – standard deviation; P25 – 25th percentile; P75 – 75th percentile.

Table 4. The normality test and statistical analysis of multiple dependent variable of Fig. 3, 4

Dependent variable	Rspo1-1 μM MP				Rspo1-NC+1 μM MP				shRspo1				1 μM MP				THV		ANOVA [§]		NPT [®]		Sig ^b	
	Shapiro-Wilk statistics		mean/median	SD/ (P25,P75)	Shapiro-Wilk statistics		mean/median	SD/ (P25,P75)	Shapiro-Wilk statistics		mean/median	SD/ (P25,P75)	Shapiro-Wilk statistics		mean/median	SD/ (P25,P75)	stat.	Sig.	stat.	Sig.	stat.	Sig.		
	stat.	Sig.			stat.	Sig.			stat.	Sig.			stat.	Sig.										
Rspo1	0.964	0.637	0.627	0.076	0.871	0.298	0.317	0.032	1.000	1.000	0.160	0.020	0.964	0.637	0.363	0.030	2.441	0.139	55.035	0.000	–	–	0.000	0.001
protein	0.797	0.107	0.956	0.089	0.855	0.253	0.323	0.037	0.750	0.000	0.130, 0.135	0.130, 0.135	0.987	0.780	0.267	0.025	–	–	–	–	10.009	0.018	0.257	0.257
β-catenin	0.949	0.567	0.623	0.051	0.987	0.780	0.207	0.025	0.964	0.637	0.147	0.015	0.964	0.637	0.197	0.015	2.554	0.126	157.786	0.000	–	–	0.000	0.080
protein	0.953	0.583	0.723	0.066	0.855	0.253	0.473	0.038	0.923	0.463	0.107	0.021	0.993	0.843	0.367	0.035	1.660	0.252	103.993	0.000	–	–	0.000	0.000
Dkk-1	0.923	0.463	0.187	0.021	0.991	0.817	0.577	0.060	0.902	0.391	0.783	0.074	0.991	0.817	0.563	0.060	1.210	0.367	56.442	0.000	–	–	0.000	0.002
protein	0.750	0.000	0.070	0.065, 0.070	1.000	1.000	0.120	0.010	0.980	0.726	0.373	0.040	0.964	0.637	0.177	0.015	–	–	–	–	10.421	0.015	0.307	0.307
Bcl-2	1.000	1.000	0.210	0.020	0.964	0.637	0.153	0.015	0.949	0.567	0.437	0.051	0.750	0.000	0.140	0.140, 0.145	–	–	–	–	9.721	0.021	0.189	0.005
protein	0.855	0.253	0.333	0.038	0.705	0.000	0.050	0.050, 0.060	0.964	0.637	0.517	0.061	0.750	0.000	0.110	0.100, 0.110	–	–	–	–	10.458	0.015	0.041	0.041
Caspase-3	0.987	0.780	0.287	0.025	0.972	0.679	0.807	0.086	0.953	0.583	0.507	0.067	0.807	0.132	0.777	0.072	1.432	0.303	40.754	0.000	–	–	0.000	0.001
protein	0.964	0.637	0.267	0.031	0.855	0.253	0.383	0.038	0.750	0.000	0.120	0.110, 0.120	0.953	0.583	0.597	0.067	–	–	–	–	10.421	0.015	0.307	0.002
Cleaved caspase-3	1.000	1.000	0.260	0.030	0.750	0.000	0.440	0.440, 0.475	0.750	0.000	0.070	0.070, 0.075	0.902	0.391	0.607	0.074	–	–	–	–	10.458	0.015	0.306	0.002
Apoptosis rate	0.901	0.389	22.747	2.349	0.924	0.467	34.463	3.817	0.977	0.710	14.013	1.583	0.935	0.507	39.007	4.230	1.534	0.279	38.068	0.000	–	–	0.002	0.000

The Shapiro-Wilk test was used as normality test. ^a Rspo1-1 μM MP group compared with Rspo1-NC+1 μM MP group; ^b shRspo1 group compared with 1 μM MP group. Other tests used: [®] Kruskal–Wallis test; [§] least significance difference test (LSD). THV – test for homogeneity of variance; shRspo1 – Rspo1 silencing mRNA with short hairpin RNA; ANOVA – analysis of variance; NPT – non-parametric test; SD – standard deviation; P25 – 25th percentile; P75 – 75th percentile; stat. – statistics; MP – methylprednisolone.

Fig. 4. The mRNA and protein expression in human osteoblast cell lines hFOB1.19 (hFOBs) transfected using lentivirus vectors. A–E. Histogram of mRNA level of R-spondin 1 (Rspo1), β -catenin, Dkk-1, Bcl-2, and caspase-3; F–K. Histogram of protein levels of Rspo1, β -catenin, Dkk-1, Bcl-2, caspase-3, and cleaved caspase-3; L. Western blot band of protein expression



* $p < 0.05$; ** $p < 0.01$; *** $p < 0.001$

($n = 3$ /group). Rspo1-NC – non-coding Rspo1 mRNA negative control; shRspo1 – Rspo1 silencing mRNA with short hairpin RNA; MP – methylprednisolone.

rhRspo1 could partially antagonize GC-induced hFOB apoptosis via the Wnt/ β -catenin pathway

The apoptosis rate of hFOB cells was significantly lower in the rhRspo1 group than in the control group, and it was reduced in the rhRspo1+1 μ M MP group compared with the 1 μ M MP group, but it did not descend to the level of the control group. The expressions of β -catenin and Bcl-2 were significantly higher, while the expressions of Dkk-1, caspase-3 and cleaved caspase-3 were significantly lower when comparing the rhRspo1 group to the control group, and the rhRspo1+1 μ M MP group to the 1 μ M MP group, and they were not restored to the level of the control group. These findings indicated that rhRspo1 could reduce the apoptosis rate of hFOB cells and partially antagonize the GC-induced hFOB apoptosis via the Wnt/ β -catenin pathway. The expression of Rspo1 was significantly lower in the rhRspo1 group than in the control group, probably indicating the feedback inhibition of exogenous rhRspo1 (Fig. 5, Table 5).

Discussion

Our results indicated that GC might be one of the causes of LCPD based on the successfully established GC-induced rabbit model of ANFH, which presented pathological process similar to LCPD. R-spondin 1 was negatively regulated by GC, which reduced the activation of the Wnt/ β -catenin pathway and promoted the occurrence of ANFH. This study provided a pre-clinical experimental basis for rhRspo1 in the treatment of LCPD.

In the present study, the animal model of ANFH was successfully established in immature rabbits, revealing pathological changes similar to LCPD, such as deformation and collapse of the femoral head, thickened cartilage and increased bony epiphyseal density.^{22,23} The expressions of Rspo1 and β -catenin were significantly decreased, while the expression of Dkk-1 was significantly increased in the bony epiphysis of the femoral head in ANFH, suggesting that the Wnt/ β -catenin pathway might be involved in the pathological process of GC-induced ANFH in immature rabbits. The expression of Rspo1 in GC-induced osteoblasts was downregulated in a time- and dose-dependent manner. The binding of Rspo1 to transmembrane receptor Frizzled (FZD) was reduced, preventing the accumulation and nuclear transfer of β -catenin, downregulating the transcription of downstream target genes, promoting osteoblast apoptosis,^{24,25} and inducing the occurrence of ANFH. Although GC and shRspo1 both can downregulate the expression of the key proteins of Wnt/ β -catenin pathway in osteoblasts and increase the apoptosis rate of osteoblasts, the apoptosis-promoting effect and the expression of pro-apoptotic factors including caspase-3, cleaved caspase-3 and anti-apoptotic factor BCL-2 were

Table 5. The normality test and statistical analysis of multiple dependent variable of Fig. 5

Dependent variable	Control			rhRspo1			1 μ M MP			rhRspo1+1 μ M MP			THV		ANOVA		NPT [®]		Sig ^c	Sig ^b	Sig ^a					
	Shapiro-Wilk		SD	Shapiro-Wilk		SD	Shapiro-Wilk		mean/median	SD/(P25, P75)	Shapiro-Wilk		mean	SD	stat.	Sig.	stat.	Sig.				stat.	Sig.			
	stat.	Sig.		stat.	Sig.		stat.	Sig.			stat.	Sig.														
Rspo1	0.992	0.824	0.815	0.091	0.999	0.930	0.242	0.024	0.984	0.762	0.113	0.012	0.796	0.105	0.445	0.045	2.757	0.112	102.139 [§]	0.000	-	-	0.000	0.000	0.000	
β -catenin	0.775	0.056	0.307	0.034	0.837	0.206	0.515	0.056	0.810	0.138	0.085	0.014	0.887	0.346	0.183	0.025	3.605	0.065	81.221 [§]	0.000	-	-	0.000	0.010	0.030	
Dkk-1	0.975	0.699	0.235	0.035	0.996	0.886	0.065	0.015	0.787	0.083	0.364	0.034	0.942	0.537	0.097	0.014	1.894	0.209	79.994 [§]	0.000	-	-	0.000	0.000	0.000	
Bcl-2	0.942	0.537	0.205	0.025	0.847	0.234	0.429	0.045	0.971	0.672	0.090	0.010	0.998	0.908	0.144	0.012	4.418	0.041	91.524 [#]	0.000	-	-	0.025	0.027	0.191	
Caspase-3	0.852	0.246	0.158	0.020	0.915	0.433	0.096	0.009	0.997	0.889	0.685	0.075	0.949	0.564	0.325	0.045	2.315	0.152	104.457 [§]	0.000	-	-	0.127	0.000	0.002	
Cleaved caspase-3	0.779	0.065	0.075	0.015	0.953	0.583	0.044	0.007	0.851	0.243	0.635	0.075	0.973	0.686	0.366	0.044	5.709	0.022	118.274 [#]	0.000	-	-	0.272	0.060	0.024	
Apoptosis rate	0.855	0.254	9.685	1.046	0.838	0.208	6.885	0.815	0.764	0.032	31.270	31.202, 34.765	0.820	0.164	20.705	2.565	-	-	-	-	10.385	0.016	0.308	0.308	0.308	0.308

The Shapiro-Wilk test was used as normality test; ^a control group compared with rhRspo1 group; ^b 1 μ M MP group compared with rhRspo1+1 μ M MP group; ^c control group compared with rhRspo1+1 μ M MP group. Other tests used: [®] Kruskal-Wallis test; [§] least significance difference test (LSD); [#] Tamhane's test. THV – test for homogeneity of variance; ANOVA – analysis of variance; NPT – non-parametric test; SD – standard deviation; P25 – 25th percentile; P75 – 75th percentile; stat. – statistics; MP – methylprednisolone.

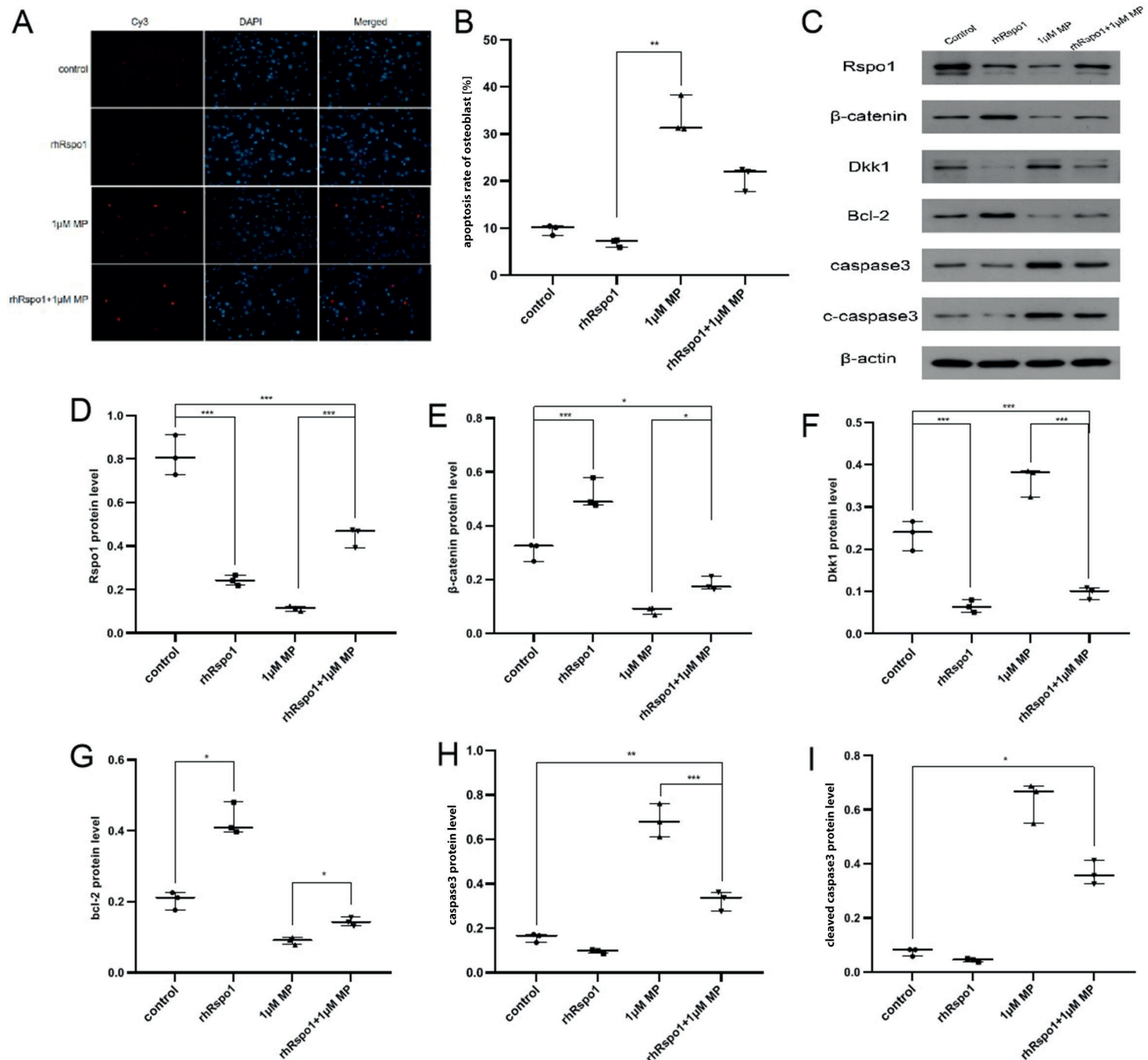


Fig. 5. Apoptosis rate and protein expression in human osteoblast cell line hFOB1.19 (hFOB) treated with R-spondin 1 (Rspo1). A. Photograph of apoptosis obtained using the terminal deoxynucleotidyl transferase dUTP nick end labeling (TUNEL) assay; B. Histogram of apoptosis rate; C. Western blot band of protein expression; D–I. Histogram of protein levels of Rspo1, β -catenin, Dkk-1, Bcl-2, caspase-3, and cleaved caspase-3

* $p < 0.05$; ** $p < 0.01$; *** $p < 0.001$ ($n = 3$ /group). rhRspo1 – recombinant human protein of R-spondin 1; MP – methylprednisolone.

obvious in the 1 μ M MP group. We further showed that shRspo1 had a greater antagonistic effect on the Wnt/ β -catenin pathway. Overexpression of *Rspo1* mRNA only activated the Wnt/ β -catenin pathway inhibited by GC and reduced osteoblast apoptosis. This suggested that GC could also promote osteoblast apoptosis through other signaling pathways or mechanisms, and *Rspo1* could only partially reverse the apoptosis-promoting effect induced by GC through the Wnt/ β -catenin pathway. Although we found that *Rspo1* could reduce GC-induced osteoblast apoptosis via the Wnt/ β -catenin pathway, the exact underlying molecular mechanism needs to be studied further.^{26,27}

We found that rhRspo1 reduced the apoptosis rate of osteoblasts by upregulating the expression of anti-apoptotic factor Bcl-2, and downregulating the expression of pro-apoptotic factors caspase-3 and cleaved caspase-3 through the Wnt/ β -catenin pathway. In addition, rhRspo1 partially antagonized the apoptosis of GC-induced osteoblasts. Whether other members of the Rspo family and other signaling molecules or pathways, as well as vascular endothelial cell apoptosis and microvascular injury, are involved in the pathological process of ANFH needs to be elucidated.^{28,29} In addition, the expression of *Rspo1* in osteoblasts treated with rhRspo1 was significantly decreased, which might be due to the feedback inhibition of exogenous rhRspo1.

Limitations

There are several limitations to this study. First, although GC is one of the causes of LCPD, the animal model of ANFH in immature rabbits was successfully induced using GC, but there is a certain difference between this model and LCPD caused by the disturbance of blood circulation of the epiphysis of the femoral head. Second, the histopathological specimens of the epiphysis of the femoral head cannot be obtained neither when the LCPD is treated operatively nor when the conservative treatment is employed, so the expression of Rspo1 in the femoral head can only be simulated in animal experiments. Third, even though the distribution of the data cannot be convincingly determined for very small samples, the authors assume that the observations come from the normal distribution, and agree that if this assumption is not true, the reported p-values and confidence intervals are unreliable and must be interpreted with caution.

Conclusions

In summary, Rspo1 reduced apoptosis of GC-induced osteoblasts via the Wnt/ β -catenin pathway in ANFH animals. Moreover, rhRspo1 could partially antagonize the apoptosis of GC-induced osteoblasts, thus providing evidence for the pre-clinical use of rhRspo1 to treat LCPD. More in vivo studies are needed to verify the therapeutic effect of rhRspo1 on ANFH.

Supplementary materials

The supplementary materials are available at <https://doi.org/10.5281/zenodo.7485276>. The package contains the following files:

Supplementary Fig. 1. Representative photos of the femoral heads in immature rabbits.

Supplementary Table 1. The original data of the manuscript.

Supplementary Table 2. The results of the ANOVA test.

ORCID iDs

Tianjiu Zhang  <https://orcid.org/0000-0002-3147-2364>

Yifa Ji  <https://orcid.org/0000-0003-1999-9689>

Song Yu  <https://orcid.org/0000-0001-6247-0751>

Nankai Wang  <https://orcid.org/0000-0003-1462-5522>

Qixiao Zhang  <https://orcid.org/0000-0002-0463-4639>

Kaicheng Guo  <https://orcid.org/0000-0001-6650-2458>

References

- Kamiya N, Kim HK. Elevation of proinflammatory cytokine HMGB1 in the synovial fluid of patients with Legg–Calvé–Perthes disease and correlation with IL-6. *JBMR Plus*. 2021;5(2):e10429. doi:10.1002/jbmr.410429
- Ren Y, Deng Z, Gokani V, et al. Anti-interleukin 6 therapy decreases hip synovitis and bone resorption and increases bone formation following ischemic osteonecrosis of the femoral head. *J Bone Miner Res*. 2021;36(2):357–368. doi:10.1002/jbmr.4191
- Johnson CP, Wang L, Tóth F, et al. Quantitative susceptibility mapping detects neovascularization of the epiphyseal cartilage after ischemic injury in a piglet model of Legg–Calvé–Perthes disease. *J Magn Reson Imaging*. 2019;50(1):106–113. doi:10.1002/jmri.26552
- Morris WZ, Liu RW, Chen E, Kim HK. Analysis of trabecular microstructure and vascular distribution of capital femoral epiphysis relevant to Legg–Calvé–Perthes disease. *J Orthop Res*. 2019;37(8):1784–1789. doi:10.1002/jor.24311
- Guan XY, Han D. Role of hypercoagulability in steroid-induced femoral head necrosis in rabbits. *J Orthop Sci*. 2010;15(3):365–370. doi:10.1007/s00776-010-1452-6
- Mulati M, Kobayashi Y, Takahashi A, et al. The long noncoding RNA Crnd regulates osteoblast proliferation through the Wnt/ β -catenin signaling pathway in mice. *Bone*. 2020;130:115076. doi:10.1016/j.bone.2019.115076
- Geng A, Wu T, Cai C, et al. A novel function of R-spondin1 in regulating estrogen receptor expression independent of Wnt/ β -catenin signaling. *eLife*. 2020;9:e56434. doi:10.7554/eLife.56434
- Clevers H, Nusse R. Wnt/ β -catenin signaling and disease. *Cell*. 2012;149(6):1192–1205. doi:10.1016/j.cell.2012.05.012
- Chen M, Han H, Zhou S, Wen Y, Chen L. Morusin induces osteogenic differentiation of bone marrow mesenchymal stem cells by canonical Wnt/ β -catenin pathway and prevents bone loss in an ovariectomized rat model. *Stem Cell Res Ther*. 2021;12(1):173. doi:10.1186/s13287-021-02239-3
- Park S, Cui J, Yu W, Wu L, Carmon KS, Liu QJ. Differential activities and mechanisms of the four R-spondins in potentiating Wnt/ β -catenin signaling. *J Biol Chem*. 2018;293(25):9759–9769. doi:10.1074/jbc.RA118.002743
- Cai C, Yu QC, Jiang W, et al. R-spondin1 is a novel hormone mediator for mammary stem cell self-renewal. *Genes Dev*. 2014;28(20):2205–2218. doi:10.1101/gad.245142.114
- Lacour F, Vezin E, Bentzinger CF, et al. R-spondin1 controls muscle cell fusion through dual regulation of antagonistic Wnt signaling pathways. *Cell Rep*. 2017;18(10):2320–2330. doi:10.1016/j.celrep.2017.02.036
- Lähde M, Heino S, Högström J, et al. Expression of R-spondin 1 in Apc mice suppresses growth of intestinal adenomas by altering Wnt and transforming growth factor beta signaling. *Gastroenterology*. 2021;160(1):245–259. doi:10.1053/j.gastro.2020.09.011
- Shi GX, Zheng XF, Zhu C, et al. Evidence of the role of R-spondin 1 and its receptor Lgr4 in the transmission of mechanical stimuli to biological signals for bone formation. *Int J Mol Sci*. 2017;18(3):564. doi:10.3390/ijms18030564
- Dai Z, Jin Y, Zheng J, et al. MiR-217 promotes cell proliferation and osteogenic differentiation of BMSCs by targeting DKK1 in steroid-associated osteonecrosis. *Biomed Pharmacother*. 2019;109:1112–1119. doi:10.1016/j.biopha.2018.10.166
- Lu W, Kim KA, Liu J, et al. R-spondin1 synergizes with Wnt3A in inducing osteoblast differentiation and osteoprotegerin expression. *FEBS Lett*. 2008;582(5):643–650. doi:10.1016/j.febslet.2008.01.035
- Kim KA, Kakitani M, Zhao J, et al. Mitogenic influence of human R-spondin1 on the intestinal epithelium. *Science*. 2005;309(5738):1256–1259. doi:10.1126/science.1112521
- Chen X, Chen L, Tan J, et al. Rspo1–LGR4 axis in BMSCs protects bone against radiation-induced injury through the mTOR-dependent autophagy pathway. *J Cell Physiol*. 2021;236(6):4273–4289. doi:10.1002/jcp.30051
- Sugano N, Atsumi T, Ohzono K, Kubo T, Hotokebuchi T, Takaoka K. The 2001 revised criteria for diagnosis, classification, and staging of idiopathic osteonecrosis of the femoral head. *J Orthop Sci*. 2002;7(5):601–605. doi:10.1007/s007760200108
- Levin G, Koga BAA, Belchior GG, Carreira ACO, Sogayar MC. Production, purification and characterization of recombinant human R-spondin1 (RSPO1) protein stably expressed in human HEK293 cells. *BMC Biotechnol*. 2020;20(1):5. doi:10.1186/s12896-020-0600-0
- Levin G, Zuber SM, Squillaro AI, Sogayar MC, Grikscheit TC, Carreira ACO. R-spondin 1 (RSPO1) increases mouse intestinal organoid unit size and survival in vitro and improves tissue-engineered small intestine formation in vivo. *Front Bioeng Biotechnol*. 2020;8:476. doi:10.3389/fbioe.2020.00476
- Kerachian MA, Séguin C, Harvey EJ. Glucocorticoids in osteonecrosis of the femoral head: A new understanding of the mechanisms of action. *J Steroid Biochem Mol Biol*. 2009;114(3–5):121–128. doi:10.1016/j.jsbmb.2009.02.007

23. Pavone V, Chisari E, Vescio A, Lizzio C, Sessa G, Testa G. Aetiology of Legg–Calvé–Perthes disease: A systematic review. *World J Orthop.* 2019;10(3):145–165. doi:10.5312/wjo.v10.i3.145
24. Wang H, Brennan TA, Russell E, et al. R-spondin 1 promotes vibration-induced bone formation in mouse models of osteoporosis. *J Mol Med.* 2013;91(12):1421–1429. doi:10.1007/s00109-013-1068-3
25. Sharma AR, Choi BS, Park JM, et al. Rspo 1 promotes osteoblast differentiation via Wnt signaling pathway. *Indian J Biochem Biophys.* 2013;50(1):19–25. PMID:23617070.
26. Gong Y, Yuan S, Sun J, et al. R-spondin 2 induces odontogenic differentiation of dental pulp stem/progenitor cells via regulation of Wnt/ β -catenin signaling. *Front Physiol.* 2020;11:918. doi:10.3389/fphys.2020.00918
27. Sato AY, Cregor M, McAndrews K, et al. Glucocorticoid-induced bone fragility is prevented in female mice by blocking Pyk2/Anoikis signaling. *Endocrinology.* 2019;160(7):1659–1673. doi:10.1210/en.2019-00237
28. Joshi PA, Waterhouse PD, Kannan N, et al. RANK signaling amplifies WNT-responsive mammary progenitors through R-spondin 1. *Stem Cell Rep.* 2015;5(1):31–44. doi:10.1016/j.stemcr.2015.05.012
29. Luo J, Han J, Li Y, Liu Y. Downregulated SOX9 mediated by miR-206 promoted cell apoptosis in Legg–Calvé–Perthes disease. *Oncol Lett.* 2017;15(1):1319–1324. doi:10.3892/ol.2017.7373

Protective effect of basic helix-loop-helix family member e40 on cerebral ischemia/reperfusion injury: Inhibition of apoptosis via repressing the transcription of pleckstrin homology-like domain family A, member 1

Li Sun^{1,A–E}, Guangsheng Gao^{1,A,C,E}, Xingsheng Wang^{2,B–D}, Xinxin Zhang^{2,B–D}, Yun Li^{1,A,E,F}

¹ Department of Critical Medicine, Jinan Central Hospital, Shandong University, China

² Department of Emergency Medicine, Graduate School, Shandong First Medical University & Shandong Academy of Medical Sciences, Jinan, China

A – research concept and design; B – collection and/or assembly of data; C – data analysis and interpretation; D – writing the article; E – critical revision of the article; F – final approval of the article

Advances in Clinical and Experimental Medicine, ISSN 1899–5276 (print), ISSN 2451–2680 (online)

Adv Clin Exp Med. 2023;32(6):655–666

Address for correspondence

Yun Li
E-mail: ylee71799@163.com

Funding sources

None declared

Conflict of interest

None declared

Received on April 25, 2022
Reviewed on September 18, 2022
Accepted on December 1, 2022

Published online on March 7, 2023

Cite as

Li Y, Sun L, Gao G, Wang X, Zhang X. Protective effect of basic helix-loop-helix family member e40 on cerebral ischemia/reperfusion injury: Inhibition of apoptosis via repressing the transcription of pleckstrin homology-like domain family A, member 1. *Adv Clin Exp Med.* 2023;32(6):655–666. doi:10.17219/acem/157071

DOI

10.17219/acem/157071

Copyright

Copyright by Author(s)

This is an article distributed under the terms of the Creative Commons Attribution 3.0 Unported (CC BY 3.0) (<https://creativecommons.org/licenses/by/3.0/>)

Abstract

Background. During ischemic stroke treatment, cerebral ischemia/reperfusion (I/R) injury results in neuronal cell death and neurological dysfunctions in brain. Previous studies indicate that basic helix-loop-helix family member e40 (BHLHE40) exerts protective effects on the pathology of neurodegenerative diseases. However, the protective function of BHLHE40 in I/R is unclear.

Objectives. This study aimed to explore the expression, role and potential mechanism of BHLHE40 after ischemia.

Materials and methods. We established models of I/R injury in rats and of oxygen-glucose deprivation/reoxygenation (OGD/R) in primary hippocampal neurons. Nissl and terminal deoxynucleotidyl transferase dUTP nick end labeling (TUNEL) staining was performed to detect neuronal injury and apoptosis. Immunofluorescence was used to detect BHLHE40 expression. Cell viability and cell damage measurements were conducted using Cell Counting Kit-8 (CCK-8) assay and lactate dehydrogenase (LDH) assay. The regulation of BHLHE40 to pleckstrin homology-like domain family A, member 1 (PHLDA1) was assessed using the dual-luciferase assay and chromatin immunoprecipitation (ChIP) assay.

Results. Cerebral I/R rats exhibited severe neuronal loss and apoptosis in hippocampal cornu Ammonis 1 (CA1) region, accompanied by downregulated BHLHE40 expression at both mRNA and protein levels, indicating that BHLHE40 may regulate the apoptosis of hippocampal neurons. The function of BHLHE40 in neuronal apoptosis during cerebral I/R was further explored by establishing an OGD/R model in vitro. Low expression of BHLHE40 was also observed in neurons treated with OGD/R. The OGD/R administration inhibited cell viability and enhanced cell apoptosis in hippocampal neurons, whereas BHLHE40 overexpression reversed those changes. Mechanistically, we demonstrated that BHLHE40 could repress PHLDA1 transcription by binding to PHLDA1 promoter. The PHLDA1 is a facilitator of neuronal damage in brain I/R injury and its upregulation reversed the effects caused by BHLHE40 overexpression in vitro.

Conclusions. The transcription factor BHLHE40 may protect against brain I/R injury through repressing cell damage via regulating PHLDA1 transcription. Thus, BHLHE40 may be a candidate gene for further study of molecular or therapeutic targets for I/R.

Key words: BHLHE40, PHLDA1, apoptosis, cerebral I/R injury, OGD/R

Background

Ischemic stroke (IS) is a serious disease endangering human health, which can lead to a disturbance in the local blood supply, eventually resulting in severe morbidity and mortality.^{1,2} Angioplasty/stenting, mechanical thrombectomy and pharmacological thrombolysis with tissue membrane activator have been confirmed to be effective interventions for IS.^{3,4} However, most IS patients still suffer from a poor prognosis due to severe neurological dysfunction. Cerebral ischemia/reperfusion (I/R) injury is one of the most prevalent complications of IS, which often occurs during thrombolysis or surgery.⁵ At present, I/R injury is a global health issue, necessitating more research into molecular processes as well as the identification of effective treatment targets.

Previous studies suggest that various neurological illnesses can lead to cognitive dysfunction⁶ and neurogenic inflammation.^{7,8} After I/R, the physiological functions in numerous organs become more vulnerable to oxidative stress, cellular damage and death.^{9,10} The process of programmed cell death (PCD) is essential in the development of the nervous system, and dysregulation of cell-death programs also occurs in ischemic disorders.¹¹ There is mounting evidence that cerebral I/R can activate a variety of cell death pathways, including necrosis, apoptosis and autophagy-associated PCD.^{11–13} One of the best-characterized types of PCD is cell apoptosis, which is considered to be the underlying cause of I/R injury.¹¹ Necroptosis and apoptosis as the 2 regulated cell death mechanisms are involved in mediating the neurologic damage in IS.^{14,15} A systematic literature review concluded that the designated hindrance of apoptosis might be a compelling treatment for different neurodegenerative infections.¹⁶ According to reports, necrostatin-1 played a therapeutic role in ischemic brain injury as a small-molecule inhibitor of necroptosis.¹⁵ Thus, targeted inhibition of pro-apoptotic factors will give a viable remedial methodology to cerebral I/R injury.

BHLHE40, also named DEC1, STRA13 or SHARP2, is a member of the basic helix-loop-helix transcription factor family, and it is reported to involve various biological processes, such as the response to hypoxia, cell differentiation, inflammatory response, and tumorigenesis.^{17–19} It has been linked to a variety of biological processes in cell lines, including the control of the cell cycle and cell death and differentiation.²⁰ The anti-apoptotic role of BHLHE40 was reported in many papers. There is evidence that BHLHE40 is abundantly expressed in different cancers and safeguards against apoptosis by inducing survivin, an anti-apoptotic protein.²¹ In colon carcinoma, BHLHE40 is highly expressed and plays an antagonizing role in serum deprivation-induced apoptosis, along with selectively inhibiting procaspase activation.²² Nevertheless, it is hazy whether BHLHE40 has a role also in neuronal apoptosis brought about by I/R injury. BHLHE40 is expressed

in different tissues and acts as a transcriptional repressor or activator to repress or activate the transcriptional regulation of downstream target genes. For instance, BHLHE40 plays an important role in controlling the mammalian circadian rhythm by inhibiting the CLOCK/BMAL1-actuated promoter.²³ BHLHE40 was able to increase the expression of TAp73 via transcriptional activation of the *TAp73* promoter.²⁴ In addition, BHLHE40 increases the promoter activation of T-box transcription factor Tbx21-mediated *Ifng*.²⁵

Pleckstrin homology-like domain family A, member 1 (PHLDA1), also known as PHRIIP, TDAG51 and DT1P1B11, exerts an important role in different pathologic states.²⁶ The importance of PHLDA1 in the process of apoptosis has been reported in a variety of cancers.^{27,28} In addition, it has been indicated that PHLDA1 inhibition ameliorates I/R induced injury, including myocardial injury and hepatic injury.^{29,30} In addition, the protective role of PHLDA1 knockdown has been described in OGD/R-injured neurons, revealing that PHLDA1 may act as a target for neuroprotective therapy. Based on these findings, we inferred that PHLDA1 might exert a central role in the nervous system.

Objectives

Bioinformatics predicted that BHLHE40 could bind to PHLDA1. On this basis, the study aimed to investigate whether PHLDA1 could serve as a transcriptional target of BHLHE40, and to uncover the protective effects of BHLHE40 on I/R injury. Moreover, the function of PHLDA1 on cell apoptosis was explored in oxygen-glucose deprivation/reoxygenation (OGD/R)-triggered primary hippocampal neurons with overexpressing PHLDA1 and BHLHE40 simultaneously.

Materials and methods

Bioinformatics analysis

JASPAR is an open-access database storing manually curated transcription factors binding profiles as position frequency matrices.³¹ The binding between the transcription factor BHLHE40 and *PHLDA1* promoter was predicted using the JASPAR website (<http://jaspar.genereg.net/>).

Animals

Male rats (Sprague Dawley, 6–8-week-old) were randomly allocated in the sham group and the I/R group. The rats were housed in a 12-hour light/dark cycle, with 45–55% humidity and temperature of 22 ± 1°C, in controlled conditions, with food and water available freely. The 4-vessel occlusion (4-VO) method was used to induce

transient cerebral ischemia. After 1 week of adaptive feeding, electrocautery was used to occlude both vertebral arteries after anesthesia with pentobarbital sodium (50 mg/kg). On the next day, both carotid arteries were ligated using microvascular clips for 10 min to instigate cerebral ischemia. After that, the aneurysm clips were removed for reperfusion and the models were established after 72 h of reperfusion. Then, the rats were sacrificed and the cerebrum tissues were isolated for subsequent investigations. Except that the bilateral common carotid arteries were not occluded, other operations in the sham group were the same as those in the I/R group. All animal procedures were approved by the committee of Jinan Central Hospital, Shandong University (approval No. JNCH2021-6).

Cell culture and lentivirus production

Hippocampal neurons obtained from the brains of newborn rats were dissociated using 0.125% trypsin (Sigma-Aldrich, St. Louis, USA) at 37°C for 15 min. Then, the cells were seeded in plates coated with 0.1 mg/mL of Poly-L-lysine (Solarbio, Beijing, China). The cells were then grown in a neurobasal medium (Gibco, Waltham, USA) containing 2% B-27 and 1% glutamine for 24 h at 37°C in a 5% CO₂ environment. Subsequently, the medium was changed every 3.5 days.

The cells were cultivated in 6-well plates and incubated at 37°C and 5% CO₂ overnight. After that, lentivirus overexpressing BHLHE40 (LV-BHLHE40) vector or containing the control vector (LV-vector) was used to infect hippocampal neurons. Additionally, lentivirus overexpressing PHLDA1 (LV-PHLDA1) vector or its control vector (LV-vector) was used to infect the hippocampal cells. To verify the regulation of BHLHE40 on PHLDA1, the cells were co-infected with LV-BHLHE40 and LV-PHLDA1.

OGD/R application

After a 72-hour lentivirus infection, OGD/R was initiated. Briefly, Dulbecco's modified Eagle's medium (DMEM) was used to replenish neurons and then the cells were placed in an anaerobic chamber filled with 85% nitrogen, 10% hydrogen and 5% CO₂ at 37°C for 4.5 h. A fresh neurobasal medium was supplanted after OGD treatment, and the neurons were then incubated at 37°C/5% CO₂ for 24 h.

Brain water content measurement

The brain was removed from 4-VO-conducted rats, and the wet weight of the brain was measured immediately. After drying in a vacuum oven at 121°C for 24 h, the brains were re-weighed for the dry weight. Finally, the degree of brain edema was calculated as follows: (wet weight – dry weight)/wet weight × 100%.

Nissl staining

Nissl staining was assessed to detect neuronal injury in the cornu Ammonis 1 (CA1) and CA3 regions of the rat hippocampus. Sections were stained with 0.5% cresyl violet for 10 min and differentiated in 0.25% acetic acid in ethanol for a few seconds. Using an optical microscope (model DP73; Olympus Corp., Tokyo, Japan), we captured the pictures at a magnification of ×40 and ×200. The Nissl-positive cells were counted using the ImageJ software (National Institutes of Health, Bethesda, USA), and the quantitative data were expressed as the percent of Nissl-positive cells (%).

TUNEL staining

The sections of neuronal cells or paraffin-embedded brain sections were permeabilized using 0.1% Triton X-100 (Beyotime Biotechnology, Shanghai, China). After that, the sections were stained with terminal deoxynucleotidyl transferase dUTP nick end labeling (TUNEL) fluorescence staining reagents at 37°C in the dark for 60 min, and then stained with DAPI (4',6-diamidino-2-phenylindole; Aladdin, Shanghai, China). Fluorescent images were captured using an optical microscope (model DP73; Olympus Corp.). Quantitative data were expressed as the percent of TUNEL-positive cells (%).

Quantitative real-time polymerase chain reaction (qRT-PCR)

Expressions of BHLHE40 and PHLDA1 mRNA were quantitatively determined with quantitative real-time polymerase chain reaction (qRT-PCR). TRIpure reagent (BioTeke, Wuxi, China) and BeyoRTTM II M-MLV reverse transcriptase (Beyotime Biotechnology) were used to isolate total RNA and synthesize cDNA respectively. For the conduction of qRT-PCR, SYBR Green (Solarbio) was used, and the data obtained from the system was determined by calculating the $2^{-\Delta\Delta CT}$ relative fold change. The mRNA levels of BHLHE40 and PHLDA1 were normalized to β -actin. The primer sequences were as follows (5'-3'): BHLHE40 F: AGCGAGGACAGCAAGGA; BHLHE40 R: CCAAGTGACCCAAAGTAGTAAG; PHLDA1 F: ACAGCCGAACCGTCCCA; PHLDA1 R: TTTGCCCTCCGCCATCA.

Western blot

Whole-cell lysates were collected in the lysis buffer and the BCA method (Beyotime Biotechnology) was used to determine the protein concentration. Then, we subjected equal amounts of protein to sodium dodecyl sulfate-polyacrylamide gel electrophoresis (SDS-PAGE) and transferred them to polyvinylidene difluoride (PVDF) membranes. Subsequently, the membrane was incubated

with specific primary antibodies (BHLHE40 (Abclonal, Wuhan, China); PHLDA1 (Affinity Biosciences, Changzhou, China); caspase-3 (Cell Signaling Technology (CST), Danvers, USA); cleaved caspase-3 (CST); Bcl-2 (Abclonal); PARP (CST); cleaved PARP (CST); BAX (Affinity); and β -actin (Beyotime Biotechnology)) at 4°C overnight and subsequently incubated with secondary antibodies (Beyotime Biotechnology) at 37°C for 1 h. The quantitative densitometric values of the proteins were normalized to that of β -actin.

Immunofluorescence

For double immunofluorescence, paraffin-embedded hippocampus sections (5 μ m) were incubated at 60°C in an oven for 2 h, followed by dewaxing and dehydrating. The sections were incubated with primary against BHLHE40 (Rabbit; Abclonal) and NeuN (Mouse; Abcam, Cambridge, UK) antibodies at 4°C overnight. Then, the sections were incubated with the secondary antibody conjugated to fluorescein isothiocyanate (FITC)-labeled goat anti-rabbit immunoglobulin G (IgG; Abcam) and cyanine 3 (Cy3)-labeled goat anti-mouse IgG (Invitrogen, Carlsbad, USA) at 37°C for 1 h. Phosphate-buffered saline (PBS) containing 0.1% Triton X-100 was used to permeabilize the fixed cells for 30 min at room temperature. The cells were incubated successively with the BHLHE40 antibody and the secondary antibody against FITC-labeled goat IgG. The number of BHLHE40-positive cells and BHLHE40/NeuN double-positive cells were counted at $\times 400$ magnification using ImageJ software.

CCK-8

A CCK-8 Cell Proliferation Detection Kit (KeyGen Biotech, Nanjing, China) was used to determine cell viability. Briefly, CCK-8 solution (10 μ L) was added and incubated at 37°C for 2 h with 3×10^3 cells seeded into 96-well culture plates. A microplate reader (Biotek, Winooski, USA) was used to measure the optical density (OD) at 450 nm.

Lactate dehydrogenase assay

The lactate dehydrogenase (LDH) assay kit (Jiancheng Bioengineering Institute, Nanjing, China) was used to detect cell damage. The LDH activity was determined by measuring the absorbance at 450 nm.

Dual-luciferase assay

To generate *PHLDA1* promoter-luciferase construct, a fragment of *PHLDA1* promoter from -1956 bp to +12 bp was amplified with PCR and cloned to pGL3 vectors. Then the pGL3 vectors were transfected with BHLHE40 overexpression (OE-BHLHE40) or control vectors (OE-vector) into the hippocampal cells using Lipofectamine 3000

(Invitrogen) according to the manufacturer's instruction. An assay kit (KeyGen Biotech) for determining luciferase activity was utilized in cells 48 h after transfection.

Chromatin immunoprecipitation assay

Chromatin immunoprecipitation (ChIP) assay was carried out using a cell chip kit (Wanleibio, Shenyang, China) according to the manufacturer's instructions. In brief, neurons were cross-linked to fix the DNA/protein complexes containing 1% formaldehyde for 10 min at ambient temperature. Glycine was added at a final concentration of 0.125 M to terminate the reaction. At 4°C, cell lysate was sonicated for 2 min, and the samples were mixed with precleared protein A/G beads for 2 h. Then, the supernatant fraction was incubated with the BHLHE40 antibody and normal IgG overnight at 4°C. After releasing the crosslink, purified DNA was subjected to PCR and analyzed using agarose gel electrophoresis. The primer sequences were as follows (5'-3'): chip *PHLDA1* F: GGGGAAAGGGAATAACA; chip *PHLDA1* R: GTCTCGGTCAAACAAGG.

Statistical analyses

Statistical significance was determined using GraphPad Prism v. 8.0 (GraphPad Software, San Diego, USA). The normality of distribution of all data was checked with D'Agostino–Pearson omnibus test. A value of $p < 0.05$ was deemed significant.

For data in 2 groups, the homogeneity of variance was examined with F test. If data complied with the normal distribution and had equal variance, p -values were calculated using unpaired t -test; if not, p -values were determined using Mann–Whitney U test.

For data from multiple groups, the homogeneity of variance was examined using Brown–Forsythe test. If data were in normal distribution and had unequal variances, p -values were calculated with one-way analysis of variance (ANOVA) followed by Tukey's post-test; if not, p -values were determined using Kruskal–Wallis test followed by Dunn's post-test.

Results

BHLHE40 is downregulated in rats undergoing cerebral I/R injury

Our study investigated the role of BHLHE40 by creating a model of brain I/R injury on rats, and we discovered that the brain water content was significantly increased in the ischemic rats compared with the control rats (Fig. 1A). The results of Nissl staining indicated that the neurons were changed after ischemia, which presented neuronal cell loss and karyopyknosis in the CA1 region

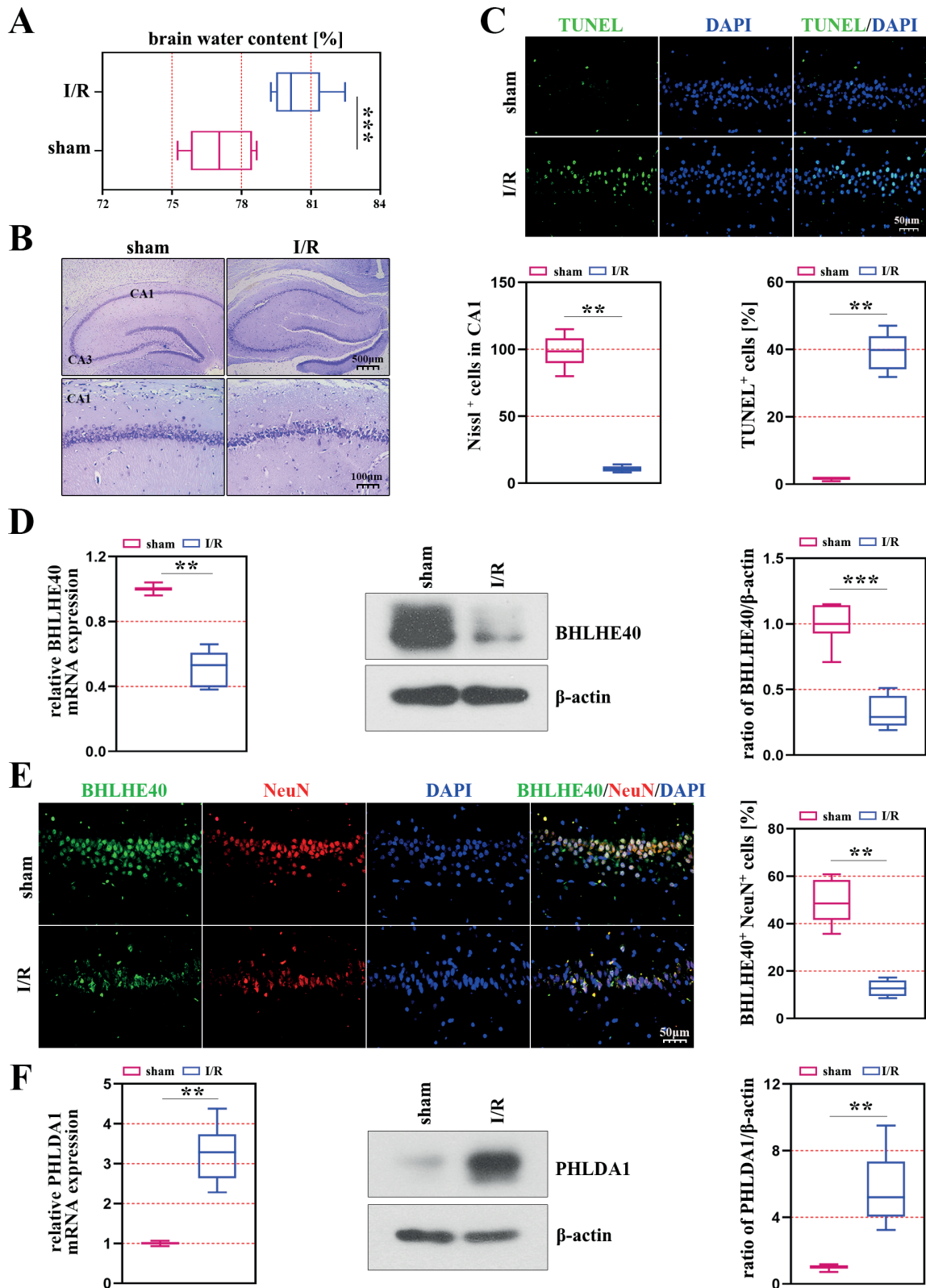


Fig. 1. The expression of BHLHE40 in the brain tissues of rats with cerebral ischemia/reperfusion (I/R) injury. The 4-vessel occlusion (4-VO) rat models were established for the following experiments. **A.** Based on wet-to-dry weight ratios, the amount of water in the brain was determined; **B.** Nissl staining was used to detect neuronal damage in the hippocampus; **C.** The apoptosis in the cornu Ammonis 1 (CA1) region of the hippocampus was detected using TUNEL staining. The Nissl-positive cells and the ratio of TUNEL-positive cells were quantified; **D.** In the hippocampal tissues, the mRNA and protein levels of BHLHE40 were measured using quantitative real-time polymerase chain reaction (qRT-PCR) and western blot, respectively. The level of BHLHE40 (normalized to β-actin) was quantified; **E.** The cells were immunofluorescently analyzed with BHLHE40 (green) and NeuN (red), and fluorescein-labeled (blue) with DAPI. The panel presents the quantification of BHLHE40-positive cells and NeuN-positive cells. **(F)** The expression of PHLDA1 was detected, and the level of PHLDA1 (normalized to β-actin) was quantified

*** $p < 0.001$.

of rats (Fig. 1B). The number of apoptotic cells was increased in the ischemic models compared with the sham group ($p < 0.001$, Fig. 1C). We found that the mRNA and protein levels of BHLHE40 had a notable decrease in rats induced with induced I/R (Fig. 1D). The results of immunofluorescence staining suggested that BHLHE40 colocalized with NeuN (a neuronal marker), and positive cells of BHLHE40 and NeuN were decreased in the CA1 region of the hippocampus after I/R injury ($p < 0.001$, Fig. 1E). As shown in Fig. 1F, the transcriptional and protein levels of PHLDA1 were markedly increased in rats induced with induced I/R.

BHLHE40 overexpression ameliorates cell damage in OGD/R-induced neurons

Using neuronal cells subjected to OGD/R, we analyzed cell damage and apoptosis to determine the role of BHLHE40 in brain I/R injury. The efficiency of lentivirus infection was verified using qRT-PCR and western blot assays (Fig. 2A). The results showed that the mRNA and protein levels of PHLDA1 were decreased after BHLHE40 overexpression (Fig. 2B). Figure 2C shows that OGD/R treatment downregulated BHLHE40 expression, while BHLHE40 overexpression significantly elevated its expression in OGD/R-induced neurons (Fig. 2C). As shown in Fig. 2D,E, the OGD/R-induced cells activated the cell viability and inhibited the LDH activity after BHLHE40 overexpression. Immunofluorescence staining showed decreased BHLHE40-positive cells in the OGD/R group (Fig. 2F).

BHLHE40 overexpression ameliorates apoptosis in OGD/R-induced neurons

The ratio of TUNEL-positive cells was significantly increased after OGD/R administration, whereas BHLHE40 overexpression inhibited the effects (Fig. 3A). The western blot analysis indicated that the protein levels of cleaved caspase-3 and cleaved PARP were markedly decreased in OGD/R-induced cells with BHLHE40 overexpression, while the levels of caspase-3 and PARP did not change (Fig. 3B – upper section). In addition, the results showed that BAX was downregulated in the presence of BHLHE40 overexpression, which enhanced the protein content of Bcl-2 (Fig. 3B – lower section).

Transcriptional regulatory effects of BHLHE40 on PHLDA1

To clarify the association between BHLHE40 and PHLDA1 in neuronal injury after OGD/R treatment, we identified PHLDA1 expression after BHLHE40 upregulation. The results of qRT-PCR and western blot assays showed that PHLDA1 expression was negatively regulated by BHLHE40 (Fig. 4A). Then, a luciferase assay was

performed using a plasmid constructed with the *PHLDA1* promoter linked to a luciferase reporter gene, and it showed that BHLHE40 repressed the luciferase activity of the *PHLDA1* promoter (Fig. 4B). Furthermore, ChIP experiments demonstrated that *PHLDA1* was the target gene of BHLHE40 (Fig. 4C).

BHLHE40 overexpression inhibits cell apoptosis of OGD/R-induced cells through controlling PHLDA1

To verify the mechanism of BHLHE40 through regulating PHLDA1 in I/R injury, the hippocampal neurons were co-infected with LV-BHLHE40 and LV-PHLDA1, and subjected to OGD/R treatment. The mRNA and protein levels of PHLDA1 verified the efficiency of lentivirus infection (Fig. 5A). As shown in Fig. 5B, the enhanced cell viability caused by BHLHE40 upregulation was inhibited in the presence of PHLDA1 overexpression. The anti-apoptotic role of BHLHE40 in OGD/R-induced neurons was observed using the TUNEL staining, whereas the ratio of TUNEL-positive cells was increased after PHLDA1 overexpression (Fig. 5C). We discovered that the inhibiting effect of BHLHE40 overexpression on PHLDA1 expression was reversed by PHLDA1 upregulation in neurons subjected to OGD/R (Fig. 5D).

Discussion

This study found that BHLHE40 was downregulated in ischemia rats and primary neurons following OGD/R treatment. To systematically identify the function of BHLHE40 in brain I/R injury, cell damage and apoptosis were measured in BHLHE40-overexpressed neurons. In vitro experiments further confirmed the direct transcriptional regulation of PHLDA1 by BHLHE40. Furthermore, BHLHE40 overexpression shielded neurons from damage from brain I/R via inhibiting PHLDA1.

It is well known that neuronal apoptosis can shape the developing brain,¹⁶ and dysregulation of apoptosis is reported to be related to the progression of neurodegenerative illnesses and chronic diseases such as ischemic stroke.³² We found that increased ratio of TUNEL-labeled cells was observed in the hippocampal CA1 region of ischemia rats, and the neurons presented karyopyknosis. Several proteins are involved in mammalian apoptosis, including genes encoding Bcl-2, the adaptor protein Apaf-1, and cysteine protease caspases.¹⁶ A series of morphological and histochemical changes occur after apoptosis, and they are mainly the result of the activation of cellular suicide cysteine proteases – the caspases.^{33,34} These enzymes subsequently participate in a cascade when pro-apoptotic signals are activated.³³ Moreover, studies have indicated that the activity of Bcl-2 family gene products is involved in cellular and neurological processes in ischemic brain

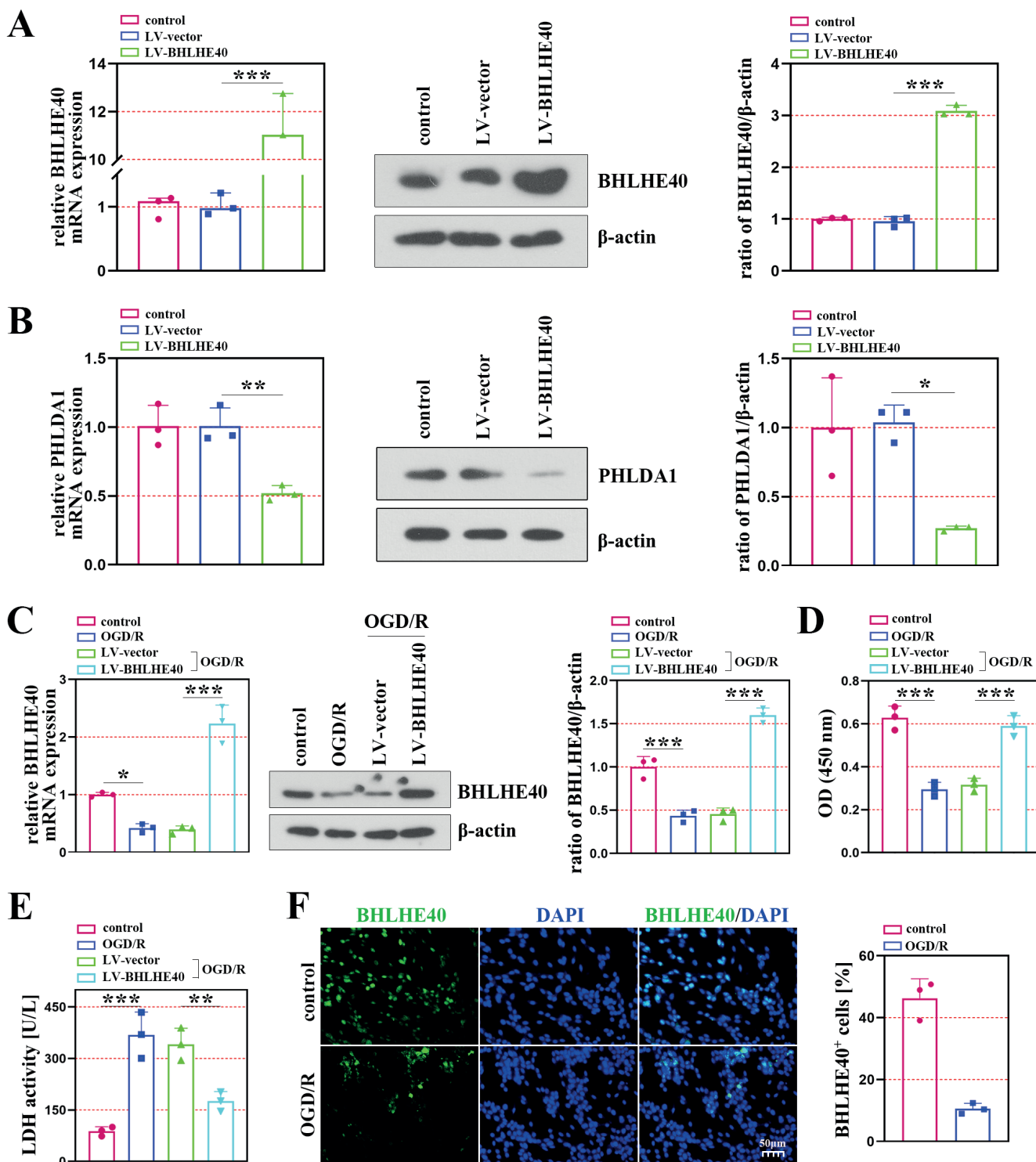


Fig. 2. Effects of BHLHE40 on cell damage in primary hippocampal neurons subject to oxygen-glucose-deprivation/reperfusion (OGD/R) injury. A,B. The expression of BHLHE40 and PHLDA1 in hippocampal neurons was measured, and their levels were quantified by normalizing to β-actin; C. The mRNA and protein levels of BHLHE40 were detected in OGD/R-induced cells, and the BHLHE40 level was quantified by normalizing to β-actin. D. Cell viability was detected with Cell Counting Kit-8 (CCK-8) assay; E. Quantification of cell injury was measured with lactate dehydrogenase (LDH) activity; F. The expression of BHLHE40 visualized with immunofluorescence staining, and the quantification of BHLHE40-positive cells

** p < 0.01; *** p < 0.001.

injury.³⁵ Consistently, our study discovered that the expression of Bcl-2 was downregulated in OGD/R-induced neurons. In addition, BAX, a pro-apoptotic member of the Bcl-2 family, is required for neuronal death,³⁶ and

PARP-1 activity is suppressed by Bcl-2 directly.³⁷ Previous study suggests that amantadine and topiramate can improve I/R injury by reducing apoptosis.³⁸ We found that the protein accumulation of cleaved caspase-3, cleaved

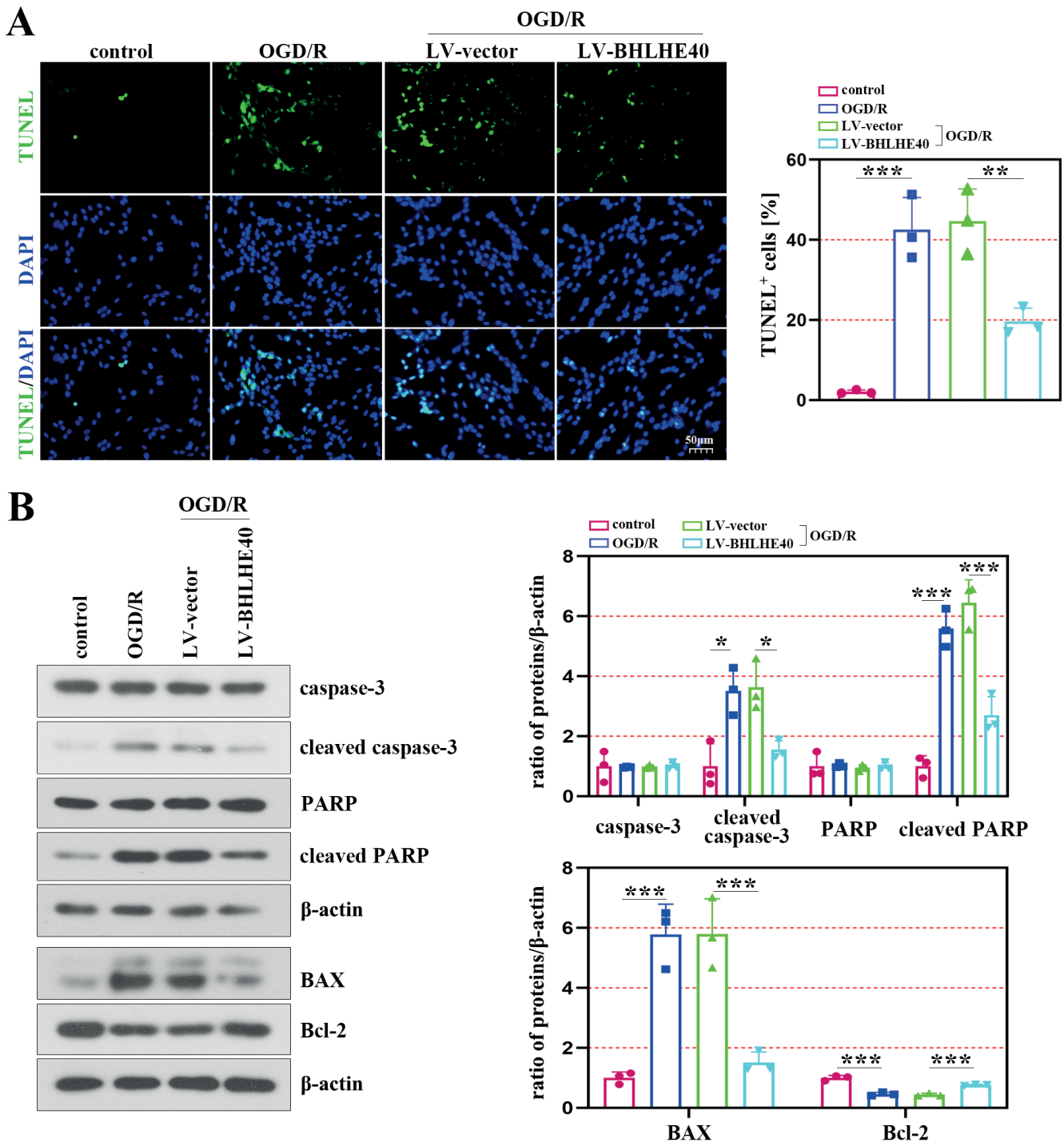


Fig. 3. Effects of BHLHE40 on apoptosis in oxygen-glucose deprivation/reoxygenation (OGD/R)-induced hippocampal neurons. A. TUNEL staining was used to detect cell apoptosis, and the ratio of TUNEL-positive cells was quantified; B. Western blot analysis for caspase-3, cleaved caspase-3, PARP, cleaved PARP, BAX, and Bcl-2, whose levels were quantified by normalizing to β -actin

* $p < 0.05$; ** $p < 0.01$; *** $p < 0.001$.

PARP and BAX was enhanced in OGD/R-induced neurons, while BHLHE40 overexpression reduced the protein amount, indicating that BHLHE40 exerted an anti-apoptotic role in I/R injury.

In addition to cellular damage, patients with brain damage present cognitive dysfunction³⁹; thus, it is imperative to develop new techniques and therapeutic schedules.

Accumulating evidence indicates that BHLHE40 exerts protective effects in different diseases. This was exemplified in the paper by Huynh et al., which reported that BHLHE40 was an essential repressor of cytokine IL-10 during *Mycobacterium tuberculosis* infection.⁴⁰ In human hepatocellular carcinoma HepG2 cells, BHLHE40 upregulation partially antagonized apoptosis after

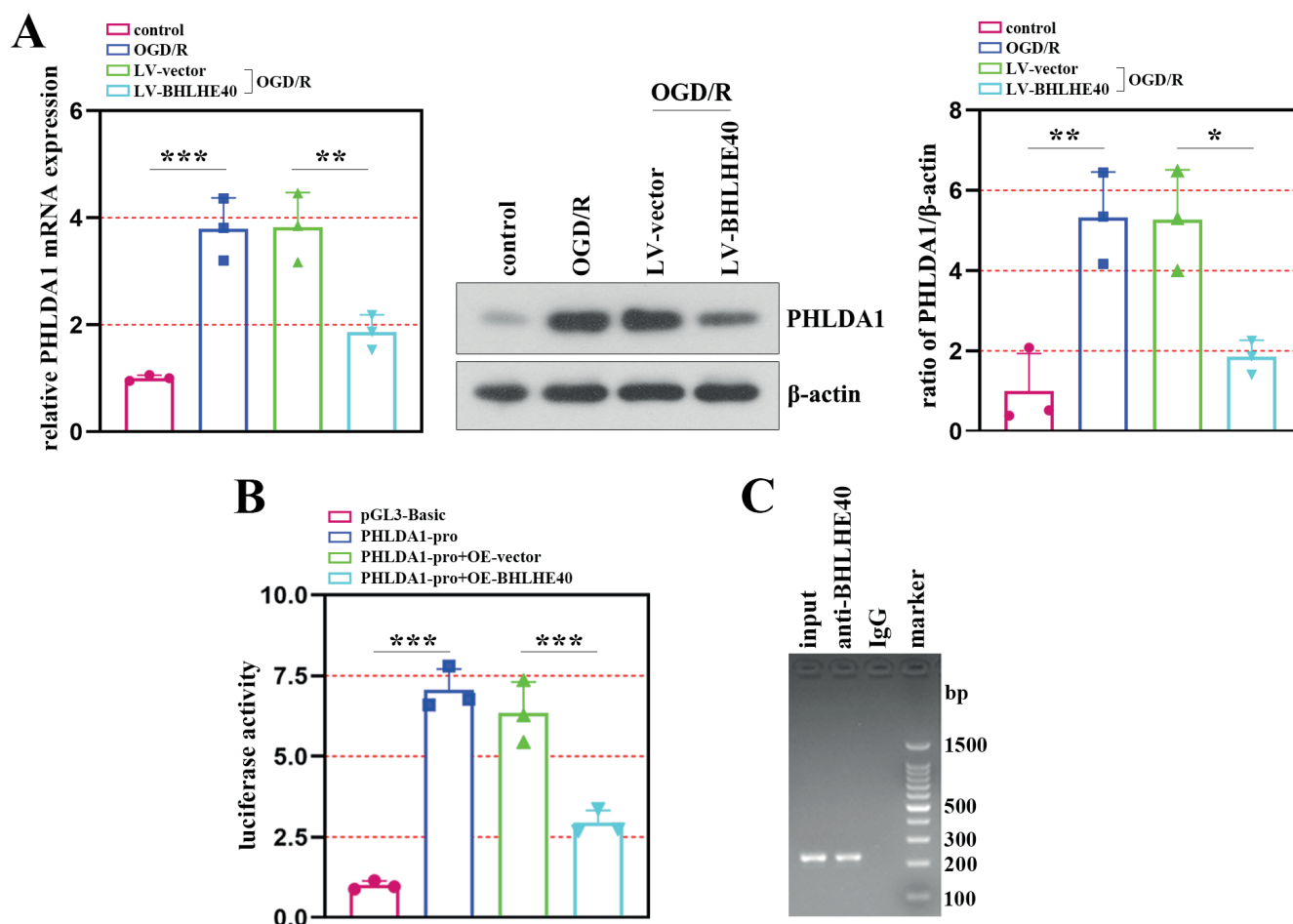


Fig. 4. Direct transcriptional regulation of PHLDA1 by BHLHE40. A. In oxygen-glucose deprivation/reoxygenation (OGD/R)-induced cells, the mRNA and protein levels of *PHLDA1* were detected after BHLHE40 overexpression. *PHLDA1* level was quantified by normalizing to β -actin; B. The relative luciferase activity of *PHLDA1* promoter in the neuronal cells; C. Chromatin immunoprecipitation (ChIP) assay using the antibody against BHLHE40 was performed in neurons

** $p < 0.01$; *** $p < 0.001$.

8-methoxypsoralen treatment and decreased the activation of caspase-3.⁴¹ Hamilton et al. found that mice lacking BHLHE40 displayed increased neuronal excitability and poorer synaptic plasticity in the hippocampal area.⁴² Similarly, our study confirmed the effects of BHLHE40 in neuroprotection, which was evidenced by the decreased protein amounts of apoptosis-related factors and cell apoptosis after BHLHE40 overexpression in neuronal cells with OGD/R treatment. In addition to the role of anti-apoptotic factor, BHLHE40 also ameliorated cell damage (according to the data from the detection of LDH activity). It was reported that BHLHE40 overexpression alleviated MPP⁺-induced neurotoxicity in Parkinson’s disease, whereas BHLHE40 silencing aggravated the symptom,⁴³ which was consistent with our work.

The most critical function of BHLHE40 is as a transcription factor to regulate the expression of downstream target genes. A few molecules have been detailed to be included within the metastasis controlled transcriptionally by BHLHE40. Studies indicate that BHLHE40 plays a pro-survival and pro-metastatic role in breast cancer cells by activating the transcription of heparin-binding

epidermal growth factor.¹⁷ Beyond that, a report by Kanda et al. suggested that BHLHE40 increased the promoter activation of T-box transcription factor Tbx21-mediated *Irfng*.²⁵ Hereon, *PHLDA1* was revealed to be repressed transcriptionally by BHLHE40, and functional investigation found that BHLHE40 overexpression inhibited cell apoptosis of OGD/R-induced cells via controlling *PHLDA1*. It is of pivotal importance to investigate the mechanism of BHLHE40 in ischemic injury.

PHLDA1, first identified by Park et al, was reported to fulfill an essential role in the induction of apoptosis in mouse T-cell hybridomas.⁴⁴ In previous studies, *PHLDA1* was markedly expressed in oxidative stress-induced cardiomyocyte and myocardial I/R wounds, and its upregulation in cardiomyocytes exacerbated oxidative stress-induced cardiomyocyte injury.²⁹ In addition, other work has shown that *PHLDA1* deficiency protects against OGD/R injury, which makes it one of the new targets for treating cerebral injury.⁴⁵ Consistently, in the study, the data showed that *PHLDA1* was upregulated in the hippocampal neurons exposed to OGD/R, and *PHLDA1* overexpression inhibited the cell viability and promoted the cell apoptosis caused

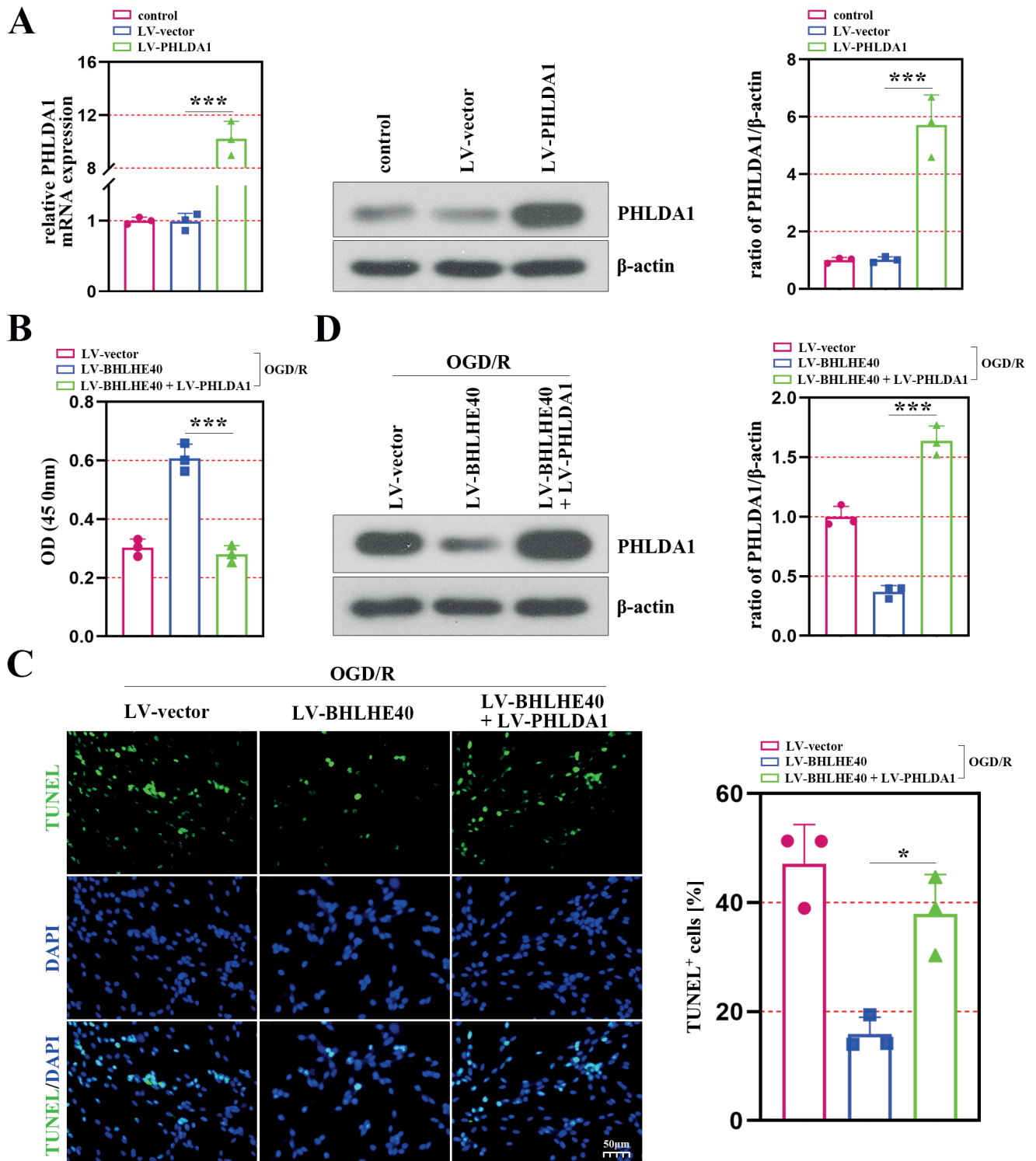


Fig. 5. BHLHE40 inhibits cell damage and apoptosis in oxygen-glucose deprivation/reoxygenation (OGD/R)-induced cells by controlling PHLDA1. A. The expression of PHLDA1 in neurons was verified, and the PHLDA1 level was quantified by normalizing to β -actin. Primary hippocampal neurons co-infected with BHLHE40 and PHLDA1 overexpressing lentiviral vectors were treated with OGD/R, and the cells were utilized for the following experiments; B. Cell viability was detected using Cell Counting Kit-8 (CCK-8) assay; C. TUNEL staining was used to detect cell apoptosis, and the ratio of TUNEL-positive cells was quantified; D. Western blot analysis for PHLDA1 in OGD-induced cells after overexpressing BHLHE40 and PHLDA1. The level of PHLDA1 (normalized to β -actin) was quantified

* $p < 0.05$; *** $p < 0.001$.

by BHLHE40 upregulation. Further studies showed that *PHLDA1* was the target gene of BHLHE40, and BHLHE40 overexpression inhibited cell damage through controlling

PHLDA1. The regulation between BHLHE40 and *PHLDA1* might provide a novel direction for the development of neuroprotective therapy. The cardiac autonomic dynamics

reported by Battaglia et al. provide a new understanding of the nervous system.⁴⁶ There is growing evidence for the protective role of neuropsychiatric disorders,^{47,48} which provides theoretical and clinical implications. Moreover, many new applications for psychiatric and neurological disorders have been reported, including non-invasive stimulation techniques^{49,50} and prognostic biomarkers.⁵¹ Whether these applications can treat cerebral I/R injury remains to be explored in future studies.

Limitations

Some limitations of the present study should be recognized. First, although we provide potential therapeutic directions for clinical treatment, there is still no evidence to prove whether our results apply to humans. Moreover, the neurons were not treated with OGD/R under different conditions, so the optimal time for the establishment of the cell model was not obtained. The statistical analysis was exploratory, and the Bonferroni correction was not applied.

Even though the distribution of the data cannot be convincingly determined for very small samples, we assume that the observations come from the normal distribution. We agree that if this assumption is not true, the reported p-values and confidence intervals are unreliable and must be interpreted with caution. The nonparametric tests only indicated significant differences between groups in Fig. 2A (BHLHE40 protein expression), Fig. 2C (BHLHE40 mRNA expression) and 5A,B (PHLDA1 protein expression).

Conclusions

In summary, neuronal loss and apoptosis were found in the hippocampal CA1 region of cerebral I/R rats, and the results suggested that BHLHE40 and PHLDA1 were respectively downregulated and upregulated in rat brains after cerebral I/R. Functional analysis suggested that BHLHE40 suppressed neuronal apoptosis and cell death, as well as increased cell viability in OGD/R-induced cells. Mechanistic analysis reveals that BHLHE40 could decrease the expression of PHLDA1 through transcriptional inhibition of the *PHLDA1* promoter, demonstrating that PHLDA1 serves as a transcriptional target of BHLHE40. These findings indicate that BHLHE40 protected against I/R damage by inhibiting PHLDA1. It is plausible that BHLHE40 may be an effective therapeutic option for cerebral I/R injury.

ORCID iDs

Li Sun  <https://orcid.org/0000-0003-4629-4983>
 Guangsheng Gao  <https://orcid.org/0000-0002-0514-6346>
 Xingsheng Wang  <https://orcid.org/0000-0002-8844-3847>
 Xinxin Zhang  <https://orcid.org/0000-0003-1748-4219>
 Yun Li  <https://orcid.org/0000-0001-6335-1164>

References

- Campbell BCV, De Silva DA, Macleod MR, et al. Ischaemic stroke. *Nat Rev Dis Primers*. 2019;5(1):70. doi:10.1038/s41572-019-0118-8
- Turner RC, Dodson SC, Rosen CL, Huber JD. The science of cerebral ischemia and the quest for neuroprotection. Navigating past failure to future success: A review. *J Neurosurg*. 2013;118(5):1072–1085. doi:10.3171/2012.11.JNS12408
- Kondziella D, Cortsen M, Eskesen V, et al. Update on acute endovascular and surgical stroke treatment. *Acta Neurol Scand*. 2013;127(1):1–9. doi:10.1111/j.1600-0404.2012.01702.x
- Chamorro A, Dirnagl U, Urra X, Planas AM. Neuroprotection in acute stroke: Targeting excitotoxicity, oxidative and nitrosative stress, and inflammation. *Lancet Neurol*. 2016;15(8):869–881. doi:10.1016/S1474-4422(16)00114-9
- Xu J, Kong X, Xiu H, Dou Y, Wu Z, Sun P. Combination of curcumin and vagus nerve stimulation attenuates cerebral ischemia/reperfusion injury-induced behavioral deficits. *Biomed Pharmacother*. 2018;103:614–620. doi:10.1016/j.biopha.2018.04.069
- Martos D, Tuka B, Tanaka M, Vécsei L, Telegdy G. Memory enhancement with kynurenic acid and its mechanisms in neurotransmission. *Biomedicines*. 2022;10(4):849. doi:10.3390/biomedicines10040849
- Spekker E, Tanaka M, Szabó Á, Vécsei L. Neurogenic inflammation: The participant in migraine and recent advancements in translational research. *Biomedicines*. 2021;10(1):76. doi:10.3390/biomedicines10010076
- Tanaka M, Tóth F, Polyák H, Szabó Á, Mándi Y, Vécsei L. Immune influencers in action: Metabolites and enzymes of the tryptophan-kynurenine metabolic pathway. *Biomedicines*. 2021;9(7):734. doi:10.3390/biomedicines9070734
- Yan HF, Tuo QZ, Yin QZ, Lei P. The pathological role of ferroptosis in ischemia/reperfusion-related injury. *Zool Res*. 2020;41(3):220–230. doi:10.24272/j.issn.2095-8137.2020.042
- Ma D, Qiao J, Qu Q, He F, Chen W, Yu B. Weighted gene co-expression network analysis to investigate the key genes implicated in global brain ischemia/reperfusion injury in rats. *Adv Clin Exp Med*. 2020;29(6):649–659. doi:10.17219/acem/121918
- Bredesen DE, Rao RV, Mehlen P. Cell death in the nervous system. *Nature*. 2006;443(7113):796–802. doi:10.1038/nature05293
- Zille M, Farr TD, Przesdzin I, et al. Visualizing cell death in experimental focal cerebral ischemia: Promises, problems and perspectives. *J Cereb Blood Flow Metab*. 2012;32(2):213–231. doi:10.1038/jcbfm.2011.150
- Qin AP, Liu CF, Qin YY, et al. Autophagy was activated in injured astrocytes and mildly decreased cell survival following glucose and oxygen deprivation and focal cerebral ischemia. *Autophagy*. 2010;6(6):738–753. doi:10.4161/auto.6.6.12573
- Naito MG, Xu D, Amin P, et al. Sequential activation of necroptosis and apoptosis cooperates to mediate vascular and neural pathology in stroke. *Proc Natl Acad Sci U S A*. 2020;117(9):4959–4970. doi:10.1073/pnas.1916427117
- Degterev A, Huang Z, Boyce M, et al. Chemical inhibitor of nonapoptotic cell death with therapeutic potential for ischemic brain injury. *Nat Chem Biol*. 2005;1(2):112–119. doi:10.1038/nchembio711
- Yuan J, Yankner BA. Apoptosis in the nervous system. *Nature*. 2000;407(6805):802–809. doi:10.1038/35037739
- Sethuraman A, Brown M, Krutilina R, et al. BHLHE40 confers a pro-survival and pro-metastatic phenotype to breast cancer cells by modulating HBEGF secretion. *Breast Cancer Res*. 2018;20(1):117. doi:10.1186/s13058-018-1046-3
- Tian J, Wu J, Chen X, et al. BHLHE40, a third transcription factor required for insulin induction of SREBP-1c mRNA in rodent liver. *eLife*. 2018;7:e36826. doi:10.7554/eLife.36826
- Yu F, Sharma S, Jankovic D, et al. The transcription factor Bhlhe40 is a switch of inflammatory versus anti-inflammatory Th1 cell fate determination. *J Exp Med*. 2018;215(7):1813–1821. doi:10.1084/jem.20170155
- Ow JR, Tan YH, Jin Y, Bahirvani AG, Taneja R. Stra13 and Sharp-1, the non-Grouchy regulators of development and disease. *Curr Top Dev Biol*. 2014;110:317–338. doi:10.1016/B978-0-12-405943-6.00009-9
- Li Y, Xie M, Yang J, et al. The expression of antiapoptotic protein survivin is transcriptionally upregulated by DEC1 primarily through multiple sp1 binding sites in the proximal promoter. *Oncogene*. 2006;25(23):3296–3306. doi:10.1038/sj.onc.1209363

22. Li Y, Zhang H, Xie M, et al. Abundant expression of Dec1/stra13/sharp2 in colon carcinoma: Its antagonizing role in serum deprivation-induced apoptosis and selective inhibition of procaspase activation. *Biochem J*. 2002;367(2):413–422. doi:10.1042/bj20020514
23. Sato F, Kawamoto T, Fujimoto K, et al. Functional analysis of the basic helix-loop-helix transcription factor DEC1 in circadian regulation: Interaction with BMAL1. *Eur J Biochem*. 2004;271(22):4409–4419. doi:10.1111/j.1432-1033.2004.04379.x
24. Qian Y, Zhang J, Jung YS, Chen X. DEC1 coordinates with HDAC8 to differentially regulate TAp73 and Δ Np73 expression. *PLoS One*. 2014;9(1):e84015. doi:10.1371/journal.pone.0084015
25. Kanda M, Yamanaka H, Kojo S, et al. Transcriptional regulator Bhlhe40 works as a cofactor of T-bet in the regulation of IFN- γ production in iNKT cells. *Proc Natl Acad Sci U S A*. 2016;113(24):E3394–E3402. doi:10.1073/pnas.1604178113
26. Nagai MA. Pleckstrin homology-like domain, family A, member 1 (PHLDA1) and cancer. *Biomed Rep*. 2016;4(3):275–281. doi:10.3892/br.2016.580
27. Xu J, Bi G, Luo Q, et al. PHLDA1 modulates the endoplasmic reticulum stress response and is required for resistance to oxidative stress-induced cell death in human ovarian cancer cells. *J Cancer*. 2021;12(18):5486–5493. doi:10.7150/jca.45262
28. Murata T, Sato T, Kamoda T, Moriyama H, Kumazawa Y, Hanada N. Differential susceptibility to hydrogen sulfide-induced apoptosis between PHLDA1-overexpressing oral cancer cell lines and oral keratinocytes: Role of PHLDA1 as an apoptosis suppressor. *Exp Cell Res*. 2014;320(2):247–257. doi:10.1016/j.yexcr.2013.10.023
29. Guo Y, Jia P, Chen Y, et al. PHLDA1 is a new therapeutic target of oxidative stress and ischemia reperfusion-induced myocardial injury. *Life Sci*. 2020;245:117347. doi:10.1016/j.lfs.2020.117347
30. Luo YH, Huang ZT, Zong KZ, et al. miR-194 ameliorates hepatic ischemia/reperfusion injury via targeting PHLDA1 in a TRAF6-dependent manner. *Int Immunopharmacol*. 2021;96:107604. doi:10.1016/j.intimp.2021.107604
31. Fornes O, Castro-Mondragon JA, Khan A, et al. JASPAR 2020: Update of the open-access database of transcription factor binding profiles. *Nucleic Acids Res*. 2019;48(D1):D87–D92. doi:10.1093/nar/gkz1001
32. Fricker M, Tolkovsky AM, Borutaite V, Coleman M, Brown GC. Neuronal cell death. *Physiol Rev*. 2018;98(2):813–880. doi:10.1152/physrev.00011.2017
33. Thornberry NA, Lazebnik Y. Caspases: Enemies within. *Science*. 1998;281(5381):1312–1316. doi:10.1126/science.281.5381.1312
34. Yuan J. The *C. elegans* cell death gene *ced-3* encodes a protein similar to mammalian interleukin-1 β -converting enzyme. *Cell*. 1993;75(4):641–652. doi:10.1016/0092-8674(93)90485-9
35. Graham SH, Chen J, Clark RSB. Bcl-2 family gene products in cerebral ischemia and traumatic brain injury. *J Neurotrauma*. 2000;17(10):831–841. doi:10.1089/neu.2000.17.831
36. Deckwerth TL, Elliott JL, Knudson CM, Johnson EM, Snider WD, Korsmeyer SJ. BAX is required for neuronal death after trophic factor deprivation and during development. *Neuron*. 1996;17(3):401–411. doi:10.1016/S0896-6273(00)80173-7
37. Dutta C, Day T, Kopp N, et al. BCL2 suppresses PARP1 function and non-apoptotic cell death. *Cancer Res*. 2012;72(16):4193–4203. doi:10.1158/0008-5472.CAN-11-4204
38. Gunduz Z, Aktas F, Vatanssev H, Solmaz M, Erdogan E. Effects of amantadine and topiramate on neuronal damage in rats with experimental cerebral ischemia-reperfusion. *Adv Clin Exp Med*. 2021;30(10):1013–1023. doi:10.17219/acem/138327
39. Battaglia S, Fabius JH, Moravkova K, Fracasso A, Borgomaneri S. The neurobiological correlates of gaze perception in healthy individuals and neurologic patients. *Biomedicines*. 2022;10(3):627. doi:10.3390/biomedicines10030627
40. Huynh JP, Lin CC, Kimmey JM, et al. Bhlhe40 is an essential repressor of IL-10 during *Mycobacterium tuberculosis* infection. *J Exp Med*. 2018;215(7):1823–1838. doi:10.1084/jem.20171704
41. Peng Y, Liu W, Xiong J, et al. Downregulation of differentiated embryonic chondrocytes 1 (DEC1) is involved in 8-methoxypsoralen-induced apoptosis in HepG2 cells. *Toxicology*. 2012;301(1–3):58–65. doi:10.1016/j.tox.2012.06.022
42. Hamilton KA, Wang Y, Raefsky SM, et al. Mice lacking the transcriptional regulator Bhlhe40 have enhanced neuronal excitability and impaired synaptic plasticity in the hippocampus. *PLoS One*. 2018;13(5):e0196223. doi:10.1371/journal.pone.0196223
43. Zhu Z, Wang YW, Ge DH, et al. Downregulation of DEC1 contributes to the neurotoxicity induced by MPP⁺ by suppressing PI3K/Akt/GSK3 β pathway. *CNS Neurosci Ther*. 2017;23(9):736–747. doi:10.1111/cns.12717
44. Park CG, Lee SY, Kandala G, Lee SY, Choi Y. A novel gene product that couples TCR signaling to Fas(CD95) expression in activation-induced cell death. *Immunity*. 1996;4(6):583–591. doi:10.1016/S1074-7613(00)80484-7
45. Yang F, Chen R. Loss of PHLDA1 has a protective role in OGD/R-injured neurons via regulation of the GSK-3 β /Nrf2 pathway. *Hum Exp Toxicol*. 2021;40(11):1909–1920. doi:10.1177/09603271211014596
46. Battaglia S, Orsolini S, Borgomaneri S, Barbieri R, Diciotti S, di Pellegrino G. Characterizing cardiac autonomic dynamics of fear learning in humans. *Psychophysiology*. 2022;59(12):e14122. doi:10.1111/psyp.14122
47. Tanaka M, Spekker E, Szabó Á, Polyák H, Vécsei L. Modelling the neurodevelopmental pathogenesis in neuropsychiatric disorders: Bioactive kynurenines and their analogues as neuroprotective agents. In celebration of 80th birthday of Professor Peter Riederer. *J Neural Transm*. 2022;129(5–6):627–642. doi:10.1007/s00702-022-02513-5
48. Battaglia S, Thayer JF. Functional interplay between central and autonomic nervous systems in human fear conditioning. *Trends Neurosci*. 2022;45(7):504–506. doi:10.1016/j.tins.2022.04.003
49. Kubis N. Non-invasive brain stimulation to enhance post-stroke recovery. *Front Neural Circuits*. 2016;10:56. doi:10.3389/fncir.2016.00056
50. Borgomaneri S, Battaglia S, Sciamanna G, Tortora F, Laricchiuta D. Memories are not written in stone: Re-writing fear memories by means of non-invasive brain stimulation and optogenetic manipulations. *Neurosci Biobehav Rev*. 2021;127:334–352. doi:10.1016/j.neubiorev.2021.04.036
51. Tanaka M, Vécsei L. Editorial of Special Issue “Crosstalk between Depression, Anxiety, and Dementia: Comorbidity in Behavioral Neurology and Neuropsychiatry.” *Biomedicines*. 2021;9(5):517. doi:10.3390/biomedicines9050517

Fluid resuscitation, but not inhaled nitric oxide, improves microcirculation in septic pigs

Małgorzata Grotowska^{1,A–D,F}, Piotr Harbut^{2,A–C,E,F}, Claes Frostell^{2,A–C,E,F}, Waldemar Goździk^{1,A–F}

¹ Department of Anaesthesiology and Intensive Therapy, University Hospital in Wrocław, Wrocław Medical University, Poland

² Department of Clinical Sciences, Division of Anesthesia and Intensive Care, Danderyd Hospital, Karolinska Institutet, Stockholm, Sweden

A – research concept and design; B – collection and/or assembly of data; C – data analysis and interpretation; D – writing the article; E – critical revision of the article; F – final approval of the article

Advances in Clinical and Experimental Medicine, ISSN 1899–5276 (print), ISSN 2451–2680 (online)

Adv Clin Exp Med. 2023;32(6):667–676

Address for correspondence

Małgorzata Grotowska

E-mail: malgorzata.grotowska@umw.edu.pl

Funding sources

This research was in part supported by grants from Claes Frostell Research & Consulting AB (Stockholm, Sweden).

Conflict of interest

None declared

Received on August 27, 2022

Reviewed on November 3, 2022

Accepted on November 18, 2022

Published online on December 8, 2022

Abstract

Background. Prolonged deterioration of microvascular flow during sepsis leads to organ dysfunction. Capillary flow restoration may prevent this complication.

Objectives. The main aim of this study was to investigate the microcirculatory effects of inhaled nitric oxide (iNO) combined with intravenous hydrocortisone in a porcine model of sepsis. The 2nd aim was to evaluate the influence of hemodynamic resuscitation with noradrenaline and crystalloids on capillary flow.

Materials and methods. Eleven piglets of Polish breed underwent surgical colon perforation to develop sepsis. They were randomly allocated to one of 3 treatment groups. Group 1 received iNO and hydrocortisone, whereas group 2 did not. Both groups were resuscitated with crystalloids and noradrenaline if hypotensive. Group 3 received no treatment at all. During a 30-hour observation, we assessed the microcirculation using sidestream dark field imaging (SDF).

Results. We found no effect of iNO with hydrocortisone on the microcirculation. Fluid and vasopressor treatment led to a higher microcirculatory flow index after 20 h of observation (3 and 2.75 in groups 1 and 2 compared to 1.9 in group 3), a greater proportion of perfused vessels (94% and 87% compared to 63% in groups 1, 2 and 3, respectively) and a greater perfused vessel density (15.2 mm/mm², 15.09 mm/mm² and 10.1 mm/mm² in groups 1, 2 and 3, respectively).

Conclusions. Crystalloid and vasopressor treatment postponed microvascular flow derangements, whereas iNO combined with intravenous hydrocortisone did not improve microvascular perfusion.

Key words: sepsis, multiorgan failure, microcirculation, inhaled nitric oxide, sidestream dark field

Cite as

Grotowska M, Harbut P, Frostell C, Goździk W. Fluid resuscitation, but not inhaled nitric oxide, improves microcirculation in septic pigs. *Adv Clin Exp Med.* 2023;32(6):667–676. doi:10.17219/acem/156700

DOI

10.17219/acem/156700

Copyright

Copyright by Author(s)

This is an article distributed under the terms of the Creative Commons Attribution 3.0 Unported (CC BY 3.0) (<https://creativecommons.org/licenses/by/3.0/>)

Background

Each year, 31 million people are hospitalized due to sepsis, and over 5 million die with this diagnosis.¹ Sepsis and its complications, including multiorgan failure, result from complex hemodynamic and cellular mechanisms, with capillary perfusion being altered. Specific changes in capillary flow may precede the more severe symptoms of sepsis and septic shock.^{2,3} Persistent microcirculatory derangement is strongly related to poor outcomes and can be observed in patients with multiorgan dysfunction even after the resolution of shock.^{4,5} Therefore, capillary flow monitoring may be helpful in the early diagnosis of sepsis, following its course and determining its prognosis.

There are multiple studies concerning septic patients and septic animal models that provide reproducible information about the microcirculation changes occurring in sepsis.^{6–8} Activation of the inflammatory response leads to the cessation of flow in some capillaries and augmentation of flow in others, resulting in heterogeneity within microvascular flow.⁹ An increased distance between perfused capillaries impedes oxygen diffusion and its delivery to cells, creating a microcirculatory shunt.¹⁰ It leads to oxygen deficits in tissues, increased lactate production, shock, and finally organ dysfunction.^{2,11,12} Therefore, microvascular resuscitation and the restoration of homogeneity of flow in capillary beds are crucial for managing sepsis and preventing its complications.

In recent years, much attention has been paid to nitric oxide (NO) and its role in microvascular flow restoration in sepsis. Generally, the release of NO is increased in septic shock. However, in some areas, NO production may be impaired, which is one of the factors leading to heterogeneity and hypoperfusion of the microvascular bed.^{13,14} There are multiple trials targeting both NO production inhibition and external NO delivery.^{15–17} The delivery of exogenous NO, a very potent vasodilator, can potentially restore microcirculation and tissue perfusion, and reduce mortality.^{17,18} Inhaled nitric oxide (iNO) is one of the donors tested not only because of its pulmonary activity but also because of its recognized peripheral effects.¹⁹

It has been previously reported that moderate doses of hydrocortisone administered in the early stages of septic shock improved capillary perfusion and increased NO delivery to tissues.²⁰ The use of hydrocortisone in septic shock seems beneficial not only due to its anti-inflammatory properties since glucocorticoids inhibit pro-inflammatory gene expression and activate anti-inflammatory protein production.²¹ It also increases vessel responsiveness to catecholamines.²² Low doses of corticosteroids can restore circulation and reduce mortality in septic shock.^{23,24} In a preliminary study on piglets exposed to prolonged endotoxin/lipopolysaccharide (LPS) infusions, it has been demonstrated that combined iNO and intravenous steroids attenuate LPS-induced kidney injury, but neither of them does it on its own.²⁵ This effect may be partially explained by the fact that iNO upregulates glucocorticoid receptors and blunts the inflammatory response.²⁶

When it comes to septic shock, intravenous fluids with vaso-pressors have been proven to resuscitate the microcirculation. However, whether hemodynamic stabilization equals microcirculatory improvement is still in question. For years, early goal-directed therapy (EGDT) has been recognized as an effective treatment in managing septic shock and reducing mortality and the probability of multiorgan failure.²⁷ Further studies have not confirmed the influence of protocol-based fluid resuscitation on mortality and morbidity reduction.^{28–30} However, in the above trials, patients received fluids before randomization. For this reason, fluid resuscitation was retained in the latest Surviving Sepsis Campaign guidelines, but the strength of this recommendation was reduced to weak.³¹ Ospina-Tascon et al. proved that early administration of fluids in sepsis may improve capillary perfusion.³² Interestingly, microcirculatory changes were independent of macrocirculatory variables. Early fluid loading without a cardiac response could increase microvascular perfusion, whereas late administration of fluids, even if associated with increased cardiac index and mean arterial pressure, did not lead to microvascular resuscitation. For this reason, hemodynamic monitoring seems insufficient in sepsis, and observation of the microcirculation seems necessary as it provides the full picture of the disease. For this purpose, in our study, we applied sidestream dark field imaging (SDF) as described elsewhere.³³

Objectives

Based on our previous experience in an experimental model of piglet endotoxemia undergoing combined therapy with iNO and intravenous hydrocortisone, we attempted to verify whether this type of therapeutic management, along with standard fluid and hemodynamic resuscitation, can improve or restore homogeneous capillary flow in septic pigs.

Our study was based on a porcine fecal peritonitis model. This model has been widely used in the study of the pathophysiology of sepsis and the impact of new therapeutic modalities on its course.^{34,35}

Materials and methods

Ethical issues

This study was approved by the Animal Research Ethics Committee of the Institute of Immunology and Experimental Therapy, Polish Academy of Science, Wrocław, Poland (permission No. 7/05) and reported in compliance with the Animal Research: Reporting of In Vivo Experiments (ARRIVE) guidelines. All methods were carried out in accordance with applicable Polish law and followed the Guide for the Care and Use of Laboratory Animals published by the National Institutes of Health (NIH) and Minimum Quality Threshold in Pre-Clinical Sepsis Studies (MQTiPSS) recommendations.^{36,37}

Throughout our research, care was taken to guarantee the maximum comfort of the animals. The depth of analgesia was adjusted to the level of pain stimuli and the depth of anesthesia was adjusted according to the level of consciousness. The animals that survived the study period were euthanized with pentobarbital.

Animal preparation

A detailed description of the instrumentation was previously presented elsewhere.³³ This study is part of a larger project covering a sequence of studies on iNO delivery to septic piglets.^{25,38–40}

The experiment was conducted in the Department of Surgery at the Wrocław University of Environmental and Life Sciences, Poland. Originally, the study group consisted of 12 female piglets of Polish breed. One of them was excluded as it developed severe hypotonia unresponsive to treatment during instrumentation and died. All animals were of the same age (2 months). Their median body weight was 18.5 kg (range: 17–22 kg).

All piglets fasted for 6 h before the experiment; however, they were allowed to drink water at will. To induce anesthesia, we administered tiletamine-zolazepam doses of $4 \text{ mg} \times \text{kg}^{-1}$ dissolved in medetomidine $0.08 \text{ mg} \times \text{kg}^{-1}$ intramuscularly. All animals were successfully intubated and mechanical ventilation was started using Servo 900C ventilators (Siemens-Eléma AB, Solna, Sweden). A ventilation protocol was based on the pressure-controlled mode with an initial inspired fraction of oxygen (FIO_2) of 0.3 and a positive end-expiratory pressure (PEEP) of $5 \text{ cm H}_2\text{O}$. During the experiment, ventilator settings were adjusted in accordance with blood gas analysis.

Following induction, general anesthesia was maintained with the intravenous infusion of ketamine ($1.5\text{--}2.4 \text{ mg} \times \text{kg}^{-1} \times \text{h}^{-1}$), medetomidine ($5.3\text{--}8.2 \mu\text{g} \times \text{kg}^{-1} \times \text{h}^{-1}$), fentanyl ($0.8\text{--}1.3 \mu\text{g} \times \text{kg}^{-1} \times \text{h}^{-1}$), and midazolam ($0.08\text{--}0.13 \text{ mg} \times \text{kg}^{-1} \times \text{h}^{-1}$). All animals received a solution of 2.5% dextrose in 0.9% saline (Glu/NaCl 1:1) at a constant rate

of $100 \text{ mL} \times \text{h}^{-1}$ to prevent hypoglycemia. In addition, all animals received 500 mg of cefuroxime (GlaxoSmithKline, Solna, Sweden) intravenously (i.v.) every 8 h to counter accidental bacterial contamination during instrumentation and as the treatment modality.

For further hemodynamic monitoring, arterial lines, central venous catheters and pulmonary artery catheters were introduced. The following hemodynamic parameters were registered: heart rate (HR), systolic arterial pressure (SAP), diastolic arterial pressure (DAP), mean arterial pressure (MAP), systolic pulmonary artery pressure (SPAP), central venous pressure (CVP), diastolic pulmonary artery pressure (DPAP), mean pulmonary artery pressure (MPAP), pulmonary capillary wedge pressure (PCWP), cardiac output (CO), cardiac index (CI), systemic vascular resistance index (SVRI), pulmonary vascular resistance index (PVRI), and stroke volume index (SVI). Access to the urinary bladder was obtained transabdominally. According to core temperature measurements, heating blankets and external cooling were used to keep temperatures within the normal range. After instrumentation, the first blood sample was taken to evaluate arterial blood gas, complete blood count, aspartate transaminase (AST), alanine transaminase (ALT), creatinine, and urea. Hemodynamic measurements and microvascular imaging were performed.

Study protocol

The timeline of interventions is presented in Fig. 1. After a 1-hour rest, all piglets underwent a surgical midline laparotomy. The descending colon was visualized, a 3-centimeter incision was performed and 1.5 g/kg of fecal content was removed, mixed with blood, and then deposited close to the diaphragm to cause a septic-like condition. Then, the laparotomy was closed and all measurements were repeated every 10 h from that moment (Fig. 1).

Next, the piglets were randomly allocated to one of 3 groups:

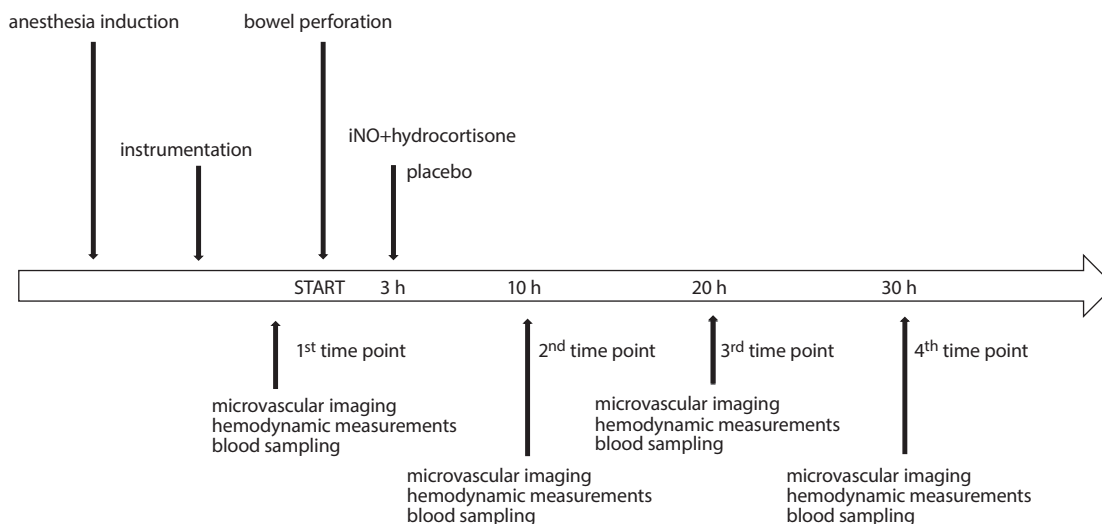


Fig. 1. Timeline of interventions and data acquisition events

Group 1 – piglets receiving iNO (800 ppm iNO in 9000 nitrogen; Pulmonox-Messer Griesheim, Bad Soden am Taunus, Germany) at a concentration of 30 ppm and hydrocortisone (75 mg i.v. every 7 h). Hypotensive piglets (MAP < 65 mm Hg for more than 3 min) were treated with a bolus of Ringer's lactate (300 mL) and norepinephrine infusion (if unresponsive to fluids) to maintain MAP \geq 65 mm Hg.

Group 2 – piglets receiving neither iNO nor hydrocortisone but treated for hypotension with fluids and noradrenaline infusion similar to group 1.

Group 3 – piglets not receiving iNO and hydrocortisone, and not resuscitated with fluids or noradrenaline infusions.

In most cases, fluid boluses were sufficient to raise the MAP above 65 mm Hg in the resuscitated groups. Only 1 pig from group 1 received noradrenaline.

Microcirculation assessment

Our study evaluated microcirculation with the MicroScan™ device (MicroVisionMedical, Amsterdam, the Netherlands) based on SDF. We assessed the microvascular bed of the sublingual region of the oral cavity using 4 different sequences at every time point. Every record was stored using a random number code and the analyzing researcher was blinded to all clinical data. To optimize image quality and avoid artifacts, we ensured maximum camera stability, removed saliva from the sublingual area using sterile gauze, and minimized pressure on the mucosa.

For the microcirculation evaluation, we used AVA v. 3.0 (MicroVision Medical BV, Amsterdam, The Netherlands), which automatically identifies vessels. It calculates total vessel density by calculating the number of vessels crossing

a grid of 6 lines (dividing the screen image into 16 equal areas). Further images were assessed using 2 semi-quantitative methods described by Boerma and De Backer.^{3,6} The analysis provided information about the proportion of perfused vessels (PPV), the perfused vessel density (PVD = PPV \times total vessel density (TVD)) and the microvascular flow index (MFI). All of the above variables were calculated separately for small vessels whose diameter was less than 20 μ m (small vessel MFI – sMFI, small vessel density – sVD, proportion of perfused small vessels – sPPV, and perfused small vessel density – sPVD).

Statistical analyses

Statistical analysis was performed using Statistica v. 13.1 PL (StatSoft Polska, Kraków, Poland). The distribution of the microcirculatory variables was tested with the Shapiro–Wilk normality test. Since they showed a non-normal distribution, data were presented as medians with interquartile range (IQR) and analyzed with non-parametric tests. Differences between groups were tested with a Kruskal–Wallis analysis of variance (ANOVA) test, which was followed by a post hoc analysis. Correlation analysis was assessed using Spearman's rho correlation coefficient. A p-value <0.05 was considered statistically significant. All values were reported as medians unless otherwise stated.

Results

All eleven piglets included in the study developed a systemic inflammatory response syndrome (SIRS) diagnosed by meeting at least 2 of its criteria – heart rate >90 bpm and

Table 1. Group characteristics demonstrating the number of animals at particular time points, number of animals that developed systemic inflammatory response syndrome (SIRS), and temperature, heart rate (HR) and white blood cell count (WBC)

Variable	Group	START	10 h	20 h	30 h
Number of animals	1	4	4	4	3
	2	4	4	3	3
	3	3	3	3	0
Number of animals with SIRS	1	0	4	4	3
	2	0	3	3	3
	3	0	3	3	–
Temperature [°C]	1	36.0 \pm 0.6	38.4 \pm 1.5	41.3 \pm 0.5	41.5 \pm 0.6
	2	36.7 \pm 0.6	39.0 \pm 1.1	41.0 \pm 0.6	41.9 \pm 0.7
	3	37.5 \pm 0.8	39.3 \pm 1.6	41.5 \pm 0.7	–
HR [bpm]	1	76 \pm 8	155 \pm 43	142 \pm 28	152 \pm 3
	2	77 \pm 13	124 \pm 15	123 \pm 12	151 \pm 33
	3	95 \pm 12	158 \pm 47	161 \pm 45	–
WBC [m/mm ³]	1	15.0 \pm 7.4	13.2 \pm 6.7	11.1 \pm 4.3	9.5 \pm 4.5
	2	18.8 \pm 2.7	13.7 \pm 5.1	18.2 \pm 6.6	9.9 \pm 5.9
	3	18.6 \pm 4.6	21.6 \pm 12.6	22.4 \pm 3.3	–

Temperature, HR and WBC are expressed as mean \pm standard deviation (M \pm SD). Group 1 – iNO + hydrocortisone; group 2 – placebo; group 3 – no resuscitation.

Table 2. Baseline microcirculatory variables. Initially, there were no differences in TVD, sTVD, PVD, sPVD, PPV, sPPV, MFI, sMFI, and the De Backer score between the groups ($p > 0.05$)

Variable	Group 1	Group 2	Group 3	p-value
TVD [mm/mm ²]	17.4 (16.8–19.0)	18.6 (17.4–21.3)	18.0 (16.0–20.3)	0.35
sVD [mm/mm ²]	16.0 (14.7–18.5)	17.4 (16.0–20.0)	16.7 (15.3–19.5)	0.30
PVD [mm/mm ²]	15.5 (13.7–16.9)	17.6 (15.4–20.1)	16.4 (14.1–18.8)	0.19
sPVD [mm/mm ²]	14.0 (12.8–15.8)	16.5 (14.1–19.0)	14.7 (12.6–18.6)	0.18
PPV [%]	91 (78–98)	94 (88–97)	91 (84–94)	0.48
sPPV [%]	92 (77–98)	93 (88–97)	91 (84–94)	0.52
MFI	2.9 (2.4–3.0)	3.0 (2.75–3.0)	2.9 (2.7–3.0)	0.86
sMFI	2.8 (2.3–3.0)	3.0 (2.6–3.0)	3.0 (2.6–3.0)	0.70
De Backer score	12.0 (10.6–13.1)	12.4 (11.1–13.6)	11.8 (10.9–13.4)	0.66

Group 1 – iNO + hydrocortisone; group 2 – placebo; group 3 – no resuscitation. TVD – total vessel density; sVD – small vessel density; PVD – perfused vessel density; sPVD – perfused small vessel density; PPV – proportion of perfused vessels; sPPV – proportion of perfused small vessels; MFI – microvascular flow index; sMFI – small vessel MFI; iNO – inhaled nitric oxide.

temperature $>38^{\circ}\text{C}$ (Table 1).⁴¹ There were no differences between the 3 studied groups in the initial microcirculatory parameters (Table 2).

iNO and hydrocortisone

The 30-hour analysis of groups 1 and 2 showed no influence of iNO and hydrocortisone on microvascular bed perfusion. In both groups, the microcirculation generally deteriorated (Fig. 2). Microvascular flow impairment after 30 h was expressed by a statistically significant drop in the MFI (from 2.9 to 2.6 in group 1, and from 3.0 to 2.3 in group 2; $p < 0.05$), sMFI (from 2.8 to 2.5 in group 1, and from 3.0 to 2.3 in group 2; $p < 0.05$), PVD (from 15.5 mm/mm² to 12.8 mm/mm² in group 1, and from 17.6 mm/mm² to 15.3 mm/mm² in group 2; $p < 0.05$), sPVD (from 14.0 mm/mm² to 12.1 mm/mm² in group 1, and from 16.5 mm/mm² to 13.6 mm/mm² in group 2; $p < 0.05$), PPV (from 78% to 52% in group 1, and from 88% to 65% in group 2; $p < 0.05$), and sPPV (from 92% to 80% in group 1, and from 93% to 85% in group 2; $p < 0.05$). There were no statistically significant differences in capillary perfusion between groups 1 and 2 after 30 h (Fig. 2).

Hemodynamic resuscitation

All piglets from group 3 died prematurely (after 12 h, 23 h and 23.5 h). For this reason, the complete analysis of all groups after 30 h could not be conducted, and it was performed 20 h after the laparotomy.

In group 3, the perfusion deteriorated to a significantly greater extent than in the other groups after 20 h of observation (Fig. 2). The median MFI was equal to 3 and 2.8 in groups 1 and 2, respectively, compared to 1.9 in group 3 ($p < 0.05$), the median PPV reached 94%, 87% and 63% in groups 1, 2 and 3, respectively ($p < 0.05$), and the median PVD was 15.2 mm/mm², 15.09 mm/mm² and 10.1 mm/mm² in groups 1, 2 and 3, respectively ($p < 0.05$).

Similar results were observed during small vessel analysis: the median sMFI reached 3.0 and 2.6 in groups 1 and 2, and 1.4 in group 3 ($p < 0.05$), the median sPPV was equal to 85%, 88% and 59% in groups 1, 2 and 3, respectively ($p < 0.05$), and the median sPVD at 20 h reached 13.9 mm/mm², 14.2 mm/mm² and 9.0 mm/mm² in groups 1, 2 and 3, respectively ($p < 0.05$). There were no significant intergroup differences in the TVD, sVD and the De Backer score at 20 h (Table 3).

Microvascular flow compared with systemic flow

Throughout the study, the only consistent correlations between microvascular flow and systemic flow were observed in group 3 (Table 4). Impairment of microvascular flow (expressed by changes in MFI and sMFI) correlated with MAP, SAP, DAP, and SVRI with $p < 0.05$ in all cases. None of these parameters depended on CO, CI, PCWP, MPAP, and SPAP. Nevertheless, they were inversely related to HR and DPAP.

Markers of organ function

In terms of the laboratory tests, only in group 3 was capillary perfusion deterioration related to a decrease in pH, base excess (BE) and urine output, and an increase in creatinine, urea and AST (with $p < 0.05$ for all the above variables; Table 5).

Discussion

Flow impairment and heterogeneity are the main pathologies accounting for microcirculatory derangements in sepsis. Endothelial dysregulation, arteriolar constriction, increased leukocyte and platelet adhesion, and the heterogeneous expression of inducible NO synthase cease the flow in some capillaries and reduces functional

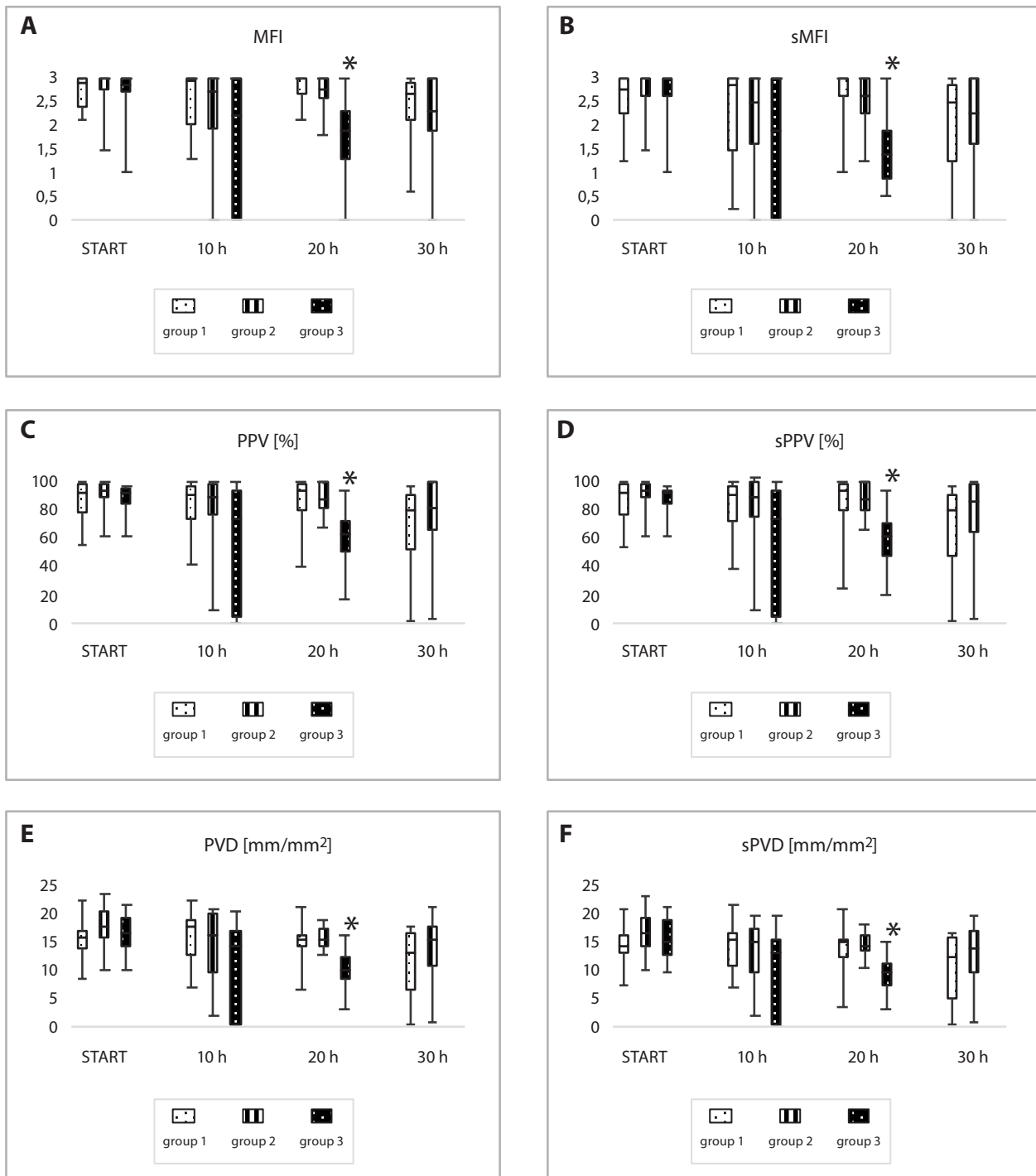


Fig. 2. Time course of microcirculatory variables in the studied groups. At 20 h of observation, significant difference (*) was seen between the groups, with a marked decrease in the microvascular flow index (MFI) (A), small vessel MFI (sMFI) (B), proportion of perfused vessels (PPV) (C), proportion of perfused small vessels (sPPV) (D), perfused vessel density (PVD) (E), and perfused small vessel density (sPVD) (F) in group 3 ($p < 0.05$). The piglets from this group died before the final endpoint (30 h). The analysis of the survivors from groups 1 and 2 showed no difference in MFI, sMFI, PPV, sPPV, PVD, and sPVD between these groups. Microcirculatory variables are presented as medians (25th–75th percentiles)

Group 1 – inhaled nitric oxide (iNO) + hydrocortisone; group 2 – placebo; group 3 – no resuscitation.

capillary density.⁹ The restoration of flow in closed capillaries by NO, a strong vasodilator, can improve tissue oxygenation and the elimination of anaerobic metabolism products. Trzeciak et al. found no effect of iNO on microcirculatory flow in adult patients with sepsis.⁴² However, iNO application was delayed and was commenced after

initial macrocirculatory resuscitation. He et al. created an ovine model of peritonitis and applied tetrahydrobiopterin (BH4, an intravenous NO donor) shortly after the injection of feces into the abdominal cavity, an event triggering sepsis.⁴³ In their study, BH4 improved microvascular flow, kidney perfusion and urine production, and

Table 3. Table demonstrating changes in TVD, sVD and De Backer scores over time. At all time points, there were no significant differences in the above variables between studied groups ($p > 0.05$). The TVD, sVD and De Backer scores did not change over time

Group	START	p-value	20 h	p-value	30 h	p-value
TVD						
iNO+hydrocortisone	17.4 (16.8–19.0)	0.35	16.3 (15.7–18.4)	0.33	17.0 (13.4–19.1)	0.08
Control	18.6 (17.4–21.3)		18.6 (15.4–19.7)		18.4 (16.6–21.0)	
No treatment	18.0 (16.0–20.3)		17.3 (14.3–19.0)		–	
sVD						
iNO+hydrocortisone	16.0 (14.7–18.5)	0.30	15.5 (14.6–16.4)	0.47	16.5 (11.9–17.4)	0.09
Control	17.4 (16.0–19.9)		15.8 (14.3–17.3)		16.9 (14.8–19.5)	
No treatment	16.7 (15.3–19.5)		15.3 (13.2–17.6)		–	
De Backer score						
iNO+hydrocortisone	12.0 (10.5–13.1)	0.66	11.0 (9.7–12.8)	0.74	11.3 (9.4–14.4)	0.78
Control	12.4 (10.8–13.6)		11.2 (9.1–13.5)		12.7 (11.3–13.7)	
No treatment	11.8 (10.8–13.4)		11.6 (10.5–13.4)		–	

Data are presented as medians (25th–75th percentiles). Group 1 – iNO + hydrocortisone; group 2 – placebo; group 3 – no resuscitation. iNO – inhaled nitric oxide; TVD – total vessel density; sVD – small vessel density.

Table 4. Spearman’s rho correlation coefficients between MFI and sMFI and hemodynamic parameters (HR, MAP, SAP, DAP, and SVRI). All correlations were statistically significant with a p-value <0.05

Flow index	HR	MAP	SAP	DAP	SVRI
MFI	–0.54	0.57	0.49	0.61	0.46
sMFI	–0.62	0.63	0.55	0.68	0.54

MFI – microvascular flow index; sMFI – small vessel MFI (sMFI); HR – heart rate; MAP – mean arterial pressure; SAP – systolic arterial pressure; DAP – diastolic arterial pressure; SVRI – systemic vascular resistance index.

Table 5. Spearman’s rho correlation coefficients between MFI and sMFI and pH, HCO₃²⁻, BE, diuresis, creatinine, urea, AST, lymphocytes, monocytes, and granulocytes. All correlations were statistically significant with a p-value <0.05

Flow index	pH	HCO ₃ ²⁻	BE	Urine output	Creatinine	Urea	AST	Lymphocytes	Monocytes	Granulocytes
MFI	0.54	0.66	0.63	–0.46	–0.48	–0.48	–0.44	–0.49	0.56	0.49
sMFI	0.52	0.66	0.66	–0.51	–0.52	–0.52	–0.50	–0.53	0.52	0.53

MFI – microvascular flow index; sMFI – small vessel MFI (sMFI); BE – base excess; AST – aspartate transaminase.

postponed the death of the treated animals. In our study, we found no effect of iNO in conjunction with hydrocortisone on the PPV, perfused capillary density and the MFI, even though iNO was started shortly after laparotomy. We hypothesize that no influence of the administered iNO on capillary recruitment and perfusion can be explained by the restricted access to closed vessels.

We observed that microcirculatory variables changed more profoundly in piglets not resuscitated with fluids and noradrenaline, with a statistically greater decrease in the MFI, sMFI, PPV, sPPV, PVD, and sPVD than in other groups. Only in this group was capillary flow strongly related to changes in hemodynamic indices during septic shock – MAP, SAP, DAP, SVRI, and HR. In groups receiving fluids and noradrenaline, hemodynamic variables were stabilized but these changes did not lead to microcirculatory flow normalization. This observation supports the theory that resuscitation of systemic flow does not resuscitate microcirculation to the same degree as the systemic circulation. Capillary flow impairment remains but

progresses at a slower pace. The discrepancies between hemodynamics and microcirculatory variables have been described by other authors.^{3,5,44} According to De Backer et al., microcirculatory derangements may precede systemic hemodynamic compromise and the relation between hemodynamic and microcirculatory indices may be loose.⁵ Still, changes in CO and MAP may influence capillary perfusion.⁵ In a single-center prospective observational study, De Backer showed that when sepsis develops at the early stages of resuscitation, hemodynamic measurements are related to microvascular flow indices, and this correlation disappears in later stages.³ In human research, observations are limited to septic and resuscitated groups and are usually compared to healthy control groups. For obvious reasons, a control non-resuscitated group cannot be permitted. It is possible that for this reason, no associations between systemic hemodynamic and capillary flow indices have been observed during the advanced stages of sepsis. This correlation only exists when sepsis proceeds undisturbed. Perhaps the search for a direct relationship

between the indicators of micro- and macrocirculation is on the wrong track. At an early stage of the therapeutic process and treatment optimization, global hemodynamics improvement does not lead to immediate microcirculatory normalization. The fact that microcirculation and systemic circulation are not coherent in resuscitated patients does not mean that hemodynamic resuscitation is not effective in terms of capillary perfusion resuscitation. As shown above, microcirculation deteriorated in the resuscitated groups, but more slowly. This suggests that resuscitation may buy time necessary for the immune system and antibiotics to overcome the infection. This observation suggests that the management of sepsis should first concentrate on the monitoring and stabilization of the systemic circulation and – at later stages – on the evaluation and resuscitation of the microcirculation.⁵ Unfortunately, we have not yet found an answer to how to resuscitate the microcirculation, and we still do not have therapeutic options to restore the microcirculation. Fluids and vasopressors are an exception and may have impact on the microcirculation. They increase the pressure differences between arterioles and venules, reduce viscosity, and potentially influence the impact of the endothelium on the morphotic elements of blood.³² These effects seem to be limited to the early stages of sepsis, as at later stages, endothelial dysfunction and leakage evolve.

In the non-resuscitated group, microcirculatory parameters were significantly related to the progress of acidosis and renal failure, as well as increases in AST, lymphocytes, granulocytes, and monocytes. This correlation was not observed in the resuscitated groups, where acidosis and organ dysfunction did not proceed as fast as in the non-treated group. In group 3, the combination of capillary perfusion deterioration and the related metabolic acidosis supports the theory that severe microcirculatory derangement plays an important role in anaerobic metabolism during sepsis. Unfortunately, for technical reasons, lactate was not monitored during the study, and important information about anaerobic metabolism was lacking.

In our study, the TVD, sVD and De Backer score did not follow any certain pattern and their changes over time were not statistically significant. This observation does not support the results presented by Massey et al. in the ProCESS trial.⁴⁵ In the above study, the TVD, PVD and De Backer scores appeared to be strongly associated with outcomes in septic patients. However, their prognostic value appeared to be significant after 72 h of observation. The observed difference in TVD and De Backer score values might result from a shorter time of observation.

Limitations

This study has several limitations. Apart from the small sample size and lack of lactate levels, our observations of microcirculatory alterations were limited to the sublingual area. The sublingual mucosa and the digestive

mucosa have the same embryologic origin and changes in their capnometry correlate quite well, showing similar alterations.^{13,46,47} Capillary perfusion in the sublingual area seems to reflect the flow in the splanchnic mucosa and is easily accessible. Nevertheless, SDF does not allow the direct in vivo observation of the microcirculation in vital organs.

Moreover, in our study, we used healthy young pigs. Human sepsis is associated with elderly age and comorbidities. For this reason, the studied group did not reflect all conditions precisely. We chose a porcine model of sepsis as there are many similarities in the immune response between pigs and humans.^{48,49} Nevertheless, in our pilot studies, we found out that small colon perforation rarely leads to sepsis and multiorgan failure. To increase the probability of provoking sepsis in the animals, we decided to use a model utilizing a larger incision and fecal deposit in the abdomen.

Conclusions

In our study, crystalloid iNO with intravenous hydrocortisone did not improve microvascular perfusion in septic pigs, whereas crystalloid and vasopressor treatment postponed microvascular flow impairment.

Supplementary data

Supplementary tables are available at <https://doi.org/10.5281/zenodo.7334314>. The package contains the following files:

Supplementary Table 1. Time course of hemodynamic variables in groups 1, 2 and 3.

Supplementary Table 2. Time course of organ/metabolic function markers in groups 1, 2 and 3.

ORCID iDs

Małgorzata Grotowska  <https://orcid.org/0000-0002-0691-8440>

Piotr Harbut  <https://orcid.org/0000-0002-0943-7837>

Claes Frostell  <https://orcid.org/0000-0002-7199-1310>

Waldemar Goździk  <https://orcid.org/0000-0001-8668-1641>

References

1. Fleischmann C, Scherag A, Adhikari NKJ, et al. Assessment of global incidence and mortality of hospital-treated sepsis: Current estimates and limitations. *Am J Respir Crit Care Med*. 2016;193(3):259–272. doi:10.1164/rccm.201504-0781OC
2. De Backer D, Orbeago Cortes D, Donadello K, Vincent JL. Pathophysiology of microcirculatory dysfunction and the pathogenesis of septic shock. *Virulence*. 2014;5(1):73–79. doi:10.4161/viru.26482
3. Trzeciak S, Dellinger RP, Parrillo JE, et al. Early microcirculatory perfusion derangements in patients with severe sepsis and septic shock: Relationship to hemodynamics, oxygen transport, and survival. *Ann Emerg Med*. 2007;49(1):88–98.e2. doi:10.1016/j.annemergmed.2006.08.021
4. Sakr Y, Dubois MJ, De Backer D, Creteur J, Vincent JL. Persistent microcirculatory alterations are associated with organ failure and death in patients with septic shock. *Crit Care Med*. 2004;32(9):1825–1831. doi:10.1097/01.CCM.0000138558.16257.3F

5. De Backer D, Ortiz JA, Salgado D. Coupling microcirculation to systemic hemodynamics. *Curr Opin Crit Care*. 2010;16(3):250–254. doi:10.1097/MCC.0b013e3283383621
6. Verdant CL, De Backer D, Bruhn A, et al. Evaluation of sublingual and gut mucosal microcirculation in sepsis: A quantitative analysis. *Crit Care Med*. 2009;37(11):2875–2881. doi:10.1097/CCM.0b013e3181b029c1
7. Wester T, Häggblad E, Awan ZA, et al. Assessments of skin and tongue microcirculation reveals major changes in porcine sepsis. *Clin Physiol Funct Imaging*. 2010;31(2):151–158. doi:10.1111/j.1475-097X.2010.00994.x
8. Kanoore Edul VS, Enrico C, Laviolle B, Risso Vazquez A, Ince C, Dubin A. Quantitative assessment of the microcirculation in healthy volunteers and in patients with septic shock. *Crit Care Med*. 2012;40(5):1443–1448. doi:10.1097/CCM.0b013e31823dae59
9. Bateman RM, Sharpe MD, Ellis CG. Bench-to-bedside review. Microvascular dysfunction in sepsis: Hemodynamics, oxygen transport, and nitric oxide. *Crit Care*. 2003;7(5):359–373. doi:10.1186/cc2353
10. Bateman RM, Tokunaga C, Kareco T, Dorscheid DR, Walley KR. Myocardial hypoxia-inducible *HIF-1 α* , *VEGF* and *GLUT1* gene expression is associated with microvascular and ICAM-1 heterogeneity during endotoxemia. *Am J Physiol Heart Circ Physiol*. 2007;293(1):H448–H456. doi:10.1152/ajpheart.00035.2007
11. Gruartmoner G, Mesquida J, Ince C. Microcirculatory monitoring in septic patients: Where do we stand? *Med Intensiva*. 2017;41(1):44–52. doi:10.1016/j.medint.2016.11.011
12. Ince C. The microcirculation is the motor of sepsis. *Crit Care*. 2005;9(Suppl 4):S13. doi:10.1186/cc3753
13. Trzeciak S, Cinel I, Phillip Dellinger R, et al. Resuscitating the microcirculation in sepsis: The central role of nitric oxide, emerging concepts for novel therapies, and challenges for clinical trials. *Acad Emerg Med*. 2008;15(5):399–413. doi:10.1111/j.1553-2712.2008.00109.x
14. Morin MJ, Unno N, Hodin RA, Fink MP. Differential expression of inducible nitric oxide synthase messenger RNA along the longitudinal and crypt-villus axes of the intestine in endotoxemic rats. *Crit Care Med*. 1998;26(7):1258–1264. doi:10.1097/00003246-199807000-00031
15. López A, Lorente JA, Steingrub J, et al. Multiple-center, randomized, placebo-controlled, double-blind study of the nitric oxide synthase inhibitor 546C88: Effect on survival in patients with septic shock. *Crit Care Med*. 2004;32(1):21–30. doi:10.1097/01.CCM.0000105581.01815.C6
16. Petros A, Lamb G, Leone A, Moncada S, Bennett D, Vallance P. Effects of a nitric oxide synthase inhibitor in humans with septic shock. *Cardiovasc Res*. 1994;28(1):34–39. doi:10.1093/cvr/28.1.34
17. Spronk PE, Ince C, Gardien MJ, Mathura KR, van Straaten HMO, Zandstra DF. Nitroglycerin in septic shock after intravascular volume resuscitation. *Lancet*. 2002;360(9343):1395–1396. doi:10.1016/S0140-6736(02)11393-6
18. Lamontagne F, Meade M, Ondiveeran HK, Lesur O, Robichaud AE. Nitric oxide donors in sepsis: A systematic review of clinical and in vivo pre-clinical data [published correction appears in *Shock*. 2011;35(4):436]. *Shock*. 2008;30(6):653–659. doi:10.1097/SHK.0b013e3181777eef
19. Goldfarb RD, Cinel I. Inhaled nitric oxide therapy for sepsis: More than just lung. *Crit Care Med*. 2007;35(1):290–292. doi:10.1097/01.CCM.0000251290.41866.2B
20. Büchele GL, Silva E, Ospina-Tascón GA, Vincent JL, De Backer D. Effects of hydrocortisone on microcirculatory alterations in patients with septic shock. *Crit Care Med*. 2009;37(4):1341–1347. doi:10.1097/CCM.0b013e3181986647
21. Barnes PJ. How corticosteroids control inflammation. *Br J Pharmacol*. 2006;148(3):245–254. doi:10.1038/sj.bjp.0706736
22. Bellissant E. Effect of hydrocortisone on phenylephrine: Mean arterial pressure dose-response relationship in septic shock. *Clin Pharmacol Ther*. 2000;68(3):293–303. doi:10.1067/mcp.2000.109354
23. Annane D. Effect of treatment with low doses of hydrocortisone and fludrocortisone on mortality in patients with septic shock. *JAMA*. 2002;288(7):862–871. doi:10.1001/jama.288.7.862
24. Lian XJ, Huang DZ, Cao YS, et al. Reevaluating the role of corticosteroids in septic shock: An updated meta-analysis of randomized controlled trials. *BioMed Res Int*. 2019;2019:3175047. doi:10.1155/2019/3175047
25. Göransson SP, Goździk W, Harbut P, et al. Organ dysfunction among piglets treated with inhaled nitric oxide and intravenous hydrocortisone during prolonged endotoxin infusion. *PLoS One*. 2014;9(5):e96594. doi:10.1371/journal.pone.0096594
26. Da J, Chen L, Hedenstierna G. Nitric oxide up-regulates the glucocorticoid receptor and blunts the inflammatory reaction in porcine endotoxin sepsis. *Crit Care Med*. 2007;35(1):26–32. doi:10.1097/01.CCM.0000250319.91575.BB
27. Rivers E, Nguyen B, Havstad S, et al. Early goal-directed therapy in the treatment of severe sepsis and septic shock. *N Engl J Med*. 2001;345(19):1368–1377. doi:10.1056/NEJMoa010307
28. Yealy DM, Kellum JA, Huang DT, et al; The ProCESS Investigators. A randomized trial of protocol-based care for early septic shock. *N Engl J Med*. 2014;370(18):1683–1693. doi:10.1056/NEJMoa1401602
29. Peake SL, Delaney A, Bailey M, et al; The ARISE Investigators and the ANZICS Clinical Trials Group. Goal-directed resuscitation for patients with early septic shock. *N Engl J Med*. 2014;371(16):1496–1506. doi:10.1056/NEJMoa1404380
30. Mouncey PR, Osborn TM, Power GS, et al. Trial of early, goal-directed resuscitation for septic shock. *N Engl J Med*. 2015;372(14):1301–1311. doi:10.1056/NEJMoa1500896
31. Evans L, Rhodes A, Alhazzani W, et al. Surviving sepsis campaign: International Guidelines for Management of Sepsis and Septic Shock 2021. *Intensive Care Med*. 2021;47(11):1181–1247. doi:10.1007/s00134-021-06506-y
32. Ospina-Tascon G, Neves AP, Occhipinti G, et al. Effects of fluids on microvascular perfusion in patients with severe sepsis. *Intensive Care Med*. 2010;36(6):949–955. doi:10.1007/s00134-010-1843-3
33. Stureson C, Nilsson J, Eriksson S. Non-invasive imaging of microcirculation: A technology review. *Med Devices (Auckl)*. 2014;7:445–452. doi:10.2147/MDER.S51426
34. National Research Council (US) Committee for the Update of the Guide for the Care and Use of Laboratory Animals. *Guide for the Care and Use of Laboratory Animals*. 8th ed. Washington, D.C., USA: National Academies Press; 2011:12910. doi:10.17226/12910
35. Mai S, Khan M, Liaw P, Fox-Robichau A. Experimental sepsis models. In: Azevedo L, ed. *Sepsis: An Ongoing and Significant Challenge*. London, UK: InTech; 2012. doi:10.5772/52876
36. Rutai A, Zsikai B, Tallósy SP, et al. A porcine sepsis model with numerical scoring for early prediction of severity. *Front Med*. 2022;9:867796. doi:10.3389/fmed.2022.867796
37. Osuchowski MF, Ayala A, Bahrami S, et al. Minimum quality threshold in pre-clinical sepsis studies (MQTiPSS): An international expert consensus initiative for improvement of animal modeling in sepsis. *Intensive Care Med*. 2018;6(1):26. doi:10.1186/s40635-018-0189-y
38. Adamik B, Frostell C, Paslawska U, et al. Platelet dysfunction in a large-animal model of endotoxemic shock: Effects of inhaled nitric oxide and low-dose steroid. *Nitric Oxide*. 2021;108:20–27. doi:10.1016/j.niox.2020.12.008
39. Skirecki T, Adamik B, Frostell C, et al. Compartment-specific differences in the activation of monocyte subpopulations are not affected by nitric oxide and glucocorticoid treatment in a model of resuscitated porcine endotoxemic shock. *J Clin Med*. 2022;11(9):2641. doi:10.3390/jcm11092641
40. Goździk W, Albert J, Harbut P, et al. Prolonged exposure to inhaled nitric oxide transiently modifies tubular function in healthy piglets and promotes tubular apoptosis. *Acta Physiol*. 2009;195(4):495–502. doi:10.1111/j.1748-1716.2008.01908.x
41. Bone RC, Balk RA, Cerra FB, et al. Definitions for sepsis and organ failure and guidelines for the use of innovative therapies in sepsis. *Chest*. 1992;101(6):1644–1655. doi:10.1378/chest.101.6.1644
42. Trzeciak S, Glaspey LJ, Dellinger RP, et al. Randomized controlled trial of inhaled nitric oxide for the treatment of microcirculatory dysfunction in patients with sepsis. *Crit Care Med*. 2014;42(12):2482–2492. doi:10.1097/CCM.0000000000000549
43. He X, Su F, Velissaris D, et al. Administration of tetrahydrobiopterin improves the microcirculation and outcome in an ovine model of septic shock. *Crit Care Med*. 2012;40(10):2833–2840. doi:10.1097/CCM.0b013e31825b88ba
44. De Backer D, Donadello K, Sakr Y, et al. Microcirculatory alterations in patients with severe sepsis: Impact of time of assessment and relationship with outcome. *Crit Care Med*. 2013;41(3):791–799. doi:10.1097/CCM.0b013e3182742e8b
45. Massey MJ, Hou PC, Filbin M, et al; ProCESS investigators. Microcirculatory perfusion disturbances in septic shock: Results from the ProCESS trial. *Crit Care*. 2018;22(1):308. doi:10.1186/s13054-018-2240-5

46. Marik PE. Sublingual capnography. *Chest*. 2001;120(3):923–927. doi:10.1378/chest.120.3.923
47. Creteur J, De Backer D, Sakr Y, Koch M, Vincent JL. Sublingual capnometry tracks microcirculatory changes in septic patients. *Intensive Care Med*. 2006;32(4):516–523. doi:10.1007/s00134-006-0070-4
48. Dawson HD, Loveland JE, Pascal G, et al. Structural and functional annotation of the porcine immunome. *BMC Genomics*. 2013;14(1):332. doi:10.1186/1471-2164-14-332
49. Jensen LK, Henriksen NL, Jensen HE. Guidelines for porcine models of human bacterial infections. *Lab Anim*. 2019;53(2):125–136. doi:10.1177/0023677218789444

Silencing of TMED5 inhibits proliferation, migration and invasion, and enhances apoptosis of hepatocellular carcinoma cells

Xianyi Cheng^{A–F}, Xiulan Deng^{B,E,F}, Huiping Zeng^{C,D,F}, Tao Zhou^{C,E,F}, Dezhi Li^{A,D,F}, Wei V. Zheng^{A,D–F}

Intervention and Cell Therapy Center, Peking University Shenzhen Hospital, China

A – research concept and design; B – collection and/or assembly of data; C – data analysis and interpretation; D – writing the article; E – critical revision of the article; F – final approval of the article

Advances in Clinical and Experimental Medicine, ISSN 1899–5276 (print), ISSN 2451–2680 (online)

Adv Clin Exp Med. 2023;32(6):677–688

Address for correspondence

Wei V. Zheng

E-mail: zhengw2013@yeah.net

Funding sources

This work was supported by the Sanming Project of Medicine in Shenzhen (grant No. SZSM201612071), the Cell Technology Center and Transformation Base, Innovation Center of Guangdong-Hong Kong-Macao Greater Bay Area, Ministry of Science and Technology of China (grant No. YCZYPT[2018]03-1), Shenzhen Key Discipline of Stem Cell Clinical Research (grant No. SZXK078), and the Scientific Research Foundation of Peking University Shenzhen Hospital (grant No. KYQD202100X).

Conflict of interest

None declared

Received on January 4, 2021

Reviewed on September 20, 2022

Accepted on November 17, 2022

Published online on December 19, 2022

Cite as

Cheng X, Deng X, Zeng H, Zhou T, Li D, Zheng WV. Silencing of TMED5 inhibits proliferation, migration and invasion, and enhances apoptosis of hepatocellular carcinoma cells. *Adv Clin Exp Med.* 2023;32(6):677–688. doi:10.17219/acem/156673

DOI

10.17219/acem/156673

Copyright

Copyright by Author(s)

This is an article distributed under the terms of the Creative Commons Attribution 3.0 Unported (CC BY 3.0) (<https://creativecommons.org/licenses/by/3.0/>)

Abstract

Background. Transmembrane P24 trafficking protein 5 (TMED5) is highly expressed in cervical and bladder cancer cell lines. Moreover, TMED5 promotes nuclear autophagy and the malignant behavior of cervical cancer cells. However, the role of TMED5 in hepatocellular carcinoma (HCC) has not been extensively reported.

Objectives. To investigate the role of TMED5 in HCC cells.

Materials and methods. Bioinformatics was used to analyze the messenger-ribonucleic acid (mRNA) expression of TMED5 in HCC and its relationship with overall survival and disease-free interval of HCC patients. After TMED5 was decreased in SMMC-7721 and Hep3B cells, they were assayed for proliferation, cell cycle, apoptosis, migration, and invasion.

Results. The expression of TMED5 mRNA in HCC tissues was higher than in adjacent normal tissues, and the overall survival of HCC patients with high TMED5 transcription levels was worse. Moreover, the overexpression of TMED5 was associated with HCC progression. The downregulation of TMED5 suppressed cell proliferation, migration and invasion, and enhanced apoptosis. Therefore, TMED5 may be involved in the regulation of the cell cycle, the mammalian target of rapamycin signaling pathway, and the transforming growth factor beta (TGF- β) signaling pathway.

Conclusions. The TMED5 has the potential to promote HCC progression. Therefore, lowering TMED5 levels could represent a potential strategy for the treatment of HCC.

Key words: proliferation, hepatocellular carcinoma, bioinformatic analysis, TMED5

Background

Hepatocellular carcinoma (HCC) is the most common form of liver cancer.¹ There are more than 700,000 new cases of HCC reported annually worldwide, which accounts for 9.2% of all new cancer cases, and more than 600,000 HCC patients die globally each year.¹ However, the early symptoms of HCC are not obvious.^{2,3} In this regard, the development of biomarkers that can be used for the early diagnosis of HCC is essential to improve the survival rate of HCC patients. Although biomarkers, such as alpha-fetoprotein (AFP), have been identified and used for clinical diagnosis, there is still a need to improve their specificity and sensitivity.⁴ Despite efforts to understand the molecular mechanisms that regulate the occurrence and development of HCC in recent decades,⁵ these mechanisms remain unclear.

Transmembrane P24 trafficking protein 5 (TMED5), also known as p28, is a newly discovered member of the γ sub-family of p24 membrane proteins.⁶ It is located in the endoplasmic reticulum, Golgi intermediate compartment and the cis-Golgi apparatus, and is involved in vesicle-mediated protein transport.⁶ It has been shown that the upregulation of TMED5 promotes nuclear autophagy and the malignant behavior of cervical cancer cells.⁷ In addition, TMED5 was found to be significantly overexpressed in the SCaBER cell line.⁸ These findings suggest that TMED5 is a potential target for certain types of cancer. However, little is known about the role of TMED5 in HCC.

Objectives

In this study, preliminary investigations into the role of TMED5 in HCC were conducted using bioinformatics analysis. The role of TMED5 in the proliferation, apoptosis, migration, and invasion of HCC cells was then explored using in vitro experiments.

Materials and methods

Bioinformatic analysis

Genes that are differentially expressed between HCC tissues and adjacent normal tissues from The Cancer Genome Atlas (TCGA; <https://portal.gdc.cancer.gov/>) were identified using the R package edgeR v. 3.30.3 (R Foundation for Statistical Computing, Vienna, Austria). A volcano map was then drawn with $p < 0.05$ and $|\log_2(\text{fold change})| > 1$ set as the threshold. The TMED5 messenger ribonucleic acid (mRNA) levels in paired and unpaired HCC tissues, and adjacent normal tissues, were retrieved from TCGA or Gene Expression Omnibus (<https://www.ncbi.nlm.nih.gov/geo/>) (GSE84005) and analyzed using the R package edgeR. The distinct expression of TMED5 was analyzed in 33 types of cancer retrieved from TCGA.

Hepatocellular carcinoma patients were divided into high- and low-expression groups based on the median value of their TMED5 levels. The overall survival (OS) and disease-free interval (DFI) were then calculated using the R package survminer v. 0.4.8 (R Foundation for Statistical Computing, Vienna, Austria), and the Kaplan–Meier survival curve was drawn. The TMED5 was combined with the tumor-node-metastasis (TNM) stage to construct a nomogram model, and a calibration curve was drawn to assess the accuracy of the model.

The clinical data of HCC patients extracted from TCGA were used for univariate and multivariate Cox proportional hazard regression.⁹ Cancer-related pathways associated with TMED5 levels in HCC were then used for gene set enrichment analysis (GSEA) using GSEA v. 4.0.0 software (Broad Institute and University of California San Diego, USA).

Cell culture and transfection

The L-02, Hep3B, HepG2, SMMC-7721, and Huh7 cells (catalog No. IM-H289, IM-H367, IM-H038, IM-H047, and IM-H040, respectively; IMMOCELL, Xiamen, China) were cultured in Dulbecco's modified Eagle's medium (catalog No. D0819; Sigma-Aldrich, St. Louis, USA), supplemented with 10% fetal bovine serum (FBS), 100 U/mL penicillin and 100 U/mL streptomycin (Gibco, Detroit, USA) at 37°C.

Three small interfering RNAs (siRNAs) targeting TMED5 were designed (Table 1) and obtained from Huzhou Hippo Biotechnology Co., LTD (HIPPOBIO; Huzhou, China). In total, 1×10^6 cells/well were seeded into 6-well plates. Then, siRNAs were transfected into cells using Lipofectamine 2000 (catalog No. 11668027; Invitrogen, Carlsbad, USA) at 100 pmol per well. Cells were collected for cell proliferation, apoptosis, migration, and invasion assays, as well as for western blotting analysis and quantitative polymerase chain reaction (qPCR) 48 h after transfection.

Table 1. The sequence of small interfering RNAs (siRNAs) of transmembrane P24 trafficking protein (TMED5)

Name	Sequence 5'-3'
siTMED5-1	AGAUGGAGUUCACACUGUAGATT
siTMED5-2	GAAGAUUGGAAGAAUAUUAUUTT
siTMED5-3	GAAACAUACAAGAAAGCAACUTT

Cell proliferation assays

To detect the effects of *TMED5* knockdown on cell proliferation, 3-(4,5-dimethylthiazol-2-yl)-2,5-diphenyltetrazolium bromide (MTT), cell cycle and colony formation assays were used. After treatment with siRNAs, SMMC-7721 and Hep3B cells were inoculated into a 96-well plate and incubated for 24 h, 48 h or 72 h. At each time point, 20 μ L of 5 mg/mL MTT reagent (catalog No. 40201ES72; Yeasen Biotechnology Co. Ltd., Shanghai, China) was added to each well of the plate according to the manufacturer's

instructions to test cell survival. Then, the absorbance was measured at 490 nm using a SpectraMax® Absorbance Reader (Molecular Devices, San Francisco, USA). The data are presented as the mean ± standard deviation (M ±SD) of sextuple wells.

After treatment with siRNAs, SMMC-7721 and Hep3B cells were seeded into 6-well plates at a density of 5×10^2 cells per well to perform the colony formation assay. When the colonies were visible to the naked eye, they were fixed with methanol for 15 min and stained with 0.5% crystal violet (catalog No. 60505ES25; Yeasen Biotechnology Co. Ltd.) in phosphate-buffered saline (PBS) for 15 min. Finally, the colonies were imaged and the numbers of colonies were counted using ImageJ 1.52v (National Institutes of Health, Bethesda, USA).

To examine the cell cycle, 1×10^6 siRNA-treated SMMC-7721 and Hep3B cells were fixed with pre-cooled 75% ethanol at 4°C for 4 h and then incubated with 0.2% Triton X-100 (catalog No. ST797; Beyotime Biotechnology, Shanghai, China) and 10 µg/mL RNase A (catalog No. ST577; Beyotime Biotechnology) in PBS at 37°C for 30 min. Next, the cells were stained with 20 µg/mL propidium iodide (PI) (catalog No. A211-01; Vazyme, Nanjing, China) and kept in the dark at 28°C for 30 min. The stained cells were then analyzed using a NovoCyte 1300 flow cytometer (ACEA Biosciences, San Diego, USA).

Apoptosis assay

After siRNA treatment, SMMC-7721 and Hep3B cells were harvested for apoptosis detection, which was performed using an Annexin V-fluorescein isothiocyanate (FITC)/7-amino-actinomycin D (7-AAD) Apoptosis Detection Kit (catalog No. A211-01; Vazyme), according to the manufacturer's instructions. Flow cytometry detection was then carried out on the cells (NovoCyte 1300), and NovoExpress software (Agilent, Santa Clara, USA) was used to analyze the flow cytometry data.

Cell migration and invasion assay

In total, 3×10^5 siRNA-treated SMMC-7721 or Hep3B cells were seeded into the upper chambers of transwell plates (catalog No. 3422, 8 µm aperture; Corning, Glendale, USA), which were pre-coated with or without 8-fold diluted Matrigel™ (catalog No. 356234; BD Biosciences, Sparks, USA) for invasion or migration assay. Then, 500 µL medium containing 10% FBS was added to the lower chamber. After 24 h of incubation, 0.5% crystal violet (in PBS) was used to stain the migrated cells and the number of migrated cells was then counted in 3 random fields using ImageJ 1.52v.

Quantitative polymerase chain reaction

Total RNA was extracted from SMMC-7721 and Hep3B cells after siRNA treatment using the Total RNA Extraction

Table 2. The primers of quantitative polymerase chain reaction (qPCR)

Name	Sequence 5'-3'	NCBI reference sequence
TMED5-F	AGAAGGAGTGCTTCTACCAGCC	NM_016040
TMED5-R	CTAAGGTTTTGCCTTCTGGAGAG	
18S-F	ACCCGTTGAACCCATTCGTGA	NR_003286
18S-R	GCCTCACTAAACCATCCAATCGG	
MAPK1-F	ACACCAACCTCTCGTACATCGG	NM_002745
MAPK1-R	TGGCAGTAGGTCTGGTCTCAA	
CDC14A-F	TAGATGGCAGCACACCCAGTGA	NM_033312
CDC14A-R	GTCCTGTCTTCCAAGACCAG	
mTOR-F	AGCATCGGATGCTTAGGAGTGG	NM_004958
mTOR-R	CAGCCAGTCATCTTTGGAGACC	
CDC27-F	ACACCTCTGTAATTGATGTGCC	NM_001256
CDC27-R	GGAGTTACCTCTCGCTATTTC	
ROCK1-F	GAAACAGTGTCCATGCTAGACG	NM_005406
ROCK1-R	GCCGCTTATTGATTCCTGCTCC	
CREBBP-F	AGTAACGGCACAGCCTCTCAGT	NM_004380
CREBBP-R	CCTGTGATACAGTGCTTCTAGG	
CDC7-F	GGAAAACCTGCCAGTCTTGCCC	NM_003503
CDC7-R	GGCACTTTGTCAAGACCTCTGG	
PIK3CA-F	GAAGCACCTGAATAGGCAAGTCG	NM_006218
PIK3CA-R	GAGCATCCATGAAATCTGGTCCG	

F – forward primer; R – reverse primer; TMED5 – transmembrane P24 trafficking protein; MAPK1 – mitogen-activated protein kinase 1; CDC – cell division cycle; mTOR – mammalian target of rapamycin; ROCK1 – Rho-associated coiled-coil containing protein kinase 1; CREBBP – cyclic adenosine monophosphate response element binding protein; PIK3CA – phosphatidylinositol-4,5-bisphosphate 3-kinase catalytic subunit alpha; NCBI – National Center for Biotechnology Information.

Reagent (catalog No. R401-01; Vazyme), and was used to synthesize complementary deoxyribonucleic acid (cDNA) using the HiScript II One-Step reverse transcriptase (RT)-PCR Kit (catalog No. P611-01; Vazyme). Quantitative polymerase chain reaction was then performed using the cDNA with a SYBR® Premix Ex Taq™ II (Takara, Kusatsu, Japan) and AriaMx Real-Time PCR System (Agilent), as previously described.¹⁰ The primers for qPCR are listed in Table 2.

Western blotting analysis

Protein extraction from the siRNA-treated SMMC-7721 and Hep3B cells was performed using radioimmunoprecipitation (RIPA) lysis solution (catalog No. P0013C; Beyotime Biotechnology) containing protease inhibitors (catalog No. ST505; Beyotime Biotechnology). Total protein concentration was quantified using a bicinchoninic acid (BCA) protein concentration determination kit (catalog No. P0012S; Beyotime Biotechnology). Western blotting was performed as previously described.¹⁰ In brief, equal amounts of total protein were resolved using 10–12% sodium dodecyl sulfate-polyacrylamide gel electrophoresis (SDS-PAGE) and then transferred to a polyvinylidene fluoride (PVDF) membrane

Table 3. The antibodies for western blot analysis

Classification	Name	Manufacturer	Catalog No.	Dilution rate
Primary antibody	TMED5 antibody	Abcam	ab254795	1:1000
	GAPDH antibody	Proteintech	60004-1-Ig	1:10,000
Secondary antibody	HRP-conjugated goat anti-mouse IgG	Proteintech	SA00001-1	1:10,000
	HRP-conjugated goat anti-rabbit IgG	Proteintech	SA00001-2	1:10,000

TMED5 – transmembrane P24 trafficking protein; GAPDH – glyceraldehyde-3-phosphate dehydrogenase; HRP – horseradish peroxidase.

(Merck Millipore, Burlington, USA). After incubation with 5% skimmed milk, primary and secondary antibodies were applied and the membranes were visualized using enhanced chemiluminescence (ECL) (Thermo Fisher Scientific, Waltham, USA). The antibodies used are shown in Table 3.

Statistical analyses

All statistical analyses were performed using IBM SPSS software v. 22.0 (IBM Corp., Armonk, USA). The normality of data was determined using the Shapiro–Wilk test or the D’Agostino–Pearson test. The Mann–Whitney U test was performed for nonparametric data between the 2 groups. The Wilcoxon matched-pairs signed rank test was used to compare nonparametric data of matched samples. One-way analysis of variance (ANOVA), followed by Tukey’s test, was used to identify the significant differences among multiple groups. An F-test for equality of variances was performed to ensure equal variance of the 2 test groups. The proportionality of the hazard function was checked based on the Schoenfeld residuals. The Kaplan–Meier survival analysis was used to evaluate the cumulative survival probability. The Cox proportional hazards regression models were used to estimate the hazard ratio of TMED5 and HCC. The Student’s unpaired t-test was used to compare the differences between the 2 groups for parametric data. The statistical significance level was set at $p < 0.05$.

Results

TMED5 is highly expressed in hepatocellular carcinoma

To investigate the function of TMED5 in HCC, the bioinformatics analysis was conducted, and it was found that the transcription of TMED5 was higher in the HCC tissues than in the normal tissues (Fig. 1A,B). The analysis of paired tumor tissues and adjacent normal tissues from TCGA and Gene Expression Omnibus further indicated that TMED5 levels were higher in the tumor tissues than in the normal tissues (Fig. 1C,D). Intriguingly, TMED5 transcription levels were lower in some tumors (e.g., thyroid carcinoma, lung adenocarcinoma, lung squamous cell carcinoma, and cholangiocarcinoma) while higher in others (e.g., HCC, cervical squamous cell carcinoma,

endocervical adenocarcinoma, and stomach adenocarcinoma), suggesting that TMED5 plays distinct roles in tumors (Fig. 1E). Thereafter, the expression levels of TMED5 in HCC cell lines were analyzed. Both mRNA and protein levels of TMED5 were higher in HCC Hep3B, HepG2, SMMC-7721, and Huh7 cell lines than in the normal liver cells L-02 cells (Fig. 1F,G). Overall, TMED5 was highly expressed in HCC.

Overexpression of TMED5 is associated with HCC progression

According to the optimal OS threshold, the HCC patients in this study ($n = 339$) were divided into low and high TMED5 expression groups to study the clinical significance of TMED5 expression. There were no significant differences between the 2 groups in terms of age ($n = 339$, $p = 0.1900$), gender ($n = 339$, $p = 0.3780$), family history of cancer ($n = 339$, $p = 0.5910$), Ishak score ($n = 339$, $p = 0.7210$), histological grade ($n = 339$, $p = 0.5440$), living status ($n = 339$, $p = 0.0594$), disease status ($n = 339$, $p = 0.2560$), or Child–Pugh score ($n = 339$, $p = 0.0878$) (Table 4). In contrast, the overexpression of TMED5 was closely related to serum AFP ($n = 339$, $p = 0.0030$), vascular invasion ($n = 339$, $p = 0.0205$), TNM stage ($n = 339$, $p = 0.0479$), and residual tumor ($n = 339$, $p = 0.0085$) (Table 4). These results indicate that TMED5 is positively associated with HCC progression.

Early hepatocellular carcinoma patients exhibiting high TMED5 levels had poor overall survival and disease-free interval

The Kaplan–Meier survival curve was used to analyze the relationship between TMED5 levels and OS or DFI in HCC patients. Patients with high TMED5 levels exhibited shorter OS (Fig. 2A). However, the level of TMED5 had no significant effect on patients’ DFI (Fig. 2B). It is worth noting that among HCC patients in TNM stages I and II, patients with high TMED5 levels had shorter OS and DFI than patients with low TMED5 levels, whereas for HCC patients in TNM stages III and IV, the relationship between TMED5 level and OS and DFI was not significant (Fig. 2C–F). These data demonstrate that high levels of TMED5 indicate a poor prognosis for HCC patients in TNM stages I or II. In addition, the multivariate analysis showed that TNM stages III (hazard ratio (HR) = 2.1, 95%

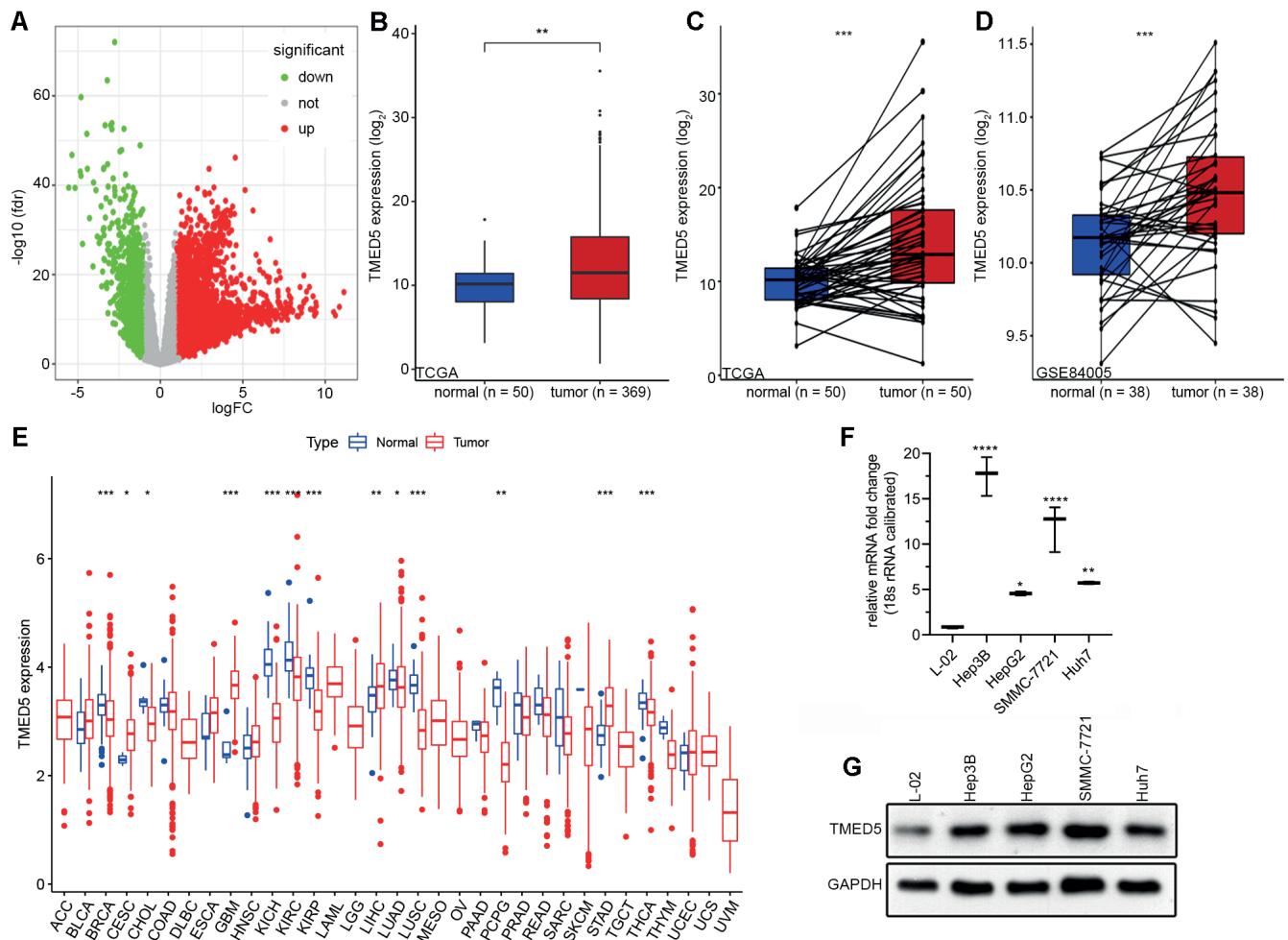


Fig. 1. Transcriptional levels of transmembrane P24 trafficking protein (TMED5) were higher in hepatocellular carcinoma (HCC) tissues than in adjacent normal tissues. **A.** Volcano map of gene expression in HCC tissues; **B.** The difference in TMED5 mRNA levels between HCC tissue (n = 369) and adjacent normal tissue (n = 50). The Mann–Whitney U test was used to analyze the data; **C,D.** The difference in TMED5 mRNA levels between HCC tissues and paired adjacent normal tissues from The Cancer Genome Atlas (TCGA) (**C**) or Gene Expression Omnibus (GSE84005) (**D**). The data were analyzed using the Wilcoxon matched-pairs signed rank test; **E.** The difference in TMED5 mRNA levels between distinct tumor tissues and corresponding adjacent normal tissues. The Mann–Whitney U test was used to analyze the data; **F,G.** Differences in TMED5 mRNA (**F**) and protein (**G**) levels between HCC cell lines and normal liver cell lines. All experiments were repeated independently 3 times. One-way analysis of variance (ANOVA) followed by the Tukey’s test was used for statistical analysis. Box plots indicate the outliers, the maximum, the minimum, the medians, the upper quartile (Q1), and the lower quartile (Q3). Outliers are defined as values that lie 1.5 times beyond the interquartile range (IQR) above Q3 and below Q1. The maximum is defined as 1.5 times the IQR above Q3. The minimum is defined as 1.5 times the IQR below Q1

* p < 0.05; ** p < 0.01; *** p < 0.001; **** p < 0.0001.

confidence interval (95% CI) = 1.23–3.6, p = 0.0060) and IV (HR = 5.64, 95% CI = 1.73–18.43, p = 0.0040) could be considered as independent prognostic indicators of OS, whereas the TMED5 level was not an independent prognostic indicator of OS (Table 5).

The nomogram and calibration curve revealed the prognostic value of TMED5 in HCC patients

To explore the prognostic value of TMED5 levels in HCC patients, TMED5 mRNA levels and TNM stage were combined to plot nomograms. The nomogram and calibration curve showed excellent consistency between predicted postoperative survival rates (1-, 3- and 5-year OS and

DFI) and observed survival rates (1-, 3- and 5-year OS and DFI; Fig. 3). The C-indices for predicting OS and DFI were 0.6173 (95% CI: 0.5887–0.6458) and 0.6403 (95% CI: 0.6137–0.6668), respectively.

Downregulation of TMED5 expression inhibited cell proliferation, migration and invasion, and enhanced apoptosis

To verify the role of TMED5 in HCC, the effect of TMED5 on HCC cell proliferation, apoptosis, migration, and invasion of SMMC-7721 and Hep3B cells was investigated, as they expressed the highest levels of TMED5. Three siRNAs of TMED5, namely siTMED5-1, siTMED5-2 and siTMED5-3, were designed. Quantitative

Table 4. Relationship between transmembrane P24 trafficking protein (TMED5) expression and the clinical parameters of patients with hepatocellular carcinoma (HCC)

Characteristics	Level	TMED5 expression			p-value ^a
		Total (n = 339)	High (n = 217)	Low (n = 122)	
Age [years]	<65	208 (61.4%)	127 (58.5%)	81 (66.4%)	0.1900
	≥65	131 (38.6%)	90 (41.5%)	82 (66.4%)	
Gender	male	231 (68.1%)	152 (70.0%)	79 (64.8%)	0.3780
	female	108 (31.9%)	65 (30.0%)	43 (35.2%)	
Family history of cancer	no	196 (57.8%)	121 (55.8%)	75 (61.5%)	0.5910
	yes	98 (28.9%)	66 (30.4%)	32 (26.2%)	
	unknown	45 (13.3%)	30 (13.8%)	15 (12.3%)	
TNM stage	I	170 (50.1%)	100 (46.1%)	70 (57.4%)	0.0479
	II	84 (24.8%)	57 (26.3%)	27 (22.1%)	
	III	81 (23.9%)	59 (27.2%)	22 (18.0%)	
	IV	4 (1.2%)	1 (0.5%)	3 (2.5%)	
Histologic grade	G1–G2	212 (62.5%)	134 (61.8%)	78 (63.9%)	0.5440
	G3–G4	125 (36.9%)	81 (37.3%)	44 (36.1%)	
	unknown	2 (0.6%)	2 (0.9%)	0 (0%)	
Ishak score	0–4	124 (36.6%)	76 (35.0%)	48 (39.3%)	0.7210
	5–6	74 (21.8%)	48 (22.1%)	26 (21.3%)	
	unknown	141 (41.6%)	93 (42.9%)	48 (39.3%)	
Child–Pugh score	A	207 (61.1%)	123 (56.7%)	84 (68.9%)	0.0878
	B–C	21 (6.2%)	15 (6.9%)	6 (4.9%)	
	unknown	111 (32.7%)	79 (36.4%)	32 (26.2%)	
Vascular invasion	none	193 (56.9%)	120 (55.3%)	73 (59.8%)	0.0205
	micro	84 (24.8%)	48 (22.1%)	36 (29.5%)	
	macro	14 (4.1%)	9 (4.1%)	5 (4.1%)	
	unknown	48 (14.2%)	40 (18.4%)	8 (6.6%)	
Alpha fetoprotein	negative	143 (42.2%)	91 (41.9%)	52 (42.6%)	0.0030
	positive	120 (35.4%)	66 (30.4%)	54 (44.3%)	
	unknown	76 (22.4%)	60 (27.6%)	16 (13.1%)	
Residual tumor	R0	301 (88.8%)	189 (87.1%)	112 (91.8%)	0.0085
	R1–R2	12 (3.5%)	5 (2.3%)	7 (5.7%)	
	unknown	26 (7.7%)	23 (10.6%)	3 (2.5%)	
Living status	alive	224 (66.1%)	135 (62.2%)	89 (73.0%)	0.0594
	dead	115 (33.9%)	82 (37.8%)	33 (27.0%)	
Disease status	no	163 (48.1%)	98 (45.2%)	65 (53.3%)	0.2560
	yes	132 (38.9%)	87 (40.1%)	45 (36.9%)	
	unknown	44 (13.0%)	32 (14.7%)	12 (9.8%)	

^a χ^2 test; TNM – tumor-node-metastasis.

polymerase chain reaction and western blotting analysis showed that siTMED5-3 had the best knockdown efficiency (Fig. 4A,B).

The results of the MTT assay indicated that *TMED5* silencing significantly inhibited cell viability ($n = 3$, $p < 0.0001$; Fig. 4C). At the same time, cell cycle analysis revealed that *TMED5* silencing induced G_0/G_1 -phase arrest. Indeed, the percentage of cells in the G_0/G_1 phase increased from $28.387 \pm 0.830\%$ to $42.363 \pm 1.699\%$ ($n = 3$, $p = 0.0002$), and from $25.963 \pm 1.930\%$ to $39.217 \pm 1.522\%$ ($n = 3$, $p = 0.0007$), for SMMC-7721 and Hep3B cells, respectively (Fig. 4D). Moreover, *TMED5* silencing suppressed colony formation, as the number of colonies was reduced from 336.000 ± 15.000 to 138.667 ± 16.653 ($n = 3$, $p = 0.0001$) for SMMC-7721 cells, and from 127.667 ± 15.631 to 46.000 ± 9.539 ($n = 3$, $p = 0.0015$) for Hep3B cells (Fig. 4E).

The *TMED5* silencing significantly increased the percentage of apoptotic cells ($5.433 \pm 0.905\%$ compared to $14.650 \pm 1.760\%$, $p = 0.0013$, for SMMC-7721; $6.550 \pm 0.462\%$ compared to $14.127 \pm 2.865\%$, $n = 3$, $p = 0.0106$, for Hep3B; Fig. 4F). Finally, the effect of *TMED5* on cell migration was investigated. As shown in Fig. 5A,B, the *TMED5* silencing reduced the number of migrated SMMC-7721 cells from 547.000 ± 12.728 to 330.000 ± 11.518 ($n = 4$, $p < 0.0001$), and the number of migrated Hep3B cells from 426.500 ± 14.201 to 225.750 ± 16.741 ($n = 4$, $p < 0.0001$). Moreover, the number of invasive cells was reduced from 138.750 ± 15.903 to 62.500 ± 10.970 ($n = 4$, $p = 0.0002$) for SMMC-7721 cells, and from 132.750 ± 17.443 to 47.750 ± 7.588 ($n = 4$, $p = 0.0001$) for Hep3B cells (Fig. 5C,D). Taken together, these findings imply that *TMED5* is involved in the proliferation, apoptosis and metastasis of HCC cells.

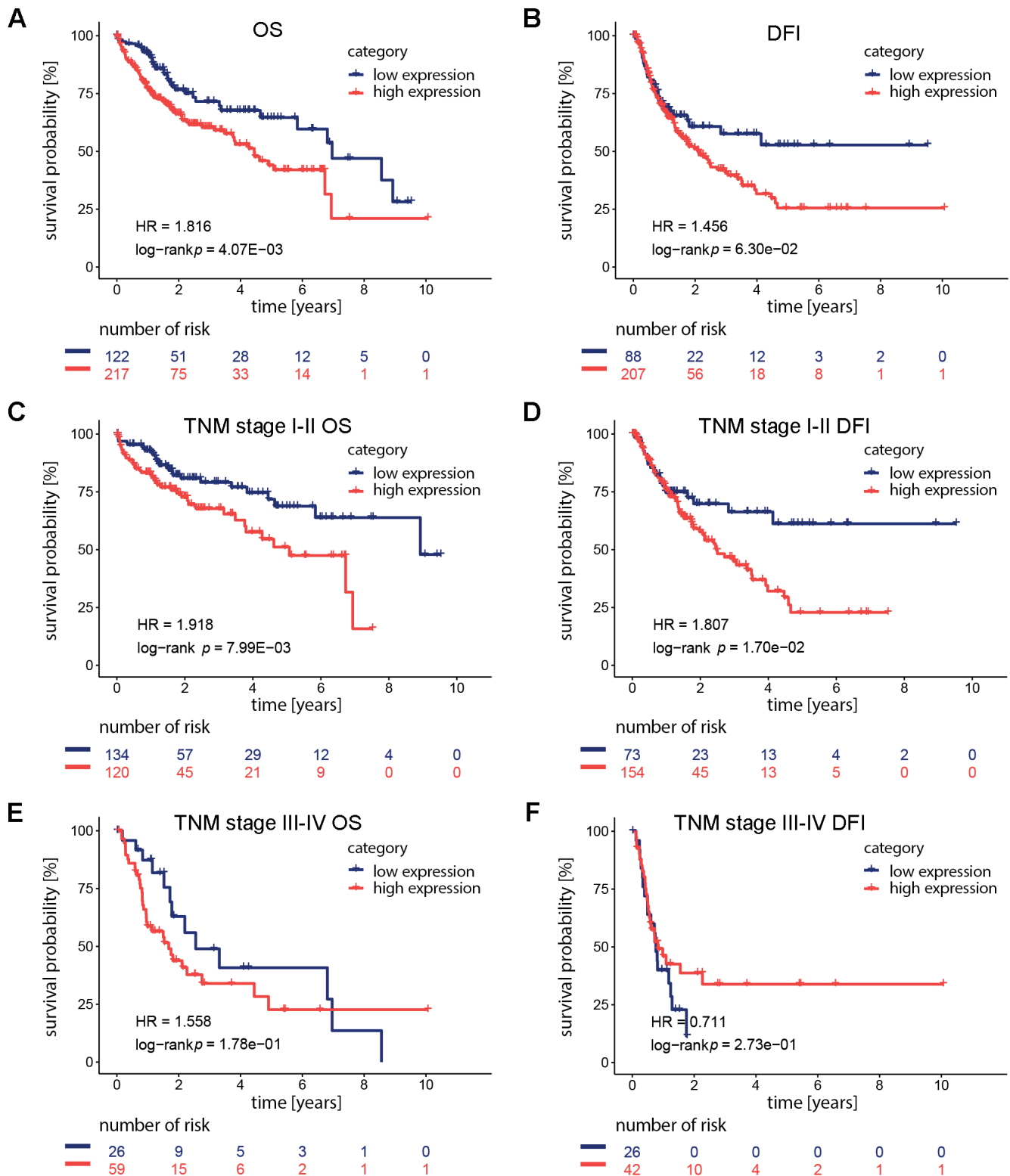


Fig. 2. Correlation between transmembrane P24 trafficking protein (TMED5) levels and overall survival (OS) and disease-free interval (DFI) in hepatocellular carcinoma (HCC) patients. A,B. The correlation between TMED5 levels and OS (A) or DFI (B) in all HCC patients was analyzed using the Kaplan–Meier (KM) curve; C,D. The correlation between TMED5 levels and OS (C) or DFI (D) in HCC patients at tumor-node-metastasis (TNM) stage I and II was analyzed using the KM curve; E,F. The correlation between TMED5 levels and OS (E) or DFI (F) in HCC patients at TNM stage I and II was analyzed using the KM curve. The log-rank test was used for statistical analysis.

HR – hazard ratio.

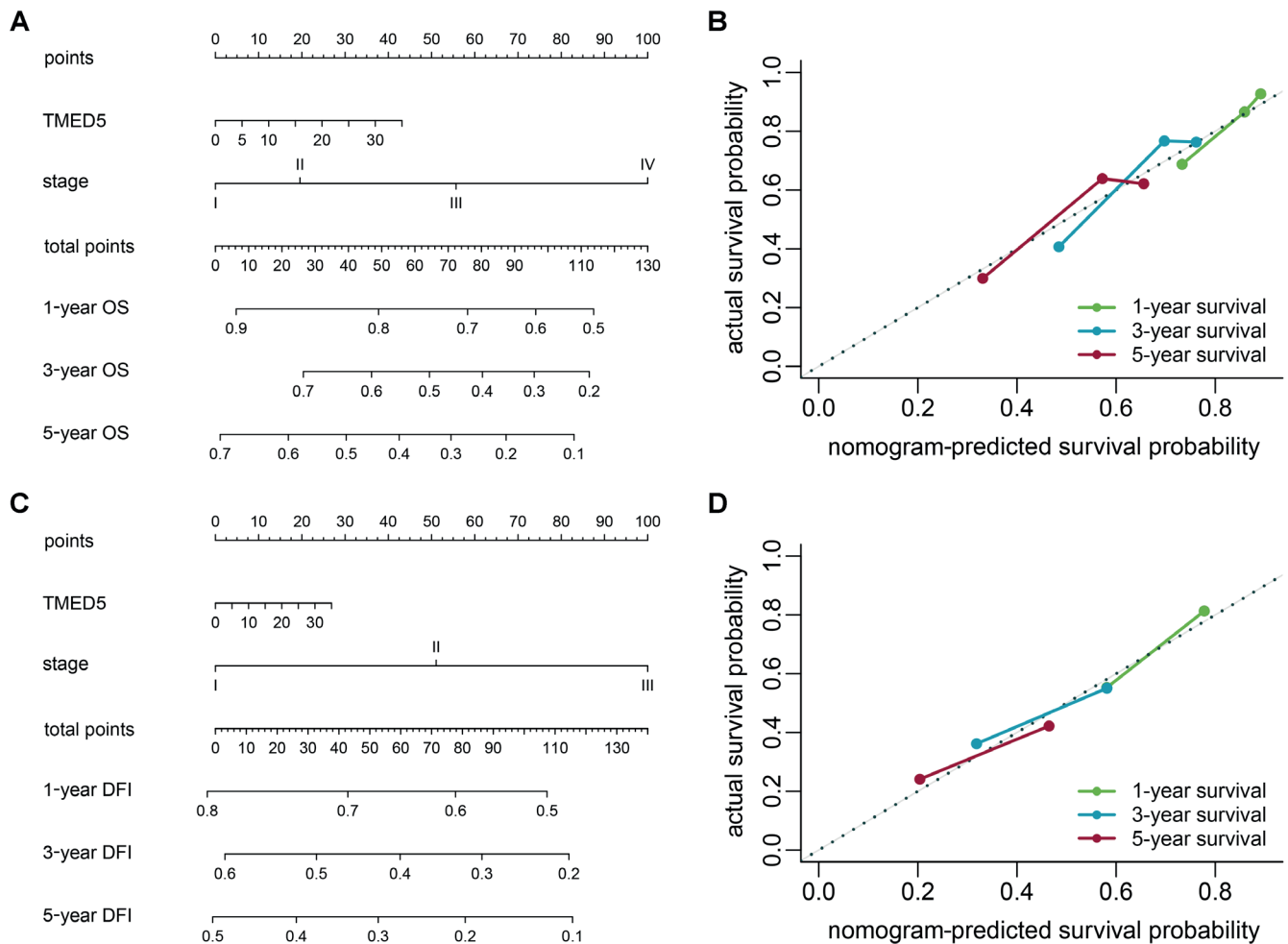


Fig. 3. Nomogram and calibration curve for hepatocellular carcinoma (HCC) patients to predict overall survival (OS) and disease-free interval (DFI). A,B. The 1-, 3- and 5-year OS in HCC patients predicted using nomogram (A) and calibration curve (B); C,D. The 1-year, 3-year, and 5-year DFI in HCC patients predicted using nomogram (C) and calibration curve (D)

TMED5 – transmembrane P24 trafficking protein.

Table 5. Cox proportional hazards regression model analysis of overall survival

Variables	Univariate analysis		Multivariate analysis	
	HR (95% CI)	p-value	HR (95% CI)	p-value
Age (≥65 years vs. <65 years)	1.23 (0.85–1.78)	0.273	–	–
Gender (female vs. male)	1.26 (0.87–1.84)	0.228	–	–
Family history of cancer (yes vs. no)	1.14 (0.76–1.69)	0.530	–	–
TNM stage (II vs. I)	1.42 (0.87–2.32)	0.160	1.22 (0.65–2.29)	0.5360
TNM stage (III vs. I)	2.72 (1.78–4.15)	<0.001	2.1 (1.23–3.6)	0.0060
TNM stage (IV vs. I)	5.44 (1.68–17.63)	0.005	5.64 (1.73–18.43)	0.0040
Histologic grade (G3–G4 vs. G1–G2)	1.14 (0.78–1.67)	0.489	–	–
Ishak score (5–6 vs. 0–4)	0.87 (0.5–1.5)	0.612	–	–
Child–Pugh score (B–C vs. A)	1.66 (0.82–3.36)	0.159	–	–
Vascular invasion (micro vs. none)	1.16 (0.72–1.88)	0.539	1.02 (0.59–1.79)	0.9360
Vascular invasion (macro vs. none)	2.52 (1.14–5.58)	0.023	2 (0.88–4.56)	0.0990
Alpha fetoprotein (positive vs. negative)	1.45 (0.92–2.28)	0.108	–	–
Residual tumor (R1–R2 vs. R0)	1.17 (0.43–3.2)	0.754	–	–
TMED5 (high vs. low)	1.1 (0.85–1.43)	0.472	–	–

Proportionality of hazard function was checked based on the Schoenfeld residuals. HR – hazard ratio; 95% CI – 95% confidence interval; TNM – tumor-node-metastasis.

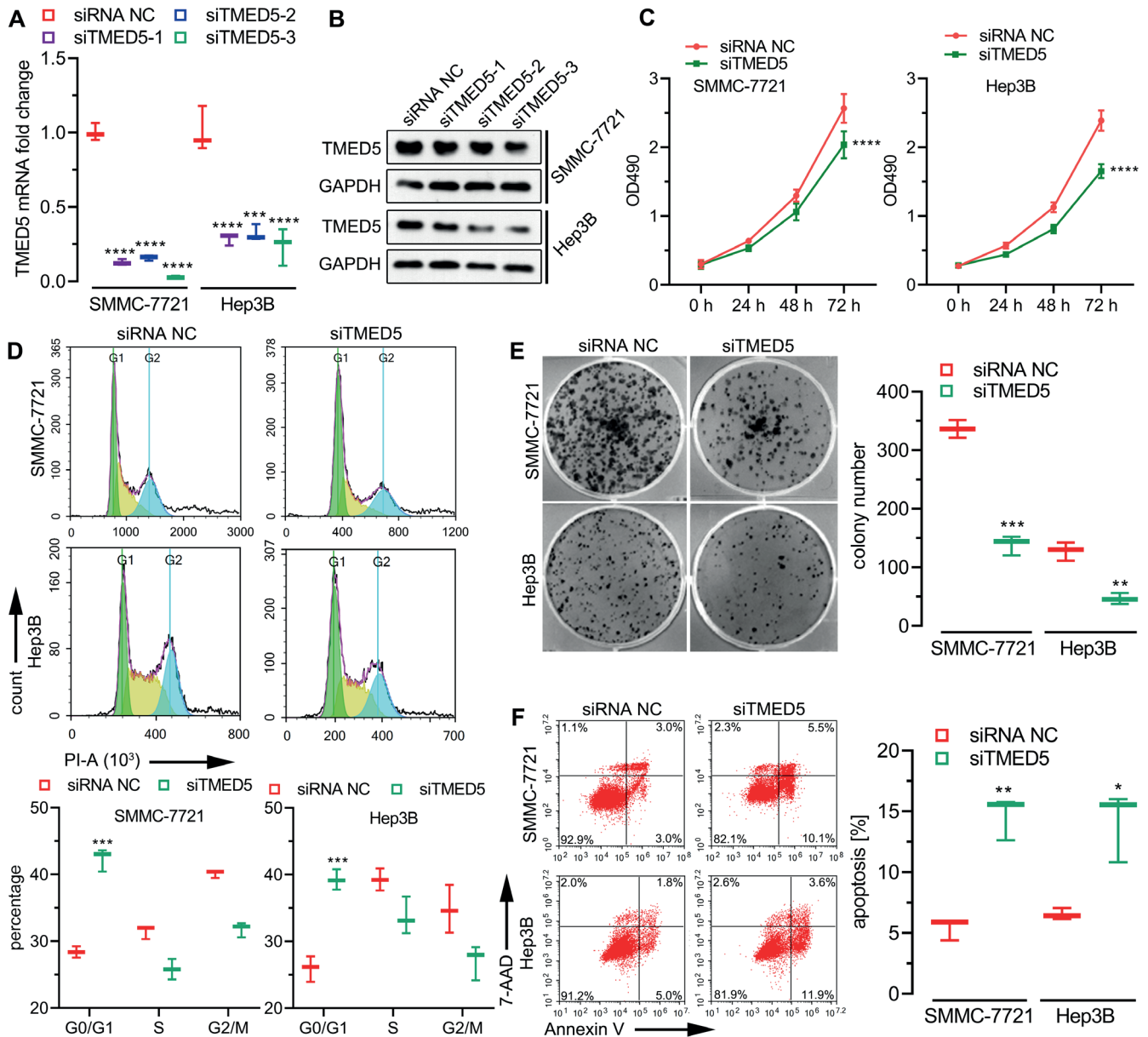


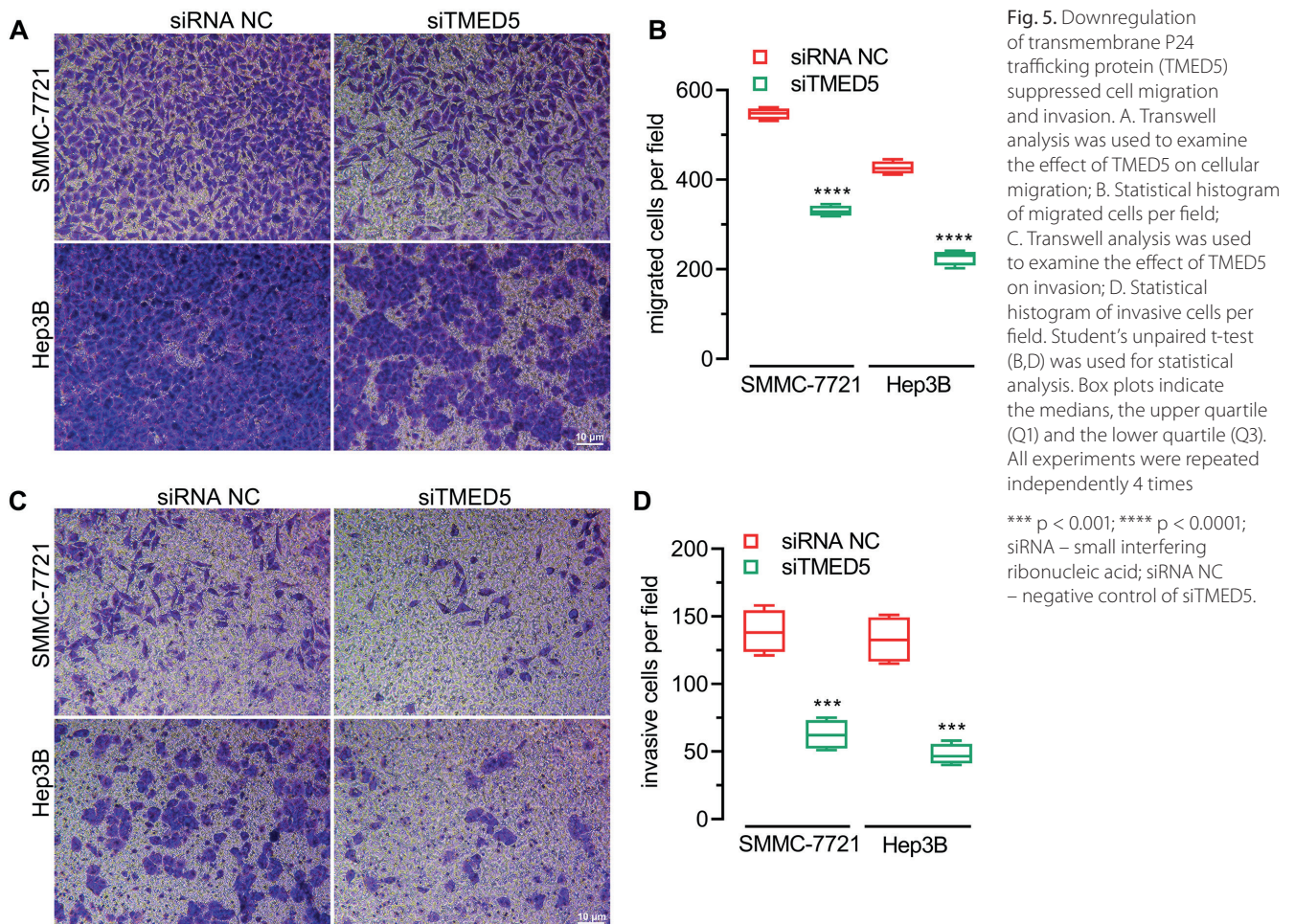
Fig. 4. Downregulation of transmembrane P24 trafficking protein (TMED5) inhibited cell proliferation and enhanced apoptosis. A. Quantitative polymerase chain reaction (qPCR) was used to detect the effect of siTMED5-1-, siTMED5-2- and siTMED5-3-mediated knockdown of *TMED5* in cells; B. Western blotting was used to detect the effect of siTMED5-1-, siTMED5-2- and siTMED5-3-mediated knockdown of *TMED5* in cells; C. MTT assay was used to detect the effect of the knockdown of *TMED5* on cell proliferation; D. The effect of TMED5 downregulation on the cell cycle was determined; E. The effect of TMED5 on colony formation was examined using a colony formation assay; F. Annexin V-fluorescein isothiocyanate (FITC) and 7-aminoactinomycin D (7-AAD) staining was used to detect the effect of TMED5 on apoptosis. One-way analysis of variance (ANOVA) followed by the Tukey's test (A), and the Student's unpaired t-test (C–F) were used for statistical analysis. Box plots indicate the medians, the upper quartile (Q1) and the lower quartile (Q3). All experiments were repeated independently 3 times.

* $p < 0.05$; ** $p < 0.01$; *** $p < 0.001$; **** $p < 0.0001$; siRNA – small interfering ribonucleic acid; siRNA NC – negative control of siTMED5.

TMED5 levels positively correlated with the cell cycle, the mammalian target of rapamycin signaling pathway and the TGF- β signaling pathway

To explore the potential biological function of TMED5 upregulation in HCC, GSEA was performed. This highlighted significant enrichment of the cell cycle, the mammalian target of rapamycin (mTOR) signaling pathway and the transforming growth factor beta (TGF- β) signaling

pathway (Fig. 6A,B). Moreover, genes co-expressed with TMED5 in HCC samples with complete mRNA and sequencing data were evaluated and validated by silencing *TMED5* in SMMC-7721 and Hep3B cells. The *TMED5* silencing resulted in a decrease in both mRNA and protein levels of ras homolog enriched in brain (RHEB), cell division cycle 14A (CDC14A), structural maintenance of chromosomes 1A (SMC1A), cell division cycle 27 (CDC27), mitogen-activated protein kinase 1 (MAPK1), mTOR, ribosomal protein S6 kinase A3 (RPS6KA3),



phosphatidylinositol-4,5-bisphosphate 3-kinase catalytic subunit alpha (PIK3CA), stromal antigen 2 (STAG2), zinc finger FYVE domain containing 16 (ZFYVE16), origin recognition complex subunit 1 (ORC1), cyclic adenosine monophosphate response element binding protein (CREBBP), cell division cycle 7 (CDC7), cullin 1 (CUL1), Rho-associated coiled-coil containing protein kinase 1 (ROCK1), and zinc finger FYVE domain containing 9 (ZFYVE9), all of which are associated with the cell cycle, mTOR signaling or TGF- β signaling (Fig. 6C,D).^{11–26}

Discussion

Effective early diagnosis is essential to improve the survival rate of HCC patients.⁴ Some genes are useful in the diagnosis and treatment of HCC, including *AFP*, heat shock protein (*HSP*), glypican-3 (*GPC-3*), Golgi protein 73 (*GP73*), Des- γ -carboxy prothrombin (*DCP*), γ -glutamyl transferase (*GGT*), *TGF- β 1*, vascular endothelial growth factor (*VEGF*), microRNA-21 (*miRNA-21*), *miRNA-29*, *miRNA-199*, and *miRNA-500*.^{4,27,28} However, it is still necessary to further understand the occurrence of, and mechanisms underlying, the development of HCC

to improve its diagnosis and treatment. In this study, it was found that high transcriptional levels of TMED5 in HCC tissues were associated with poor OS in patients, suggesting that TMED5 is involved in HCC progression.

The Golgi apparatus, which is an essential organelle for protein transport and secretion, plays an important role in cellular life.²⁹ Also, there are many pro-apoptotic factors and mitosis-related molecules in the Golgi membrane.²⁹ Several stimuli that promote cell death cause fragmentation of the Golgi apparatus and the subsequent induction of apoptosis and autophagy.²⁹ Therefore, Golgi function has a fundamental impact on the survival of cancer cells,²⁹ which indicates that the Golgi apparatus is a potential target for anticancer therapies. The TMED5 is a component of the Golgi apparatus essential for its maintenance and acts in the early stages of the secretory pathway.⁶ However, studies investigating the role of TMED5 in cancer are limited. Yang et al. revealed that TMED5 was upregulated in cervical cancer cells and promoted nuclear autophagy and malignant behavior,⁷ suggesting that TMED5 may play an important role in the progression of cancer. In this study, TMED5 promoted proliferation and metastasis but suppressed apoptosis in HCC cells, indicating that *TMED5* serves as an oncogene in HCC. Nevertheless, the molecular

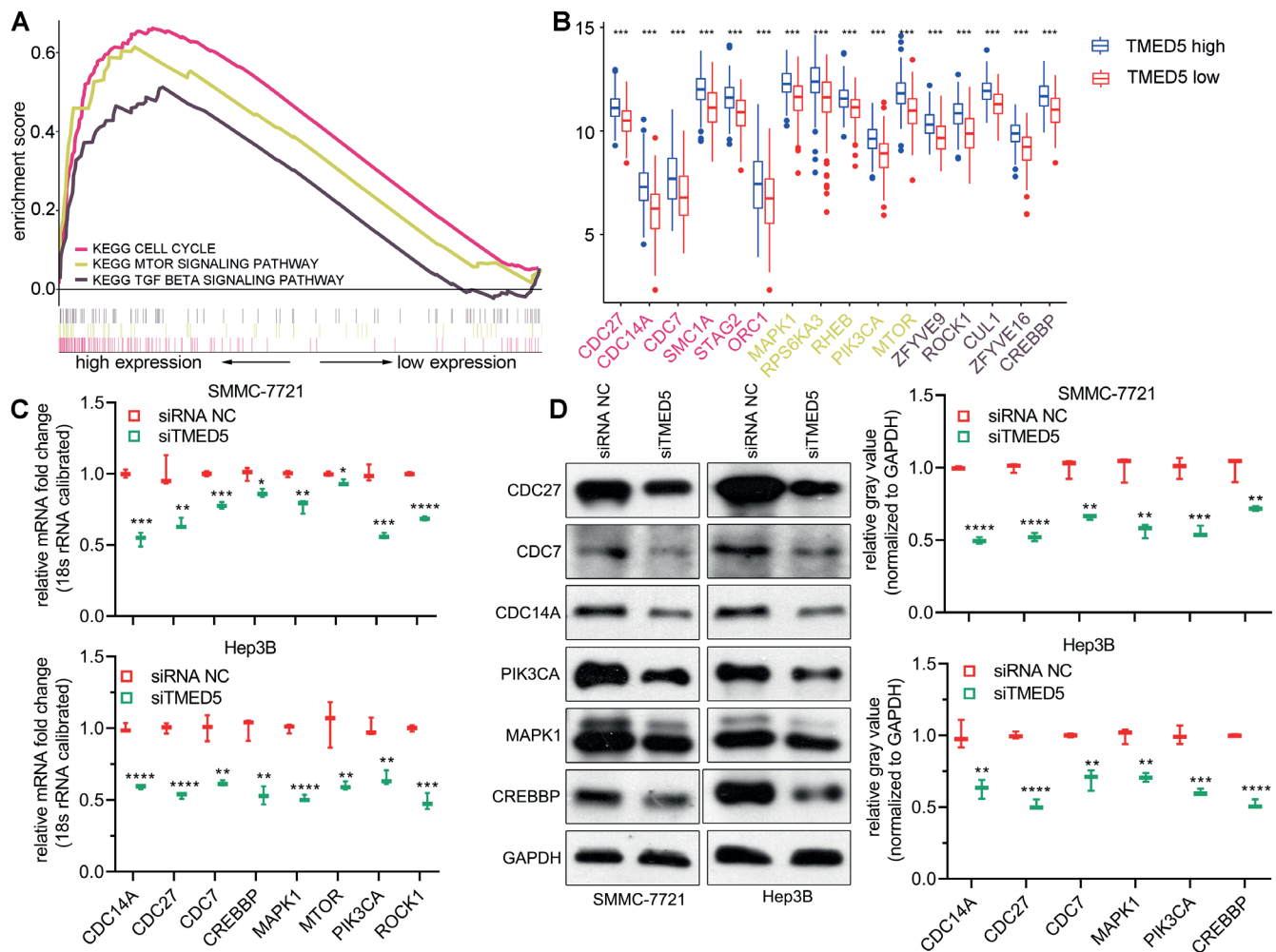


Fig. 6. Transmembrane P24 trafficking protein (TMED5) was positively correlated with the cell cycle, the mammalian target of rapamycin (mTOR) signaling pathway and the tumor growth factor beta (TGF- β) signaling pathway. **A.** The activation gene sets related to the cell cycle, mTOR signaling pathway and TGF- β signaling pathway are shown in the gene set enrichment analysis (GSEA) enrichment curve; **B.** The correlation between the expression of genes related to the cell cycle, mTOR signaling pathway and TGF- β signaling pathway, and the expression of TMED5 in HCC; **C, D.** The expression of CDC14A, CDC27, MAPK1, mTOR, PIK3CA, CREBBP, CDC7, and ROCK1 after *TMED5* silencing in SMMC-7721 and Hep3B cells. Mann-Whitney U test (**B**) and Student's unpaired t-test (**C**) were used for statistical analysis. Box plots indicate the outliers, the maximum, the minimum, the medians, the upper quartile (Q1), and the lower quartile (Q3). Outliers are defined as values that lie 1.5 times beyond the interquartile range (IQR) above Q3 and below Q1. The maximum is defined as 1.5 times the IQR above Q3. The minimum is defined as 1.5 times the IQR below Q1. All experiments were performed independently 3 times

* $p < 0.05$; ** $p < 0.01$; *** $p < 0.001$; **** $p < 0.0001$.

mechanism by which TMED5 promotes HCC progression is still unknown. We have shown that *TMED5* knockdown reduced the expression level of genes including *RHEB*, *CDC14A*, *SMC1A*, *CDC27*, *MAPK1*, *mTOR*, *RPS6KA3*, *PIK3CA*, *STAG2*, *ZFYVE16*, *ORC1*, *CREBBP*, *CDC7*, *CUL1*, *ROCK1*, and *ZFYVE9*, all of which are involved in cell cycle progression, mTOR signaling or TGF- β signaling,^{11–26} and whose abnormalities are closely related to the pathogenesis of cancers.^{30–32}

A previous study had revealed that TMED5 was up-regulated by MIR-G-1 (a type of miRNA) in cervical cancer cells in a G-rich RNA sequence binding factor 1 (GRSF1)-dependent manner, which promoted nuclear autophagy, malignant behavior and interaction with Wnt

family member 7B (WNT7B), thereby activating the classic WNT-catenin beta 1 (CTNNB1)/ β -catenin signaling pathway.⁷ However, whether TMED5 promotes the transcription of the aforementioned genes through the activation of the WNT7B/ β -catenin signaling pathway or other signaling pathways needs further investigation.

Limitations

Limitations of this study include the lack of animal experiments to further verify the findings. The detailed mechanism of action of TMED5 in the cell cycle, mTOR signaling pathway and TGF- β signaling pathway also require further investigation.

Conclusions

This study demonstrated that high transcriptional levels of TMED5 in HCC tissues were related to poor OS in HCC patients. Moreover, the downregulation of TMED5 expression in HCC cells inhibited proliferation, migration and invasion, and enhanced apoptosis. As such, TMED5 is a potential regulator of the cell cycle, mTOR signaling pathway and TGF- β signaling pathway, and has the potential to promote HCC.

ORCID iDs

Xianyi Cheng  <https://orcid.org/0000-0003-4265-6916>
 Xiulan Deng  <https://orcid.org/0000-0003-3214-006X>
 Huiping Zeng  <https://orcid.org/0000-0001-8567-4810>
 Tao Zhou  <https://orcid.org/0000-0003-1547-0462>
 Dezhi Li  <https://orcid.org/0000-0002-4500-7439>
 Wei V. Zheng  <https://orcid.org/0000-0002-8942-1543>

References

- Sagnelli E, Macera M, Russo A, Coppola N, Sagnelli C. Epidemiological and etiological variations in hepatocellular carcinoma. *Infection*. 2020;48(1):7–17. doi:10.1007/s15010-019-01345-y
- Waller LP. Hepatocellular carcinoma: A comprehensive review. *World J Hepatol*. 2015;7(26):2648–2663. doi:10.4254/wjh.v7.i26.2648
- Zhao YJ, Ju Q, Li GC. Tumor markers for hepatocellular carcinoma. *Mol Clin Oncol*. 2013;1(4):593–598. doi:10.3892/mco.2013.119
- Tak H, Kang H, Ji E, Hong Y, Kim W, Lee EK. Potential use of TIA-1, MFF, microRNA-200a-3p, and microRNA-27 as a novel marker for hepatocellular carcinoma. *Biochem Biophys Res Commun*. 2018;497(4):1117–1122. doi:10.1016/j.bbrc.2018.02.189
- Li D, Zhang J, Li J. Role of miRNA sponges in hepatocellular carcinoma. *Clin Chim Acta*. 2020;500:10–19. doi:10.1016/j.cca.2019.09.013
- Koegler E, Bonnon C, Waldmeier L, Mitrovic S, Halbeisen R, Hauri HP. p28, a novel ERGIC/cis Golgi protein, required for Golgi ribbon formation. *Traffic*. 2010;11(1):70–89. doi:10.1111/j.1600-0854.2009.01009.x
- Yang Z, Sun Q, Guo J, et al. GRSF1-mediated MIR-G-1 promotes malignant behavior and nuclear autophagy by directly upregulating TMED5 and LMNB1 in cervical cancer cells. *Autophagy*. 2019;15(4):668–685. doi:10.1080/15548627.2018.1539590
- Scaravilli M, Asero P, Tammela TL, Visakorpi T, Saramäki OR. Mapping of the chromosomal amplification 1p21-22 in bladder cancer. *BMC Res Notes*. 2014;7(1):547. doi:10.1186/1756-0500-7-547
- Goldman M, Craft B, Swatloski T, et al. The UCSC Cancer Genomics Browser: Update 2015. *Nucleic Acids Res*. 2015;43(D1):D812–D817. doi:10.1093/nar/gku1073
- Xu X, Zheng S. MiR-887-3p negatively regulates STARD13 and promotes pancreatic cancer progression. *Cancer Manag Res*. 2020;12:6137–6147. doi:10.2147/CMAR.S260542
- Jin L, Williamson A, Banerjee S, Philipp I, Rape M. Mechanism of ubiquitin-chain formation by the human anaphase-promoting complex. *Cell*. 2008;133(4):653–665. doi:10.1016/j.cell.2008.04.012
- Yazdi PT, Wang Y, Zhao S, Patel N, Lee EYHP, Qin J. SMC1 is a downstream effector in the ATM/NBS1 branch of the human S-phase checkpoint. *Genes Dev*. 2002;16(5):571–582. doi:10.1101/gad.970702
- Imtiaz A, Belyantseva IA, Beirl AJ, et al. CDC14A phosphatase is essential for hearing and male fertility in mouse and human. *Hum Mol Genet*. 2018;27(5):780–798. doi:10.1093/hmg/ddx440
- Sancak Y, Bar-Peled L, Zoncu R, Markhard AL, Nada S, Sabatini DM. Regulator-Rag complex targets mTORC1 to the lysosomal surface and is necessary for its activation by amino acids. *Cell*. 2010;141(2):290–303. doi:10.1016/j.cell.2010.02.024
- Wortzel I, Seger R. The ERK cascade: Distinct functions within various subcellular organelles. *Genes Cancer*. 2011;2(3):195–209. doi:10.1177/1947601911407328
- Cheng X, Ma X, Zhu Q, et al. Pacer is a mediator of mTORC1 and GSK3-TIP60 signaling in regulation of autophagosome maturation and lipid metabolism. *Mol Cell*. 2019;73(4):788–802.e7. doi:10.1016/j.molcel.2018.12.017
- Zhou Y, Yamada N, Tanaka T, et al. Crucial roles of RSK in cell motility by catalysing serine phosphorylation of EphA2. *Nat Commun*. 2015;6(1):7679. doi:10.1038/ncomms8679
- Di Donato N, Rump A, Mirzaa GM, et al. Identification and characterization of a novel constitutional PIK3CA mutation in a child lacking the typical segmental overgrowth of PIK3CA-related overgrowth spectrum. *Hum Mutat*. 2016;37(3):242–245. doi:10.1002/humu.22933
- Prieto I, Pezzi N, Buesa JM, et al. STAG2 and Rad21 mammalian mitotic cohesins are implicated in meiosis. *EMBO Rep*. 2002;3(6):543–550. doi:10.1093/embo-reports/kvf108
- Seet LF, Liu N, Hanson BJ, Hong W. Endofin recruits TOM1 to endosomes. *J Biol Chem*. 2004;279(6):4670–4679. doi:10.1074/jbc.M311228200
- Tocilj A, On KF, Yuan Z, et al. Structure of the active form of human origin recognition complex and its ATPase motor module. *eLife*. 2017;6:e20818. doi:10.7554/eLife.20818
- Iyer-Bierhoff A, Krogh N, Tessarz P, Ruppert T, Nielsen H, Grummt I. SIRT7-dependent deacetylation of fibrillarin controls histone H2A methylation and rRNA synthesis during the cell cycle. *Cell Rep*. 2018;25(11):2946–2954.e5. doi:10.1016/j.celrep.2018.11.051
- Montagnoli A. Drf1, a novel regulatory subunit for human Cdc7 kinase. *EMBO J*. 2002;21(12):3171–3181. doi:10.1093/emboj/cdf290
- Scott DC, Rhee DY, Duda DM, et al. Two distinct types of E3 ligases work in unison to regulate substrate ubiquitylation. *Cell*. 2016;166(5):1198–1214.e24. doi:10.1016/j.cell.2016.07.027
- Niemann MCE, Bartrina I, Ashikov A, et al. Arabidopsis ROCK1 transports UDP-GlcNAc/UDP-GalNAc and regulates ER protein quality control and cytokinin activity. *Proc Natl Acad Sci U S A*. 2015;112(1):291–296. doi:10.1073/pnas.1419050112
- Lin HK, Bergmann S, Pandolfi PP. Cytoplasmic PML function in TGF- β signalling. *Nature*. 2004;431(7005):205–211. doi:10.1038/nature02783
- Arai T, Kobayashi A, Ohya A, et al. Assessment of treatment outcomes based on tumor marker trends in patients with recurrent hepatocellular carcinoma undergoing trans-catheter arterial chemo-embolization. *Int J Clin Oncol*. 2014;19(5):871–879. doi:10.1007/s10147-013-0634-6
- Asaoka Y, Tateishi R, Nakagomi R, et al. Frequency of and predictive factors for vascular invasion after radiofrequency ablation for hepatocellular carcinoma. *PLoS One*. 2014;9(11):e111662. doi:10.1371/journal.pone.0111662
- Migita T, Inoue S. Implications of the Golgi apparatus in prostate cancer. *Int J Biochem Cell Biol*. 2012;44(11):1872–1876. doi:10.1016/j.biocel.2012.06.004
- Phan TG, Croucher PL. The dormant cancer cell life cycle. *Nat Rev Cancer*. 2020;20(7):398–411. doi:10.1038/s41568-020-0263-0
- Ayuk SM, Abrahamse H. mTOR signaling pathway in cancer targets photodynamic therapy in vitro. *Cells*. 2019;8(5):431. doi:10.3390/cells8050431
- Colak S, ten Dijke P. Targeting TGF- β signaling in cancer. *Trends Cancer*. 2017;3(1):56–71. doi:10.1016/j.trecan.2016.11.008

Hsa-circ-0000098 promotes the progression of hepatocellular carcinoma by regulation of miR-136-5p/MMP2 axis

Yunfei Cheng^{A–F}

Department of Hepatobiliary Surgery, Xiantao First People's Hospital, China

A – research concept and design; B – collection and/or assembly of data; C – data analysis and interpretation; D – writing the article; E – critical revision of the article; F – final approval of the article

Advances in Clinical and Experimental Medicine, ISSN 1899–5276 (print), ISSN 2451–2680 (online)

Adv Clin Exp Med. 2023;32(6):689–700

Address for correspondence

Yunfei Cheng
E-mail: yun7feic@163.com

Funding sources

None declared

Conflict of interest

None declared

Received on October 19, 2021
Reviewed on November 12, 2021
Accepted on December 1, 2022

Published online on March 7, 2023

Abstract

Background. Many papers revealed the abnormal expression of circular RNA (circRNA), a kind of non-coding RNA, in mammals. However, the potential functional mechanisms are still unknown.

Objectives. In this paper, we aimed to elucidate the function and mechanisms of hsa-circ-0000098 in hepatocellular carcinoma (HCC).

Materials and methods. Bioinformatics was used to analyze the Gene Expression Omnibus (GEO) database (GSE97332) and predict the targeted gene site of miR-136-5p. The starBase online database was utilized to predict that *MMP2* is the downstream target gene of miR-136-5p. The expression of hsa_circ_0000098, miR-136-5p and matrix metalloproteinase 2 (MMP2) in HCC tissues or cells was detected using quantitative real-time polymerase chain reaction (qRT-PCR) method. The migration and invasion abilities of processing cells were measured with transwell assay. The luciferase reporter assay was carried out to verify the targets of hsa_circ_0000098, MMP2 and miR-136-5p. The western blot assay was performed to detect the expression of MMP2, MMP9, E-cadherin, and N-cadherin.

Results. According to the analysis of GEO database of GSE97332, hsa_circ_0000098 had a prominent expression in HCC tissues. A continued analysis of relevant patients has verified that the high expression of hsa_circ_0000098 is present in HCC tissues with relative to poor prognosis. We also proved that the migration and invasion abilities of HCC cell lines can be inhibited by silencing hsa_circ_0000098. In view of the above findings, we continued to study the hsa_circ_0000098 mechanism of action in HCC. The study revealed that hsa_circ_0000098 can sponge miR-136-5p and then regulate *MMP2*, which is a downstream target gene of miR-136-5p, in order to promote HCC metastasis by regulation of miR-136-5p/MMP2 axis.

Conclusions. Our data showed that hsa_circ_0000098 facilitates the migration, invasion and malignant progression of HCC. On the other hand, we demonstrated that the mechanism of action of hsa_circ_0000098 in HCC might be due to the regulation of miR-136-5p/MMP2 axis.

Key words: hepatocellular carcinoma, MMP2, miR-136, hsa_circ_0000098

Cite as

Cheng Y. Hsa-circ-0000098 promotes the progression of hepatocellular carcinoma by regulation of miR-136-5p/MMP2 axis. *Adv Clin Exp Med.* 2023;32(6):689–700. doi:10.17219/acem/157063

DOI

10.17219/acem/157063

Copyright

Copyright by Author(s)

This is an article distributed under the terms of the Creative Commons Attribution 3.0 Unported (CC BY 3.0) (<https://creativecommons.org/licenses/by/3.0/>)

Background

Liver cancer is a malignant disease responsible for the majority of disease-induced deaths worldwide.¹ As a kind of hepatic malignancy, hepatocellular carcinoma (HCC) has become the 3rd leading cause of mortality and the 6th most common malignancy.² In the initial stage, liver cancer has hidden characteristics so that most people ignore the disease and get a belated diagnosis. Gene expression therapy or transplant is the common therapeutic method.³ Despite tremendous efforts invested in the past few decades, surgical techniques and chemoradiotherapy regimens that are used to cure HCC result in a limited prognostic improvement. The 5-year survival rate of HCC patients is not satisfactory.^{4,5} Although some reports indicate that many genes are related to the carcinogenicity of HCC,⁶ there is no convincing evidence to expound the exact molecular mechanism. Therefore, it is important for researchers to explore the pathogenic process and molecular mechanism of HCC.

Circular RNAs (circRNAs), an important class of non-coding RNAs (ncRNAs), can participate in numerous physiological processes,⁷ including encoding proteins,⁸ sponging miRNA⁹ and regulating gene transcription.¹⁰ Gene expression can be regulated by ncRNAs at the transcriptional and post-transcriptional level, thus various ncRNAs play fundamental roles in the metastasis and tumorigenesis of HCC.¹¹ On the other hand, different from usual linear RNAs, circRNAs have covalently closed loop structures without the polyadenylation tail, which are more stable when interacting with RNA exonuclease.^{12,13} Circular RNAs are broadly expressed in mammals and their expression is related to various human diseases, especially cancer.¹⁴ They are correlated with metastasis, drug resistance and tumorigenesis.¹⁵ In the past few years, it has been reported that lots of circRNAs (hsa_cir_0007874,¹⁶ hsa_ccirc_0000847¹⁷) have been reported to be involved in HCC and regulate the progression of the disease.¹⁴ Furthermore, there are studies indicating that circRNAs (hsa_circ_002059, hsa_circ_0000096^{18,19}) can govern the migration and proliferation of gastric cancer cells according to the modulation of gene expression of matrix metalloproteinase-2 (MMP2), MMP9 and E-cadherin. However, functional mechanisms of circRNAs need further research.

Objectives

In this study, we performed an integrated analysis of circ_0000098, a kind of circRNA that has not been mentioned in the previous studies, to figure out the molecular and functional mechanisms for the diagnosis and therapy of HCC.

Materials and methods

Cell culture and samples

Four HCC cell lines (Hep3B, Huh7, MHCC97L, and SK-hep1) which are representative cell lines in HCC research, and normal human liver cell line (THLE-21) were purchased from American Type Culture Collection (ATCC, Manassas, USA). The cells were cultured in Dulbecco's modified Eagle's medium (DMEM; Thermo Fisher Scientific, Waltham, USA) containing 10% fetal bovine serum (FBS; Gibco, Waltham, USA), 100 units/mL of penicillin, 100 µg/mL of streptomycin (Invitrogen, Carlsbad, USA), and 2 mM of L-glutamine in a humidified atmosphere containing 5% CO₂ at 37°C. The tumor and adjacent noncancerous specimens were surgically dissected from 64 patients with HCC at Xiantao First People's Hospital Affiliated to Yangtze University, Jingzhou, China. All the procedures were performed according to the Declaration of Helsinki. The protocols were discussed with the patients and written informed consent was obtained before the surgical collection of the samples. Samples were immediately stored at -80°C until further use. The study was approved by the ethical review committee of Xiantao First People's Hospital Affiliated to Yangtze University (approval No. KY-E-2020-8-10).

Cell transfections

The vector responsible for lentiviral overexpression in circ_0000098 was transfected into Hep3B and SK-hep1 cell lines by adding puromycin into the stable cells. We performed circRNA knockdown using validated Stealth RNAi siRNA against circ_0000098 (Invitrogen), according to the manufacturer's instructions. In brief, 4×10⁵ cells were seeded in 60-millimeter plates, and siRNA treatment was performed the next day. A total of 100 µL transfection reagent mixture Lipofectamine™ 2000 (Thermo Fisher Scientific) was obtained after mixing 20 nM of transfection solutions with HiPerFect Transfection Reagent (Qiagen, Valencia, USA) and serum free media. The amount used and serum free media were used according to the instruction manual of the HiPerFect Transfection Reagent. Then, the transfection complexes were fed by incubating the mixture solution for 15 min. Subsequently, cells were inoculated with 10 µL solutions, the mixture solution was incubated at 37°C for 48 h and cells were collected 72 h after transfection for subsequent experimentation. The procedures were followed by gene silencing.

Nuclear/cytoplasmic fractionation and quantitative real-time polymerase chain reaction assay

The extraction of nuclear and cytoplasmic RNA from tumor samples was performed using the extraction reagent (Pierce™ 660nm Protein Assay Reagent; Thermo Fisher Scientific). The amount of used liver cancer cells was equal

to 1×10^7 and the principal method complied with the manufacturer's instructions. RiboLock RNase inhibitors were introduced and the isolation of total RNA was performed using whole-cell lysates of RNase R achieved using RN-Aesay mini kits (Qiagen). The circumstantial experimental method was performed as following. A total of 250 μ L of each fraction were instilled with 750 μ L of TRIzol Reagent for RNA extraction. The cDNA synthesis was performed using 1 μ g total RNA in 20 μ L reaction volumes by means of All-In-One 5X RT MasterMix (Takara, Shiga, Japan). The *U6* was used as a reference gene of miR-136-5p, and *GAPDH* was used as a reference gene of hsa_circ_0000098 and MMP2. Relative gene expression was measured using the $2^{-\Delta\Delta Ct}$ method. The primer sequences were as following:

hsa_circ_0000098 forward:
5'-GGTGTAATTGCTTCTGCCATCA-3',
reverse: 5'-GTCCAGCCAAAATGGCAGTG-3';
miR-136-5p forward:
5'-ACACTCCAGCTGGGACTCCATTTGTTTT-3',
reverse: 5'-CCAGTGCAGGGTCCGAGGT-3';
MMP2 forward: 5'-GTGAAGTATGGGAACGCCG-3',
reverse: 5'-GCCGTA CTGCCATCCTTCT-3';
GAPDH forward: 5'-GAAAGCTGCCGGTACTAA-3',
reverse: 5'-GCGCCCAATACGACCAAATC-3';
U6 forward: 5'-CTCGCTTCGGCAGCAC-3',
reverse: 5'-AACGCTTACGAATTTGCGT-3'.

RNA pull-down assay

For RNA pull-down assay, biotinylated miR-136-5p probe was obtained from RiboBio (Guangzhou, China). The C-1 magnetic beads (Thermo Fisher Scientific) were used to incubate with the probe in order to acquire probe-coated beads. Then, they were incubated with cell lysates Hep3B and SK-hep1 at 4°C. After the washing of RNA complexes, quantitative real-time polymerase chain reaction (qRT-PCR) assay was performed to determine the expression of miR-136-5p and MMP2.

RNA immunoprecipitation assay

The RNA immunoprecipitation assay (RIPA) was performed using EZMagna RIP kit obtained from EMD Millipore (Burlington, USA). The relevant experiments were carried out in accordance with the manufacturer's guidelines. Briefly, cells (Hep3B, SK-hep1) were lysed with RIPA lysis buffer. The supernatant was harvested after the centrifugation and cultured with magnetic beads conjugated to human anti-Ago2 antibody (Abcam, Cambridge, USA) or anti-IgG antibody (Abcam). Finally, the expression of hsa_circ_0000098 and miR-136-5p was detected using qRT-PCR assay.

Transwell assay

Transwell chambers (Corning Company, Corning, USA) were used to evaluate the migration and invasion abilities

of HCC cells. In brief, liver cancer cells (about 1×10^4 cells) were resuspended and planted into upper chambers with or without the addition of Matrigel (BD Bioscience, Waltham, USA). At the same time, 800 μ L medium with 30% FBS was added to the lower chambers. All chambers were incubated for 24 h at 37°C. Subsequently, transmigrated cells were set in the chambers. Then, crystal violet (Sigma-Aldrich, St. Louis, USA) was utilized to stain the cells. Finally, Nikon Diaphot inverted microscope (Nikon Corp., Tokyo, Japan) was utilized to count and photograph the migrated or invaded cells.

Western blot

Cells were lysed with RIPA lysis buffer, and BCA Protein Assay Kit (Beyotime Biotechnology, Beijing, China) was utilized to quantify them. Total proteins (40 μ g) were charged to sodium dodecyl-sulfate polyacrylamide gel electrophoresis (SDS-PAGE) gel and transferred onto a polyvinylidene difluoride (PVDF) membrane (EMD Millipore). The membrane was blocked with 5% skim milk and incubated with MMP2 (cat. No. AF1420), MMP9 (cat. No. AF5234), E-cadherin (cat. No. AF6759), and N-cadherin (cat. No. AF0243) antibodies (1:1000; Beyotime Biotechnology). After incubation, the secondary antibody horseradish peroxidase (HRP)-labeled Goat Anti-Rabbit IgG (H+L) (cat. No. A0208, 1:1000; Beyotime Biotechnology) was utilized to incubate the membrane. The membrane was then visualized with an electrochemiluminescence (ECL) reagent (Beyotime Biotechnology). Glyceraldehyde-3-phosphate dehydrogenase (GAPDH, cat. No. AF1186; Beyotime Biotechnology) was used as an internal control.

Dual-luciferase reporter assay

The hsa_circ_0000098 and MMP2 wild type (hsa_circ_0000098 wt and MMP2 wt) and mutant type (hsa_circ_0000098 mut and MMP2 mut) reporter vectors were set by Beijing TransGen Biotech Co. Ltd. (Beijing, China). The reporter plasmids were co-transfected with either miR-136-5p mimics or negative mimics control into Hep3B cells. After transfection for 48 h, the cells were lysed and the relevant luciferase activities were detected using a dual-luciferase reporter assay system (Promega, Madison, USA).

Statistical analyses

The IBM SPSS v. 20.0 (IBM Corp., Armonk, USA) was used to perform the statistical analyses. The Student's t test and one-way analysis of variance (ANOVA) followed by the Tukey's post hoc test were utilized to analyze 2 or multiple groups, respectively. The survival curves were assessed by the Kaplan–Meier (K–M) analysis. The log-rank test was used to analyze the difference between K–M curves. The χ^2 test was used to examine the correlation between hsa-circ-0000098 expression and clinical data.

The normality of the data and the homogeneity of variance between the groups were tested using the Shapiro–Wilk test and the Levene’s test, respectively. The value of $p > 0.05$ indicated that the assumption of normality of data and homogeneity of variance was consistent, and further parameter testing could be performed. The number of independent replications in all the experiments amounted to 3. The data are shown as mean \pm standard deviation ($M \pm SD$). The value of $p < 0.05$ was considered statistically significant. The results of the statistical analyses are presented in Table 1.

Results

High expression of hsa_circ_0000098 in HCC gives rise to worse prognosis

In order to investigate the impact of hsa_circ_0000098 on the development of HCC, 64 HCC patients have been chosen for this study. Their biopsied HCC and para-carcinoma tissues were collected and analyzed. To investigate the hsa_circ_0000098 expression profiles in HCC, we analyzed the microarray data from Gene Expression Omnibus (GEO) database GSE97332. Compared with normal tissues, hsa_circ_0000098 was highly expressed in HCC tumor

tissues, and the heat map and volcano plot both indicated the diversity of circRNAs (Fig. 1A). The qRT-PCR indicated that hsa_circ_0000098 was highly expressed in HCC tissues (Fig. 1B; $t = 14.88$, degrees of freedom (df) = 126, $p < 0.001$). Furthermore, in order to examine the difference in the hsa_circ_0000098 expression between HCC cells and normal cells, several HCC cell lines (Hep3B, Huh7, MHCC97L, SK-hep1) were compared with normal human liver cell (THLE-21). The results show that hsa_circ_0000098 has a high expression in all HCC cell lines, while the normal liver cell, THLE-21, shows an inferior expression ($F(4,10) = 161.7$, $p < 0.001$; Fig. 1C). As for Fig. 1D, we selected the median expression value of the HCC tissues in Fig. 1B as the cutoff value, and patients with HCC were divided into hsa_circ_0000098 high expression group ($n = 32$) and low expression group ($n = 32$). The K–M survivorship curve indicated that the prognostic survival rate of hsa_circ_0000098 high expression group is distinctly lower than that of the low expression group. Overall, the above data show that hsa_circ_0000098 is highly expressed in HCC, which gives rise to worse prognosis.

The relevant clinicopathological characteristics of patients are presented in Table 2, according to the degree of hsa_circ_0000098 expression after the χ^2 testing. The results revealed that the expression of hsa_circ_0000098 is closely related to tumor size ($p = 0.024$), tumor-node-metastasis

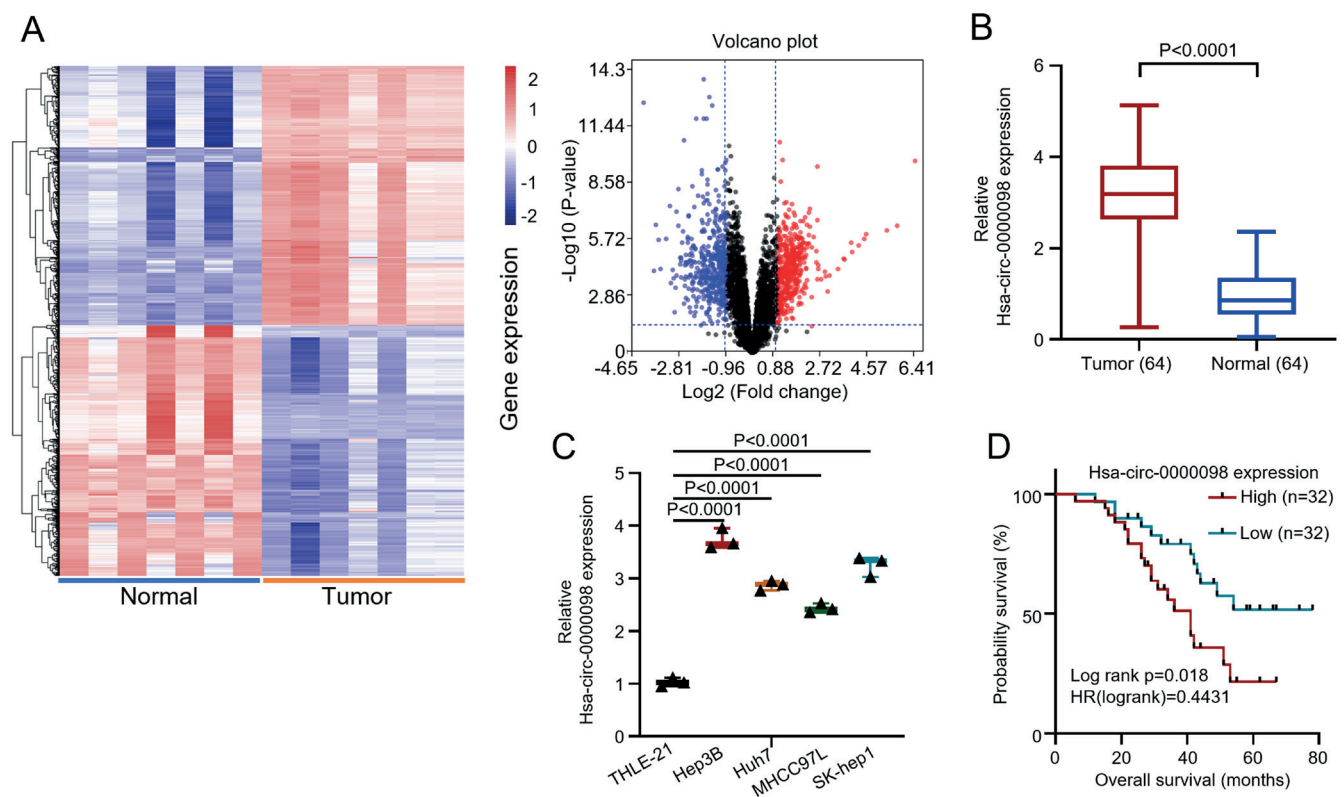


Fig. 1. Upregulated expression of hsa-circ-0000098 in hepatocellular carcinoma (HCC) tissue and cell lines. A. Hsa_circ_0000098 is highly expressed in liver cancer tissues from Gene Expression Omnibus (GEO) database. The heat map and volcano plots of circular RNAs (circRNAs) based on GSE97332; B. The expression level of hsa_circ_0000098 in 64 pairs of HCC tissues detected using quantitative real-time polymerase chain reaction (qRT-PCR). The Student’s t-test was utilized to analyze the 2 groups; C. The expression level of hsa_circ_0000098 in HCC cell lines (Hep3B, Huh7, MHCC97L, SK-hep1) and normal liver cell (THLE-21) was detected using qRT-PCR method. One-way analysis of variance (ANOVA) followed by the Tukey’s post hoc test were utilized to analyze multiple groups; D. The Kaplan–Meier (K–M) plotter was used to evaluate overall survival in HCC patients according to the expression of hsa_circ_0000098

Table 1. The results of Student's t-test and ANOVA

Figure	Method	F(df ₁ ,df ₂)	t	df	p _{SK}	p _L	p-value
Fig. 1B	Student's t-test	–	14.88	126	0.6374	0.4782	0.0001
Fig. 1C	ANOVA	F(4,10) = 161.7	–	–	0.3067	0.8670	0.0001
Fig. 2A (left)	ANOVA	F(2,6) = 346.3	–	–	0.9914	0.8775	0.0001
Fig. 2A (right)	ANOVA	F(2,6) = 442.1	–	–	0.9933	0.7664	0.0001
Fig. 2B (left)	ANOVA	F(2,6) = 159.4	–	–	0.7450	0.5141	0.0001
Fig. 2B (right)	ANOVA	F(2,6) = 349.4	–	–	0.5882	0.9434	0.0001
Fig. 2C (left)	ANOVA	F(2,6) = 813.6	–	–	0.2353	0.7973	0.0001
Fig. 2C (right)	ANOVA	F(2,6) = 300.9	–	–	0.6636	0.5491	0.0001
Fig. 3A (left)	ANOVA	F(2,12) = 234.9	–	–	0.7168	0.9750	0.0001
Fig. 3A (right)	ANOVA	F(1,12) = 142.6	–	–	0.8580	0.9747	0.0001
Fig. 3B	ANOVA	F(1,8) = 53.46	–	–	0.4385	0.3219	0.0001
Fig. 3C (left #1)	ANOVA	F(2,6) = 991.6	–	–	0.7155	0.5264	0.0001
Fig. 3C (left #2)	ANOVA	F(2,6) = 1099	–	–	0.3601	0.7117	0.0001
Fig. 3C (right #1)	ANOVA	F(2,6) = 402.4	–	–	0.5764	0.4504	0.0001
Fig. 3C (right #2)	ANOVA	F(2,6) = 2692	–	–	0.2478	0.1642	0.0001
Fig. 3D (left)	ANOVA	F(2,6) = 184.4	–	–	0.5168	0.6208	0.0001
Fig. 3D (right)	ANOVA	F(2,6) = 1048	–	–	0.9179	0.4489	0.0001
Fig. 3E	Student's t-test	–	10.78	126	0.4797	0.3356	0.0001
Fig. 3F	ANOVA	F(1,8) = 95.55	–	–	0.2764	0.4743	0.0001
Fig. 3G (left)	ANOVA	F(2,6) = 201	–	–	0.3336	0.8895	0.0001
Fig. 3G (right)	ANOVA	F(2,6) = 494.8	–	–	0.4209	0.3090	0.0001
Fig. 3H	Student's t-test	–	11.16	126	0.4972	0.6855	0.0001
Fig. 4A (left)	Student's t-test	–	45.51	4	0.5472	0.9981	0.0001
Fig. 4A (right)	Student's t-test	–	17	4	0.5506	0.9863	0.0001
Fig. 4B (left)	Student's t-test	–	56.28	4	0.2113	0.9987	0.0001
Fig. 4B (right)	Student's t-test	–	36.25	4	0.2072	0.9970	0.0001
Fig. 4C (left)	ANOVA	F(2,6) = 163.7	–	–	0.4326	0.6676	0.0001
Fig. 4C (right)	ANOVA	F(2,6) = 72.01	–	–	0.7013	0.5325	0.0001
Fig. 4D (left)	ANOVA	F(2,6) = 659	–	–	0.3611	0.7111	0.0001
Fig. 4D (right)	ANOVA	F(2,6) = 238.3	–	–	0.5107	0.9788	0.0001
Fig. 4E (left)	ANOVA	F(2,6) = 839.9	–	–	0.1701	0.8475	0.0001
Fig. 4E (right)	ANOVA	F(2,6) = 462	–	–	0.4776	0.9537	0.0001

ANOVA – analysis of variance; df – degrees of freedom; t – Student's t-test results; p_{SK} – Shapiro–Wilk test; p_L – Levene's test; df₁ – degrees of freedom of miR-NC compared to miR-136-5p mimics group; df₂ – degrees of freedom of miR-136-5p mimics compared to miR-136-5p mimics+Oe-circ group (p < 0.05 was considered statistically significant).

(TNM) stage (p = 0.024), differentiation (p = 0.035), and lymph node metastasis (p = 0.045). Inversely, the expression of hsa_circ_0000098 does not correlate with patient's age and gender.

Silence of hsa_circ_0000098 inhibits cell migration and invasion in vitro

In order to explore the relationship between severe HCC and hsa_circ_0000098, an established knockdown method was conducted in order to silence the hsa_circ_0000098 expression. First, Hep3B and SK-hep1 with the highest expression of hsa_circ_0000098 (Fig. 1C) were chosen

as experimental targets to be silenced by 2 designed shRNAs (sh-circ#1 and sh-circ#2). Figure 2A (F(2,6) = 346.3, p < 0.001, and F(2,6) = 442.1, p < 0.001) indicates that compared with short hairpin RNA negative control (sh-NC), sh-circ#1 and sh-circ#2 can effectively knock out more than 70% of hsa_circ_0000098 from Hep3B and SK-hep1 cells. The hsa_circ_0000098 was successfully knocked down. Subsequently, the transwell assay with or without pre-coated Matrigel was used to detect the migration and invasion abilities of Hep3B and SK-hep1 cells. The results proved that after the knockdown of hsa_circ_0000098, the migration and invasion abilities of Hep3B and SK-hep1 cells decreased (F(2,6) = 159.4, p < 0.001, and

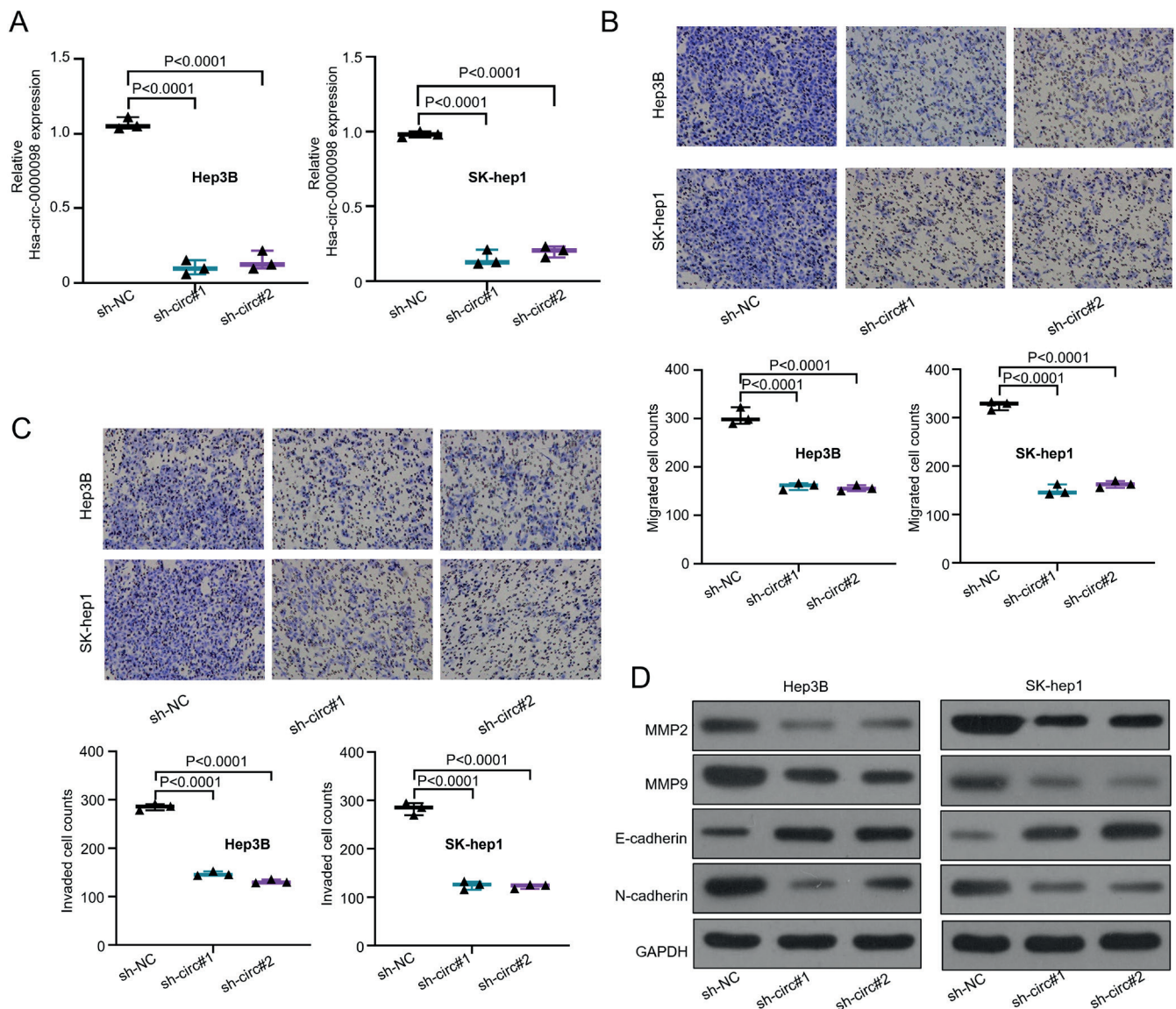


Fig. 2. Silencing of hsa-circ-0000098 inhibits hepatocellular carcinoma (HCC) cell migration and invasion in vitro. A. The knockdown efficiency of hsa_circ_0000098 measured using quantitative real-time polymerase chain reaction (qRT-PCR). Targeted shRNAs were designed according to the results presented in Fig. 1C. One-way analysis of variance (ANOVA) followed by the Tukey's post hoc test were utilized to analyze multiple groups; B. The migration ability of Hep3B and SK-hep1 cells based on the transwell assay (without pre-coated Matrigel). One-way ANOVA followed by the Tukey's post hoc test were utilized to analyze multiple groups; C. The invasion ability of Hep3B and SK-hep1 cells based on the transwell assay (with pre-coated Matrigel). One-way ANOVA followed by the Tukey's post hoc test were utilized to analyze multiple groups; D. The expression of MMP2, MMP9, E-cadherin, and N-cadherin detected with western blot assay based on Hep3B and SK-hep1 cells

$F(2,6) = 349.4$, $p < 0.001$, Fig. 2B; $F(2,6) = 813.6$, $p < 0.001$, and $F(2,6) = 300.9$, $p < 0.001$; Fig. 2C).

On the other hand, matrix metalloproteinases (like MMP2 and MMP9) can degrade almost all protein compositions in the extracellular matrix (ECM) and destroy the histological barriers of tumor cell invasion, playing a vital role in the tumor migration and invasion. Additionally, the tumor progression and migration are linked to E-cadherin and N-cadherin. Hence, through western blot assay, we detected the expression of MMP2, MMP9, E-cadherin, and N-cadherin in Hep3B and SK-hep1 cells transfected with sh-NC, sh-circ#1 and sh-circ#2. The expression of MMP2, MMP9 and N-cadherin shows a distinct

decrease after the knockdown of hsa_circ_0000098 both in Hep3B and SK-hep1 cells (Fig. 2D). The expression of E-cadherin shows a distinct increase. The results suggest that hsa_circ_0000098 has an important role in HCC migration and invasion.

Hsa-circ-0000098 is expressed in cytoplasm and functions as ceRNA through sponge mir-136-5p/MMP2 signal axis

The circRNA has the potential to act as a competitive endogenous RNA (ceRNA) to sponge miRNAs and mitigate

the inhibitory effect on the targeted mRNA expression.²⁰ In order to explore the hsa_circ_0000098 mechanism of action in HCC, we performed a series of experiments. First, the location of the highest hsa_circ_0000098 expression was estimated using qRT-PCR through nuclear/cytoplasmic fractionation. The graph presented in Fig. 3A ($F(2,12) = 234.9, p < 0.001$, and $F(2,12) = 440.3, p < 0.001$, and $F(1,12) = 50.04, p < 0.001$, and $F(1,12) = 142.6, p < 0.001$) indicates that most of hsa_circ_0000098 can be detected in the cytoplasm. However, the mature miRNAs are also present in the cytoplasm and there is the possibility of hsa_circ_0000098 to comb with miRNAs. The U6 and GAPDH were set as internal references of nucleus and cytoplasm, respectively. Then, we used a bioinformatics database (circRNA interactome: <https://circinteractome.irp.nia.nih.gov/>) to predict the potential target miRNA. We found that hsa_circ_0000098 can target miR-136-5p (Fig. 3B). Subsequently, the luciferase assay was conducted with Hep3B cells to confirm the prediction (Fig. 3C). The results indicate that compared with miRNA negative control (miR-NC), the overexpressed miR-136-5p can inhibit the luciferase activity of hsa_circ_0000098 wt in Hep3B cells. However, when we mutated circRNA, which was the binding site of predicted miR-136-5p, the corresponding inhibition disappeared ($F(1,8) = 53.46, p = 0.0001$; Fig. 3B). Then, the RIPA-qRT-PCR method was performed on Hep3B and SK-hep1 cells ($F(2,6) = 991.6, p = 0.0001$; $F(2,6) = 1099, p = 0.0001$; $F(2,6) = 402.4, p = 0.0001$; $F(2,6) = 2692, p = 0.0001$; Fig. 3C). The results

show that hsa_circ_0000098 could bind to miR-136-5p, whereas the beads coupled with AGO2 pulled down significantly greater hsa_circ_0000098 and miR-136-5p than the IgG control. The results presented in Fig. 3D ($F(2,6) = 184.4, p < 0.001$, and $F(2,6) = 1048, p < 0.001$) indicate that both sh-circ#1 and sh-circ#2 can increase the expression of miR-136-5p in Hep3B and SK-hep1 cells. The qRT-PCR indicated that miR-136-5p is down-regulated in HCC tissues ($t = 10.78, df = 126, p < 0.001$; Fig. 1E). Figure 3F presents the consequence of 3'-UTR of the *MMP2* gene on the binding site of miR-136-5p. The analysis was predicted using starBase on-line database (<http://starbase.sysu.edu.cn>). On the other hand, the luciferase assay was undertaken with Hep3B ($F(1,8) = 95.55, p < 0.001$; Fig. 3F). The results suggest that compared with miR-NC, the overexpressed miR-136-5p can inhibit the luciferase activity of *MMP2* wt in Hep3B cells. However, when the binding site of predicted miR-136-5p was mutated, the corresponding inhibition disappeared. Finally, the variation of *MMP2* expression in Hep3B and SK-hep1 cells was measured using qRT-PCR, after the knockdown of hsa_circ_0000098. The results indicate that in both Hep3B and SK-hep1 cells, sh-circ#1 and sh-circ#2 can decrease the expression of *MMP2* ($F(2,6) = 201, p < 0.001$; $F(2,6) = 494.8, p < 0.001$; Fig. 3G). Similar to hsa_circ_0000098, *MMP2* was upregulated in HCC tissue ($t = 11.16, df = 126, p = 0.0001$; Fig. 3H). The sh-NC was used to make comparisons with sh-circ#1 and sh-circ#2.

Table 2. Relationship between hsa_circ_0000098 expression and the clinicopathological parameters in HCC tissue samples

Clinicopathological characteristics	Hsa-circ-0000098 high expression (n = 32)	Hsa-circ-0000098 low expression (n = 32)	χ^2	p-value
Gender				
Male	15	16	0.063	0.802
Female	17	16		
Age				
≤50	17	20	0.577	0.448
>50	15	12		
Tumor size				
T1 + T2	10	19	5.107	0.024
T3 + T4	22	13		
Differentiation				
Poor	7	15	4.433	0.035
Moderate + high	25	17		
Lymph node metastasis				
Negative	11	19	4.016	0.045
Positive	21	13		
TNM stages				
I + II	10	19	5.107	0.024
III + IV	22	13		

HCC – hepatocellular carcinoma; TNM – tumor-node-metastasis.

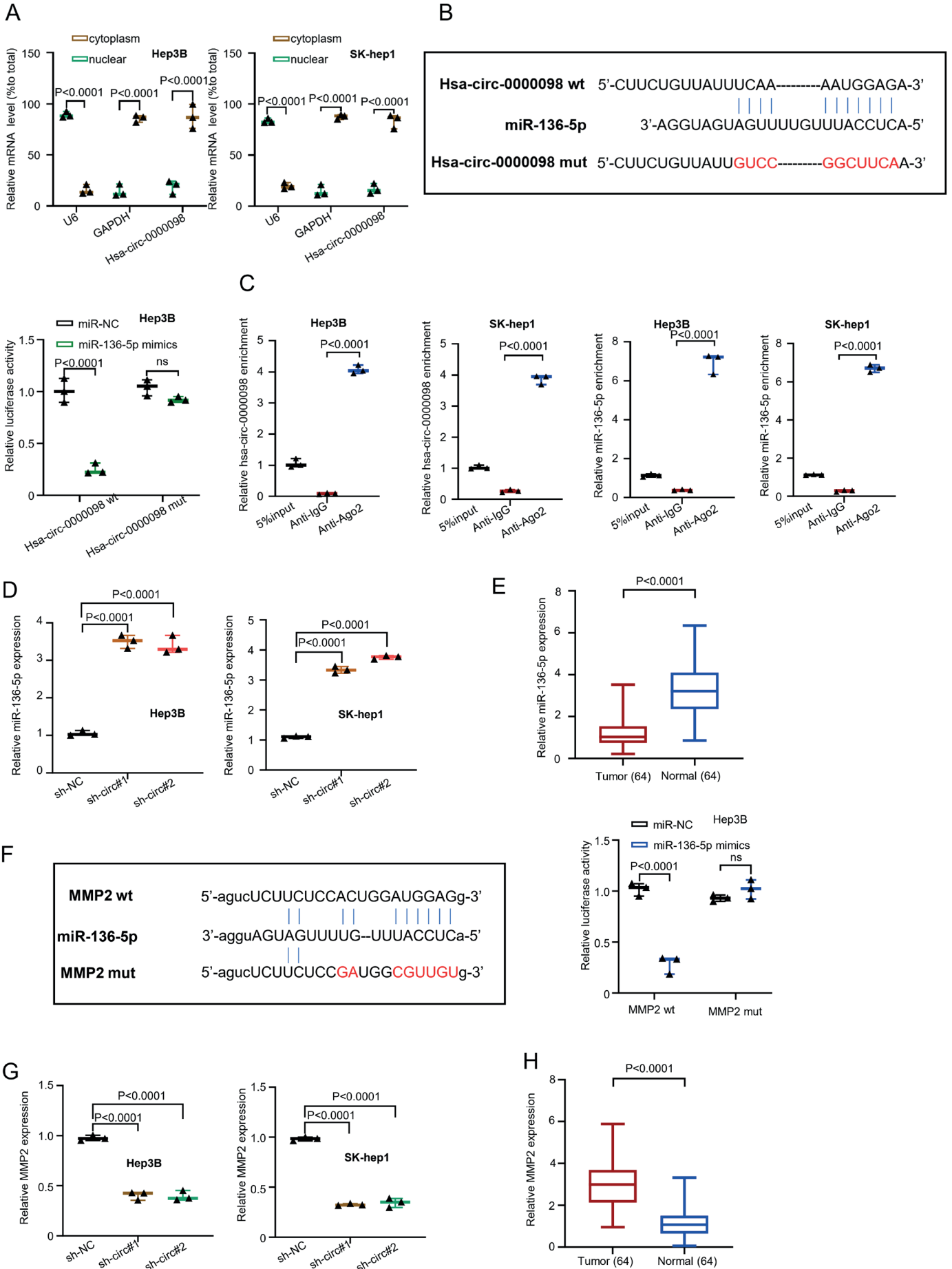


Fig. 3. Hsa_circ_0000098 was expressed in cytoplasm and functions as competitive endogenous RNA (ceRNA) through sponge miR-136-5p/MMP2 signal axis. A. The expression of hsa_circ_0000098 in cytoplasm and nucleus detected with quantitative real-time polymerase chain reaction (qRT-PCR), based on Hep3B and SK-hep1 cells. One-way analysis of variance (ANOVA) followed by the Tukey's post hoc test were utilized to analyze multiple groups; B. The predicted binding sites between hsa_circ_0000098 and miR-136-5p were confirmed with luciferase reporter gene assay in Hep3B. One-way ANOVA followed by the Tukey's post hoc test were utilized to analyze multiple groups; C. RNA immunoprecipitation assay (RIPA)-qRT-PCR method was used in Hep3B and SK-hep1 cells to measure the difference in anti-IgG and anti-Ago2. One-way ANOVA followed by the Tukey's post hoc test were utilized to analyze multiple groups; D. The expression of miR-136-5p in Hep3B and SK-hep1 cells after the knockdown of hsa_circ_0000098 detected using qRT-PCR method. One-way ANOVA followed by the Tukey's post hoc test were utilized to analyze multiple groups; E. The expression level of miR-136-5p in 64 pairs of HCC tissues detected using qRT-PCR. The Student's t-test was utilized to analyze the 2 groups; F. The binding sites of miR-136-5p on MMP2 were confirmed and utilized to conduct the luciferase reporter gene assay. One-way ANOVA followed by the Tukey's post hoc test were utilized to analyze multiple groups; G. The expression of MMP2 in Hep3B and SK-hep1 cells after the knockdown of hsa_circ_0000098 detected using qRT-PCR method; H. The expression level of MMP2 in 64 pairs of HCC tissues detected with qRT-PCR. The Student's t-test was utilized to analyze the 2 groups

Hsa_circ_0000098 promotes HCC migration and invasion by regulating miR-136-5p/MMP2 axis

The described experiments proved that hsa_circ_0000098 plays a critical role in HCC cell migration and invasion. Yet, the exact regulatory mechanism is still unknown. In view of this and previous studies, we designed a series of experiments to examine the relevant mechanism. Synthesized miR-136-5p mimics were overexpressed in Hep3B and SK-hep1 cells. Thus, qRT-PCR method was used to evaluate the efficiency of overexpression. The used symbols and abbreviations are as follows: t_1 – Student's t-test results of miR-NC compared to miR-136-5p mimics group; t_2 – t-test results of miR-136-5p mimics compared to miR-136-5p mimics+Oe-circ group; df_1 – degrees of freedom of miR-NC compared to miR-136-5p mimics group; df_2 – degrees of freedom of miR-136-5p mimics compared to miR-136-5p mimics+Oe-circ group ($p < 0.05$ was considered statistically significant); p_1 – p-value of miR-NC compared to miR-136-5p mimics group; p_2 – p-value of miR-136-5p mimics compared to miR-136-5p mimics+Oe-circ group.

The results indicate that miR-136-5p mimics, compared with miR-NC, can be overexpressed in both Hep3B and SK-hep1 cells ($t_1 = 45.51$, $df_1 = 4$, $p_1 < 0.001$; $t_2 = 17$, $df_2 = 4$, $p_2 < 0.001$; Fig. 4A). Then, the overexpressed hsa_circ_0000098 (Oe-circ) was constructed by transfecting Hep3B and SK-hep1 cells. Figure 4B ($t_1 = 56.28$, $df_1 = 4$, $p_1 < 0.001$; $t_1 = 36.25$, $df_1 = 4$, $p_1 < 0.001$) displays the results of the evaluation of the efficiency of overexpression: compared with vector, Oe-circ can be effectively overexpressed with hsa_circ_0000098 in Hep3B and SK-hep1 cells. Thus, after the overexpression of miR-136-5p, we detected the expression variation of MMP2. The results revealed that the overexpressed miR-136-5p decreases the expression of MMP2 ($F(2,6) = 163.7$, $p = 0.0001$; $F(2,6) = 72.01$, $p = 0.0001$; Fig. 4C). After the co-transfection of Oe-circ, the expression of MMP2 has increased. The transwell assay was used to detect the migration and invasion abilities of different groups (miR-NC, miR-136-5p mimics and miR-136-5p mimics+Oe-circ) in Hep3B and SK-hep1 cells. The similar results presented in Fig. 4D ($F(2,6) = 659$, $p_{SK} = 0.3611$; $p_L = 0.7111$ (p_{SK} – Shapiro–Wilk test; p_L – Levene's test); $F(2,6) = 238.3$, $p < 0.001$) and Fig. 4E ($F(2,6) = 839.9$, $p < 0.001$, and $F(2,6) = 462$, $p < 0.001$)

indicate that the overexpressed miR-136-5p can decrease the migration and invasion abilities of these 2 cell lines, while after the co-transfection of Oe-circ, the migration and invasion abilities of Hep3B and SK-hep1 cells increase (Fig. 4D,E). Finally, the western blot assay was used to detect the expression of MMP2, MMP9, E-cadherin, and N-cadherin in different groups (miR-NC, miR-136-5p mimics, miR-136-5p mimics+Oe-circ) in Hep3B and SK-hep1 cells. The results show that miR-136-5p decreased the expression of MMP2, MMP9 and N-cadherin, and increased the expression of E-cadherin (Fig. 4F); however, after the co-transfection of Oe-circ, the expression of MMP2, MMP9 and N-cadherin increased and the expression of E-cadherin decreased, which corresponds with our assumptions.

Discussion

Hepatocellular carcinoma is the 3rd leading cause of the cancer-related mortality worldwide. It is a multifactorial disease caused by various risk factors such as cirrhosis, alcohol abuse, viral infections, and others.^{21–24} The circRNAs have drawn attention as oncogenes or suppressors of cancer progression.^{16,25} Since circRNAs are nonlinear reverse splicing structures, they are more stable even under the dispose of RNase R.^{19,26–28} Until now, the studies have described circRNAs as ceRNAs which can sponge miRNA in order to regulate mRNA expression in HCC.^{27,29,30} For example, circRNA hsa_circRNA_104348 promotes HCC progression through modulating miR-187-3p/RTKN2 axis and activating Wnt/ β -catenin pathway.³¹ The circRNA-5692 inhibits the progression of HCC by sponging miR-328-5p to improve the expression of DAB2IP.³² The circRNA-104718 acts as a competing endogenous RNA and promotes HCC progression through microRNA-218-5p/TXNDC5 signaling pathway.³³ However, the specific function and mechanism of hsa_circ_0000098 associated with tumorigenesis and progression of HCC are still unclear. In this study, we designed a series of experiments to explore the specific role of hsa_circ_0000098 in HCC and confirmed that hsa_circ_0000098 is highly expressed in HCC. Afterwards, the in vitro studies confirmed that hsa_circ_0000098 is extremely involved in the HCC progression.

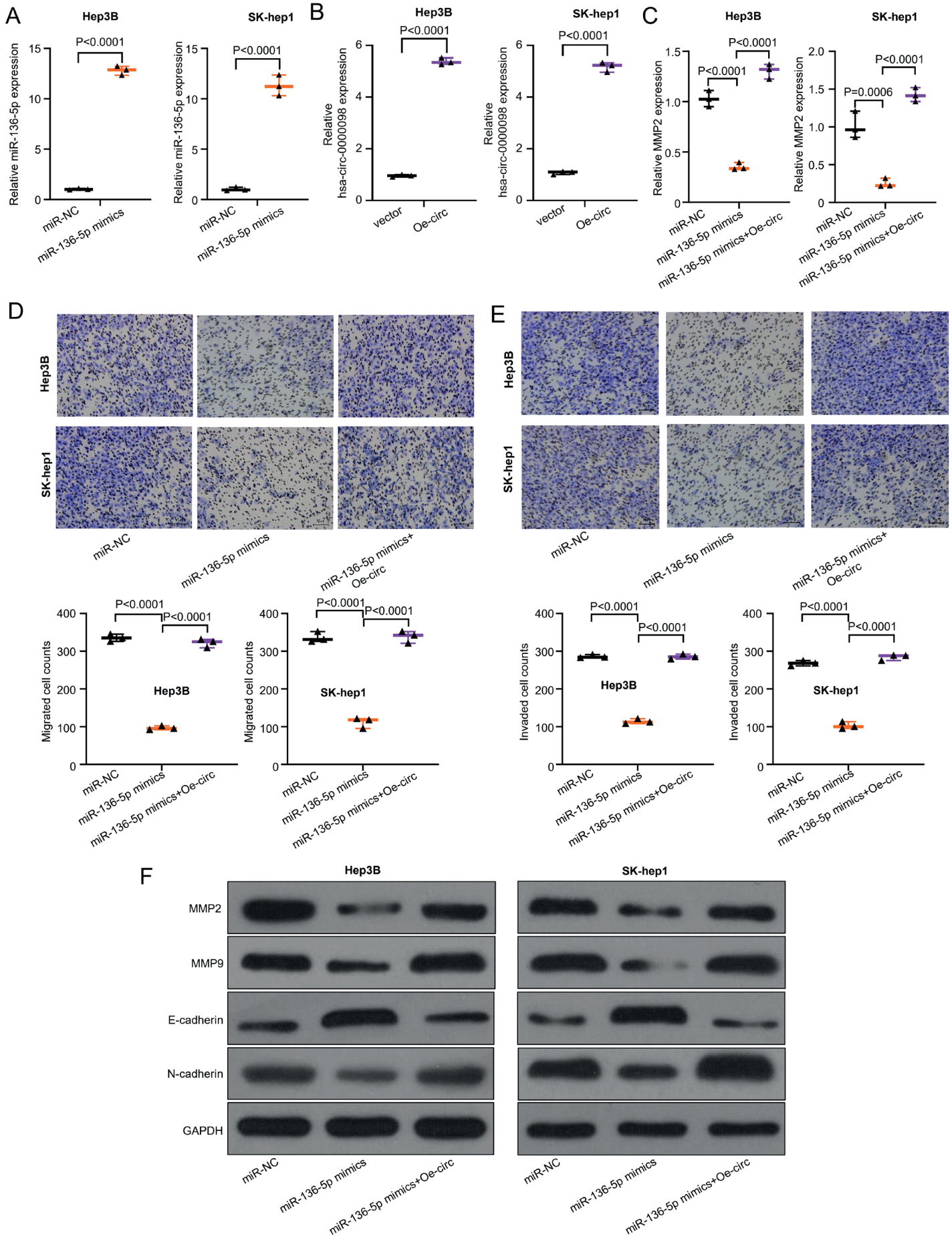


Fig. 4. Hsa_circ_0000098 promotes hepatocellular carcinoma (HCC) migration and invasion by regulation of miR-136-5p/MMP2 axis. A. The overexpression of synthesized miR-136-5p mimics in Hep3B and SK-hep1 cells detected with quantitative real-time polymerase chain reaction (qRT-PCR). The Student's t-test was utilized to analyze the 2 groups; B. The transfection of the overexpressed miR-136-5p in Hep3B and SK-hep1 cells detected using qRT-PCR method. The Student's t-test was utilized to analyze the 2 groups; C. The expression of MMP2 was detected after the overexpression of miR-136-5p in Hep3B and SK-hep1 cells had been detected using qRT-PCR method. One-way analysis of variance (ANOVA) followed by the Tukey's post hoc test were utilized to analyze multiple groups; D. The migration ability of Hep3B and SK-hep1 cells, with different groups (miRNA negative control (miR-NC), miR-136-5p mimics, miR-136-5p mimics + overexpressed hsa_circ_0000098 (Oe-circ)), based on the transwell assay (without pre-coated Matrigel). One-way ANOVA followed by the Tukey's post hoc test were utilized to analyze multiple groups; E. The invasion ability of Hep3B and SK-hep1 cells, with different groups (miR-NC, miR-136-5p mimics, miR-136-5p mimics+Oe-circ), detected using the transwell assay (without pre-coated Matrigel). One-way ANOVA followed by the Tukey's post hoc test were utilized to analyze multiple groups; F. The expression of MMP2, MMP9, E-cadherin, and N-cadherin in Hep3B and SK-hep1 cells, with different groups (miR-NC, miR-136-5p mimics, miR-136-5p mimics+Oe-circ), detected using the western blot assay

In view of the above conclusions, we continued to study the mechanism of action of hsa_circ_0000098 in HCC. CircInteractome online database predicted that hsa_circ_0000098 can sponge miR-136-5p. To the best of our knowledge, miR-136-5p was reported to have a low expression in liver cancer.^{3,34} Additionally, miR-136-5p has an impact on carcinomatosis in various cancers (colorectal carcinoma,³⁵ gallbladder carcinoma,³⁶ human T-cell leukemia virus type 1 (HTLV-1),³⁷ thyroid cancer,³⁸ oral squamous cell carcinoma³⁹). Remarkably, miR-136-5p has been identified to be downregulated in HCC. For instance, silencing of lncRNA LEF1-AS1 prevents the progression of HCC via the crosstalk with miR-136-5p/WNK1.⁴⁰ The *miR-136-5p* is a target gene for circ_0027089, thereby modulating NACC1 to aggravate HCC is associated with hepatitis B virus.⁴¹ In our study, miR-136-5p was downregulated in HCC tissues, which is consistent with the literature on the subject.

The downstream target gene of miR-136-5p is predicted to be *MMP2*, which is one of the prominent members of MMP family. The *MMP2* and *MMP9* are usually highly expressed in malignant tumors and take part in the degradation of tumor ECM and base, assisting tumor cells in breaking the metastasis barriers.⁴² Dorandish et al. revealed that *MMP2* is the predominant regulator of cytotoxic effects brought about by A β in lung cancer cells,⁴³ especially in HCC.⁴⁴ Hence, *MMP2* and *MMP9* play crucial roles in the migration and invasion of tumor cells.

Epithelial–mesenchymal transition (EMT) is a biological process in which epithelial cells transform and exhibit a mesenchymal phenotype via a specific program.⁴⁵ It has been shown that EMT exhibits a significant effect on malignant tumors, which could transform epithelial cells to obtain migration and invasion abilities associated with malignancy.⁴⁶ Thereby, it is important to investigate the molecular mechanism underlying the EMT process by N-cadherin and E-cadherin expression. In the present study, the results revealed that N-cadherin decreased and E-cadherin increased after the co-transfection of sh-circ, which means that the knockdown could suppress the ability to migrate and invade.

In conclusion, hsa_circ_0000098, highly expressed in HCC, can mediate the migration, invasion and malignant progression of liver cancer. This might be due to the regulation of miR-136-5p/MMP2 axis. This study has also provided inspiration for relieving pain of HCC patients. For

the first time, we made efforts in exploring the relationship and mechanism of action between hsa_circ_0000098 and HCC, which will pave the way for the subsequent study.

Limitations

The study did not verify the signal pathways studied in in vivo experiments. Subsequent research should focus on in vivo experiments to provide more reliable data and strategic treatment for future clinical studies.

Conclusions

Our data demonstrated that hsa_circ_0000098 is highly expressed in HCC, which facilitates the migration, invasion and malignant progression of cancer cells. On the other hand, we also proved that the mechanism of action of hsa_circ_0000098 in HCC might be due to the regulation of miR-136-5p/MMP2 axis.

Data availability

All supporting data are available from the corresponding author upon request.

ORCID iDs

Yunfei Cheng  <https://orcid.org/0000-0001-8289-6258>

References

- Zhang H, Deng T, Ge S, et al. Exosome circRNA secreted from adipocytes promotes the growth of hepatocellular carcinoma by targeting deubiquitination-related USP7. *Oncogene*. 2019;38(15):2844–2859. doi:10.1038/s41388-018-0619-z
- Ziogas IA, Tsoufas G. Advances and challenges in laparoscopic surgery in the management of hepatocellular carcinoma. *World J Gastrointest Surg*. 2017;9(12):233–245. doi:10.4240/wjgs.v9.i12.233
- Ding H, Ye ZH, Wen DY, et al. Downregulation of miR-136-5p in hepatocellular carcinoma and its clinicopathological significance. *Mol Med Rep*. 2017;16(4):5393–5405. doi:10.3892/mmr.2017.7275
- Forner A, Bruix J. Hepatocellular carcinoma: Authors' reply. *Lancet*. 2012;380(9840):470–471. doi:10.1016/S0140-6736(12)61286-0
- Sayiner M, Golabi P, Younossi ZM. Disease burden of hepatocellular carcinoma: A global perspective. *Dig Dis Sci*. 2019;64(4):910–917. doi:10.1007/s10620-019-05537-2
- Yin L, Cai Z, Zhu B, Xu C. Identification of key pathways and genes in the dynamic progression of HCC based on WGCNA. *Genes (Basel)*. 2018;9(2):92. doi:10.3390/genes9020092
- Ding J, Zhou W, Li X, Sun M, Ding J, Zhu Q. Tandem DNase: A new tool for circRNA suppression. *Biol Chem*. 2019;400(2):247–253. doi:10.1515/hsz-2018-0232

8. Gao Y, Zhang J, Zhao F. Circular RNA identification based on multiple seed matching. *Brief Bioinform.* 2018;19(5):803–810. doi:10.1093/bib/bbx014
9. Hansen TB, Jensen TI, Clausen BH, et al. Natural RNA circles function as efficient microRNA sponges. *Nature.* 2013;495(7441):384–388. doi:10.1038/nature11993
10. Wilusz JE, Sharp PA. A circuitous route to noncoding RNA. *Science.* 2013;340(6131):440–441. doi:10.1126/science.1238522
11. Zhang H, Sheng C, Yin Y, et al. PABPC1 interacts with AGO2 and is responsible for the microRNA mediated gene silencing in high grade hepatocellular carcinoma. *Cancer Lett.* 2015;367(1):49–57. doi:10.1016/j.canlet.2015.07.010
12. Suzuki H, Tsukahara T. A view of pre-mRNA splicing from RNase R resistant RNAs. *Int J Mol Sci.* 2014;15(6):9331–9342. doi:10.3390/ijms15069331
13. Lin X, Chen Y. Identification of potentially functional circRNA-miRNA-mRNA regulatory network in hepatocellular carcinoma by integrated microarray analysis. *Med Sci Monit Basic Res.* 2018;24:70–78. doi:10.12659/MSMBR.909737
14. Li X, Ding J, Wang X, Cheng Z, Zhu Q. NUDT21 regulates circRNA cyclization and ceRNA crosstalk in hepatocellular carcinoma. *Oncogene.* 2020;39(4):891–904. doi:10.1038/s41388-019-1030-0
15. Xu S, Zhou L, Ponnusamy M, et al. A comprehensive review of circRNA: From purification and identification to disease marker potential. *PeerJ.* 2018;6:e5503. doi:10.7717/peerj.5503
16. Han D, Li J, Wang H, et al. Circular RNA circMTO1 acts as the sponge of microRNA-9 to suppress hepatocellular carcinoma progression. *Hepatology.* 2017;66(4):1151–1164. doi:10.1002/hep.29270
17. Zhang X, Luo P, Jing W, Zhou H, Liang C, Tu J. circSMAD2 inhibits the epithelial–mesenchymal transition by targeting miR-629 in hepatocellular carcinoma. *Onco Targets Ther.* 2018;11:2853–2863. doi:10.2147/OTT.S158008
18. Li P, Chen S, Chen H, et al. Using circular RNA as a novel type of biomarker in the screening of gastric cancer. *Clin Chim Acta.* 2015;444:132–136. doi:10.1016/j.cca.2015.02.018
19. Li P, Chen H, Chen S, et al. Circular RNA 0000096 affects cell growth and migration in gastric cancer. *Br J Cancer.* 2017;116(5):626–633. doi:10.1038/bjc.2016.451
20. Wang F, Nazarali AJ, Ji S. Circular RNAs as potential biomarkers for cancer diagnosis and therapy. *Am J Cancer Res.* 2016;6(6):1167–1176. PMID:27429839. PMCID:PMC4937728.
21. Huang XB, Li J, Zheng L, et al. Bioinformatics analysis reveals potential candidate drugs for HCC. *Pathol Oncol Res.* 2013;19(2):251–258. doi:10.1007/s12253-012-9576-y
22. Pinter M, Scheiner B, Peck-Radosavljevic M. Immunotherapy for advanced hepatocellular carcinoma: A focus on special subgroups. *Gut.* 2021;70(1):204–214. doi:10.1136/gutjnl-2020-321702
23. Garrido A, Djouder N. Cirrhosis: A questioned risk factor for hepatocellular carcinoma. *Trends Cancer.* 2021;7(1):29–36. doi:10.1016/j.trecan.2020.08.005
24. Lu L, Jiang J, Zhan M, et al. Targeting neoantigens in hepatocellular carcinoma for immunotherapy: A futile strategy? *Hepatology.* 2021;73(1):414–421. doi:10.1002/hep.31279
25. Arnaiz E, Sole C, Manterola L, Iparraguirre L, Otaegui D, Lawrie CH. CircRNAs and cancer: Biomarkers and master regulators. *Semin Cancer Biol.* 2019;58:90–99. doi:10.1016/j.semcancer.2018.12.002
26. Memczak S, Jens M, Elefsinioti A, et al. Circular RNAs are a large class of animal RNAs with regulatory potency. *Nature.* 2013;495(7441):333–338. doi:10.1038/nature11928
27. Kristensen LS, Andersen MS, Stagsted LVW, Ebbesen KK, Hansen TB, Kjems J. The biogenesis, biology and characterization of circular RNAs. *Nat Rev Genet.* 2019;20(11):675–691. doi:10.1038/s41576-019-0158-7
28. Tsitsipatis D, Grammatikakis I, Driscoll RK, et al. AUF1 ligand circPCNX reduces cell proliferation by competing with p21 mRNA to increase p21 production. *Nucleic Acids Res.* 2021;49(3):1631–1646. doi:10.1093/nar/gkaa1246
29. Patop IL, Wüst S, Kadener S. Past, present, and future of circRNAs. *EMBO J.* 2019;38(16):e100836. doi:10.15252/embj.2018100836
30. Gasparini S, Licursi V, Presutti C, Mannironi C. The secret garden of neuronal circRNAs. *Cells.* 2020;9(8):1815. doi:10.3390/cells9081815
31. Huang G, Liang M, Liu H, et al. CircRNA hsa_circRNA_104348 promotes hepatocellular carcinoma progression through modulating miR-187-3p/RTKN2 axis and activating Wnt/ β -catenin pathway. *Cell Death Dis.* 2020;11(12):1065. doi:10.1038/s41419-020-03276-1
32. Liu Z, Yu Y, Huang Z, et al. CircRNA-5692 inhibits the progression of hepatocellular carcinoma by sponging miR-328-5p to enhance DAB2IP expression. *Cell Death Dis.* 2019;10(12):900. doi:10.1038/s41419-019-2089-9
33. Yu J, Yang M, Zhou B, et al. CircRNA-104718 acts as competing endogenous RNA and promotes hepatocellular carcinoma progression through microRNA-218-5p/TXNDC5 signaling pathway. *Clin Sci (Lond).* 2019;133(13):1487–1503. doi:10.1042/CS20190394
34. Shiu TY, Lin HH, Shih YL, et al. CRNDE-h transcript/miR-136-5p axis regulates interleukin enhancer binding factor 2 expression to promote hepatocellular carcinoma cell proliferation. *Life Sci.* 2021;284:119708. doi:10.1016/j.lfs.2021.119708
35. Yuan Q, Cao G, Li J, Zhang Y, Yang W. MicroRNA-136 inhibits colon cancer cell proliferation and invasion through targeting liver receptor homolog-1/Wnt signaling. *Gene.* 2017;628:48–55. doi:10.1016/j.gene.2017.07.031
36. Niu J, Li Z, Li F. Overexpressed microRNA-136 works as a cancer suppressor in gallbladder cancer through suppression of JNK signaling pathway via inhibition of MAP2K4. *Am J Physiol Gastrointest Liver Physiol.* 2019;317(5):G670–G681. doi:10.1152/ajpgi.00055.2019
37. Fayyad-Kazan M, Eldirani R, Hamade E, et al. Circulating miR-29c, miR-30c, miR-193a-5p and miR-885-5p: Novel potential biomarkers for HTLV-1 infection diagnosis. *Infect Genet Evol.* 2019;74:103938. doi:10.1016/j.meegid.2019.103938
38. Xiong Y, Kotian S, Zeiger MA, Zhang L, Kebebew E. miR-126-3p inhibits thyroid cancer cell growth and metastasis, and is associated with aggressive thyroid cancer. *PLoS One.* 2015;10(8):e0130496. doi:10.1371/journal.pone.0130496
39. Al Rawi N, Elmabrouk N, Abu Kou R, Mkadmi S, Rizvi Z, Hamdoon Z. The role of differentially expressed salivary microRNA in oral squamous cell carcinoma: A systematic review. *Arch Oral Biol.* 2021;125:105108. doi:10.1016/j.archoralbio.2021.105108
40. Dong H, Jian P, Yu M, Wang L. Silencing of long noncoding RNA LEF1-AS1 prevents the progression of hepatocellular carcinoma via the crosstalk with microRNA-136-5p/WNK1. *J Cell Physiol.* 2020;235(10):6548–6562. doi:10.1002/jcp.29503
41. He W, Zhu X, Tang X, Xiang X, Yu J, Sun H. Circ_0027089 regulates NACC1 by targeting miR-136-5p to aggravate the development of hepatitis B virus-related hepatocellular carcinoma. *Anticancer Drugs.* 2022;33(1):e336–e348. doi:10.1097/CAD.0000000000001211
42. Das S, De S, Sengupta S. Post-transcriptional regulation of MMP2 mRNA by its interaction with miR-20a and nucleolin in breast cancer cell lines. *Mol Biol Rep.* 2021;48(3):2315–2324. doi:10.1007/s11033-021-06261-9
43. Dorandish S, Williams A, Atali S, et al. Regulation of amyloid- β levels by matrix metalloproteinase-2/9 (MMP2/9) in the media of lung cancer cells. *Sci Rep.* 2021;11(1):9708. doi:10.1038/s41598-021-88574-0
44. Khalil HH, Osman HA, Teleb M, et al. Engineered s-triazine-based dendrimer-honokiol conjugates as targeted MMP-2/9 inhibitors for halting hepatocellular carcinoma. *ChemMedChem.* 2021;16(24):3701–3719. doi:10.1002/cmdc.202100465
45. Li Y, Zhang T, Qin S, et al. Investigational drugs in HIV: Pros and cons of entry and fusion inhibitors (review). *Mol Med Rep.* 2019;19(3):1987–1995. doi:10.3892/mmr.2019.9838
46. Kim CW, Hwang KA, Choi KC. Anti-metastatic potential of resveratrol and its metabolites by the inhibition of epithelial-mesenchymal transition, migration, and invasion of malignant cancer cells. *Phytomedicine.* 2016;23(14):1787–1796. doi:10.1016/j.phymed.2016.10.016

The clinical research study for fosaprepitant to prevent chemotherapy-induced nausea and vomiting: A review

Fei Xue^{1,D}, Xin Liu^{2,D}, Xiao Qi^{3,D}, Jiajing Zhou^{4,D}, Yongjun Liu^{5,E}

¹ Traditional Chinese Medicine General Practice Department, Yantai Hospital of Traditional Chinese Medicine, China

² Research and Development Department, Shandong Xianglong Pharmaceutical Research Institute Co., Ltd, Yantai, China

³ Respiratory Department, Yantai Hospital of Traditional Chinese Medicine, China

⁴ Oncology Department, Yantai Hospital of Traditional Chinese Medicine, China

⁵ Department of Traditional Chinese Medicine, Shandong Drug and Food Vocational College, Weihai, China

A – research concept and design; B – collection and/or assembly of data; C – data analysis and interpretation;

D – writing the article; E – critical revision of the article; F – final approval of the article

Advances in Clinical and Experimental Medicine, ISSN 1899–5276 (print), ISSN 2451–2680 (online)

Adv Clin Exp Med. 2023;32(6):701–706

Address for correspondence

Yongjun Liu

E-mail: liuyongjun189@163.com

Funding sources

None declared

Conflict of interest

None declared

Received on May 17, 2022

Reviewed on November 18, 2022

Accepted on December 1, 2022

Published online on April 7, 2023

Abstract

In recent years, chemotherapy-induced nausea and vomiting (CINV) has become the most common adverse effect of chemotherapy in oncology patients. The CINV may reduce the quality of life in mild cases, or even make the patients resist or delay further treatment. Fosaprepitant is a newly marketed neurokinin-1 receptor antagonist (NK-1RA), which can be combined with 5-hydroxytryptamine 3 receptor antagonists (5-HT3RAs) and dexamethasone to prevent chemotherapy-induced vomiting. The dimeglumine salt form of fosaprepitant can be utilized as an intravenous injectable drug, which surpasses aprepitant's oral administration limits. Fosaprepitant is effective and safe in the control of CINV in cancer patients receiving highly emetogenic chemotherapy (HEC), and may be an alternative option for antiemetic therapy. In general, fosaprepitant is worthy of clinical promotion and has a large market potential. This article reviews the clinical studies on fosaprepitant conducted in recent years, with the aim of providing a basis for the rational clinical selection of antiemetic drugs.

Key words: neurokinin-1 receptor antagonist, fosaprepitant, efficacy and safety, clinical research, chemotherapy-induced nausea and vomiting

Cite as

Xue F, Liu X, Qi X, Zhou J, Liu Y. The clinical research study for fosaprepitant to prevent chemotherapy-induced nausea and vomiting: A review. *Adv Clin Exp Med.* 2023;32(6):701–706. doi:10.17219/acem/157061

DOI

10.17219/acem/157061

Copyright

Copyright by Author(s)

This is an article distributed under the terms of the Creative Commons Attribution 3.0 Unported (CC BY 3.0) (<https://creativecommons.org/licenses/by/3.0/>)

Introduction

The treatment of malignant tumors has improved rapidly in recent years. Though there have been many breakthroughs in targeted therapeutics in oncology that are less emetogenic, chemotherapeutics have not been completely replaced. Chemotherapy-induced nausea and vomiting (CINV) are one of the most prevalent side effects of treatment, and severe vomiting can have a negative impact on subsequent therapeutic efficacy.¹ Children present a more severe response compared to adults.² If not managed effectively, CINV can affect patients by causing dehydration, malnutrition and electrolyte imbalance. These side effects can significantly impact patient's quality of life and instill fear of chemotherapy. The prevalence of nausea and vomiting is related to several factors, including the emetogenicity of the chemotherapy regimen, the dose and rate of administration of the chemotherapy agents, various environmental triggers, and patient-related factors. The pathogenesis involves multiple organ systems, the central nervous system, the gastrointestinal tract, and neurotransmitters.³ Highly emetogenic chemotherapy (HEC) is defined as drugs that cause vomiting in more than 90% of patients without any emetic prophylaxis, whereas moderately emetogenic chemotherapy (MEC) is defined as drugs that cause nausea and vomiting in 30–90% of patients without any emetic prophylaxis.⁴

Neurokinin-1 receptor antagonists (NK-1RAs) in combination with 5-hydroxytryptamine 3 receptor antagonists (5-HT₃RAs) and dexamethasone have been suggested by domestic and international standards to prevent and minimize CINV in patients.⁴ The NK-1RAs are a novel kind of anti-nausea medication with high selectivity and affinity. These medications work by competitively binding to the NK-1R, which can block the binding of substance P and prevent the emetic signal from being transmitted. The release of 5-HT^{3,5,6} is the focus of acute CINV, whereas the release of substance P is the focus of delayed CINV. All NK-1RAs are effective but exhibit important differences in efficacy against acute and delayed CINV. For delayed CINV compared to acute CINV, the benefit of NK-1RA-containing 3-drug regimens is greater than that of 2-drug regimens. Fosaprepitant, a subsequently developed aprepitant precursor drug, is given intravenously (i.v.) and is rapidly converted to aprepitant through the hydrolysis of phosphatase enzymes widely present in the body, which can mediate the blockage of substance P.⁷ In China, the NK-1RA medications primarily contain aprepitant (oral) and fosaprepitant (injection). The clinical trials for aprepitant are conducted more often due to its earlier availability in the market. However, because fosaprepitant is new to the Chinese market, studies have been limited to children. The dimeglumine salt form of the novel anti-nausea medicine, fosaprepitant, can be utilized as an i.v. injectable drug, which is able to surpass the oral administration limit of aprepitant. The bioavailability is unaffected by vomiting;

therefore, it can be utilized in patients with oral mucositis who are unable to take medications orally.⁸

Objectives

This review compiles the domestic and international clinical investigations on the anti-nausea effects of fosaprepitant, and serves as a guide for choosing anti-nausea medications in the clinic.

Methodology

Studies from the years 2003–2022 were included in our review. The studies were identified using the following keywords: “fosaprepitant”, “aprepitant”, “CINV”, “HEC”, “MEC”, and “NK-1RA”. Several representative articles were screened to analyze and summarize the clinical therapeutic effects of fosaprepitant. The data and conclusions from clinical trials were discussed. The data are presented along historical and medical drug development routes.

The clinical efficacy of fosaprepitant in preventing HEC-induced nausea and vomiting in adults

Fosaprepitant is used to prevent acute and delayed nausea and vomiting associated with HEC, and delayed nausea and vomiting associated with initial and recurrent courses of MEC in adults when used in combination with other antiemetic medicines.⁹ In a study conducted in China, 626 cancer patients who were administered HEC were randomly assigned to 2 groups: aprepitant (aprepitant+granisetron+dexamethasone) or fosaprepitant (fosaprepitant+granisetron+dexamethasone).¹⁰ The results showed that there were no differences in the complete response (CR) rate of the acute phase (AP), delayed phase (DP) and overall phase (OP) ($p > 0.05$) between the 2 treatments, and both drugs were well tolerated. In the OP, the CR rate was achieved by 293 (89.33%) patients in the fosaprepitant group and by 294 (92.74%) patients in the aprepitant group. During the AP and DP, the CR rates in the fosaprepitant group were 95.73% and 91.16%, respectively. Thus, fosaprepitant was found to be beneficial in controlling HEC-related nausea and vomiting in Chinese patients. Saito et al. studied 347 adult patients in Japan who received chemotherapy, including cisplatin (≥ 70 mg/m²), and were randomly divided into fosaprepitant and control groups.¹¹ The results showed that the fosaprepitant regimen was more effective than the control regimen in both the AP ($p = 0.0006$) and the DP ($p = 0.0025$).

Both of the studies were similar in regard to the CR rates observed during the AP. In contrast to the findings

Table 1. The clinical efficacy of fosaprepitant in preventing HEC

Study	Day	Cisplatin dose (mean)	Group	Antiemetic doses	CR (%) (acute phase (AP))	CR (%) (delay phase (DP))	CR (%) (overall phase (OP))
Yang et al. ¹⁰ n = 645	day 1 (before chemotherapy)	non-cisplatin HEC regimen (148 people) or cisplatin 60–80 mg/m ² (497 people)	fosaprepitant group	fosaprepitant 150 mg i.v. plus granisetron 3 mg i.v. plus dexamethasone 6 mg orally or i.v.	fosaprepitant group: 95.73% aprepitant group: 95.90%	fosaprepitant group: 95.73% aprepitant group: 93.38%	fosaprepitant group: 89.33% aprepitant group: 92.74%
			aprepitant group	aprepitant 125 mg orally plus granisetron 3 mg i.v. plus dexamethasone 6 mg orally or i.v.			
	day 2–3		fosaprepitant group	dexamethasone 3.75 mg orally every 12 h			
			aprepitant group	aprepitant 80 mg orally plus dexamethasone 3.75 mg orally			
	day 4		fosaprepitant group	dexamethasone 3.75 mg orally every 12 h			
			aprepitant group	dexamethasone 3.75 mg orally			
Saito et al. ¹¹ n = 347	day 1 (before chemotherapy)	cisplatin 76.2 mg/m ²	fosaprepitant group	fosaprepitant 150 mg i.v. plus granisetron 40 µg/kg i.v. plus dexamethasone i.v.	fosaprepitant group: 94% control group: 81%	fosaprepitant group: 65% control group: 49%	fosaprepitant group: 64% control group: 47%
			control group	placebo i.v. plus granisetron 40 µg/kg i.v. plus dexamethasone i.v.			
	day 2–3		fosaprepitant group	dexamethasone i.v.			
			control group	dexamethasone i.v.			

i.v. – intravenously; CR – complete response; HEC – highly emetogenic chemotherapy.

in Chinese patients, the CR rates in Japanese patients were different in the DP. The dose of cisplatin could have been a substantial factor causing the disparity. In the Japanese research, the target population was given cisplatin at a mean dose of 76.2 mg/m². In contrast, the Chinese patients were given a non-cisplatin HEC regimen or cisplatin at ≥60 mg/m², which is defined as HEC under treatment standards (Table 1).

The clinical efficacy of fosaprepitant in preventing MEC-induced nausea and vomiting in adults

Fosaprepitant can prevent MEC-induced nausea and vomiting, especially during the DP. Weinstein et al. selected patients aged ≥18 years who received non-cyclophosphamide MEC.¹² All patients were assigned to treatment with fosaprepitant combined with ondansetron and dexamethasone (the observation group) or with ondansetron and dexamethasone alone (the control group). The study showed that fosaprepitant significantly enhanced CR in the DP (78.9% compared to 68.5%; *p* < 0.001) and OP (77.1% compared to 66.9%; *p* < 0.001), but not in the AP (93.2% compared to 91.0%; *p* = 0.184), compared to control. Thus, the anti-nausea efficacy of fosaprepitant was comparable between the observation and control groups for acute vomiting, whereas the efficacy was considerable

for delayed vomiting. The adverse response was mild, and the fosaprepitant regimen was generally well tolerated. Weinstein et al. randomly allocated patients undergoing the first day of planned i.v. anthracycline-cyclophosphamide-based MEC chemotherapy with oral ondansetron and oral dexamethasone plus a single dose of i.v. fosaprepitant (150 mg) or placebo, and found that a single dose of fosaprepitant was effective and safe in preventing CINV in different types of cancer.¹³

The clinical efficacy of fosaprepitant in preventing CINV in pediatric patients

Under the current standard of care, antiemetic regimens are more effective in adults than in children. When compared to adults, children exhibit differences in bioavailability, absorption, volume of distribution, and hepatic and renal clearance. Another factor is the widespread use of multiple-day chemotherapy regimens in pediatric patients, which are used less frequently in adult patients.¹⁴ However, some studies have shown that fosaprepitant can effectively prevent the CINV associated with MEC in pediatric patients. Radhakrishnan et al. selected patients aged 1–12 years who received MEC from the India Cancer Institute.¹⁵ Patients were randomly divided into an observation group and a control group. In that study,

patients in the fosaprepitant arm received 3 mg/kg (maximum 150 mg) of fosaprepitant as a 30-minute i.v. infusion in 100 mL of normal saline. The study showed that the CR for acute vomiting in the observation group (86%) was considerably higher than in the control group (60%; $p < 0.001$), and the CR for delayed vomiting in the observation group (79%) was significantly higher than in the control group (5%; $p < 0.001$). Overall, the CR in the observation group (70%) was higher than in the control group (40%; $p < 0.001$), which indicates that the anti-nausea efficacy of fosaprepitant was significant. In addition, the adverse response was mild and tolerable.¹⁵

In a Chinese trial on the prevention of CINV with the use of fosaprepitant in children with tumors, a total of 122 children were enrolled (62 in the fosaprepitant group and 60 in the aprepitant group).¹⁶ In this study, patients aged 2–12 years received fosaprepitant at a dose of 3 mg/kg (maximum 150 mg). The proportions of AP, DP and OP reaching CR (no vomiting rate) were 88.5%, 71.3% and 65.6%, respectively. Fosaprepitant also had a greater CR than aprepitant in preventing acute vomiting ($p < 0.05$). There were no differences between the 2 groups in terms of adverse responses, and the drugs were well tolerated.

Recently, from August 2015 to January 2017, a retrospective chart review characterized the usage of fosaprepitant in patients aged from 10 months to 18 years at a single hospital.¹⁷ The study included 35 patients who got fosaprepitant at a dose of 4 mg/kg (maximum 150 mg) for CINV prophylaxis. A follow-up phone call was made to 10 patients aged ≥ 5 who received fosaprepitant after October 2016 to assess the control of delayed CINV. During the AP, 89% exhibited complete control of emesis, while 63% presented complete control during the DP, and 60% exhibited overall control of emesis. These results provide evidence that fosaprepitant is safe and effective in the prevention of CINV in pediatric patients as young as 10 months. However, because the above studies were all single-center, small sample clinical trials, more randomized controlled multi-center clinical trials are needed to determine the efficacy and safety of fosaprepitant for the treatment of CINV in pediatric patients.

In April 2018, the U.S. Food and Drug Administration (FDA) approved the use of fosaprepitant in children over the age of 6 months.⁹ The FDA recommends fosaprepitant doses of 5 mg/kg (age: 6 months–2 years) and 4 mg/kg (age: 2–12 years) capped at 150 mg and infused over 1 h. On day 1, children under the age of 12 receive 3 mg/kg fosaprepitant (maximum: 115 mg) administered over 1 h, followed by an oral 2 mg/kg aprepitant suspension (maximum: 80 mg) on days 2 and 3.

According to pharmacokinetic studies, children under the age of 12 convert fosaprepitant to aprepitant in the blood more slowly than adults and have a lower mean area under the curve (AUC). Hence, children under the age of 12 required greater doses to achieve exposures comparable to adults.¹⁴

Efficacy comparison for fosaprepitant and aprepitant

Aprepitant is a NK-1RA and fosaprepitant is a prodrug of aprepitant that is activated in the bloodstream after i.v. delivery. In contrast to aprepitant, fosaprepitant may be beneficial for individuals who are unable to take oral antiemetics during a bout of nausea or vomiting.¹⁸ In order to compare the efficacy and safety of fosaprepitant and aprepitant, Zhang et al. designed a randomized, double-blind, non-inferiority clinical study in which 644 patients receiving cisplatin-based chemotherapy were randomized to fosaprepitant or aprepitant groups. In this study, it was found that the antiemetic effects of fosaprepitant and aprepitant were comparable (71.96% compared to 69.35%, $p = 0.4894$).¹⁹ Therefore, these 2 drugs have the potential to have a positive impact on daily life by easing the completion of a patient's clinically prescribed chemotherapy treatment.

According to a randomized controlled trial, the use of aprepitant and fosaprepitant for the treatment of CINV in patients with gynecological cancer showed no significant differences between the 2 groups in the AP and DP of cycle 1 chemotherapy.²⁰ This study also showed that both i.v. fosaprepitant and oral aprepitant were effective in preventing vomiting, and had a beneficial effect on patients' quality of life. In another study conducted in Japan, a 5-day administration of aprepitant and a single administration of fosaprepitant for the prevention of nausea and vomiting caused by cisplatin-induced HEC were compared.²¹ The results showed no significant differences between groups in the rate of complete remission and the complete control rate of vomiting during the entire treatment period. Nausea scores in both groups tended to increase from day 3, but there was no statistical significance between groups.

These results demonstrate that a single dose of fosaprepitant improves the antiemetic effects of conventional 5-HT₃RA and corticosteroid therapy compared to standard therapy alone, and may have an efficacy comparable to the recommended 3-day aprepitant regimen.

Safety and drug interactions for fosaprepitant

Fatigue, diarrhea, constipation, sleeplessness, vertigo, local pain at the injection site, and other side effects of fosaprepitant can occur throughout the therapeutic process. Other adverse responses are minor and acceptable ($p > 0.05$),¹² and the incidence of diarrhea and vertigo is lower than in the control group ($p < 0.05$). Other adverse responses, including hiccups, headache and serious adverse event (SAE; anaphylactic reaction) to the medication, were reported by only a few children in one of the pediatric cancer treatment studies, and there was no mortality in the first cycle.¹⁴

Drug interactions associated with fosaprepitant should be considered when selecting an antiemetic therapy. A report by Patel et al. stated that concomitant administration of aprepitant and alcohol can cause impaired cognitive function, the simultaneous use of aprepitant with vincristine and isocyclophosphamide can cause neurotoxicity, and a combination with quetiapine can induce drowsiness.²² They have also shown that there may be local reactions at the infusion site when fosaprepitant and anthracycline drugs are given via the same peripheral i.v. route.²² In general, adverse effects of fosaprepitant are slight, the drug is significantly safe for children, women, the elderly and patients with renal insufficiency, and there is no need to change their prescribed dosage.

Discussion

More than 90% of the vomiting caused by chemotherapy medicines is delayed vomiting, with a prevalence of more than 60%. This usually relates to inadequate control of acute CINV or the use of cisplatin, Cytoxan, Paraplatin, or doxorubicin. The severity of the vomiting reaches its peak after 2–4 days of chemotherapy. Although the frequency of delayed vomiting is not as high as acute vomiting, it is difficult to control and normally lasts long. As a result, preventing delayed vomiting remains a challenge.²³

The ability of NK-1RAs to bind to the NK-1R with great selectivity and potency in order to inhibit the activity of substance P offers a new treatment option for CINV.²⁴ The NK-1RAs have a considerable anti-nausea effect. Most people can tolerate these drugs because they are safe and induce only minor adverse reactions. The i.v. injection of fosaprepitant, the phosphate prodrug of aprepitant, is more practical for patients during nausea and vomiting than the administration of oral antiemetics. The efficacy of a single dose of fosaprepitant is comparable to that of aprepitant, allowing the antiemetic regimen to be simplified. Fosaprepitant has become one of the most important medications in antiemetic therapy. At present, the brand name “fosaprepitant” is still not available in the Chinese market. Jiangsu Hansoh Pharmaceutical Group Co., Ltd. produces genericized fosaprepitant (Tannen), which is the first injectable NK-1RA licensed for sale in China. According to clinical research, fosaprepitant (Tannen) is well tolerated and has a similar safety profile to aprepitant.²⁰ The launch of domestic fosaprepitant will give Chinese patients more options for CINV treatment. However, there are still very few domestic clinical studies for fosaprepitant, particularly in children. More clinical trials are needed to support the appropriate usage of NK-1RAs in clinics.

Other recently developed antiemetics, such as Zyprexa, Akynzeo and Varubi, are approved for marketing. In order to prevent CINV in adults receiving cisplatin and other highly emetic single agents, as well as in adults receiving anthracycline combined with cyclophosphamide, the updated

American Society of Clinical Oncology (ASCO) antiemetic guidelines advise the addition of olanzapine (Zyprexa) to a NK-1RA, a 5-HT₃RA and dexamethasone.²⁵

Two published phase 3 studies compared olanzapine with aprepitant (both in combination with a 5-HT₃RA and dexamethasone). Both studies showed that the 2 treatment plans had equal effects on CINV during the immediate period (0–24 h after chemotherapy), but olanzapine was superior to aprepitant at controlling nausea during the later phase (0–120 h after chemotherapy).^{26,27}

For the prevention of immediate and delayed nausea and vomiting brought on by moderately and highly emetogenic cancer chemotherapy, netupitant/palonosetron (NEPA/Akynzeo) is recommended in the EU for adults. In one trial, patients receiving cisplatin-based HEC were randomized to either NEPA (plus dexamethasone) or aprepitant (plus granisetron and dexamethasone) groups. The NEPA showed non-inferiority to aprepitant for the key efficacy end objective over the course of CINV (73.8% compared to 72.4%).²⁸

Rolapitant (Varubi) is also a novel NK-1RA that was approved by FDA in 2015 for the prevention of delayed CINV with MEC and HEC. It has definite advantages over aprepitant and NEPA. First, it has no CYP3A4 inhibitory or inducing effects, which restricts the ability to alter the dose of dexamethasone, a requirement for the use of aprepitant and NEPA. Unlike aprepitant, rolapitant is administered as a one-time dose.²⁹

Future studies should be conducted in this area because it is unclear whether employing a NK-1RA will increase the effectiveness of nausea control. In comparison to existing agents, newer ones may provide important advantages in terms of better nausea control, tolerability, formulation options, and therapeutic plasma levels during the AP of CINV. These newer agents also give clinicians more opportunities to maximize the advantages of this significant class of antiemetics.³⁰

Limitations

This article only describes the efficacy of fosaprepitant in adults and children. The use of this medication in special populations (elderly, hepatic and renal insufficiency, etc.) has been less studied, thus caution should be exercised in its use. More prospective clinical studies are needed to prove its efficacy and safety, and the efficacy of fosaprepitant and aprepitant in controlling various types of vomiting remains controversial, requiring more clinical trials or meta-analyses to confirm.

Conclusions

Fosaprepitant is effective and safe in the treatment of cancer patients receiving HEC. As an antiemetic therapy, this may be a better option. In general, fosaprepitant has a large market potential and is worthy of clinical promotion.

ORCID iDs

Fei Xue  <https://orcid.org/0009-0003-3128-2629>

Xin Liu  <https://orcid.org/0000-0001-8675-3692>

Xiao Qi  <https://orcid.org/0009-0004-4506-4742>

Jiajing Zhou  <https://orcid.org/0000-0003-4322-754X>

Yongjun Liu  <https://orcid.org/0000-0003-2049-7416>

References

- Soefje SA. Strategies to improve CINV outcomes in managed care. *Am J Manag Care*. 2018;24(18 Suppl):S398–S404. PMID:30328691.
- Jordan K, Roila F, Molassiotis A, Maranzano E, Clark-Snow RA, Feyrer P. Antiemetics in children receiving chemotherapy: MASCC/ESMO guideline update 2009. *Support Care Cancer*. 2011;19(51):37–42. doi:10.1007/s00520-010-0994-7
- Di Liso E. Chemotherapy-induced nausea and vomiting. In: Cascella M, John Stones M, eds. *Suggestions for Addressing Clinical and Non-Clinical Issues in Palliative Care*. London, UK: IntechOpen; 2021. doi:10.5772/intechopen.96194
- Berger MJ, Ettinger DS, Aston J, et al. NCCN Guidelines Insights: Antiemesis, Version 2. 2017. *J Natl Compr Canc Netw*. 2017;15(7):883–893. doi:10.6004/jnccn.2017.0117
- Jordan K, Hinke A, Grothey A, et al. A meta-analysis comparing the efficacy of four 5-HT₃-receptor antagonists for acute chemotherapy-induced emesis. *Support Care Cancer*. 2007;15(9):1023–1033. doi:10.1007/s00520-006-0186-7
- Hesketh PJ, Van Belle S, Aapro M, et al. Differential involvement of neurotransmitters through the time course of cisplatin-induced emesis as revealed by therapy with specific receptor antagonists. *Eur J Cancer*. 2003;39(8):1074–1080. doi:10.1016/S0959-8049(02)00674-3
- Ruhlmann CH, Herrstedt J. Fosaprepitant for the prevention of chemotherapy-induced nausea and vomiting. *Expert Rev Anticancer Ther*. 2012;12(2):139–150. doi:10.1586/era.11.199
- Aziz F. Neurokinin-1 receptor antagonists for chemotherapy-induced nausea and vomiting. *Ann Palliat Med*. 2012;1(2):130–136. doi:10.3978/j.issn.2224-5820.2012.07.10
- U.S. Food and Drug Administration (FDA). EMEND (fosaprepitant) for injection, for intravenous use. Initial U.S. Approval. 2008. https://www.accessdata.fda.gov/drugsatfda_docs/label/2018/022023s0171bl.pdf. Accessed April 16, 2022.
- Yang LQ, Sun XC, Qin SK, et al. Efficacy and safety of fosaprepitant in the prevention of nausea and vomiting following highly emetogenic chemotherapy in Chinese people: A randomized, double-blind, phase III study. *Eur J Cancer Care*. 2017;26(6):e12668. doi:10.1111/ecc.12668
- Saito H, Yoshizawa H, Yoshimori K, et al. Efficacy and safety of single-dose fosaprepitant in the prevention of chemotherapy-induced nausea and vomiting in patients receiving high-dose cisplatin: A multicentre, randomised, double-blind, placebo-controlled phase 3 trial. *Ann Oncol*. 2013;24(4):1067–1073. doi:10.1093/annonc/mds541
- Weinstein C, Jordan K, Green SA, et al. Single-dose fosaprepitant for the prevention of chemotherapy-induced nausea and vomiting associated with moderately emetogenic chemotherapy: Results of a randomized, double-blind phase III trial. *Ann Oncol*. 2016;27(1):172–178. doi:10.1093/annonc/mdv482
- Weinstein C, Jordan K, Green S, et al. Single-dose fosaprepitant for the prevention of chemotherapy-induced nausea and vomiting in patients receiving moderately emetogenic chemotherapy regimens: A subgroup analysis from a randomized clinical trial of response in subjects by cancer type. *BMC Cancer*. 2020;20(1):918. doi:10.1186/s12885-020-07259-5
- Mora J, Valero M, DiCristina C, Jin M, Chain A, Bickham K. Pharmacokinetics/pharmacodynamics, safety, and tolerability of fosaprepitant for the prevention of chemotherapy-induced nausea and vomiting in pediatric cancer patients. *Pediatr Blood Cancer*. 2019;66(6):e27690. doi:10.1002/pbc.27690
- Radhakrishnan V, Joshi A, Ramamoorthy J, et al. Intravenous fosaprepitant for the prevention of chemotherapy-induced vomiting in children: A double-blind, placebo-controlled, phase III randomized trial. *Pediatr Blood Cancer*. 2019;66(3):e27551. doi:10.1002/pbc.27551
- Yuan DM, Li Q, Zhang Q, et al. Efficacy and safety of neurokinin-1 receptor antagonists for prevention of chemotherapy-induced nausea and vomiting: Systematic review and meta-analysis of randomized controlled trials. *Asia Pac J Cancer Prev*. 2016;17(4):1661–1675. doi:10.7314/APJCP.2016.17.4.1661
- Timaues S, Elder J, Franco K. Evaluation of the use of fosaprepitant for the prevention of chemotherapy-induced nausea and vomiting in pediatric patients. *J Pediatr Hematol Oncol*. 2018;40(7):527–531. doi:10.1097/MPH.0000000000001213
- Langford P. Fosaprepitant and aprepitant: An update of the evidence for their place in the prevention of chemotherapy-induced nausea and vomiting. *Core Evid*. 2010;5:77–90. doi:10.2147/CE.S6012
- Zhang Z, Yang Y, Lu P, et al. Fosaprepitant versus aprepitant in the prevention of chemotherapy-induced nausea and vomiting in patients receiving cisplatin-based chemotherapy: A multicenter, randomized, double-blind, double-simulated, positive-controlled phase III trial. *Ann Transl Med*. 2020;8(5):234–234. doi:10.21037/atm.2019.12.158
- Micha JP, Rettenmaier MA, Brown JV, et al. A randomized controlled pilot study comparing the impact of aprepitant and fosaprepitant on chemotherapy induced nausea and vomiting in patients treated for gynecologic cancer. *Int J Gynecol Cancer*. 2016;26(2):389–393. doi:10.1097/IGC.0000000000000593
- Ando Y, Hayashi T, Ito K, et al. Comparison between 5-day aprepitant and single-dose fosaprepitant meglumine for preventing nausea and vomiting induced by cisplatin-based chemotherapy. *Support Care Cancer*. 2016;24(2):871–878. doi:10.1007/s00520-015-2856-9
- Patel P, Leeder JS, Piquette-Miller M, Dupuis LL. Aprepitant and fosaprepitant drug interactions: A systematic review. *Br J Clin Pharmacol*. 2017;83(10):2148–2162. doi:10.1111/bcp.13322
- Roila F, Herrstedt J, Aapro M, et al. Guideline update for MASCC and ESMO in the prevention of chemotherapy- and radiotherapy-induced nausea and vomiting: Results of the Perugia consensus conference. *Ann Oncol*. 2010;21(Suppl 5):v232–v243. doi:10.1093/annonc/mdq194
- Shillingburg A, Biondo L. Aprepitant and fosaprepitant use in children and adolescents at an academic medical center. *J Pediatr Pharmacol Ther*. 2014;19(2):127–131. doi:10.5863/1551-6776-19.2.127
- Hesketh PJ, Kris MG, Basch E, et al. Antiemetics: American Society of Clinical Oncology Clinical Practice Guideline update. *J Clin Oncol*. 2017;35(28):3240–3261. doi:10.1200/JCO.2017.74.4789
- Tan L, Liu J, Liu X, et al. Clinical research of olanzapine for prevention of chemotherapy-induced nausea and vomiting. *J Exp Clin Cancer Res*. 2009;28(1):131. doi:10.1186/1756-9966-28-131
- Navari RM, Gray SE, Kerr AC. Olanzapine versus aprepitant for the prevention of chemotherapy-induced nausea and vomiting: A randomized phase III trial. *J Support Oncol*. 2011;9(5):188–195. doi:10.1016/j.suponc.2011.05.002
- Zhang L, Lu S, Feng J, et al. A randomized phase III study evaluating the efficacy of single-dose NEPA, a fixed antiemetic combination of netupitant and palonosetron, versus an aprepitant regimen for prevention of chemotherapy-induced nausea and vomiting (CINV) in patients receiving highly emetogenic chemotherapy (HEC). *Ann Oncol*. 2018;29(2):452–458. doi:10.1093/annonc/mdx698
- Heo YA, Deeks ED. Rolapitant: A review in chemotherapy-induced nausea and vomiting. *Drugs*. 2017;77(15):1687–1694. doi:10.1007/s40265-017-0816-z
- Navari RM, Schwartzberg LS. Evolving role of neurokinin 1-receptor antagonists for chemotherapy-induced nausea and vomiting. *Onco Targets Ther*. 2018;11:6459–6478. doi:10.2147/OTT.S158570

Review of the epidemiology, pathogenesis and prevention of atrial fibrillation after pacemaker implantation

Yeshun Wu^{A–D}, Hongqing Xu^{A–C}, Xiaoming Tu^E, Zhenyan Gao^{E,F}

Department of Cardiology, Quzhou Affiliated Hospital of Wenzhou Medical University – Quzhou People's Hospital, China

A – research concept and design; B – collection and/or assembly of data; C – data analysis and interpretation; D – writing the article; E – critical revision of the article; F – final approval of the article

Advances in Clinical and Experimental Medicine, ISSN 1899–5276 (print), ISSN 2451–2680 (online)

Adv Clin Exp Med. 2023;32(6):707–718

Address for correspondence

Zhenyan Gao
E-mail: gaozhenyan80@163.com

Funding sources

This work was funded by Guiding Scientific and Technological Project of Quzhou (grant No. 2021007) and Clinical Research Fund Project of Zhejiang Medical Association (grant No. 2021ZYC-A46).

Conflict of interest

None declared

Acknowledgements

We would like to thank Servier Medical Art (<https://smart.servier.com>) for providing graphical elements required to design Fig. 1.

Received on September 28, 2022

Reviewed on November 27, 2022

Accepted on December 7, 2022

Published online on March 6, 2023

Abstract

Cardiac pacemaker implantation is an important treatment for symptomatic bradycardia. However, epidemiological data show that the incidence of atrial fibrillation (AF) is significantly higher in patients with implanted pacemakers than in the general population, which may be related to the preoperative presence of multiple risk factors for AF, improvement of diagnostic sensitivity and the pacemaker itself. The pathogenesis of AF after the implantation of pacemaker is related to cardiac electrical remodeling, structural remodeling, inflammation, and autonomic nervous disorder, which are induced by the pacemaker. Moreover, different pacing modes and pacing sites have various effects on the pathogenesis of postoperative AF. Recent studies have reported that reducing the proportion of ventricular pacing, improving the pacing site and setting up special pacing procedures might be highly useful in prevention of AF after pacemaker implantation. This article reviews the epidemiology, pathogenesis, influencing factors, and preventive measures regarding AF after pacemaker surgery.

Key words: pathogenesis, atrial fibrillation, pacemaker implantation, pacing modes, pacing sites

Cite as

Wu Y, Xu H, Tu X, Gao Z. Review of the epidemiology, pathogenesis and prevention of atrial fibrillation after pacemaker implantation [published online as ahead of print on January March 6, 2023]. *Adv Clin Exp Med.* 2023;32(6):707–718. doi:10.17219/acem/157239

DOI

10.17219/acem/157239

Copyright

Copyright by Author(s)

This is an article distributed under the terms of the Creative Commons Attribution 3.0 Unported (CC BY 3.0) (<https://creativecommons.org/licenses/by/3.0/>)

Introduction

Cardiac pacemaker implantation is an important treatment for symptomatic bradycardia.¹ In recent years, the prevalence of atrial fibrillation (AF) after pacemaker implantation has gradually increased, which may be related to the preprocedural presence of multiple risk factors for AF, improvement of diagnostic sensitivity and the pacemaker itself.^{2–4} The parameters and mode setting after the pacemaker implantation, such as atrial and/or ventricular pacing mode, atrioventricular (AV) interval and AV synchronization, may prevent AF, but they might also contribute to the initiation and maintenance of AF.^{2,5} This article reviews the epidemiology, pathogenesis, influencing factors, and preventive measures regarding AF after pacemaker surgery.

Epidemiology

Atrial fibrillation is age-related, and the results of various studies have demonstrated that its incidence increases with age.⁶ Similarly, in elderly patients, sinus node and AV node diseases requiring permanent pacemaker implantation are more common. Previous findings suggest that the annual incidence of AF after pacemaker implantation is $\geq 5\%$, the annual incidence of chronic persistent AF is approx. 3%, the average cumulative incidence of AF is as high as 24.5–40%, and the average cumulative incidence of chronic AF is approx. 20%, which are all significantly higher than for people without pacemaker.^{7,8} After analyzing several large-scale clinical trials,^{9–14} we concluded that the incidence of AF varied significantly across studies, possibly because of the different study populations, follow-up times, AF-endpoint definitions, and pacing modes.

The mode selection (MOST) trial¹³ selected patients with sick sinus syndrome, whereas the United Kingdom Pacing and Cardiovascular Events (UKPACE) trial¹⁴ excluded the sick sinus population and selected patients with AV block who were >70 years old. In the Physical Activity Scale for the Elderly (PASE) trial,¹¹ the average follow-up time of all elderly patients enrolled was 18 months, and the incidence of AF after pacemaker implantation was 18%. The MOST trial¹³ found that the incidence rate of AF was 22.5% after 33 months of follow-up, and the Canadian Trial of Physiological Pacing (CTOPP)⁹ had a follow-up time of 42 months, during which the annual rate of AF was 6.0%. Furthermore, the AF-endpoint definition varied among the studies, which may be the main reason for the great differences in the results. The Search AV Extension and Managed Ventricular Pacing for Promoting Atrioventricular Conduction (SAVE PACE) trial¹² defined AF as persistent AF lasting ≥ 22 h per day for >7 consecutive days; the Danish Multicenter Randomized Trial on Single Lead Atrial versus Dual Chamber Pacing in Sick Sinus Syndrome

(DANPACE) trial¹⁰ included the incidence of paroxysmal and chronic persistent AF, in which paroxysmal AF was defined as AF first identified in follow-up electrocardiogram (ECG) or pacemaker recording, and persistent AF was defined as AF found in at least 2 consecutive follow-up ECGs; the MOST trial¹³ and PASE trial¹¹ did not distinguish the types of AF and only based their AF definitions on the results of 1 ECG examination. Finally, there were also significant differences in the pacing modes among the studies. The MOST trial¹³ and PASE trial¹¹ mainly observed the effects of rate-adaptive ventricular pacing (VVIR) and rate-adaptive dual-chamber pacing (DDDR) on AF, and the prospective multicenter SAVE PACE clinical trial¹² was the first to evaluate dual-chamber minimal ventricular pacing.

Diagnostic value of pacemakers in AF

The above studies have shown that the incidence of AF was higher with than without pacemaker implantation, which may be related to the pacemaker improving the sensitivity of AF diagnosis and the impact of the pacemaker on AF.^{2–4} For patients with implanted pacemakers, the device automatically records and stores the atrial high-rate episodes (AHREs) based on programmable detection algorithms. Studies have shown that AHREs are a reliable indicator for monitoring atrial arrhythmias.^{15,16} Kaufman et al. conducted a detailed statistical analysis of 2580 patients with pacemaker implantation, and the results showed that when AF was defined as an atrial-wave frequency >190 beats/min and a duration >6 min, the diagnostic accuracy was 82.7%, and the false positive rate was 17.3%; if the duration of AHRE was extended to 30 min, 6 h and 12 h, the false positive rate decreased to 6.8%, 3.3% and 1.8%, respectively; if the atrial wave frequency was defined as >250 times/min, the diagnostic accuracy for AF would be further improved.¹⁷ Sanna also argued that pacemakers could better detect the occurrence of AF than routine ECG and Holter monitoring.¹⁸

Although AHREs are associated with the incidence of clinical AF, they also have important independent predictive value for thrombotic stroke and early death.^{19,20} In the 2019 American Heart Association (AHA)/American College of Cardiology (ACC)/Heart Rhythm Society (HRS), the 2020 European Society of Cardiology (ESC), and the 2020 Canadian Cardiovascular Society (CCS)/Canadian Heart Rhythm Society (CHRS) AF guidelines,^{21–23} regular evaluation for AHREs among patients with cardiac implantable electronic devices is recommended (class I), which could prompt further evaluation to document clinically relevant AF characteristics and guide anticoagulation treatment decisions. However, the threshold duration of AHREs that warrants anticoagulation is unclear, whereas a wide range of AHRE duration cutoffs (from

10–20 s to >24 h) is reported in studies on the association of subclinical AF with thromboembolism. A meta-study of 18,943 patients found a significantly increased risk of thromboembolic events in patients with an AHRE burden >6 min compared with the no-AHRE group (hazard ratio (HR): 1.82; 95% confidence interval (95% CI): 1.32–2.51), and there was no clear linear relationship between the increasing burden of AF and risk of stroke.²⁴ In Atrial Fibrillation Reduction Atrial Pacing Trial (ASSERT),²⁵ AHRE duration >24 h significantly increased the risk of ischemic stroke or systemic embolism (adjusted HR: 3.24, 95% CI: 1.51–6.95, $p = 0.003$) with an event rate of 3.08%/year. There was no increased risk of stroke for AHRE duration between 6 min and 24 h. Hence, the 2019 AHA/ACC/HRS and the 2020 ESC guidelines recommend complete cardiovascular evaluation with the AHRE duration, ECG recording, thromboembolic risk assessment, and preferences to determine whether to initiate long-term anticoagulation, while the CCS/CHRS guidelines recommend that patients with AHRE duration >24 h be treated with anticoagulation if they have stroke risk factors.

Related studies have reported that the incidence of AHREs after pacemaker implantation was approx. 10% in half a year and approx. 35% in 2.5 years.²⁶ Kawakami et al. found that 48% of patients had at least 1 AHRE during a follow-up period of 52 ± 30 months.²⁷ Implantable devices, such as cardiac pacemakers, can increase the incidence of AHREs, which may be associated with P-wave dispersion in sinus rhythm.²⁸ Due to the loss of AV synchrony and irregular ventricular cycle, pacemaker-related new-onset AF leads to reduced cardiac output and acute hemodynamic changes, thus increasing the risk of worsening heart failure and reducing patient survival.^{29,30}

Mechanism of pacemaker implantation-induced AF

Cardiac electrical remodeling

The nonphysical ectopic pacing of the heart caused by a pacemaker would cause a disorder in the electrical excitation sequence and frequency, and then lead to abnormal changes in cardiac electrical characteristics, including ion channels, electrical coupling and electrical conduction properties. The opening and closing of ion channels in the myocardial cell membrane cause ion transmembrane movement and form an action potential, which produces electrical excitation under the action of cardiac electrical coupling.³¹ However, pacemaker-mediated cardiac pacing cannot completely simulate the pacing mode in the physiological state. As an ectopic pacing, it is easy to cause action potential remodeling and abnormal changes in ion channels in the myocardial cell

membrane, thus leading to myocardial electrical disturbance.^{32,33} Reduction of transient outward K^+ current (Ito), which plays a key role in the first phase of action potential repolarization, is the most important of the changes in ion channels after pacemaker implantation. The decrease in Ito would cause imbalances of potassium and calcium concentrations inside and outside of cells and lead to abnormal changes in electrical conductivity.³⁴ A long-term electrical remodeling would result in more complex variability in cardiomyocyte transmembrane ion flux, including inactivation of the fast sodium channel (INa), increased expression of slowly activating delayed rectifier potassium (IKs) channels and decreased density of Ito channels and L-type calcium (ICa-L) channels; all 3 disrupt the normal electrophysiological coordination of myocardium.^{35–37} Moreover, persistent changes in the properties of ion channels would lead to abnormal myocardial excitation–contraction coupling and changes in the number and distribution of gap junction proteins (such as connexin 43) between cardiomyocytes.^{37,38} Therefore, it can be inferred that abnormal changes in ion channels in the myocardial membrane and electrical coupling caused by pacemakers eventually promote re-entry and lead to AF (Fig. 1). In addition, long-term exogenous electrode stimulation produced by a pacemaker causes the enlargement of the left atrium and leads to myocardial stretch, which has been proven to slow myocardial electrical conduction velocity, shorten the effective refractory period and increase the conduction anisotropy in the atrium.^{39–41}

Cardiac structural remodeling

Cardiac structural remodeling caused by pacemaker implantation is an adaptive response of the heart to hemodynamic changes or other exogenous factors, including cardiomyocyte hypertrophy, apoptosis and interstitial fibrosis, which would result in cardiac dilation and dysfunction (Fig. 1).^{42,43}

The mechanism of cardiomyocyte apoptosis caused by pacemaker implantation includes 2 main aspects. On the one hand, abnormal electrical excitation caused by pacemaker implantation leads to changes in cardiac mechanical contraction. Under the influence of long-term nonphysiological electrical excitation and mechanical contraction, cardiomyocytes in the electrode implantation site and its adjacent areas undergo a series of abnormal changes, including cardiomyocyte arrangement disorder, endoplasmic reticulum aggregation, mitochondrial morphological variation, calcification, and even apoptosis.⁴⁴ On the other hand, the hemodynamic changes caused by permanent pacemaker implantation contribute to increased atrial afterload, which leads to compensatory hypertrophy of cardiomyocytes, and induce the release of a series of neuroendocrine substances (such as tumor necrosis factor alpha (TNF- α) and angiotensin II), and leads to cardiomyocyte apoptosis.^{42,45,46} Hypertrophy and

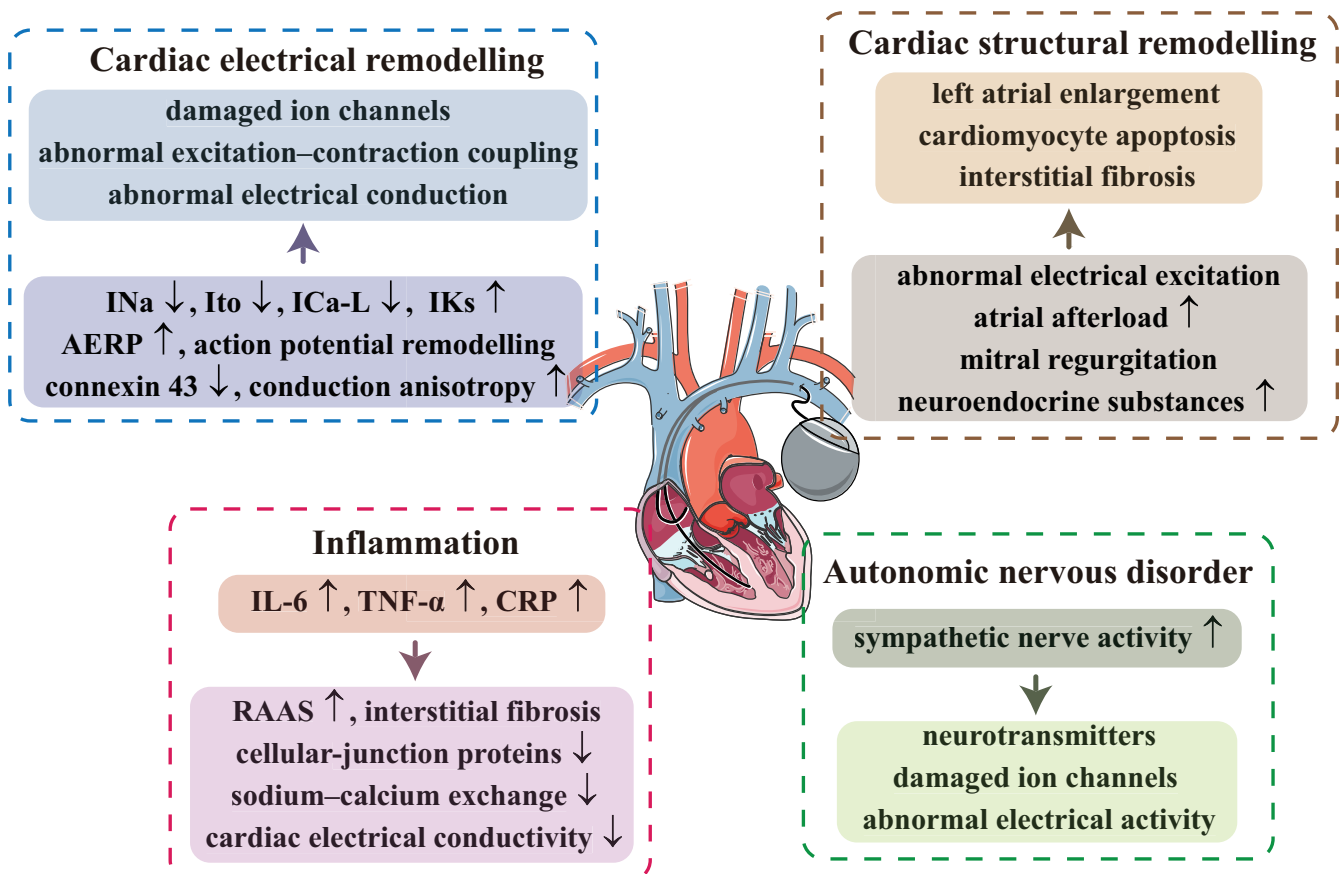


Fig. 1. Mechanism of pacemaker implantation-induced atrial fibrillation (AF)

AERP – atrial effective refractory period; CRP – C-reactive protein; ICa-L – L-type calcium channel; IKs – slowly activating delayed rectifier potassium; IL-6 – interleukin 6; INa – fast sodium channel; Ito – transient outward K⁺ current channel; RAAS – renin–angiotensin–aldosterone system; TNF- α – tumor necrosis factor alpha.

apoptosis of cardiomyocytes in the atrial region can cause abnormal changes in local electrical conductivity and eventually lead to AF. Permanent pacemaker implantation can cause changes in myocardial stroma. The myocardial interstitium is mainly filled with fibroblasts, which have electrophysiological characteristics different from those of the surrounding cardiomyocytes. Interstitial fibrosis promotes abnormal changes in cell coupling as well as the nonuniform and multidirectional transmission of electrical pulses, ultimately leading to AF.^{47,48}

Under the action of various nonphysiological electrical stimulations, the atrial connective tissue tends toward fibrosis and redistribution, and the atrial morphological structure changes in order to compensate for the effect of various exogenous mechanical, chemical and electrical stimulations caused by the implantation of pacemaker.^{43,49} The long-term left and right ventricular systolic and diastolic asynchrony and the change in AV pacing sequence caused by pacemaker implantation leads to hemodynamic changes, such as increased left ventricular end-diastolic pressure, decreased ventricular stroke volume and decreased ejection fraction in terms of mechanical outcomes, resulting in increased left atrial (LA) afterload and an enlarged left atrium.^{43,50} Furthermore, abnormal AV systole

and diastole would contribute to mitral regurgitation, and increase LA diastolic filling and LA preload, ultimately leading to left atrium enlargement.⁵¹ As a result of clinical observation, the incidence of AF is significantly higher in patients with LA enlargement, and there is a clear causal relationship between the two.^{52,53}

Inflammation

Many studies have shown that inflammation is closely related to AF.^{54,55} The exogenous stimulation of electrodes and wires of the pacemaker can induce an inflammatory response.⁵⁶ Previous studies have found that the inflammatory mediators such as interleukin 6 (IL-6) and TNF- α could downregulate the expression of cellular junction proteins and promote abnormal changes in cardiac electrical conductivity.⁵⁷ Moreover, C-reactive protein (CRP), a core expression of the inflammatory response, can bind to phosphatidylcholine on the surface of the cardiomyocyte membrane, thereby affecting sodium–calcium exchange and leading to cardiac electrical remodelling.^{58,59} Therefore, the release of inflammatory mediators induced by exogenous stimulation from the implantation of a pacemaker may lead to AF by regulating local cardiomyocyte

junctional proteins and intracellular calcium homeostasis (Fig. 1). Additionally, a long-term pacemaker implantation induces atrial enlargement, and the resulting stretch can strongly stimulate the release of angiotensin II.^{60,61} The activation of the renin–angiotensin–aldosterone system could be involved in the inflammatory response, which promotes interstitial fibrosis and eventually leads to AF (Fig. 1).^{60,61}

Autonomic nervous disorder

An important cause of the occurrence and development of AF is abnormal autonomic nerve function.^{62,63} It can lead to abnormal release of various neurotransmitters and regulate the ion permeability of the cardiomyocyte membrane, causing damage to some ion channel activities and changes in cellular electrical activity, which finally contributes to AF by affecting trigger potential, autonomy and re-entry.^{62,63} Right ventricular pacing (RVP) can strongly enhance sympathetic nerve activity, whereas dual-chamber (DDD) pacing has a similar role in the autonomic nervous system.^{64,65} Therefore, pacemaker implantation can induce AF through autonomic nervous disorder (Fig. 1).

Effects of different pacing modes on AF

Pacing modes are mainly divided into 2 categories: single-chamber pacing (atrial (AAI) and ventricular single chamber (VVI) pacing) and dual-chamber pacing (DDD pacing).^{66,67} Given that the better understanding of natural course of conduction disturbances in patients with pacemakers have rendered AAI pacing clinically obsolete, and VVI pacing is inapplicable in patients without preprocedural AF, they are not to be discussed.

Dual-chamber pacing can maintain synchronization of AV conduction, and thus it has been considered a physiological pacing mode. However, a series of large-scale clinical trials, such as CTOPP, MOST and UKPACE, challenged this traditional thinking.^{13,14,68} It has been found that compared with single-chamber pacing, DDD pacing cannot reduce mortality or major cardiovascular events.^{13,14,68} Electrophysiological studies of the left atrium found that most patients exhibited intra-atrial conduction block, especially the elderly and those with an enlarged left atrium.^{69,70} When the intra-atrial block is 70 ms in sinus rhythm, it may be prolonged to 120 ms during right atrial (RA) pacing. Furthermore, the intra-atrial block can delay LA activation by ≥ 130 ms.⁷¹ If the AV interval is set to 120 ms (the factory default value for most pacemakers), the AV interval of the left atrium and ventricle will be very short or even negative; that is, the left atrium would be activated after the left ventricle.^{71,72} Given the short AV interval setting, DDD pacing patients received a large number of unnecessary

RVP, so the seemingly physiological dual-chamber pacing can cause a distinctly “non-physiological” hemodynamic state.^{73,74}

In the MOST trial, 2010 patients were implanted with DDD or VVI pacemakers, respectively. The rate of AF was observed in 1399 patients (69.6%). Of these 1339, 707 (52.8%) were randomly assigned to the DDD group and 632 (47.2%) to the VVI group. After 6 years of follow-up, there were no significant differences in various clinical endpoints between the VVI and DDD groups, and the difference in the incidence of AF was 2.1% ($p > 0.05$). In the VVI group, RVP accounted for 58% of the total ventricular events, whereas in the DDD group, it accounted for 90%, especially in patients with pure sinoatrial node disorder. In a further subgroup analysis, Sweeney et al. studied the relationship between the RVP ratio and the incidence of AF.¹³ In the VVI group, the incidence of AF was 21% in patients with a RVP ratio $< 10\%$ and 29% in patients with a RVP ratio of 50–90%. The association was stronger in the DDD group. The incidence of AF was 16% in patients with a pacing ratio $< 10\%$ and 32% in patients with a pacing ratio of 50–90%. Moreover, Cheung et al. found that in patients with a DDD pacemaker implanted for sick sinus syndrome, a cumulative RVP ratio $\geq 50\%$ increased the risk of AF by twofold (HR: 2.2, 95% CI: 1.0–4.7, $p = 0.04$).⁷⁵ Wu et al. came to a similar conclusion.⁷⁶

Relationship between atrial pacing site and AF

In addition to the pacing mode, the location of the atrial electrodes can also influence the AF occurrence. Atrial electrical asynchrony can be induced during atrial appendage or high RA pacing. Also, the pacing P-wave reflected on the ECG is wider than the sinus P-wave.⁷⁷ Moreover, compared with pacing at the low atrial septum (LAS) near the coronary sinus ostium or the high atrial septum near the Bachmann’s bundle, atrial appendage or high RA pacing was more likely to induce AF.^{78,79} During atrial septal pacing, the P-wave is even narrower than the sinus P-wave, possibly due to the Bachmann’s bundle linking to the connecting fibres in the atria and coronary sinus.^{78,80} Therefore, in DDD mode, the incidence of AF is lower in the pacing near the Bachmann’s bundle than in the right atrial appendage (RAA) pacing. Similarly, atrial overdrive pacing is more effective in preventing AF in the lower atrial septum than in the RAA.⁷⁹ Furthermore, the RAA or high RA pacing would prolong AV conduction, resulting in left AV asynchrony (P-wave is located in the T-wave on the ECG) causing pseudo-pacemaker syndrome.⁸¹ During low atrial septal pacing, the duration of AV conduction is shortened, so that under the same AV interval setting, compared with RA pacing, the RVP ratio will be significantly reduced, which can effectively prevent AF.^{79,82}

Prevention of AF after pacemaker implantation

The occurrence of AF affects cardiac pacemaker function and increases the risk of embolic events and heart failure, thus significantly reducing the quality of life of patients and causing a huge economic burden. Therefore, it is of great clinical importance to effectively prevent AF after the implantation of a permanent pacemaker.

Reducing the percentage of RVP

Long-term RVP can cause systolic and diastolic asynchrony in various segments of the ventricular wall, which results in decreased ventricular systolic function, increased mitral regurgitation and increased atrial pressure, thereby promoting the occurrence and maintenance of AF.^{83,84} Right ventricular pacing with retrograde AV conduction would significantly increase the atrial pressure and cause pulmonary venous reflux, resulting in significant pulmonary vein dilatation, which may be a potential inducement of AF.⁸⁵ Even in the absence of retrograde AV conduction, sinus atrial activation can periodically appear after right ventricular (RV) activation, similarly to RVP with retrograde transmission. Another predisposing factor for AF is mitral regurgitation during RVP, which can increase pulmonary wedge pressure and the risk of AF.⁸⁶ Elevated brain natriuretic peptide (BNP) during RVP may reflect increased atrial pressure and the potential risk of AF.⁸⁷ In addition, animal and human experiments have shown that RVP can increase the ratio of myocardial oxygen consumption to left ventricular output and myocardial oxygen consumption, which can aggravate myocardial ischemia and heart failure, thereby promoting AF.^{88,89} Furthermore, long-term AV asynchrony leads to mechanical and electrical remodeling of the atrium, which is conducive to AF and the formation of LA appendage thrombosis. A 10-year follow-up study showed that the incidence of AF was 85.7%

in VVI mode compared to 37.4% in non-VVI mode, which confirmed that RVP is more likely to induce AF than AAI or DDD pacing.⁹⁰

Several pacemaker companies have successively developed various functions to reduce RVP, such as AV Search+, Managed Ventricular Pacing (MVP), ventricular intrinsic preference algorithm, and dynamic AV delay (Fig. 2). Although these programs are named differently, the basic principle of preventing AF is to reduce unnecessary ventricular pacing.^{83,91} The SAVE PACe trial enrolled 1065 patients with sick sinus syndrome, randomized to the conventional dual-chamber pacing group and dual-chamber minimal ventricular pacing group.¹² During an average follow-up of 1.7 ± 1.0 year, the results showed that the median percentage of RVP in the conventional pacing group was 99%, and 68 patients in the group (12.7%) developed persistent AF, whereas the median percentage of RVP in the minimal ventricular pacing group was 9.1%, and 42 (7.9%) patients developed persistent AF ($p < 0.001$ and $p = 0.004$, respectively). Minimal RVP could greatly reduce the risk of ventricular dyssynchrony and persistent AF, with an absolute risk reduction of 4.8% and a relative risk reduction of 40.0%. The MINimize Right Ventricular Pacing to Prevent Atrial Fibrillation and Heart Failure (MINERVA) trial also showed that MVP significantly reduced mortality, need for hospitalization for cardiovascular events and the incidence of permanent AF.⁹² Conversely, a meta-analysis by Shurrab et al. demonstrated that compared with standard DDD pacing, ventricular pacing reduction modalities did not reduce the incidence of persistent AF, nor did they reduce the hospitalization and mortality rates for heart failure.⁹³ The poor prognosis may be related to the significant prolongation of the AV interval allowed by MVP.⁹⁴ Pacing in the DDD mode likely prevented further episodes of atrial tachycardia by preventing long AV intervals, unlike the MVP mode, which permits long AV intervals as long as a ventricular event occurs before the subsequent atrial-paced or atrial-sensed event.

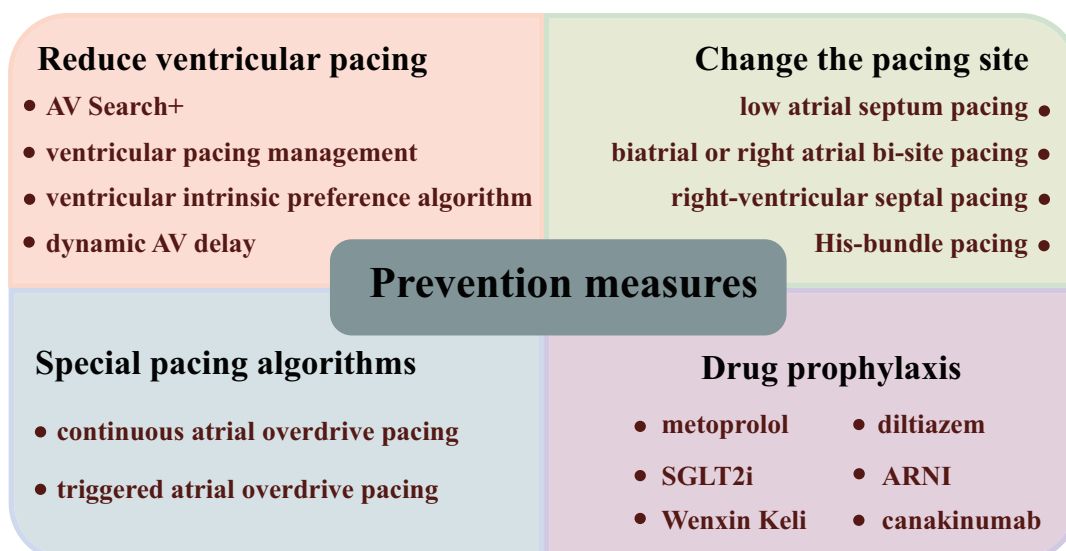


Fig. 2. Prevention of atrial fibrillation (AF) after pacemaker implantation

ARNI – angiotensin receptor-neprilysin inhibitor; AV – atrioventricular; SGLT2i – sodium glucose cotransporter 2 inhibitors.

Changing the pacing site

The RAA contains the pectinate muscle, in which the pacing electrodes are easy to place, so it is the traditional atrial pacing site. However, studies have shown that RAA pacing changes the normal atrial pacing conduction sequence, increases the intra-atrial conduction time and makes the left and right atria asynchronous, which contributes to mitral valve regurgitation, increases the LA pressure and eventually leads to atrial structural and mechanical remodeling and an increased incidence of AF.^{95,96} Therefore, scholars have proposed reducing burden of AF after pacemaker implantation by changing the atrial pacing site (Fig. 2).

At present, the feasible atrial pacing sites mainly include LAS pacing and multisite atrial pacing (biatrial or RA bi-site pacing). Minamiguchi et al. found that compared with RAA pacing, LAS pacing could reduce the incidence of AF after pacemaker implantation in patients with sick sinus syndrome from 19.0% to 5.9%, and prevent persistent AF.⁹⁷ Zhang et al. agreed that LAS pacing can reduce AF burden, and proved the safety of septal pacing.⁹⁸ Multisite atrial pacing mainly refers to biatrial pacing and RA bi-site pacing, and its electrophysiological mechanisms for the prevention of AF include the following: improving atrial depolarization and/or repolarization and ameliorating anisotropic conduction in the atrium, shortening the intra-atrial conduction time and restoring the synchronization of electrical activity in both atria, and shortening the atrial refractory period and reducing the dispersion of the atrial refractory period.^{99,100} For patients with intra-atrial block, i.e., the P-wave time in the ECG >120 ms, the benefit of multisite atrial pacing is more obvious. Moreover, biatrial pacing can eliminate premature atrial contraction (an inducement of AF), and prevent AF initiation with programmed atrial stimulation.¹⁰¹ In a study by Lewicka-Nowak et al. on RA bi-site pacing in 97 patients with sick sinus syndrome, AF was converted to sinus rhythm by preprocedural administration of drugs or electrical cardioversion, and the atrial electrodes were then implanted into the Bachmann's bundle and coronary sinus.¹⁰² After 2 years of follow-up, compared with sinus rhythm, the P-wave time of RA bi-site pacing was significantly shortened, and 90% of the patients showed no AF after surgery. However, some studies have found that RA bi-site pacing could not significantly reduce the incidence of AF, but due to the more complicated and subtle operation, it increased the operation time and X-ray exposure, as well as the dislocation rate of the atrial electrodes.⁷⁷ Moreover, it should be noted that the programmed atrial stimulation is not routinely programmed nor endorsed by guidelines. Therefore, further studies are needed.

The ventricular pacing sites also affect the incidence of AF after the implantation of a pacemaker. In patients with RVP, apical activation of the heart gradually spreads

to the bottom, causing a significant delay in left ventricular contraction.¹⁰³ More ideal ventricular pacing sites, such as the ventricular septum, His bundle or left bundle area, can achieve pacing through the His–Purkinje system and make the ventricular activation close to the physiological conduction sequence, thus enabling synchronization between the left and right ventricles to be maintained, which could help in keeping smooth hemodynamics (Fig. 2).^{104–106} A meta-analysis noted that RV septal pacing resulted in narrower QRS complexes than apical pacing, which improved interventricular dyssynchrony and left ventricular ejection fraction (LVEF), ultimately reducing the incidence of AF.¹⁰⁷ Compared with RV apical pacing, RV outflow tract pacing is closer to the physiological state, which has the advantages of ventricular synchronous activation, reduced myocardial perforation complications, shorter QRS wave duration, and better hemodynamics.¹⁰⁸ Furthermore, a retrospective study of patients receiving different ventricular sites found that patients who received His-bundle pacing had a lower rate of AF occurrence (16.9%) than those who received RV septal and RV apical pacing (25.7% and 28.0%, respectively).¹⁰⁹ Another prospective cohort study indicated that, during a mean follow-up of 11.1 months, left bundle pacing resulted in a significantly lower incidence of new-onset AF (7.4% compared to 17.0%, $p < 0.001$) than RVP. Moreover, after adjusting for confounding factors predisposing to AF, only left bundle pacing was an independent protective factor for decreasing the risk of new-onset AF.¹¹⁰ Researchers are constantly looking for new ventricular pacing sites to avoid asynchronous contraction between ventricles, so as to reduce the risk of AF after pacemaker implantation. His-bundle pacing and left bundle branch area pacing are the 2 most common physiological pacing strategies.^{111,112} We look forward to more clinical evidence and experimental data to confirm their benefits.

Algorithms to prevent AF

Several pacemaker companies have introduced special pacing algorithms to prevent AF attacks, mainly in 2 categories: continuous atrial overdrive pacing (CAOP) and triggered atrial overdrive pacing (Fig. 2). The possible mechanisms are as follows: 1) suppressing premature atrial contractions and short bursts of atrial tachycardia through atrial overdrive pacing, thereby eliminating triggering factors of AF; 2) atrial pacing reducing repolarization time; 3) improving bradycardia and long interval to prevent bradycardia-related AF; and 4) shortening the compensatory interval after premature atrial contraction and reducing the short–long sequences.^{113,114}

Lewalter et al. observed the heart rhythm before the onset of AF in 126 patients and demonstrated that the AF diagnostics and preventive algorithms could reduce the AF burden by 28% in patients whose AF was mainly triggered by premature atrial contractions.¹¹⁵ Similarly,

the MINERVA trial evaluated the role of atrial antitachycardia pacing (Reactive ATP) in the development of AF and found that Reactive ATP could reduce the progression of atrial tachyarrhythmias to permanent AF.⁹² Moreover, the results of the Study for Atrial Fibrillation Reduction (SAFARI) and the diabetes outcome progression trial (ADOPT) studies both showed that atrial overdrive pacing could significantly lower the risk of AF.^{116,117}

However, there are problems with these algorithms. Continuous atrial overdrive pacing aims to prevent the occurrence of AF by increasing the atrial pacing frequency and shortening the compensatory interval after bradycardia and premature atrial contraction. However, symptoms such as heart palpitations may occur.^{118,119} The ASSERT trial followed up 2343 patients with DDD pacemaker implantation for 2.5 years, and the results showed that atrial overdrive pacing did not reduce the incidence of AF, whereas COAP could accelerate battery depletion and increase the reoperation rate.¹¹⁸ The multicenter randomized controlled Septal Pacing for Atrial Fibrillation Suppression Evaluation (SAFE) trial also found no significant benefits of an atrial overdrive pacing program on reducing persistent AF.¹²⁰

Drug prophylaxis

The use of combinations of antiarrhythmic drugs to maintain sinus rhythm or reduce the incidence of AF after pacemaker implantation is advocated (Fig. 2). Metoprolol, a β_1 -selective adrenoceptor antagonist, can effectively increase the activity of the vagus nerve and maintain the balance of cardiac autonomic nerve function.^{121,122} Metoprolol can also inhibit the stimulating effect of endogenous catecholamines on the heart and prolong the refractory period of myocardium, sinoatrial node and AV node, thereby reducing the burden of AF.^{121,122} Diltiazem, a non-dihydropyridines calcium channel blocker, can reduce heart rate and sympathetic activity by inhibiting the calcium influx of sinoatrial and AV nodes and decrease left atrium pressure by lowering peripheral blood pressure stress, which could indirectly prevent the onset of AF.¹²³

Sodium glucose cotransporter 2 inhibitors (SGLT2i) and angiotensin receptor-neprilysin inhibitor (ARNI) reduce the risk of heart failure and new data show that they can prevent AF.^{124,125} In a diabetic rat model, Shao et al. demonstrated that SGLT2i treatment could significantly ameliorate atrial structural and electrical remodeling as well as improve mitochondrial function and mitochondrial biogenesis. Hence, it may be potentially used in the prevention of AF.¹²⁶ Similarly, ARNI could effectively decrease LA fibrosis in mice, as well as reduce atrial inhomogeneous conduction in patients with heart failure, which had potential therapeutic value in preventing the incidence of AF.^{127,128} Moreover, recent studies have reported that drugs that can improve abnormal changes in ion channels may have a role in preventing AF after pacemaker implantation. For

example, Wenxin Keli, a classical Chinese patent medicine, has a selective inhibitory effect on the atrial ion channels and could effectively decrease the incidence of AF.^{129,130} Moreover, it is the first Chinese antiarrhythmic medicine to be approved by the China Food and Drug Administration (CFDA), and it has been increasingly used as an alternative approach for AF treatment globally.¹³¹ Canakinumab, a human monoclonal antibody, significantly reduced the levels of inflammatory mediators, such as IL-6 and IL-1 β .^{132,133} Since inflammatory signaling pathways are associated with the pathogenesis of AF, anti-inflammatory treatment, such as canakinumab, could prevent postprocedural AF,^{134,135} which further supports this novel cytokine-based therapy. Modulation of the autonomic nervous system is also helpful because spinal cord stimulation can suppress AF by inhibiting autonomic nerve remodeling.^{136,137} In the future, the deepening research on the pathogenesis of AF after pacemaker implantation will inspire more effective and practical prevention methods.

Conclusions

The incidence of AF after pacemaker implantation is relatively high. Various types of exogenous stimulation provided by pacemaker implantation and the resulting cardiac electrical remodeling, structural remodeling, inflammation, and autonomic nervous disorder are all related to the occurrence of postprocedural AF. Moreover, different pacing modes and sites have various effects on the incidence of postprocedural AF. It is of great significance to explore clinical measures in order to reduce the incidence of AF after pacemaker implantation. However, it should be emphasized that optimizing the pacing site and mode may reduce the incidence of postprocedural AF, but there are still few long-term large-scale clinical studies in progress. The safety and effectiveness of special pacing algorithms remain controversial. The impact of the above measures on postprocedural AF is complex and requires additional research.

ORCID iDs

Yeshun Wu  <https://orcid.org/0000-0002-8986-9014>
 Hongqing Xu  <https://orcid.org/0000-0002-2622-2280>
 Xiaoming Tu  <https://orcid.org/0000-0003-1148-9641>
 Zhenyan Gao  <https://orcid.org/0000-0001-6503-5560>

References

1. Biffi M, Capobianco C, Spadotto A, et al. Pacing devices to treat bradycardia: Current status and future perspectives. *Exp Rev Med Devices*. 2021;18(2):161–177. doi:10.1080/17434440.2021.1866543
2. Bukari A, Wali E, Deshmukh A, et al. Prevalence and predictors of atrial arrhythmias in patients with sinus node dysfunction and atrial pacing. *J Interv Card Electrophysiol*. 2018;53(3):365–371. doi:10.1007/s10840-018-0463-7
3. Chu SY, Jiang J, Wang YL, Sheng QH, Zhou J, Ding YS. Pacemaker-detected atrial fibrillation burden and risk of ischemic stroke or thromboembolic events: A cohort study. *Heart Lung*. 2020;49(1):66–72. doi:10.1016/j.hrtng.2019.07.007

4. Tayal B, Riahi S, Sogaard P, et al. Risk of atrial fibrillation after pacemaker implantation: A nationwide Danish registry-based follow-up study. *J Electrocardiol.* 2020;63:153–158. doi:10.1016/j.jelectrocard.2019.09.021
5. Boriani G, Sakamoto Y, Botto G, et al. Prevention of long-lasting atrial fibrillation through antitachycardia pacing in DDDR pacemakers. *Int J Clin Pract.* 2021;75(3):e13820. doi:10.1111/ijcp.13820
6. Kornej J, Börschel CS, Benjamin EJ, Schnabel RB. Epidemiology of atrial fibrillation in the 21st century: Novel methods and new insights. *Circ Res.* 2020;127(1):4–20. doi:10.1161/CIRCRESAHA.120.316340
7. Chen XL, Ren XJ, Liang Z, Han ZH, Zhang T, Luo Z. Analyses of risk factors and prognosis for new-onset atrial fibrillation in elderly patients after dual-chamber pacemaker implantation. *J Geriatr Cardiol.* 2018;15(10):628–633. doi:10.11909/j.jisn.1671-5411.2018.10.008
8. Nielsen JC. Mortality and incidence of atrial fibrillation in paced patients. *J Cardiovasc Electrophysiol.* 2002;13(S1):S17–S22. doi:10.1111/j.1540-8167.2002.tb01948.x
9. Connolly SJ, Kerr CR, Gent M, et al. Effects of physiologic pacing versus ventricular pacing on the risk of stroke and death due to cardiovascular causes. *N Engl J Med.* 2000;342(19):1385–1391. doi:10.1056/NEJM200005113421902
10. Nielsen JC, Thomsen PEB, Hojberg S, et al. A comparison of single-lead atrial pacing with dual-chamber pacing in sick sinus syndrome. *Eur Heart J.* 2011;32(6):686–696. doi:10.1093/eurheartj/ehr022
11. Stambler BS, Ellenbogen KA, Orav EJ, et al. Predictors and clinical impact of atrial fibrillation after pacemaker implantation in elderly patients treated with dual chamber versus ventricular pacing. *Pacing Clin Electrophysiol.* 2003;26(10):2000–2007. doi:10.1046/j.1460-9592.2003.00309.x
12. Sweeney MO, Bank AJ, Nsah E, et al. Minimizing ventricular pacing to reduce atrial fibrillation in sinus-node disease. *N Engl J Med.* 2007;357(10):1000–1008. doi:10.1056/NEJMoa071880
13. Sweeney MO, Hellkamp AS, Ellenbogen KA, et al. Adverse effect of ventricular pacing on heart failure and atrial fibrillation among patients with normal baseline QRS duration in a clinical trial of pacemaker therapy for sinus node dysfunction. *Circulation.* 2003;107(23):2932–2937. doi:10.1161/01.CIR.0000072769.17295.B1
14. Toff WD, Camm AJ, Skehan JD. Single-chamber versus dual-chamber pacing for high-grade atrioventricular block. *N Engl J Med.* 2005;353(2):145–155. doi:10.1056/NEJMoa042283
15. Khan AA, Boriani G, Lip GYH. Are atrial high rate episodes (AHREs) a precursor to atrial fibrillation? *Clin Res Cardiol.* 2020;109(4):409–416. doi:10.1007/s00392-019-01545-4
16. Simu G, Rosu R, Cismaru G, et al. Atrial high-rate episodes: A comprehensive review. *Cardiovasc J Afr.* 2021;32(2):48–53. doi:10.5830/CVJA-2020-052
17. Kaufman ES, Israel CW, Nair GM, et al. Positive predictive value of device-detected atrial high-rate episodes at different rates and durations: An analysis from ASSERT. *Heart Rhythm.* 2012;9(8):1241–1246. doi:10.1016/j.hrthm.2012.03.017
18. Sanna T. Long-term monitoring to detect atrial fibrillation with the indwelling implantable cardiac monitors. *Int J Stroke.* 2018;13(9):893–904. doi:10.1177/1747493018790023
19. Bertaglia E, Blank B, Blomström-Lundqvist C, et al. Atrial high-rate episodes: Prevalence, stroke risk, implications for management, and clinical gaps in evidence. *EP Europace.* 2019;21(10):1459–1467. doi:10.1093/europace/euz172
20. Camm AJ, Simantirakis E, Goette A, et al. Atrial high-rate episodes and stroke prevention. *EP Europace.* 2017;19(2):169–179. doi:10.1093/europace/euw279
21. January CT, Wann LS, Calkins H, et al. 2019 AHA/ACC/HRS Focused Update of the 2014 AHA/ACC/HRS Guideline for the Management of Patients With Atrial Fibrillation: A Report of the American College of Cardiology/American Heart Association Task Force on Clinical Practice Guidelines and the Heart Rhythm Society in Collaboration With the Society of Thoracic Surgeons. *Circulation.* 2019;140(2):e125–e151. doi:10.1161/CIR.0000000000000665
22. Hindricks G, Potpara T, Dagres N, et al. 2020 ESC Guidelines for the diagnosis and management of atrial fibrillation developed in collaboration with the European Association for Cardio-Thoracic Surgery (EACTS). *Eur Heart J.* 2021;42(5):373–498. doi:10.1093/eurheartj/ehaa612
23. Andrade JG, Aguilar M, Atzema C, et al. The 2020 Canadian Cardiovascular Society/Canadian Heart Rhythm Society Comprehensive Guidelines for the Management of Atrial Fibrillation. *Can J Cardiol.* 2020;36(12):1847–1948. doi:10.1016/j.cjca.2020.09.001
24. Uittenbogaart SB, Lucassen WAM, van Etten-Jamaludin FS, de Groot JR, van Weert HCPM. Burden of atrial high-rate episodes and risk of stroke: A systematic review. *EP Europace.* 2018;20(9):1420–1427. doi:10.1093/europace/eux356
25. Van Gelder IC, Healey JS, Crijns HJGM, et al. Duration of device-detected subclinical atrial fibrillation and occurrence of stroke in ASSERT. *Eur Heart J.* 2017;38(17):1339–1344. doi:10.1093/eurheartj/ehx042
26. Healey JS, Connolly SJ, Gold MR, et al. Subclinical atrial fibrillation and the risk of stroke. *N Engl J Med.* 2012;366(2):120–129. doi:10.1056/NEJMoa1105575
27. Kawakami H, Nagai T, Saito M, et al. Clinical significance of atrial high-rate episodes for thromboembolic events in Japanese population. *Heart Asia.* 2017;9(2):e010954. doi:10.1136/heartasia-2017-010954
28. Nishinara R, Niwano S, Oikawa J, et al. Novel predictor for new-onset atrial high-rate episode in patients with a dual-chamber pacemaker. *Circ Rep.* 2021;3(9):497–503. doi:10.1253/circrep.CR-21-0096
29. Ogino Y, Ishikawa T, Ishigami T, et al. Characteristics and prognosis of pacemaker-identified new-onset atrial fibrillation in Japanese people. *Circ J.* 2017;81(6):794–798. doi:10.1253/circj.CJ-16-1018
30. Tanawuttivat T, Lande J, Smeets P, et al. Atrial fibrillation burden and subsequent heart failure events in patients with cardiac resynchronization therapy devices. *J Cardiovasc Electrophysiol.* 2020;31(6):1519–1526. doi:10.1111/jce.14444
31. Brandenburg S, Arakel EC, Schwappach B, Lehnart SE. The molecular and functional identities of atrial cardiomyocytes in health and disease. *Biochim Biophys Acta.* 2016;1863(7):1882–1893. doi:10.1016/j.bbamcr.2015.11.025
32. Liaquat MT, Ahmed I, Alzahrani T. Pacemaker malfunction. In: *StatPearls.* Treasure Island, USA: StatPearls Publishing; 2022. <http://www.ncbi.nlm.nih.gov/books/NBK553149/>. Accessed December 7, 2022.
33. Saito Y, Nakamura K, Ito H. Cell-based biological pacemakers: Progress and problems. *Acta Med Okayama.* 2018;72(1):1–7. doi:10.18926/AMO/55656
34. Ni H, Zhang H, Grandi E, Narayan SM, Giles WR. Transient outward K⁺ current can strongly modulate action potential duration and initiate alternans in the human atrium. *Am J Physiol Heart Circ Physiol.* 2019;316(3):H527–H542. doi:10.1152/ajpheart.00251.2018
35. Greiser M, Schotten U. Dynamic remodeling of intracellular Ca²⁺ signaling during atrial fibrillation. *J Mol Cell Cardiol.* 2013;58:134–142. doi:10.1016/j.yjmcc.2012.12.020
36. Nattel S, Dobrev D. Electrophysiological and molecular mechanisms of paroxysmal atrial fibrillation. *Nat Rev Cardiol.* 2016;13(10):575–590. doi:10.1038/nrcardio.2016.118
37. Nattel S, Heijman J, Zhou L, Dobrev D. Molecular basis of atrial fibrillation pathophysiology and therapy: A translational perspective. *Circ Res.* 2020;127(1):51–72. doi:10.1161/CIRCRESAHA.120.316363
38. Dzeshka MS, Lip GYH, Snezhitskiy V, Shantsila E. Cardiac fibrosis in patients with atrial fibrillation. *J Am Coll Cardiol.* 2015;66(8):943–959. doi:10.1016/j.jacc.2015.06.1313
39. Lai D, Xu L, Cheng J, et al. Stretch current-induced abnormal impulses in CaMKII δ knockout mouse ventricular myocytes. *J Cardiovasc Electrophysiol.* 2013;24(4):457–463. doi:10.1111/jce.12060
40. Walters TE, Lee G, Spence S, et al. Acute atrial stretch results in conduction slowing and complex signals at the pulmonary vein to left atrial junction: Insights into the mechanism of pulmonary vein arrhythmogenesis. *Circ Arrhythm Electrophysiol.* 2014;7(6):1189–1197. doi:10.1161/CIRCEP.114.001894
41. Yang S, Mei B, Liu H, et al. A modified beagle model of inducible atrial fibrillation using a right atrium pacemaker. *Braz J Cardiovasc Surg.* 2020;35(5):713–721. doi:10.21470/1678-9741-2019-0363
42. Ferrari ADL, Borges AP, Albuquerque LC, et al. Cardiac pacing induced cardiomyopathy: Myth or reality sustained by evidence? *Rev Bras Cir Cardiovasc.* 2014;29(3):402–413. doi:10.5935/1678-9741.20140104
43. Merchant FM, Mittal S. Pacing induced cardiomyopathy. *J Cardiovasc Electrophysiol.* 2020;31(1):286–292. doi:10.1111/jce.14277
44. Xu H, Gao J, Wang F. Altered mitochondrial expression genes in patients receiving right ventricular apical pacing. *Exp Mol Pathol.* 2016;100(3):469–475. doi:10.1016/j.yexmp.2016.05.005

45. Deshmukh A, Lakshmanadoss U, Deshmukh P. Hemodynamics of His bundle pacing. *Card Electrophysiol Clin*. 2018;10(3):503–509. doi:10.1016/j.ccep.2018.05.014
46. Zhang YY, Wu DY, Fu NK, Lu FM, Xu J. Neuroendocrine and haemodynamic changes in single-lead atrial pacing and dual-chamber pacing modes. *J Int Med Res*. 2013;41(4):1057–1066. doi:10.1177/0300060513489798
47. Jalife J, Kaur K. Atrial remodeling, fibrosis, and atrial fibrillation. *Trends Cardiovasc Med*. 2015;25(6):475–484. doi:10.1016/j.tcm.2014.12.015
48. Reese-Petersen AL, Olesen MS, Karsdal MA, Svendsen JH, Genovese F. Atrial fibrillation and cardiac fibrosis: A review on the potential of extracellular matrix proteins as biomarkers. *Matrix Biol*. 2020;91–92:188–203. doi:10.1016/j.matbio.2020.03.005
49. Merchant FM. Pacing-induced cardiomyopathy: Just the tip of the iceberg? *Eur Heart J*. 2019;40(44):3649–3650. doi:10.1093/eurheartj/ehz715
50. Khurshid S, Frankel DS. Pacing-induced cardiomyopathy. *Card Electrophysiol Clin*. 2021;13(4):741–753. doi:10.1016/j.ccep.2021.06.009
51. Fanari Z, Hammami S, Hammami MB, Hammami S, Shuraih M. The effects of right ventricular apical pacing with transvenous pacemaker and implantable cardioverter defibrillator on mitral and tricuspid regurgitation. *J Electrocardiol*. 2015;48(5):791–797. doi:10.1016/j.jelectrocard.2015.07.002
52. Iscan S, Eygi B, Besir Y, et al. Inflammation, atrial fibrillation and cardiac surgery: Current medical and invasive approaches for the treatment of atrial fibrillation. *Curr Pharm Des*. 2018;24(3):310–322. doi:10.2174/1381612824666180131120859
53. Olsen FJ, Møgelvang R, Jensen GB, Jensen JS, Biering-Sørensen T. Relationship between left atrial functional measures and incident atrial fibrillation in the general population. *JACC Cardiovasc Imaging*. 2019;12(6):981–989. doi:10.1016/j.jcmg.2017.12.016
54. Scott L, Li N, Dobrev D. Role of inflammatory signaling in atrial fibrillation. *Int J Cardiol*. 2019;287:195–200. doi:10.1016/j.ijcard.2018.10.020
55. Vyas V, Hunter RJ, Longhi MP, Finlay MC. Inflammation and adiposity: New frontiers in atrial fibrillation. *EP Europace*. 2020;22(11):1609–1618. doi:10.1093/europace/eaab214
56. Pacheco KA. Allergy to surgical implants. *Clinic Rev Allerg Immunol*. 2019;56(1):72–85. doi:10.1007/s12016-018-8707-y
57. Liew R, Khairunnisa K, Gu Y, et al. Role of tumor necrosis factor- α in the pathogenesis of atrial fibrosis and development of an arrhythmogenic substrate. *Circ J*. 2013;77(5):1171–1179. doi:10.1253/circj.CJ-12-1155
58. Acampa M, Lazzarini PE, Guideri F, Tassi R, Lo Monaco A, Martini G. Inflammation and atrial electrical remodelling in patients with embolic strokes of undetermined source. *Heart Lung Circ*. 2019;28(6):917–922. doi:10.1016/j.hlc.2018.04.294
59. da Silva RMFL. Influence of inflammation and atherosclerosis in atrial fibrillation. *Curr Atheroscler Rep*. 2017;19(1):2. doi:10.1007/s11883-017-0639-0
60. Wijesurendra RS, Casadei B. Mechanisms of atrial fibrillation. *Heart*. 2019;105(24):1860–1867. doi:10.1136/heartjnl-2018-314267
61. Yongjun Q, Huanzhang S, Wenxia Z, Hong T, Xijun X. From changes in local RAAS to structural remodeling of the left atrium: A beautiful cycle in atrial fibrillation. *Herz*. 2015;40(3):514–520. doi:10.1007/s00059-013-4032-7
62. Carnagarin R, Kiuchi MG, Ho JK, Matthews VB, Schlaich MP. Sympathetic nervous system activation and its modulation: Role in atrial fibrillation. *Front Neurosci*. 2019;12:1058. doi:10.3389/fnins.2018.01058
63. Qin M, Zeng C, Liu X. The cardiac autonomic nervous system: A target for modulation of atrial fibrillation. *Clin Cardiol*. 2019;42(6):644–652. doi:10.1002/clc.23190
64. Chiladakis JA, Kalogeropoulos A, Manolis AS. Autonomic responses to single- and dual-chamber pacing. *Am J Cardiol*. 2004;93(8):985–989. doi:10.1016/j.amjcard.2003.12.052
65. Elder DH, Lang CC, Choy AM. Pacing-induced heart disease: Understanding the pathophysiology and improving outcomes. *Exp Rev Cardiovasc Ther*. 2011;9(7):877–886. doi:10.1586/erc.11.82
66. DeForge WF. Cardiac pacemakers: A basic review of the history and current technology. *J Vet Cardiol*. 2019;22:4–50. doi:10.1016/j.jvc.2019.01.001
67. Mulpuru SK, Madhavan M, McLeod CJ, Cha YM, Friedman PA. Cardiac pacemakers: Function, troubleshooting, and management. *J Am Coll Cardiol*. 2017;69(2):189–210. doi:10.1016/j.jacc.2016.10.061
68. Kerr CR, Connolly SJ, Abdollah H, et al. Canadian trial of physiological pacing: Effects of physiological pacing during long-term follow-up. *Circulation*. 2004;109(3):357–362. doi:10.1161/01.CIR.0000109490.72104.EE
69. Reiffel JA. Intra-atrial block: Definition and relationship to atrial fibrillation and other adverse outcomes. *J Atrial Fibril*. 2019;12(2):2234. doi:10.4022/jafib.2234
70. Spies F, Knecht S, Zeljkovic I, et al. First-degree atrioventricular block in patients with atrial fibrillation and atrial flutter: The prevalence of intra-atrial conduction delay. *J Interv Card Electrophysiol*. 2021;61(2):421–425. doi:10.1007/s10840-020-00838-3
71. Bohm A. Prolonged PR interval despite a programmed short sensed AV delay: The role of intra-atrial conduction time. *Europace*. 2002;4(3):329–331. doi:10.1053/eupc.2002.0244
72. Khaykin Y, Exner D, Birnie D, Sapp J, Aggarwal S, Sambelashvili A. Adjusting the timing of left-ventricular pacing using electrocardiogram and device electrograms. *EP Europace*. 2011;13(10):1464–1470. doi:10.1093/europace/eur146
73. Kim WH, Joung B, Shim J, et al. Long-term outcome of single-chamber atrial pacing compared with dual-chamber pacing in patients with sinus-node dysfunction and intact atrioventricular node conduction. *Yonsei Med J*. 2010;51(6):832. doi:10.3349/ymj.2010.51.6.832
74. Statescu C, Sascau RA, Maciuc V, Arsenescu Georgescu C. Programming an optimal atrioventricular interval in a dual chamber pacemaker regional population. *Maedica (Bucur)*. 2011;6(4):272–276. PMID:22879840. PMCID:PMC3391943.
75. Cheung JW, Keating RJ, Stein KM, et al. Newly detected atrial fibrillation following dual chamber pacemaker implantation. *J Cardiovasc Electrophysiol*. 2006;17(12):1323–1328. doi:10.1111/j.1540-8167.2006.00648.x
76. Wu Z, Chen X, Ge J, Su Y. The risk factors of new-onset atrial fibrillation after pacemaker implantation. *Herz*. 2021;46(51):61–68. doi:10.1007/s00059-019-04869-z
77. Roithinger FX, Abou-Harb M, Pachinger O, Hintringer F. The effect of the atrial pacing site on the total atrial activation time. *Pacing Clin Electrophysiol*. 2001;24(3):316–322. doi:10.1046/j.1460-9592.2001.00316.x
78. Kliš M, Sławuta A, Gajek J. Antiarrhythmic properties of atrial pacing. *Adv Clin Exp Med*. 2017;26(2):351–357. doi:10.17219/acem/61429
79. Verlato R, Botto GL, Massa R, et al. Efficacy of low interatrial septum and right atrial appendage pacing for prevention of permanent atrial fibrillation in patients with sinus node disease: Results from the Electrophysiology-Guided Pacing Site Selection (EPASS) Study. *Circ Arrhythm Electrophysiol*. 2011;4(6):844–850. doi:10.1161/CIRCEP.110.957126
80. Sławuta A, Kliš M, Skoczyński P, Bańkowski T, Moszczyńska-Stulin J, Gajek J. Bachmann's bundle pacing not only improves interatrial conduction but also reduces the need for ventricular pacing. *Adv Clin Exp Med*. 2016;25(5):845–850. doi:10.17219/acem/63351
81. Hettrick DA, Mittelstadt JR, Kehl F, et al. Atrial pacing lead location alters the hemodynamic effects of atrial-ventricular delay in dogs with pacing induced cardiomyopathy. *Pacing Clin Electrophysiol*. 2003;26(4 Pt 1):853–861. doi:10.1046/j.1460-9592.2003.t01-1-00150.x
82. Watabe T, Abe H, Kohno R, et al. Atrial pacing site and atrioventricular conduction in patients paced for sinus node disease: Atrial pacing site and AV conduction. *J Cardiovasc Electrophysiol*. 2014;25(11):1224–1231. doi:10.1111/jce.12476
83. Akerström F, Pachón M, Puchol A, et al. Chronic right ventricular apical pacing: Adverse effects and current therapeutic strategies to minimize them. *Int J Cardiol*. 2014;173(3):351–360. doi:10.1016/j.ijcard.2014.03.079
84. Iqbal AM, Jamal SF. Pacemaker syndrome. In: *StatPearls*. Treasure Island, USA: StatPearls Publishing; 2022. <http://www.ncbi.nlm.nih.gov/books/NBK536976/>. Accessed December 7, 2022.
85. Liu T, Li G. Pulmonary vein dilatation: Another possible crosslink between left atrial enlargement and atrial fibrillation? *Int J Cardiol*. 2008;123(2):193–194. doi:10.1016/j.ijcard.2006.11.135
86. Ratanasit N, Karaketklang K, Krittayaphong R. Left atrial volume index as an independent determinant of pulmonary hypertension in patients with chronic organic mitral regurgitation. *BMC Cardiovasc Disord*. 2016;16(1):141. doi:10.1186/s12872-016-0306-3

87. Kodama Y, Kuraoka A, Ishikawa Y, et al. Outcome of patients with functional single ventricular heart after pacemaker implantation: What makes it poor, and what can we do? *Heart Rhythm*. 2019;16(12):1870–1874. doi:10.1016/j.hrthm.2019.06.019
88. Ståhlberg M, Nakagawa R, Bedja D, et al. Chronic atrial and ventricular pacing in the mouse: Application to model cardiac dyssynchrony and resynchronization in heart failure. *Circ Heart Fail*. 2019;12(2):e005655. doi:10.1161/CIRCHEARTFAILURE.118.005655
89. Tayal B, Fruelund P, Sogaard P, et al. Incidence of heart failure after pacemaker implantation: A nationwide Danish registry-based follow-up study. *Eur Heart J*. 2019;40(44):3641–3648. doi:10.1093/eurheartj/ehz584
90. Abedin Z. Incidence of new onset atrial fibrillation in patients with permanent pacemakers and the relation to the pacing mode. *Med Sci Monit*. 2014;20:268–273. doi:10.12659/MSM.890052
91. Jankelson L, Bordachar P, Strik M, Ploux S, Chinitz L. Reducing right ventricular pacing burden: Algorithms, benefits, and risks. *EP Europace*. 2019;21(4):539–547. doi:10.1093/europace/euy263
92. Boriani G, Tukkie R, Manolis AS, et al. Atrial antitachycardia pacing and managed ventricular pacing in bradycardia patients with paroxysmal or persistent atrial tachyarrhythmias: The MINERVA randomized multicentre international trial. *Eur Heart J*. 2014;35(35):2352–2362. doi:10.1093/eurheartj/ehu165
93. Shurrab M, Healey JS, Haj-Yahia S, et al. Reduction in unnecessary ventricular pacing fails to affect hard clinical outcomes in patients with preserved left ventricular function: A meta-analysis. *Europace*. 2016;19(2):282–288. doi:10.1093/europace/euw221
94. Frisch DR, Kenia AS, Walinsky P, Balog J. Managed ventricular pacing facilitating atrioventricular nodal reentrant tachycardia. *Pacing Clin Electrophysiol*. 2014;37(11):1568–1571. doi:10.1111/pace.12318
95. Das A. Electrocardiographic features: Various atrial site pacing. *Indian Heart J*. 2017;69(5):675–680. doi:10.1016/j.ihj.2017.08.030
96. Ramdjan TT, van der Does LJ, Knops P, Res JC, de Groot NM. Right versus left atrial pacing in patients with sick sinus syndrome and paroxysmal atrial fibrillation (Riverleft study): Study protocol for randomized controlled trial. *Trials*. 2014;15(1):445. doi:10.1186/1745-6215-15-445
97. Minamiguchi H, Nanto S, Onishi T, Watanabe T, Uematsu M, Komuro I. Low atrial septal pacing with dual-chamber pacemakers reduces atrial fibrillation in sick sinus syndrome. *J Cardiol*. 2011;57(2):223–230. doi:10.1016/j.jjcc.2010.11.002
98. Zhang L, Jiang H, Wang W, et al. Interatrial septum versus right atrial appendage pacing for prevention of atrial fibrillation: A meta-analysis of randomized controlled trials. *Herz*. 2018;43(5):438–446. doi:10.1007/s00059-017-4589-7
99. Burri H, Bennani I, Domenichini G, et al. Batrial pacing improves atrial haemodynamics and atrioventricular timing compared with pacing from the right atrial appendage. *Europace*. 2011;13(9):1262–1267. doi:10.1093/europace/eur099
100. Rubaj A, Rucinski P, Kutarski A, et al. Cardiac hemodynamics and proinflammatory cytokines during biatrial and right atrial appendage pacing in patients with interatrial block. *J Interv Card Electrophysiol*. 2013;37(2):147–154. doi:10.1007/s10840-013-9792-8
101. Nagarakanti R, Slee A, Saksena S. Left atrial reverse remodeling and prevention of progression of atrial fibrillation with atrial resynchronization device therapy utilizing dual-site right atrial pacing in patients with atrial fibrillation refractory to antiarrhythmic drugs or catheter ablation. *J Interv Card Electrophysiol*. 2014;40(3):245–254. doi:10.1007/s10840-014-9931-x
102. Lewicka-Nowak E, Kutarski A, Dabrowska-Kugacka A, Rucinski P, Zagodzón P, Raczak G. A novel method of multisite atrial pacing, incorporating Bachmann's bundle area and coronary sinus ostium, for electrical atrial resynchronization in patients with recurrent atrial fibrillation. *Europace*. 2007;9(9):805–811. doi:10.1093/europace/eum152
103. Hayashi K, Kohno R, Fujino Y, et al. Pacing from the right ventricular septum and development of new atrial fibrillation in paced patients with atrioventricular block and preserved left ventricular function. *Circ J*. 2016;80(11):2302–2309. doi:10.1253/circj.CJ-16-0640
104. Chen X, Qian Z, Zou F, et al. Differentiating left bundle branch pacing and left ventricular septal pacing: An algorithm based on intracardiac electrophysiology. *Cardiovasc Electrophysiol*. 2022;33(3):448–457. doi:10.1111/jce.15350
105. Heckman LIB, Luermans JGLM, Curila K, et al. Comparing ventricular synchrony in left bundle branch and left ventricular septal pacing in pacemaker patients. *J Clin Med*. 2021;10(4):822. doi:10.3390/jcm10040822
106. Vetta F, Marinaccio L, Vetta G. Alternative sites of ventricular pacing: His bundle pacing. *Monaldi Arch Chest Dis*. 2020;90(2). doi:10.4081/monaldi.2020.1251
107. Weizong W, Zhongsu W, Yujiao Z, et al. Effects of right ventricular nonapical pacing on cardiac function: A meta-analysis of randomized controlled trials. *Pacing Clin Electrophysiol*. 2013;36(8):1032–1051. doi:10.1111/pace.12112
108. Curila K, Jurak P, Halamek J, et al. Ventricular activation pattern assessment during right ventricular pacing: Ultra-high-frequency ECG study. *J Cardiovasc Electrophysiol*. 2021;32(5):1385–1394. doi:10.1111/jce.14985
109. Pastore G, Zanon F, Baracca E, et al. The risk of atrial fibrillation during right ventricular pacing. *Europace*. 2016;18(3):353–358. doi:10.1093/europace/euv268
110. Zhu H, Li X, Wang Z, et al. New-onset atrial fibrillation following left bundle branch area pacing vs. right ventricular pacing: A two-centre prospective cohort study [published online as ahead of print on August 9, 2022]. *EP Europace*. 2022. doi:10.1093/europace/eaac132
111. Sharma PS, Patel NR, Ravi V, et al. Clinical outcomes of left bundle branch area pacing compared to right ventricular pacing: Results from the Geisinger–Rush Conduction System Pacing Registry. *Heart Rhythm*. 2022;19(1):3–11. doi:10.1016/j.hrthm.2021.08.033
112. Su L, Wang S, Wu S, et al. Long-term safety and feasibility of left bundle branch pacing in a large single-center study. *Circ Arrhythm Electrophysiol*. 2021;14(2):e009261. doi:10.1161/CIRCEP.120.009261
113. Knight BP, Gersh BJ, Carlson MD, et al. Role of permanent pacing to prevent atrial fibrillation: Science advisory From the American Heart Association Council on Clinical Cardiology (Subcommittee on Electrocardiography and Arrhythmias) and the Quality of Care and Outcomes Research Interdisciplinary Working Group, in Collaboration With the Heart Rhythm Society. *Circulation*. 2005;111(2):240–243. doi:10.1161/01.CIR.0000151800.84945.47
114. Mitchell A. How do atrial pacing algorithms prevent atrial arrhythmias? *Europace*. 2004;6(4):351–362. doi:10.1016/j.eupc.2004.03.005
115. Lewalter T, Yang A, Pfeiffer D, et al. Individualized selection of pacing algorithms for the prevention of recurrent atrial fibrillation: Results from the VIP registry. *Pacing Clin Electrophysiol*. 2006;29(2):124–134. doi:10.1111/j.1540-8159.2006.00305.x
116. Carlson MD, Ip J, Messenger J, et al. A new pacemaker algorithm for the treatment of atrial fibrillation. *J Am Coll Cardiol*. 2003;42(4):627–633. doi:10.1016/S0735-1097(03)00780-0
117. Gold MR, Adler S, Fauchier L, et al. Impact of atrial prevention pacing on atrial fibrillation burden: Primary results of the Study of Atrial Fibrillation Reduction (SAFARI) trial. *Heart Rhythm*. 2009;6(3):295–301. doi:10.1016/j.hrthm.2008.11.033
118. Hohnloser SH, Healey JS, Gold MR, et al. Atrial overdrive pacing to prevent atrial fibrillation: Insights from ASSERT. *Heart Rhythm*. 2012;9(10):1667–1673. doi:10.1016/j.hrthm.2012.06.012
119. Kantharia BK, Freedman RA, Hoekenga D, et al. Increased base rate of atrial pacing for prevention of atrial fibrillation after implantation of a dual-chamber pacemaker: Insights from the Atrial Overdrive Pacing Study. *Europace*. 2007;9(11):1024–1030. doi:10.1093/europace/eum170
120. Lau CP, Tachapong N, Wang CC, et al. Prospective randomized study to assess the efficacy of site and rate of atrial pacing on long-term progression of atrial fibrillation in sick sinus syndrome: Septal Pacing for Atrial Fibrillation Suppression Evaluation (SAFE) Study. *Circulation*. 2013;128(7):687–693. doi:10.1161/CIRCULATIONAHA.113.001644
121. Dézsi CA, Szentes V. The real role of β -blockers in daily cardiovascular therapy. *Am J Cardiovasc Drugs*. 2017;17(5):361–373. doi:10.1007/s40256-017-0221-8
122. Vinereanu D, Spinar J, Pathak A, Kozłowski D. Role of metoprolol succinate in the treatment of heart failure and atrial fibrillation: A systematic review. *Am J Ther*. 2020;27(2):e183–e193. doi:10.1097/MJT.0000000000001043
123. Lan Q, Wu F, Han B, Ma L, Han J, Yao Y. Intravenous diltiazem versus metoprolol for atrial fibrillation with rapid ventricular rate: A meta-analysis. *Am J Emerg Med*. 2022;51:248–256. doi:10.1016/j.ajem.2021.08.082

124. Bonora BM, Raschi E, Avogaro A, Fadini GP. SGLT-2 inhibitors and atrial fibrillation in the Food and Drug Administration adverse event reporting system. *Cardiovasc Diabetol.* 2021;20(1):39. doi:10.1186/s12933-021-01243-4
125. De Vecchis R, Paccone A, Di Maio M. Upstream therapy for atrial fibrillation prevention: The role of sacubitril/valsartan. *Cardiol Res.* 2020;11(4):213–218. doi:10.14740/cr1073
126. Shao Q, Meng L, Lee S, et al. Empagliflozin, a sodium glucose co-transporter-2 inhibitor, alleviates atrial remodeling and improves mitochondrial function in high-fat diet/streptozotocin-induced diabetic rats. *Cardiovasc Diabetol.* 2019;18(1):165. doi:10.1186/s12933-019-0964-4
127. Okutucu S, Fatihoglu SG, Sabanoglu C, et al. Effects of angiotensin receptor neprilysin inhibition on P-wave dispersion in heart failure with reduced ejection fraction. *Herz.* 2021;46(Suppl 1):69–74. doi:10.1007/s00059-019-04872-4
128. Suo Y, Yuan M, Li H, et al. Sacubitril/valsartan improves left atrial and left atrial appendage function in patients with atrial fibrillation and in pressure overload-induced mice. *Front Pharmacol.* 2019;10:1285. doi:10.3389/fphar.2019.01285
129. Rodriguez A, Hunter CL, Premuroso C, et al. Safety and efficacy of prehospital diltiazem for atrial fibrillation with rapid ventricular response. *Prehosp Disaster Med.* 2019;34(3):297–302. doi:10.1017/S1049023X19004278
130. Shi S, Chu Y, Jia Q, Hu Y. Comparative efficacy and safety of wenxin granule combined with antiarrhythmic drugs for atrial fibrillation: A protocol for a systematic review and network meta-analysis. *Medicine (Baltimore).* 2021;100(3):e24434. doi:10.1097/MD.00000000000024434
131. Tian G, Sun Y, Liu S, et al. Therapeutic effects of Wenxin Keli in cardiovascular diseases: An experimental and mechanism overview. *Front Pharmacol.* 2018;9:1005. doi:10.3389/fphar.2018.01005
132. Arnold DD, Yalamanoglu A, Boyman O. Systematic review of safety and efficacy of IL-1-targeted biologics in treating immune-mediated disorders. *Front Immunol.* 2022;13:888392. doi:10.3389/fimmu.2022.888392
133. Capucci A, Cipolletta L, Guerra F, Giannini I. Emerging pharmacotherapies for the treatment of atrial fibrillation. *Expert Opin Emerg Drugs.* 2018;23(1):25–36. doi:10.1080/14728214.2018.1446941
134. Nomani H, Saei S, Johnston TP, Sahebkar A, Mohammadpour AH. The efficacy of anti-inflammatory agents in the prevention of atrial fibrillation recurrences. *Curr Med Chem.* 2020;28(1):137–151. doi:10.2174/1389450121666200302095103
135. Scott L, Li N, Dobrev D. Role of inflammatory signaling in atrial fibrillation. *Int J Cardiol.* 2019;287:195–200. doi:10.1016/j.ijcard.2018.10.020
136. Bashir M, Bhagra A, Kapa S, MacLeod C. Modulation of the autonomic nervous system through mind and body practices as a treatment for atrial fibrillation. *Rev Cardiovasc Med.* 2019;20(3):129. doi:10.31083/j.rcm.2019.03.517
137. Wang S, Zhou X, Huang B, et al. Spinal cord stimulation suppresses atrial fibrillation by inhibiting autonomic remodeling. *Heart Rhythm.* 2016;13(1):274–281. doi:10.1016/j.hrthm.2015.08.018